THE AMERICAN PHYSICAL SOCIETY

OFFICERS OF THE SOCIETY

President:	D. C. Miller,	Case School of Applied Science, Cleveland, Ohio
Vice-President:	E. T. Coulton	Princeton University, Princeton, N.J.
Secretary:	H. W. Webb	Columbia University, New York City.
Treasurer:	G. B. Pegram	Columbia University, New York City.
Editor:	John T. Tate	Minneapolis, Minn.
Local Secretary for the Pacific Coast:	S. J. Waterman	Stanford University, Calif.

THE PHYSICAL REVIEW

Published monthly Two volumes annually

First series. From July 1, 1893 to January 1, 1913, the Review was conducted by Edward L. Nichols, Ernest Merritt and Frederick Bedell, with the financial support of Cornell University. The first four volumes were issued annually; subsequent volumes, semi-annually; thirty-five volumes in all.

Second series. On January 1, 1913, the Review was transferred to the American Physical Society as announced on the first page of the new series which was then begun. Since then it has been conducted by a Board of Editors elected by the Society. Semi-annual volumes begin in January and July.

Contributors are referred to page 2 of the advertisements for further information.

Annual Subscriptions, throughout the Postal Union, $7.00 in advance.

Single Copies, $1.25.

Canadian Edition, 1916-1920, $6.00, in advance.

Back Volumes, $6.00 per volume; Back Numbers, $1.25 per copy. Postage is due in addition on foreign orders; otherwise postage is extra. No foreign subscriptions are supplied. The Review offers to purchase a limited number of First Series, Vol. 1, No. 1 (at $1.25 each); Second Series, Vol. 7, No. 1, January 1916; Vol. 7, February 1916 and Vol. 9, No. 1, February 1917 (at $1.25 each); Vol. 10, No. 1, January 1918 (at $.75 each).

Advertisements. Rates will be supplied by the Editor on request. Copy for each number must be received at Corning before the 1st of the preceding month; the copy is sent until new copy is received. Send communications direct to the publisher, Cornell Publishing Co., Ithaca, New York.

Discount of ten per cent is allowed subscription agencies and members of the American Physical Society.

Communications [illegible] to receive the Review, [illegible] should be addressed to the Treasurer; [illegible] to the Editor. The regular [illegible] not [illegible] if complaint is received within three months of date of issue.

Communications should be addressed to the Physical Review, 2209 University Ave. S. E., Minneapolis, Minn.

Entered at the postoffice at Ithaca, N.Y., as second class matter. Acceptance for mailing at special rate of postage provided for in section 1103, Act of October 3, 1917, authorized September 4, 1918.

First Series *July, 1926* *Vol. 28, No. 1*

THE

PHYSICAL REVIEW

THE DURATION OF RADIATION EXCITED IN HYDROGEN BY 10.2 VOLT ELECTRON IMPACTS

By Francis G. Slack

Abstract

By the use of a four electrode tube, in which high frequency voltages are applied in phase to the grids of the excitation and photo-electric systems, the life of the $2P$ state in hydrogen, excited by 10.2 volt electron impacts, was measured. Because of the small amount of hydrogen dissociated by the hot cathode it is improbable that absorption and re-radiation played any part. A discussion of other possible errors leads to the conclusion that the observed effects are due to the persistence of the radiation. The experimental results, which were obtained with tubes of different dimensions and for pressures from .075 to .25 mm, check well with those calculated on the assumption that starting at the instant of impact the radiation falls off exponentially. The exponential constant found was $.83\times10^{8}$ sec^{-1}. Unless the form of the curve is the result of a lag in the photo-electric effect, as seems improbable, the average duration of the radiation resulting from the 10.2 volt electron impact in hydrogen is $\tau=1.2\times10^{-8}$ sec. If the photo-electric lag is effective this is the maximum value of τ. Preliminary measurements made for the 11.9 volt radiation, attributed to the hydrogen molecule, indicate an approximate value of $\tau=3.5\times10^{-8}$ sec.

DIRECT measurements of the time associated with the decay of radiation[1] have been made by Wien[2] and by Dempster.[3] These measurements were made by means of a canal ray tube. Atoms were excited by high voltage in one chamber of the tube and passed through a narrow opening into a second chamber where the radiation was observed to decay exponentially and the time constant was computed from the observed data. Interpretation of the results was made difficult because the atoms were completely ionized in the excitation chamber and it was impossible to determine just when the atom arrived at any one state or by what processes the normal state was finally reached.

In this investigation an attempt has been made to avoid such complications and to obtain a direct measurement of the rate of decay

[1] Foote and Mohler, "The Origin of Spectra," Chap. IV.

[2] W. Wien, Ann. d. Physik **73**, 483 (1924).

[3] A. J. Dempster, Astrophys. J. **57**, 193 (1923).

of radiation in hydrogen when excited to the $2P$ state by simple electron impact. The measurement was made for the simplest possible transformation and on the simplest type of atom, only the excitation of the first line of the Lyman Series ($\lambda = 1216$) being possible under the conditions of the experiment.

METHOD

The method used is that devised and described by Webb.[4] In a four electrode tube, the hot cathode F and accelerating grid G made up the exciting system while the photo-electric grid H and photo-electric plate P served as the receiving system (see Fig. 1). The voltages on these systems were so arranged that the formation of positive ions was prevented and no electrons were allowed to pass from one system to the other. Therefore the photo-electric system responded only to radiation. A d. c. potential of 10.2 volts impressed between F and G gave the electrons, emitted from the hot cathode F, a velocity just below that necessary to excite the hydrogen atom to the $2P$ state. An a.c. voltage, of about 2.0 volts peak value, superimposed on this d.c. bias excited the atom only during the positive half of the voltage cycle, no excitation being possible in the negative half-cycle. A voltage of the same frequency, magnitude, and phase applied to the photo-electric system between H and P reversed the photo-electric current in alternate half-cycles. These electrical connections are shown in Fig. 2. The accompanying curves, (a), (b), (c) and (d) of Fig. 2 show the processes involved. The solid curves of (a) and (c) represent the sinusoidal voltages as applied to the excitation system at 60 cycles and at 10^7 cycles respectively. The dotted curves represent the resulting radiation present throughout the cycle, assuming an exponential law of decay. At 60 cycles, because of the long period, the persistence is negligible, while at sufficiently high frequencies (10^7 cycles in this case) a measurable part of the radiation persists into the negative half-cycle. Curves (b) and (d) show the effect of this on the photo-electric system. The solid lines represent the applied voltages between H and P at 60 cycles and 10^7 cycles; the dotted lines represent the photo-electric current due to the incident radiation. At 60 cycles, as no appreciable radiation persists into the negative half-cycle, no negative current affects the electrometer. At higher frequencies the distribution of the same energy over more than the initial half-cycle reduces the positive current and at the same time contributes a negative current during the negative half-cycle, resulting in a decrease of current

[4] H. W. Webb, Phys. Rev. **24**, 113 (1924); Phys. Rev. **21**, 479 (1923).

to the electrometer. By measuring the current for various frequencies the current-frequency relation is obtained. These data are sufficient to check the assumed exponential law of decay and to determine the exponential constant.

Apparatus

Two tubes, designated as tube 1 and tube 2, were used. These gave identical results. A schematic diagram of tube 2 is shown in Fig. 1.

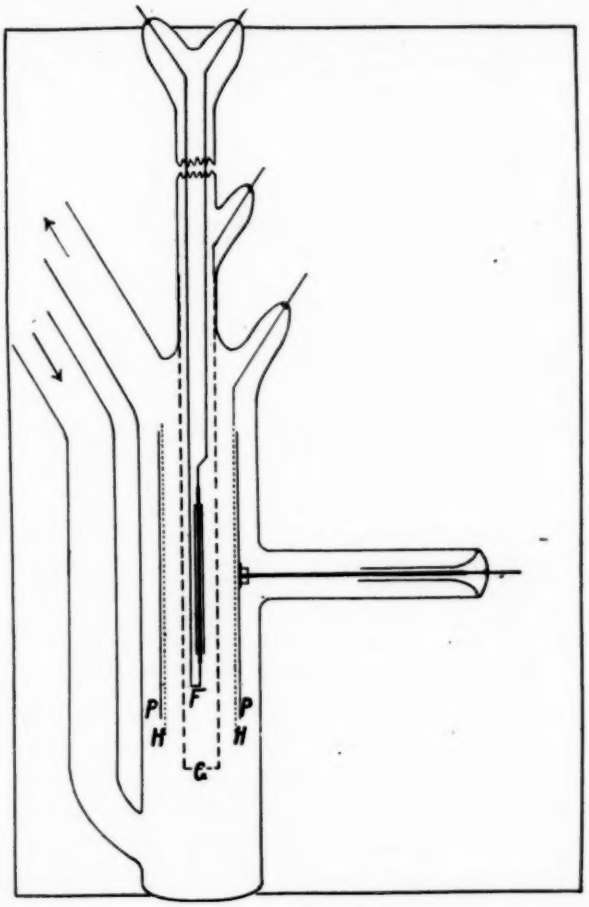

Fig. 1. Schematic diagram of experimental tube 2. Drawn to scale.

The two tubes differed in the spacing of the grids and in the nature of the photo-electric grids *H*. In both tubes the cathode *F* consisted of an equipotential sheath of barium-and-strontium-oxide-coated platinum insulated from the platinum heater by mica. The dimensions of the surfaces were approximately 2×25 mm. A current of about 5

amperes was used through the heating unit which kept the surface at a bright red. This caused sufficient dissociation of the hydrogen to make possible the needed amount of excitation. The cylindrical accelerating grids G were made of nickel gauze of 1.6 mm spacing and were supported in the neck of the tube. The photo-electric system was co-axial with the excitation grid. The plate P was a cylinder of nickel sheet supported by the nickel electrometer lead which was held rigidly by the glass seal. The photo-electric grids H in both tubes were supported by the photo-electric plate and insulated from it by

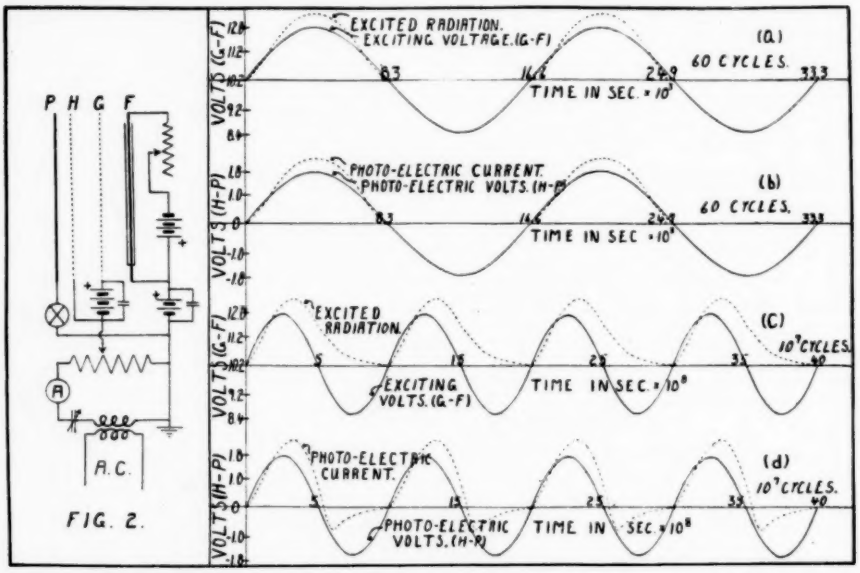

Fig. 2. Electrical connections for persistence measurements. Curves (*a*), (*b*), (*c*), and (*d*) show the processes involved in measurements.

quartz separators. In tube 1 this grid H was made of the same nickel gauze as was used for the accelerating grids G. The quartz separators were 3.2 mm thick. In tube 2 a special grid was made by drilling a nickel plate with a drill of .32 mm diameter, the holes being spaced 1 mm apart and the grid separated from the plate by 1 mm quartz separators. This was done to prevent possible overlapping of the electric fields and to simplify the paths of the electrons. The dimensions of the tubes were as follows:

	Exciting grid G		P.E. grid H.		P.E. plate P	
	Inside diam.	Length	Inside diam.	Length	Inside diam.	Length
Tube 1	1.12 cm	13.5cm	2.40cm	8.0cm	3.20cm	7.5cm
Tube 2	.95cm	14.0cm	1.90cm	8.4cm	2.12cm	7.6cm

The tubes were so constructed that a steady stream of gas could be passed through and in all cases measurements were taken with a flow of hydrogen through the tube. The hydrogen was generated electrolytically at a pressure of about 2 cm kept constant by an automatic relay. After being thoroughly dried by passing through calcium chloride and phosphorus pentoxide drying tubes, the gas passed through a capillary tube sealed into a stopcock with De Khotinsky cement, and then through a liquid air trap into the experimental tube. Upon leaving the tube it passed through a second liquid air trap and capillary to a mercury diffusion pump which was kept in continual operation. A McLeod gauge connected by a T between this second trap and capillary was used to measure the pressure. The two capillaries one on either side of the experimental tube were used to reduce the pressure gradient in the tube. For the purpose of pumping out the system, by-passes, normally closed by stop-cocks, were provided around these capillaries.

Great care was necessary to keep mercury and other contaminations such as vapor from grease joints out of the tube and the tube itself was not connected into the system until liquid air had been put on both the inlet and outlet freeze-out traps. The tube was then baked at about 300 °C for several hours and liquid air kept on the freeze-out traps continually until the tube was removed.

Voltages were applied to the grids by dry cells and the filament was heated by a six-volt storage battery. Alternating voltages were supplied by the 60 cycle lighting circuit or by a 5 watt vacuum tube oscillator. The voltages applied to the grids, normally from 1.5 to 2.0 volts peak value were tapped off a potentiometer. This consisted of a fine platinum wire stretched along the axis of a brass tube, and was part of a tuned circuit coupled with a Hartley oscillating circuit by a variable coupler. These voltages were measured by means of a vacuum tube voltmeter which had been calibrated by known d.c. and 60 cycle voltages. The grid of this tube was tied directly to the grids of the experimental tube and the voltage indication was given by the current from grid to filament read on a micro-ammeter. A Radiotron UV-201 was used with a plate voltage of 23 volts. The frequencies were measured by a General Radio Co. precision wave-meter with special coils calibrated for the higher frequencies. The electrometer used for measuring the photo-electric current was of the Dolezalek type and had a sensitivity of about 8000 mm per volt.

Experimental

It was necessary for interpreting the results to determine the d.c. characteristics of the tube during each run. The connections used in taking these curves are shown in Fig. 3a. Fig. 3b shows the characteristics of the excitation system and is taken with a constant voltage between H and P. Below 10.2 volts the curve shows "stray" energy due probably to light from the filament. At 10.2 volts we find the characteristic "break" due to resonance radiation from the hydrogen atom.[5] In taking this curve which is typical of all those taken the following voltages were used: $P=0$, $H=2.8$, $F=4.2$, and G variable.

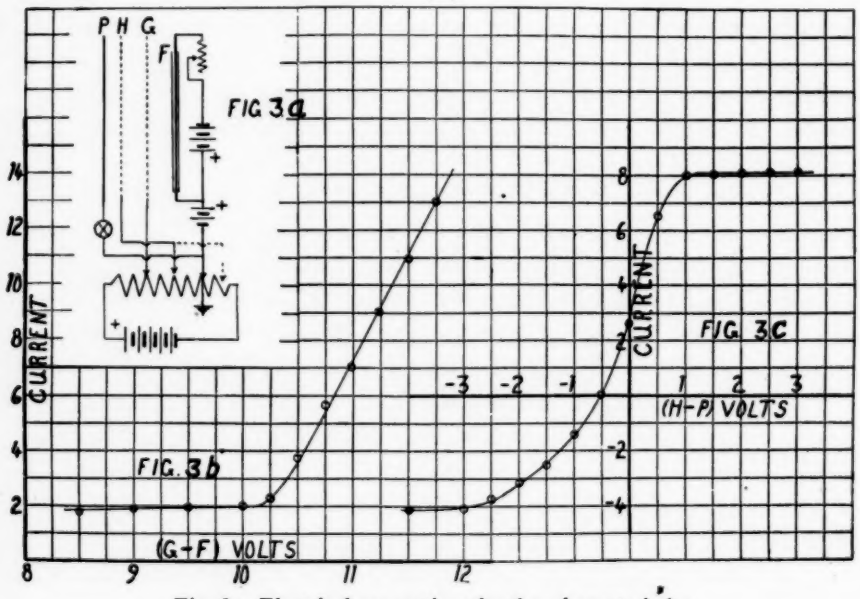

Fig. 3a. Electrical connections for d.c. characteristics.
Fig. 3b. D.C. characteristics of excitation system.
Fig. 3c. D.C. characteristics of photo-electric system.

Fig. 3c is typical of the photo-electric characteristic curves taken with the d.c. voltages $P=0$, H variable, $F=4.2$, and $G=14.7$. This curve shows saturation for the photo-electrons passing from plate to grid with H positive and for the reverse photo-electric current when H is negative with respect to P. The latter accounts for the reverse current due to radiation persisting into the negative half-cycle when a.c. voltages are applied to both systems as explained above.

[5] Horton and Davies, Phil. Mag. **46**, 872 (1923);
K. T. Compton, Phys. Rev. **20**, 283 (1922);
P. S. Olmstead and K. T. Compton, Phys. Rev. **22**, 559 (1923).

In taking the measurements to determine the persistence of the radiation *P* and *F* were kept at the above voltages. A d.c. voltage of 10.2 furnished by small flashlight cells, paralleled with a condenser, of 0.1 m.f. capacity, was put on *G* (Fig. 2). An a.c. voltage superimposed on this bias gave sufficient velocity to the electrons to excite resonance radiation in the positive half-cycle only. The photo-electric grid *H* was connected to *G* by as short a connection as possible, that is, just outside the biasing battery. Thus the same a.c. voltage was impressed on *H* and *G* in phase. The grid of the vacuum tube voltmeter was also connected to this common connection of *H* and *G*.

In making these measurements the rate of charging of the electrometer was measured, and the ratio of the current at each frequency to the corresponding current at 60 cycles, taken as 100 percent, was then found. It was in general necessary to take several measurements alternating between the higher frequency and 60 cycles to establish this current ratio. In addition for each frequency two tests were made as a check on the operation of the apparatus. High frequency surges, harmonics, double peaked waves, or other difficulties, met with in attempting to impress pure sine waves on the grids at the high frequencies used, made these tests necessary. The first of these tests consisted in impressing the a.c. voltage on the excitation grid *G* only, with a d.c. voltage of about 3.0 volts on *H*. In this case the electrometer current at 60 cycles and at higher frequencies should remain the same because the same total amount of radiation should be produced by the voltages on *G* regardless of frequency and all would be recorded as positive photo-electric current. In the second test a d.c. voltage sufficient to excite the resonance radiation was impressed on *G* with a.c. only on the photo-electric system. In this case also the current should not vary with the frequency. In case either of these tests gave differences between the 60 cycle and the higher frequency measurement of more than one percent the data were discarded and in practically every such case some direct cause for such action was discovered and remedied.

Data were taken with the two tubes described under varied conditions of filament current and electrometer shunt, and with tube 2 at pressures varying from .075 mm to .25 mm.

Results

The indicated points on the curve in Fig. 4 represent the experimental data. The points indicated by solid circles were taken with tube 1;

those indicated by the crossed circles with tube 2 at a pressure of .25 mm, and those by the plain circles with tube 2 at .075 mm. Since only three or four points could be measured in any one run and since the d.c. characteristic curves of the excitation and photo-electric systems varied slightly from day to day the following approximate correction was applied to the data before plotting so as to make the results comparable; the shape of the d.c. photo-electric characteristic was assumed constant and all data were corrected to correspond to the same ratio of positive and negative saturation currents.

The result shown in this curve can best be explained by assuming the law of decay of the radiation to be exponential, starting at the instant of impact. The relation between the rate of excitation and time, which is obtained by combining the d.c. excitation characteristic with the a.c. sine voltage wave used to produce radiation, is represented by a curve practically sinusoidal in the positive half-cycle; if we neglect the radiation due to "stray" energy it vanishes for the negative half-cycle. Then, using only positive values of the sine, the expression

$$I_0(\sin 2\pi f t_1)e^{-k(t-t_1)}dt_1$$

represents the intensity of radiation falling on the photo-electric system at any time t resulting from the excitation $I_0(\sin 2\pi f\, t_1)dt_1$ produced in the interval dt_1 at the time t_1, where k is a constant depending on the mean life of the radiation. Denoting by I the total intensity of the radiation falling on the photo-electric system at the time t, we have

$$I=\int_0^t I_0(\sin 2\pi f t_1)e^{-k(t-t_1)}dt_1$$

which gives for values of $t<1/2f$

$$I=\frac{I_0}{4\pi^2f^2+k^2}[k\sin 2\pi ft-2\pi f\cos 2\pi ft+2\pi fe^{-kt}]$$

and for $t>1/2f$

$$I=\frac{2\pi fI_0}{4\pi^2f^2+k^2}[e^{-k(t-1/2f)}+e^{-kt}]$$

With the aid of these expressions curves may be plotted for any values of k showing the relation between the intensity of radiation arriving at the photo-electric system and the time for various frequencies. (See the dotted curves of (a) and (c) in Fig. 2.) By summing up the energy in the various periods and multiplying by the frequency (f) the

total energy arriving at the photo-electric system per second in the positive half-cycles and in the negative half-cycles may be determined.

The photo-electric characteristics to which all experimental results were reduced before plotting was such that the result of applying an a.c. voltage to the photo-electric system could be approximated very closely by multiplying the total radiation arriving at the photo-electric system in the positive half-cycles by four and subtracting from it that arriving in the negative half-cycles multiplied by one. Thus we may obtain a value of the resultant current for each frequency and the ratios of these currents to that computed similarly for 60 cycles gives ratios determining the current-frequency relation resulting from the assumed exponential law of decay. By trial the value of k giving a current-frequency curve best agreeing with the experimental data

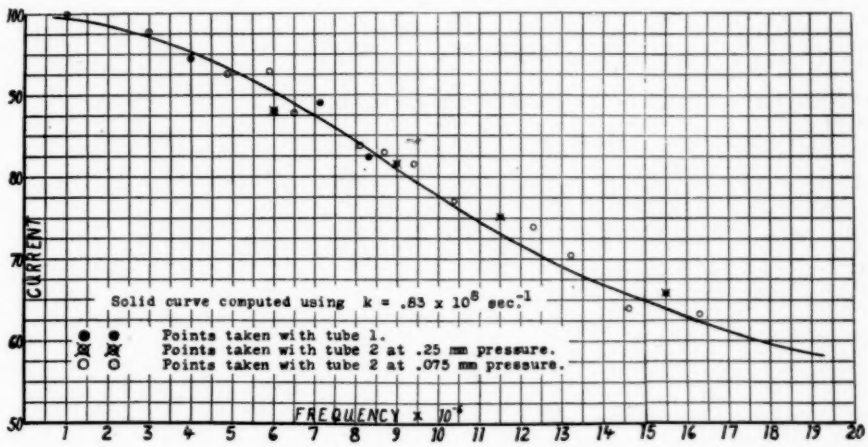
100
90
80
70
60
50
CURRENT
Solid curve computed using k = .83 x 10^8 sec.^-1
Points taken with tube 1.
Points taken with tube 2 at .25 mm pressure.
Points taken with tube 2 at .075 mm pressure.
FREQUENCY x 10^-4
1 2 3 4 5 6 7 8 9 10 11 12 13 14 15 16 17 18 19 20

Fig. 4. Graph of experimental results.

was found. The solid curve of Fig. 4 is computed using this value, $k = .83 \times 10^8$ sec.$^{-1}$. The agreement is such as to justify the assumption of an exponential decay.

To verify this, complete calculations free from approximations have been carried out and the results are shown in Table I. In order to determine accurately the effect of the radiation falling on the photo-electric system it is necessary to combine the d.c. photo-electric voltage-current characteristic curve shown in Fig. 3c with the curve of sine voltage impressed on the grid H to form a new curve which is used as an operator on the curves described above, showing the relation between the radiation arriving at the photo-electric system and time. From this combination of curves, which can only be obtained by a

graphical method, the value of the current for each frequency, stated in percent of the corresponding current at 60 cycles is obtained and the results thus computed are tabulated in column four of Table I. Column three of this table represents the corresponding experimental data. A slight correction has been made for "stray" energy as indicated by the form of the d.c. characteristic curve below 10.2 volts. The correction is made by subtracting from the electrometer readings a quantity proportional to the initial level and assumes that this energy contributes to the total radiation uniformly during the entire cycle. The agree-

TABLE I

Remarks	Frequency $\times 10^{-6}$	Experimental current corrected for initial energy Percent	Computed current $k = .83 \times 10^8$ Percent	Diff. Percent
Sept. 11, 1925				
Tube 2	5.90	91.3	91.2	.1
$p = .075$ mm	8.70	78.7	80.5	−1.8
July 3, 1925	8.33	84.0	88.2	−4.2
Tube 1	7.15	90.0	90.5	− .5
$p = .09$ mm	3.94	95.0	96.0	−1.0
Oct. 25, 1925	3.00	96.3	93.5	2.8
Tube 2	8.10	71.0	72.0	−1.0
Bias on grid H	10.4	60.0	61.0	−1.0
$p = .11$ mm				
Oct. 30 and 31	4.90	91.6	91.4	.2
Tube 2	6.50	87.2	89.5	−2.3
$p = .10$ mm	9.40	81.5	79.5	2.0
	14.6	62.2	66.0	−3.8
	12.3	71.7	70.3	1.4
Nov. 8, 1925	13.2	73.5	72.0	1.5
Tube 2	16.3	67.0	66.6	.4
$p = .10$ mm				
Nov. 20, 1925	9.0	80.0	79.5	.5
Tube 2	11.5	73.2	72.0	1.2
$p = .25$ mm	6.0	87.0	90.5	−3.5
	15.5	63.5	64.5	−1.0

ment between the experimental and computed results may readily be seen. The differences between these values are shown in the last column and indicate on the average an agreement better than two percent. The constant $k = .83 \times 10^8$ sec.$^{-1}$ used above in computing the solid curve of Fig. 4 was also used in computing the values given in column four and it was found that a variation from this value of k as great as one percent gives an agreement not nearly so good. In the table under "Remarks" are recorded the date on which the data were taken, the tube used, the pressure p at which the hydrogen was passed through

the tube, and any variation in the circuits used. Column two gives the frequencies at which the measurements were taken and for which the computations were made.

The results given in the table and indicated by the curve show a close agreement between the computed data and that found experimentally even with tubes of very different dimensions and for pressures varying from .075 mm to .25 mm. Apparently the assumptions that the radiation begins immediately upon impact and decays exponentially with the exponential constant $k=.83\times10^8$ sec.$^{-1}$ describe the processes involved. This gives the reciprocal of k, $\tau=1.2\times10^{-8}$ sec., for the average duration of radiation in hydrogen excited to the $2P$ state by 10.2 volt electron impacts. It should be noted that this experiment gives no indication of the behavior of the electron during this period of time, a part of which may be spent by the electron in an idle state.

Errors. There is possibility of several errors in the method involved in these measurements but a careful study and the results of tests show that it is improbable that any of these play even a small part. (a) *Phase shift between voltages impressed on the grids*: To give the results found a shift of from 30 to 60 degrees in the phase would be required. Phase shifts of this amount seem impossible in view of the precautions taken. Furthermore, no effects could be observed when the length of leads, the position of the batteries, etc., were altered for the purpose of investigating the possibility of trouble of this nature. Finally calculation shows that the observed results would not be consistent with the values of inductance or capacity required for these shifts. (b) *Effect of electron velocities:* At the pressure used the mean velocity of the electron under the voltages used was sufficient for it to traverse the distance between the photo-electric plate and grid in less than one-thirtieth of a half-cycle even at the highest frequencies used. Thus the effect of electrons caught in the reversing field was negligible. This is also borne out by the fact that the same results were obtained with tubes of different dimensions and at different pressures. (c) *Absorption and re-radiation:* It is improbable that this process played any part due to the limited amount of dissociated hydrogen present.

If the time required for an electron to be released from a surface by photo-electric action were of the order of 10^{-8} sec. or more, which seems improbable from other considerations, the duration of this photo-electric lag would affect the time constant measured and it would be possible to state only that $\tau=1.2\times10^{-8}$ sec. represents a maximum value of the duration of the excited radiation. Further experiments

in this laboratory are contemplated in which different materials will be used in the photo-electric systems in order to determine if this gives any measurable change in the results.

W. Wien[2] found by his canal ray method times of the order of 2×10^{-8} sec. for the average life of Hα and Hβ and for several radiations of shorter wave-length. His result for the life of $H\alpha$ is in good agreement with that computed by the classical theory assuming a linear oscillator, but according to this theory shorter times should be found for the shorter wave-lengths. The theory gives for the mean duration of the 10.2 volt radiation about 7×10^{-10} sec. which is much shorter than the life, 1.2×10^{-8} sec., found in the present investigation.

Preliminary measurements have been made on the first resonance radiation attributed to the hydrogen molecule by Horton and Davies.[3] A much cooler cathode was used which did not dissociate sufficient hydrogen to give appreciable radiation at 10.2 volts. It was thus possible to work only with the molecular radiation which starts at 11.9 volts. The results indicate a life for this radiation not less than 3.5×10^{-5} sec.

In conclusion I wish to express my indebtedness to Professor Harold W. Webb, at whose suggestion and under whose guidance this work was done. Thanks are also due to Mr. J. Horace Coulliette for assistance in adjusting the apparatus.

PHOENIX PHYSICAL LABORATORIES,
COLUMBIA UNIVERSITY,
April 15, 1926.

THE ABSORPTION SPECTRA OF SOME HYDRIDE COMPOUNDS IN THE ULTRA-VIOLET

By E. Hulthèn and R. V. Zumstein

Abstract

The vapor of the metal was heated to about 1700°C in a carbon tube and hydrogen slowly admitted. Under these conditions several hydride bands were absorbed. The four bands found for *copper* hydride confirm the analysis of Frerichs. Eight *silver* hydride bands were absorbed which enabled us to form the n_1n_2 scheme. The five *gold* hydride bands found confirm and extend the work of Bengtsson and three new bands, farther down in the ultra-violet, indicate a new electronic level. Three *aluminum* hydride bands were absorbed which support the analysis of Eriksson and Hulthèn. On nearly all our plates the OH bands at 3064 and 2852 were absorbed. Some bands were found which may be due to the oxides of calcium and silver. We were unable to observe absorption at the CdH and CH bands which are shaded toward the violet.

DURING recent years, a rapid advance has been made in the analysis of band spectra, from which important conclusions have been drawn about the structure of molecules. One of the most fundamental conclusions is that the electronic states of the molecules are analogous to those of the atoms, i. e. in band spectra there are terms analogous to the s, p, d, $\cdots$ terms of line spectra. We refer to the works of Birge[1] and of Mulliken[2] for a complete discussion of these hypotheses. A large amount of theoretical work in band spectra is based on the analysis of the *emission* bands of N_2, CO, CO^+, BO, CN and the large number of MeH compounds. When attempts were made to place all of the emission bands of a molecule on an energy diagram, there has frequently been a feeling of uncertainty in regard to the normal state. In other words—where is the level of zero energy? This question may be best answered by experiments on the excitation of the bands by electronic impacts or the study of the absorption spectrum of the molecule.

While we were studying the absorption spectrum of copper vapor in the visible part of the spectrum, very beautiful absorption bands were observed which were recognized as the well known copper hydride bands. The copper was heated in a small carbon tube to about 1700°C. No attempt was made to exclude the atmosphere from the tube. The vapor pressure of copper at 1500°C is about 1 mm of mercury and of

[1] R. T. Birge, Nature, Feb. 27 (1926).
[2] R. S. Mulliken, Phys. Rev. **26**, 561 (1925).

the water vapor of the atmosphere about 2 cm. If the copper hydride molecule is formed according to the chemical equation,

$$Cu+H_2O=CuH+OH$$

then we should expect a group of absorption bands due to the OH molecule. Such was found to be the case. The so-called "water vapor" bands at 3064 and 2852 were easily recognized in absorption. They are now attributed to the OH molecule and not to water vapor. In a recent study of the spectrum of the copper spark under water, Stücklen[3] reported that these OH bands were absorbed. The theoretical importance of the hydride bands is due especially to the wide spacing of the lines, resulting from the small inertia moments. This allows one to study the structure of the bands with a quartz spectroscope which is perhaps the only instrument that could be used below 2500A. They also form a large class of band spectra, well known in emission and with a similar structure for all elements in the same group of the periodic table.

We have undertaken a study of several hydride bands in absorption using the same experimental method that has been employed in studying the absorption spectra of metallic vapors in the ultra-violet. This method has been fully described elsewhere.[4] The metal is placed in a small carbon tube and the tube is heated with an oxy-acetylene torch to the highest temperature possible (about 1700°C). The tube is partly surrounded with concave carbon pieces which utilize the heat of the torch to best advantage and also reduce the loss of heat by radiation. Hydrogen is admitted to the hot tube directly over the surface of the metal. There are two conditions which must be fulfilled in order to obtain the hydride molecules. The atoms of the metal must be present as indicated by the strong absorption lines of these atoms which are always observed along with the hydride bands. The second condition is perhaps the presence of atomic hydrogen. The intensity of the absorption of the hydride bands is very greatly influenced by the rate of inflow of the hydrogen. We do not know if the atomic hydrogen is produced by a purely thermal dissociation of H_2 or H_2O molecules or if there is a catalytic action due to the hot surface of the metal. As an experimental fact we find that when the hydrogen is rapidly passed through the tube (indicated by bubbling the gas through a wash bottle), the hydride bands are faint. This is partly due to the removal of the metallic atoms by the stream of hydrogen and perhaps

[3] H. Stücklen, Zeits. f. Physik **33**, 562 (1925).
[4] Zumstein, Phys. Rev. **25**, 523; **26**, 765 (1925).

also the concentration of the atomic hydrogen is less because of recombination. If on the other hand the hydrogen enters the tube very slowly (about one bubble per second) the hydride bands are also weak although the absorption lines of the metallic atoms are strong. This may be due to the unfavorable influence of the atmospheric oxygen. At some intermediate rate of flow of the hydrogen, which depends on the particular metal, the concentration of the hydride molecules is a maximum. The dispersion of our spectroscope is 12A per mm at 5700A and 2.6A per mm at 2500A. The exposures were between 5 and 20 seconds.

We will now mention an experiment which illustrates the advantages of studying hydride spectra in absorption rather than emission. An exposure of 20 minutes was sufficient to give the OH bands at 3064A from the cone of an oxy-hydrogen flame in *emission*. When this flame was placed between our source of light and the spectroscope we obtained these bands in absorption with 5 seconds exposure. Supposing that the *a priori* probabilities for the transitions of the molecule between the excited and the normal states are the same in both directions, the times of exposure in our experiment are very roughly, inversely proportional to the number of OH molecules in both states. Thus the number of OH molecules in an excited state and which would be capable of emitting the band is a very small fraction of the number in the normal state which are able to absorb it. In fact the general faintness with which the hydride spectra appear in emission is a characteristic property of these bands. Several hours exposure are necessary to photograph them with a large grating. This seems to be due to the instability of the hydride molecule.

We have obtained the absorption spectra of the hydrides of (a) Cu, Ag, Au, Al, O and have tried to get those of (b) Cd, Ca, B, Tl, C, N, Pb, Sn. Regarding the (a) group of elements, we may state that the well known emission spectra of these compounds also appear in absorption. We were also able to extend our knowledge of the term schemes of AgH and AuH leading us to important conclusions about their electronic states. These results will be discussed in detail for the individual molecules. For the (b) group, we found no traces of hydride absorption bands* although for most of these elements the bands are

* *Note on calcium absorption.* When we tried to observe the absorption of the CaH bands in the red, we obtained instead the absorption of some of the complicated band groups which appear in emission from the Ca and $CaCl_2$ flame and arc spectra. Thus we obtained the characteristic group of bands at λ5934.3–5969 and the intense groups 6179.4–6185 and 6205.7–6211.8. This indicates that these groups belong to a Ca_2 molecule or a compound with oxygen or carbon (see Kayser and Konen Handbuch 7, p. 175).

known in emission. This failure may be due to at least three reasons. First: It seems very probable that for most of the (b) group the temperature that could be used was too low to give atomic hydrogen. At high temperatures the vapor was so dense that practically no light could pass through. However for cadmium, carbon and tin the conditions seemed to be favorable for the production of hydride molecules. Second: It is known from experiments on the absorption of tin vapor[5] that under the conditions of our experiments, we only obtain atoms in excited states which differ from the normal state by $\Delta\nu = 10{,}000$ cm^{-1}. Also from the present experiments we only find hydride absorption bands from vibrational states less than 5,000 cm^{-1} from the normal state. If therefore the final state of the CH and CdH bands is an excited state differing in frequency from the normal state by more than 10,000 cm^{-1}, then we could not have observed them in absorption. Third: According to a general rule of Birge[6] and Mecke,[7] band spectra degraded toward the red are emitted by molecules having a more stable final state and bands degraded towards the violet a more stable initial state. All hydride bands emitted by the elements of the second group (Mg, Ca, − Zn, Cd, Hg) are degraded toward the violet and the structural investigations of these spectra all show a very unstable final state of the molecule. Probably these molecules only remain a very short time in the less excited states and thus their absorption spectra must be more difficult to obtain. This view is strongly supported by the fact that all band spectra of *dipoles* which we found in absorption, CuH, AgH, AuH, AlH, OH and also the absorption bands of O_2 are degraded toward the red and thus they fulfill the conditions mentioned above.

The emission bands of Cu, Ag and Au hydrides[8,9,10,11] are all shaded toward the red and homologous in structure. With the exception of the components due to the isotope effect from the metal, they are of very simple structure containing only one P and one R branch. In what follows, we denote the electronic frequency of a band system by ν_0, the vibrational quantum numbers of the initial states by n_1 and those of the final states by n_2 (referring to the emission process).

[5] Zumstein, Phys. Rev. **27**, 150 (1926).
[6] R. T. Birge, Phys. Rev. **25**, 240 (1925).
[7] R. Mecke, Zeits. f. Physik **32**, 833 (1925).
[8] R. Frerichs, Zeits. f. Physik **20**, 170 (1923).
[9] E. Bengtsson, Zeits. f. Physik **20**, 229 (1923).
[10] E. Bengtsson, Arkiv f. Math. Astronomioch Fysik **18**, 27 (1925).
[11] E. Bengtsson and E. Svensson, C. R. **180**, 274 (1925).

Copper hydride. In Table I are given the wave-lengths of the heads of the bands of the CuH spectrum as arranged by Frerichs. In this scheme, the bands 4280 and 4006 of the first row ($n_2=0$), were very strongly absorbed. Our failure to observe absorption of the 3777 band is due in part to the small dispersion of our quartz spectrograph in this region. The other CuH absorption bands were all observed with a large glass spectrograph. Faint absorption was also observed at the bands 4328 and 4063 of the second row ($n_2=1$). Our experiments thus confirm the arrangement of Frerichs and show that the $n_2=0$ level is the normal state of the CuH molecule. H. Stücklen found a single absorption band at 2240 in the spectrum of the copper spark under water but did not find it in the copper arc in air or hydrogen. We find the same band strongly absorbed in our experiments. It is also re-

TABLE I

Band system of copper hydride.
(Wave-lengths of band heads. Underlined bands were absorbed.)

n_2	$n_1=0$	1	2	3
0	4280	4006	3777	
1	4650	4328	4063	
2		4690	4380	4124
3			4734	

versed in a 100 ampere copper arc in air. This band is probably due to a copper hydride, however the large inertia moment as calculated from the 2240 band shows that the molecule is not the same as the one which absorbs the long wave system. Stücklen has suggested a CuH_2 molecule.

Silver hydride. We know of two very strong silver hydride bands in emission at λ3330 and 3358. They have recently been measured and analyzed by Bengtsson and Svensson[11] who found that these bands have no common initial or final states. Eder and Valenta in their atlas, give the flame spectrum of AgCl and indicate band heads at 3515, 3540, 3577 and a group of longer wave-length at 3750, 3810, 3900, 4102. We find the bands 3330 and 3358 beautifully developed in absorption and also two faint groups of bands at 3179, 3220 and 3516, 3544, 3583, 3638. The last group is apparently the same as the bands found by Eder and Valenta in emission. From the grouping of the bands we are able to obtain the n_1n_2 scheme of Table II. The figures above the wave-lengths of the heads denote the intensities of the bands in

absorption. We notice a remarkable symmetry in the intensity distribution around the O group (3330, 3358) which is characteristic for

TABLE II

Band system of silver hydride

(Wave-length of band heads. Numbers above band head denote intensity of absorption and those below, the frequency of the zero line.)

n_2	$n_1=0$	1	2	3
0	(10) 3330 (29900)	(1) 3179* (31389)	....	....
1	(2) 3516	(6) 3358 (29696)	(2) 3220*	....
2	3750	(3) 3544		(1) x
3	....	3810	(2) 3583	....
4	....	....	3900	(1) 3638*

* New bands.
x Head of this band hid by silver absorption line λ3280

many band spectra (N_2, AlO, etc.). In order to verify this arrangement of the bands, we have analyzed the structure of λ3179. In Table III

TABLE III

Silver hydride band λ3179.4
Wave numbers are reduced to vacuum

m	3179.4 R	3179.4 P	3179.4 Δ_1	3179.4 Δ_2	3358 Δ_1	3330 Δ_2
1	x	.....	.....	.....	.....	.....
2	31407.6	31376.5	31.1	.....	.....	.....
3	16.6	60.6	56.0	63.1	56.8	63.6
4	24.8	44.5	80.3	89.0	80.0	88.8
5	30.1	27.6	103.5	113.9	102.6	114.3
6	35.6	10.9	124.7	138.9	125.3	139.2
7	38.5	292.2	146.3	164.2	147.7	164.2
8	41.4	71.4	170.0	187.7	170.0	189.2
9	42.8	50.8	192.0	212.4	192.8	214.2
10	42.8	29.0	213.8	238.2	*	239.2
11	41.4	04.6	236.8	262.4	236.5	263.7
12	38.5	180.4	258.1	287.3	257.9	288.0
13	33.7	54.1	279.6	311.6	279.6	312.2
14	28.2	26.9	301.3	335.0	301.3	336.1
15	20.8	098.7	322.1	358.9	322.4	359.9
16	11.8	69.3	342.5	.....	343.3	.....

x not observed.

the wave numbers of the lines are given as we have arranged them in a P and R branch. If the arrangement of Table II is correct, the initial

states of 3358 and 3179 should be identical as well as the final states of 3330 and 3179. This comparison can be made by forming the initial and final rotational terms of the bands thus:[12]

$$P(m) = F(m-1) - f(m)$$
$$R(m) = F(m+1) - f(m)$$

from which $R(m) - P(m) = F(m+1) - F(m-1) = \Delta_1$

and $R(m-1) - P(m+1) = f(m+1) - f(m-1) = \Delta_2$

Accordingly the Δ_1 values should be the same for 3358 and 3179 and the Δ_2 values for 3330 and 3179. In Table III the Δ_1 and Δ_2 values are given for the bands 3358 and 3330 as calculated from the measurements of Bengtsson and Svensson and we find an agreement within the errors of measurements (approx. 1.0 cm^{-1}). It is to be noted that the emission bands found by Eder and Valenta at 3750, 3810, 3900 also find a place in this scheme.

Other silver bands. We observed a system of absorption bands having double heads at λ2661.91, 61.46 – 2660.22, 59.90 – 2658.63, 58.18 – 2657.19, 56.64. The bands are shaded toward the red and the intensity of the long wave component much greater than that of the short wave one of the doublet. They do not show a fine structure and are perhaps due to an AgO compound as they resemble the CuO bands in the visible. We also observed in absorption a group of nearly equidistant lines (or band heads?) at 2571.78, 69.85, 68.01, 66.02, 64.06, 62.34 but hesitate about the origin of this isolated band or group of bands.

Gold Hydride. The band spectrum of gold hydride in emission has been studied by Bengtsson.[10] Since the gold vapor seemed to be very inert toward the atmospheric oxygen and therefore more suitable for study by our method, we have devoted most attention to the gold hydride spectra. Thus we found of the seven bands observed by Bengtsson λ4436, 4339, 4068, 3973, 3745, 3652, 3457 only 3973, 3652 and 3457 were absorbed as one would expect. These bands correspond to the final states $n_2 = 0,1$ in Bengtsson's scheme of the spectrum. We also found two new bands with heads at λ3298.1 and 3170.0. The wave numbers of the lines of these bands are given in Table IV, columns 1 and 2. In order to find the relation between these bands and those of Bengtsson, we may form their initial and final rotational terms Δ_1 and Δ_2 as we did for silver and compare them with the corresponding Δ values calculated by Bengtsson. These values are collected in Table V. From the agreement between the Δ_2 values of λ3652, 3457, 3298 and

[12] E. Hulthèn, Ann. d. Physik **71**, 43 (1923).

TABLE IV

Gold hydride bands (ν_{vac} of lines observed)

m	λ3298.1		λ3170.0		λ2773.3		λ2612.8		λ2511.7	
	P	*R*	*P*	*R*	*P*	*R*	*P*	*R*	*P*	*R*
1		*		*		36025.1		*		39788.3
2	30277.1	30309.1	31508.6	31536.8	.....	34.4	38216.8	38251.5	39762.1	96.2
3	59.4	11.4	489.9	38.2	.....	41.5	00.9	55.8	46.4	802.0
4	37.5	09.1	65.3	33.8	35965.3	45.4	180.8	59.5	24.8	02.0
5	11.9	*	37.6	26.9	44.4	48.1	58.2	61.9	00.7	02.0
6	182.2	296.1	06.1	11.0	21.2	48.1	34.3	59.5	673.6	796.2
7	48.2	84.5	368.8	492.0	895.9	45.4	06.3	55.8	44.2	88.3
8	11.9	*	26.1	69.3	68.4	39.2	076.0	46.0	11.3	74.2
9	070.7	46.9	279.8	40.4	38.6	32.1	41.0	35.4	575.6	62.1
10	25.6	21.1	28.8	07.8	06.7	22.0	06.2	20.8	35.2	46.4
11	29976.4	192.0	172.1	368.8	*	10.6	37967.2	05.3	493.4	24.8
12	25.8	60.4	11.0	26.1	734.2	35997.9	24.5	185.6	48.2	00.7
13	866.8	22.0	044.3	276.6	.....	78.2	880.2	63.4	00.0	673.6
14	08.4	082.7	30973.8	23.5	.....	58.4	33.2	39.1	347.0	44.2
15	743.2	38.0	898.1	164.3	.....	36.5	784.9	10.6	94.0	09.4
16	675.3	29987.2	16.6	099.8	.....	11.7	32.7	079.9	36.0	570.7
17	03.7	31.9	.....	29.5	.....	884.6	676.0	45.7	174.1	29.4
18	.....	873.0	.....	30953.0	.....	*	18.2	07.9	09.4	484.5
19	.....	11.5	.....	.....	.....	22.8	560.0	37967.2	043.1	35.6
20	.....	743.2	.....	.....	.....	788.8	495.9	24.5	38972.7	384.5
21	.....	669.8	.....	.....	.....	52.6	28.5	880.2	897.8	29.5
22	.....	593.9	.....	.....	.....	13.0	*	33.2	17.6	268.4
23	.....	.....	.....	.....	.....	.....	288.7	779.5	738.7	*
24	.....	.....	.....	.....	.....	.....	12.1	23.2	656.3	143.2
25	.....	.....	.....	.....	.....	.....	.....	665.8	.....	072.3
26	.....	.....	.....	.....	.....	.....	.....	04.6	.....	.....

* Not observed because of reversal in source of light.

TABLE V A

Gold hydride bands—Table of Δ values (long wave system).

	λ3652		λ3457		λ3298		λ3170	
	$n_1=0$	$n_2=0$	$n_1=1$	$n_2=0$	$n_1=2$	$n_2=0$	$n_1=3$	$n_2=0$
m	Δ_1	Δ_2	Δ_1	Δ_2	Δ_1	Δ_2	Δ_1	Δ_2
2	.....	.....	.....	.....	32.0	.....	28.2	.....
3	.....	.....	.....	.....	52.0	71.6	48.3	71.5
4	.....	.....	.....	.....	71.6	99.5	68.5	100.6
5	.....	.....	.....	.....	*	126.9	89.3	127.7
6	.....	.....	.....	.....	113.9	*	104.9	158.1
7	.....	.....	.....	.....	136.3	184.2	123.2	184.9
8	.....	213.2	.....	213.0	*	213.8	143.2	212.2
9	198.0	240.8	187.4	240.3	176.2	*	160.6	240.5
10	220.3	268.8	208.3	268.4	195.5	270.5	179.0	268.3
11	243.1	296.6	230.4	296.0	215.6	295.3	196.7	296.8
12	265.7	324.4	251.7	324.3	234.6	325.2	215.1	324.5
13	287.9	351.8	273.6	351.7	255.2	352.0	232.2	352.3
14	309.8	379.3	294.5	378.9	274.3	378.8	249.7	378.5
15	332.0	405.8	314.1	407.1	294.8	407.4	266.2	406.9
16	353.5	433.0	334.6	434.2	311.9	434.3	283.2	.....
17	375.8	460.3	354.9	460.8	328.2	.....	.....	.....
18	396.6	487.5	.....	487.2	.....	.....	.....	.....
19	417.5	513.4	.....	.....	.....	.....	.....	.....
20	438.3	539.4	.....	.....	.....	.....	.....	.....
21	458.3	565.4	.....	.....	.....	.....	.....	.....
22	478.3	591.1	.....	.....	.....	.....	.....	.....
23	498.1	616.0	.....	.....	.....	.....	.....	.....
24	517.1	640.9	.....	.....	.....	.....	.....	.....

TABLE V B

Gold hydride bands—Table of Δ values (short wave system).

	λ2773.8		λ2612.8		λ2511.7	
	$n_1'=0$	$n_2=1$	$n_1'=0$	$n_2=0$	$n_1'=1$	$n_2=0$
m	Δ_1	Δ_2	Δ_1	Δ_2	Δ_1	Δ_2
2	.....	.....	34.7	.....	34.1	41.9
3	.....	69.1	54.9	70.7	55.6	71.4
4	80.1	97.1	78.7	97.6	77.2	101.3
5	103.7	124.2	103.7	125.2	101.3	128.4
6	126.9	152.2	125.2	155.1	122.6	157.8
7	149.5	179.7	149.5	183.5	144.1	184.9
8	170.8	206.8	170.0	214.8	162.9	212.7
9	193.5	232.5	194.4	239.8	186.5	239.0
10	215.3	*	214.6	268.2	211.2	268.7
11	.....	287.8	238.1	296.3	231.4	298.2
12	260.7	.....	261.1	325.1	252.5	324.8
13	.....	.....	283.2	352.4	273.6	353.7
14	.....	.....	305.9	378.5	297.2	379.6
15	.....	.....	325.7	406.4	315.4	408.2
16	.....	.....	347.2	434.6	334.7	435.3
17	.....	.....	369.7	461.7	355.3	461.3
18	.....	.....	389.7	485.7	375.1	486.3
19	.....	.....	407.2	512.0	392.5	511.8
20	.....	.....	428.6	538.7	411.8	537.8
21	.....	.....	451.7	*	431.7	566.9
22	.....	.....	*	591.5	450.8	590.8
23	.....	.....	490.8	621.1	*	622.1
24	.....	.....	511.1	.....	486.9	.....

3170, we conclude that these four bands have the same final state $n_2=0$. Both from their Δ_1 values and the distribution of the 0 lines (ν_0 values are given in Table VI), we conclude that they belong to a set of vibrational states $n_1=0, 1, 2, 3$.

Farther out in the ultra-violet, we found three new bands at λ2773.9, 2612.3 and 2511.7 which have the same structure as the bands of Bengtsson. Their lines are given in columns 3, 4, 5 of Table IV. Comparing the Δ values of these bands with those of the Bengtsson bands (Table V B) we find that 2612.3 and 2511.7 belong to the state $n_2=0$ and 2773.3 to $n_2=1$. From their Δ_1 values we conclude that 2773.3 and 2612.3 have the same initial state. This system is widely separated from the long wave system ($\Delta\nu$ approx. 10,000 cm^{-1}). We therefore conclude that it belong to *a new excited electronic level of the* AuH *molecule* ($n_1'=0, 1$).

TABLE VI

Band systems of gold hydride

(Wave-lengths of band heads. Underlined bands were absorbed. Numbers below band heads are frequencies of zero lines.)

n_2	$n_1=0$	1	2	3	$n_1'=0$	1
0	3652 (27342)	3457 (28894)	3298* (30291)	3170* (31523)	2612* (38230)	2511* (39778)
1	3973 (25127)	3745 (26679)	....	....	2773* (36014)	....
2	4339 (22980)	4068 (24530)	....	....	....	....
3	....	4436 (22452)	....	....	....	....

* New bands, not found in emission.

In Fig. 1 we have compared our results of the CuH, AgH and AuH absorption spectra, showing the electronic levels. If we consider the homologous structure of the spectra of these compounds, we may expect to find a new state in CuH and AgH corresponding to the second excited state in AuH. In spite of several attempts we did not find a new band system for either of these hydrides. It seems certain that such systems exist and that they could be found by improving the experimental methods.

The electronic levels of gold hydride, Fig. 1, approximately fit a Rydberg formula. From the analysis of the structure of the bands, we find that the rotational terms can be approximately represented by Kratzer's formula:[13]

$$W_r^m = B^n(m-\epsilon)^2+2\delta(m-\epsilon)+\cdots$$

[13] A. Kratzer Ann. d. Physik **71**, 72 (1923).

ϵ is 1/2 for all the states of CuH, AgH and AuH. According to the theory,[14] ϵ is closely connected with the electronic system of the molecule so that its value in some way indicates the nature of the electronic terms. It therefore seems probable that all the electronic levels indicated in Fig. 1 are *s* terms. This violates the selection principle for line spectra; however Birge[1] has pointed out that the selection principle may not hold so rigidly in band spectra.

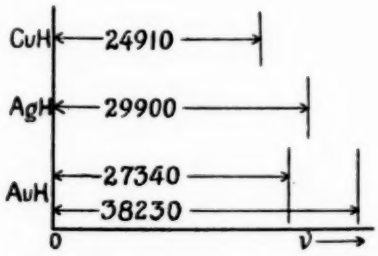

Fig. 1. Electronic energy levels in CuH, AgH, and AuH.

There is a close parallel between the nuclear distances (r) and the vibrational frequencies (ω) of the normal and the excited states of AuH. We have calculated from Tables V and VI that

$$r_2 = 1.56 \times 10^{-8}\ \text{cm},\ \omega_2 = 2256\ \text{cm}^{-1}$$
$$r_1 = 1.72 \times 10^{-8}\ \text{cm},\ \omega_1 = 1626\ \text{cm}^{-1}$$
$$r_1' = 1.74 \times 10^{-8}\ \text{cm},\ \omega_1' \sim 1600\ \text{cm}^{-1}$$

This shows that the molecule is most stable in the normal state. The emitting electron, when in the normal state, therefore plays an important part in binding the nucleii to the electron system of the molecule. In the excited states, this binding effect is decreased which is additional evidence that we are dealing with *s* terms. For ZnH, CdH, and HgH the electron in the excited states moves in $2p_{1,2}$ orbits, and makes the excited molecule more stable than the normal molecule.

Aluminum hydride. These bands have recently been studied in emission and analyzed by Eriksson and Hulthèn.[15] Four bands having *P*, *Q* and *R* branches were arranged thus:

n_2	$n_1=0$	1
0	4241	4067
1	4568	4354

[14] R. S. Mulliken, Proc. Natl. Acad. Sci. **12**, 144 (1926.)
[15] G. Eriksson and E. Hulthèn, Zeits. f. Physik **34**, 775 (1925).

They noted that the λ4241 band was reversed in the arc and also a very curious effect. The series of lines of the bands become remarkably broad and vanish at a certain rotational state of the excited molecule ($m=24$ for $n_1=0$ and $m=13$ for $n_1=1$). The three absorption bands 4241, 4067, 4354 were strongly absorbed and showed the same effect.

INTERNATIONAL EDUCATION BOARD (E. H.),
NATIONAL RESEARCH FELLOWSHIP (R. V. Z.),
PHYSICS DEPARTMENT,
UNIVERSITY OF MICHIGAN,
March 27, 1926.

BAND SERIES IN INFRA-RED ABSORPTION SPECTRA OF ORGANIC COMPOUNDS. II

By Joseph W. Ellis

Abstract

The absorption bands of secondary intensity occurring, in addition to the more pronounced members of the previously described C-H series, in the short wave-length infra-red spectra of methyl iodide, methylene chloride, methylene bromide, methylene iodide, chloroform and bromoform are accounted for on the basis of linear C–Cl, C–Br, and C–I series starting at 16.8μ, 17.2μ and 17.5μ respectively; and on the basis of simple additive combinations between these frequencies and those of the C–H series.

IN PART I of this paper[1] it has been shown that the numerous bands occurring in the nearer infra-red absorption spectra of carbon-hydrogen compounds can be arranged into series of three types: a non-linear series attributed to C-H vibrations, a linear series attributed to C-C vibrations, and combination series resulting from direct addition of frequencies of these two. There have just come to the writer's attention two papers by Bonino[2] which contribute to the identification of the well-known band near 3.4μ as a member of a C-H series. This band, assumed by the author to be the second member of a C-H series, lies in a region of the spectrum which is easily accessible and which is relatively free from overlapping bands due to other molecular sources. Bonino selected this band around which to measure molecular absorption coefficients in homologous series, in particular, four ketones and several compounds formed by successive halogen substitutions into the ethane molecule. In the case of the ketones he found the molecular absorption coefficient to increase regularly with the number of hydrogen atoms present in the molecule; in the case of the halogen compounds the coefficient decreased regularly with additional substitutions of the halogen atoms. Bonino's work contains slightly more convincing evidence of the independent absorption by a C-H group than a similar earlier investigation by Henri[3] in which the latter measured the molecular absorption coefficient of a series of alcohols in this same spectral region. Although this coefficient increased regularly throughout the homologous series, Henri had to assume that part of it

[1] Ellis, Phys. Rev. **27**, 298 (1926).
[2] G. B. Bonino, Gaz. chim. italiana **55**, 335 and 348 (1925).
[3] V. Henri, Études de Photochimie (1919).

was due to the O-H group and part, following Coblentz, to CH_2 and CH_3 groups.

Further evidence, indicating the absorption by a single group within the molecule, is found in a recent article by Salant[4] in which he identifies bands near 6.1μ and 3μ as the first two members of a N-H series. The evidence is made convincing by the disappearance of the 3μ band characteristic of the di-alkyl amines in the tri-alkyl amines, which lack the N-H bond.

In the present paper an attempt is made to identify and arrange into series bands which arise because of the presence of halogen atoms within the molecule. Only those compounds are considered which result from a substitution of one, two or three halogen atoms into the methane molecule, thus eliminating the possibility of any C-C bands. The six substances used were: methyl iodide, CH_3I; methylene chloride, CH_2Cl_2; methylene bromide, CH_2Br_2; methylene iodide, CH_2I_2; chloroform, $CHCl_3$; bromoform, $CHBr_3$. Since the investigation was limited to liquids, methyl chloride and methyl bromide, which are vapors at ordinary temperatures, and iodoform, which is a solid, were not studied.

TABLE I

Calculated and observed wave-lengths of a C-H series.

n	calc. $\nu_n \times 10^{-12}$	calc. λ_n	methylene chloride CH_2Cl_2	chloroform $CHCl_3$	methylene bromide CH_2Br_2	bromo-form $CHBr_3$	methyl iodide CH_3I	methy-lene iodide CH_2I_2
1	46.6	6.44	‡	6.8 *	‡	‡	*	‡
2	91.6	3.28	‡	3.32	‡	‡	3.4	‡
3	135.2	2.22	2.27	2.22 †	‡	2.27 *	2.23 *	2.32 *
4	177.0	1.695	1.675*	1.66 *	1.68*	1.67 *	1.66 *	1.68 *
5	217.5	1.379	1.36 *	1.385*	1.37*	1.40 *	1.35 *	1.37
6	255.9	1.172	1.15 *	1.145*	1.15*	1.15 *	1.15 *	1.15 *
7	293.4	1.022	1.03 *	1.015*	1.03*	1.015*	.....	1.03 *
8	328.8	0.912	0.935*	0.890*	0.89*	0.890*	0.895*	0.895*

* Has another band superposed upon it.
† Occurs as a point of inflection only.
‡ No reliable measurements recorded.

In Table I is shown the agreement between the C-H bands observed in the spectra of the six substances mentioned and the wave-lengths calculated from the formula already given (1):

$$\nu_n \times 10^{-12} = 47.37n - 0.783n^2$$

In Fig. 1 are shown the absorption curves to 2.5μ previously published in this journal.[5] Fig. 2 shows the additional details which are brought

[4] E. O. Salant, Proc. Nat. Acad. of Sci. **12**, 74 (1926).
[5] Ellis, Phys. Rev. **23**, 48 (1924).

out in the spectrum of chloroform by increasing the thickness of the absorbing cell. Figs. 3 and 4 show the absorption produced in the region 2μ to 3μ by 0.5 mm cells of five of these substances. These

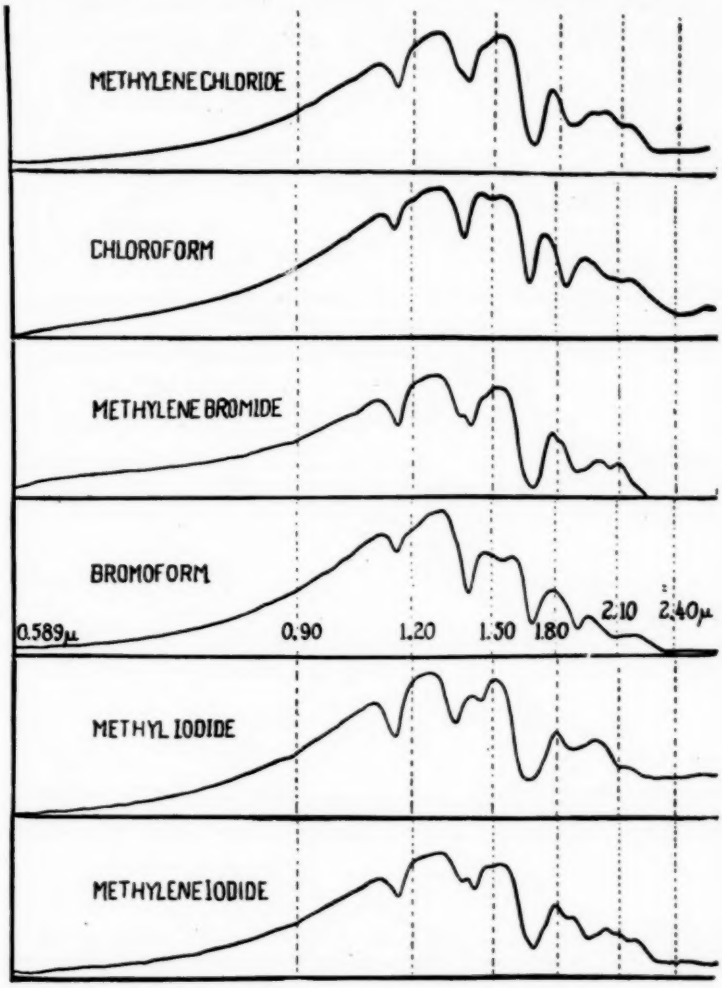

Fig. 1. Absorption spectra obtained with a recording spectrograph with flint glass prisms. Absorbing cell = 11 mm.

curves were obtained with a recording quartz spectrograph previously described.[6]

It has been pointed out in Part I of this paper that Márton[7] has independently discovered the existence of the non-linear series of

[6] Ellis, J.O.S.A. & R.S.I. **11**, 647 (1925).
[7] Márton, Zeits. f. Phys. Chem. **117**, 97 (1925).

prominent bands previously attributed by the author to C-H oscillations. In this same report Márton, using data obtained by himself, Coblentz, and the writer, attempts to account for the other bands in the spectrum of chloroform on the basis of a linear series starting at 8.35μ and combinations between this and the above mentioned non-linear series.

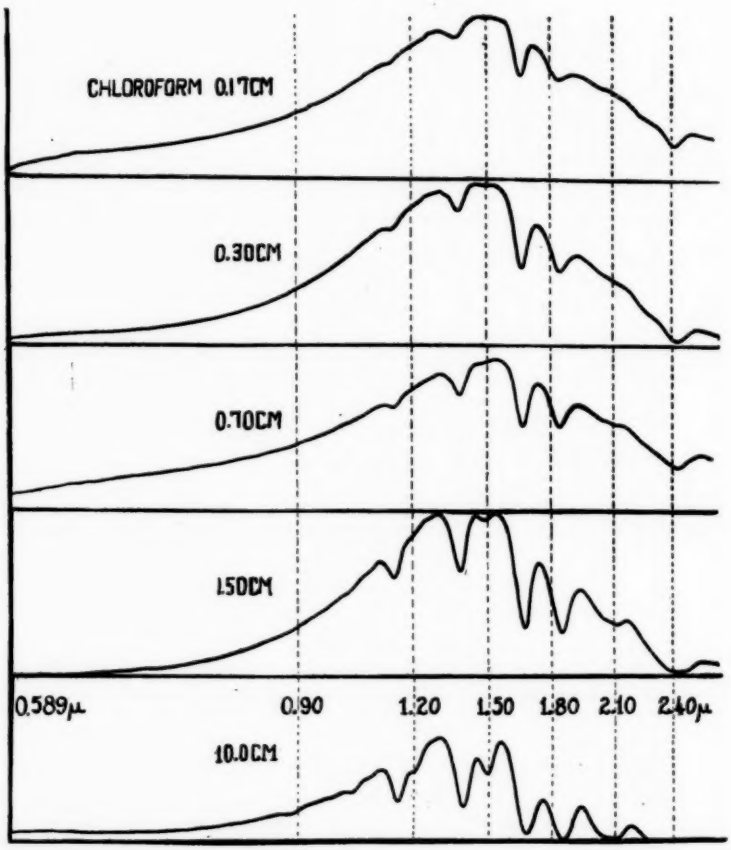

Fig. 2. Effect of increasing thickness of absorbing cell.

The choice of 8.35μ as the wave-length value of the initial member of the series in the spectrum of chloroform is natural, since it is the most outstanding band. However, a series starting at this frequency will not account for the many bands of secondary intensity appearing in Figs. 1, 2 and 3. But by assuming a linear series starting at about twice this value, namely 16.8μ, it is possible to identify all of these bands as members of such a series or of simple combination series of the type

already mentioned. Moreover, the spectrum of methylene chloride shows the same absorption maxima, although there are apparent external differences between the spectra of these two substances. Such differences should be anticipated because of different intensity ratios

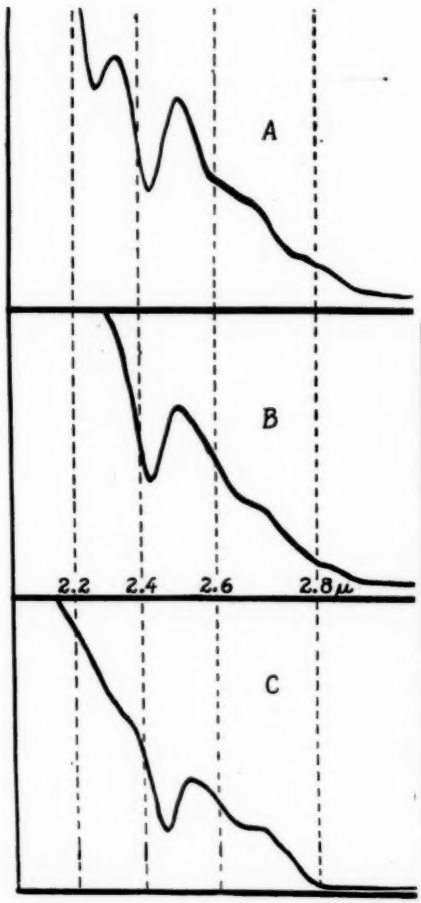

Fig. 3

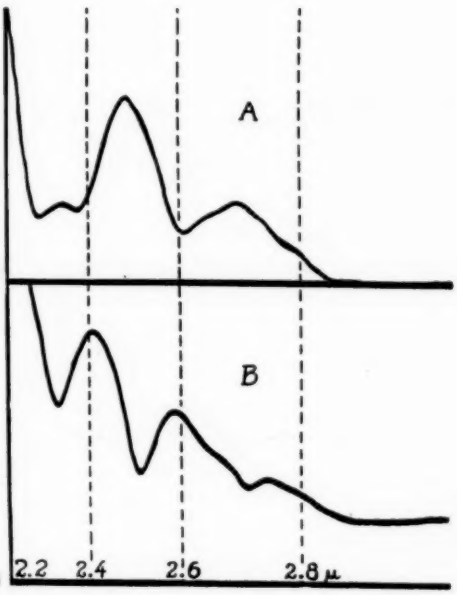

Fig. 4

Fig. 3. Absorption spectra obtained with a recording spectrograph with quartz prisms. $A = 0.5$ mm of methylene chloride; $B = 0.5$ mm of chloroform; $C = 0.5$ mm of bromoform.

Fig. 4. $A = 0.5$ mm of methyl iodide. $B = 0.5$ mm of methylene iodide.

among the bands, since chloroform contains one atom of hydrogen and three atoms of chlorine, while methylene chloride contains two of each.

Table II gives the agreement between the calculated and observed wave-length values of a series starting at 16.8μ which is attributed to

TABLE II

Calculated and observed wave-lengths of a C-Cl series.

n	calc. $\nu_n \times 10^{-12}$	calc. λ_n	methylene chloride CH_2Cl_2	chloroform $CHCl_3$
1	17.9	16.8	†	†
2	35.7	8.4	‡	8.35
3	53.6	5.6	‡	5.40 M
4	71.4	4.2	‡	4.15 M 4.4 *
5	89.3	3.34	‡	3.32 *
6	107.1	2.80	2.80	2.80
7	125.0	2.40	2.42	2.42
8	142.8	2.10	2.10 *	2.12
9	160.7	1.865	1.87 *	1.845*
10	178.5	1.68	1.765*	1.66 *
11	196.3	1.525	.....	1.50
12	214.2	1.40	1.39 *	1.385*
13	232.1	1.29	.....	1.28
14	249.9	1.20	1.20	1.20
15	267.8	1.12	1.15 *	1.145*
16	285.6	1.05	1.03 *	1.022*
17	303.5	0.99	.....	0.98
18	321.3	0.933	0.935*	0.935*
19	339.2	0.885	0.890*	0.890*

* Has another band superposed upon it.
‡ No reliable measurements recorded.
† Region never investigated.
M Obtained by Márton.

C-Cl oscillations. Table III gives the agreement between calculated and observed bands of combination series. In this case ν_n and ν'_{n1} refer

TABLE III

Combination bands of C-H and C-Cl series.

	calc. $\nu_c \times 10^{-12}$	calc. λ	methylene chloride	chloroform
$\nu_1+\nu_1'$	64.5	4.68	‡	4.4 *
$\nu_1+\nu_2'$	82.4	3.65	‡	3.75
$\nu_1+\nu_3'$	100.3	2.99	‡	.....
$\nu_1+\nu_4'$	118.2	2.55	2.57	2.55
$\nu_1+\nu_5'$	136.1	2.21	2.27 *	2.22 *
$\nu_1+\nu_6'$	154.0	1.95	1.98 *	.....
$\nu_1+\nu_7'$	171.9	1.75	.....	.....
$\nu_2+\nu_1'$	109.5	2.74	2.76	2.73
$\nu_2+\nu_2'$	127.4	2.36	2.27 *	†
$\nu_2+\nu_3'$	145.3	2.07	2.10 *	2.055*
$\nu_2+\nu_4'$	163.2	1.84	1.84 *	1.845*
$\nu_2+\nu_5'$	181.1	1.66	1.68 *	1.66 *
$\nu_2+\nu_6'$	199.0	1.51	.....	1.50 *
$\nu_2+\nu_7'$	216.9	1.38	1.39 *	1.385*
$\nu_3+\nu_1'$	153.1	1.96	1.98 *	.....
$\nu_3+\nu_2'$	171.0	1.76	.....	.....
$\nu_3+\nu_3'$	188.9	1.59	*	1.58 †
$\nu_3+\nu_4'$	206.8	1.45	1.455	1.385*

* Superposed upon another band.
† Occurs as a point of inflection only.
‡ No reliable measurements recorded.

to members of C-H and C-Cl series respectively. All values above 3μ except as otherwise indicated, are from measurements by Coblentz, while values below 3μ are from the curves of Figs. 1, 2 and 3.

Comparisons among the curves of Fig. 1 indicate that series similar to the one attributed to C-Cl might be found for C-Br and C-I oscillations. The slight shifts toward longer wave-lengths of the halogen bands when chlorine is replaced by bromine, and bromine by iodine, indicate that values slightly greater than 16.8μ must be assumed for the initial members. Tables IV and VI give agreements between observed and calculated wave-lengths on the assumption of a C-Br series

TABLE IV

Calculated and observed wave-lengths of a C-Br series.

n	calc. $\nu_n \times 10^{-12}$	calc. λ	methylene bromide CH_2Br_2	bromoform $CHBr_3$
1	17.5	17.2	§	§
2	34.9	8.6	‡	‡
3	52.4	5.73	‡	‡
4	69.8	4.30	‡	‡
5	87.3	3.42	‡	‡
6	104.6	2.87	‡	‡
7	122.0	2.46	‡	2.47
8	139.5	2.15	2.16	2.15
9	156.9	1.91	1.92	1.90
10	174.6	1.72	1.68 †	1.67 *
11	192.0	1.56	.....	1.55
12	209.6	1.43	1.405	1.40 *
13	227.0	1.32	.....	1.285
14	244.5	1.225	1.22	1.22
15	262.0	1.145	1.15*	1.15 *
16	278.5	1.07	.....	1.08
17	297.0	1.01	.....	1.02
18	314.0	0.955	.....	0.97

* Superposed upon another band.
† Occurs as a point of inflection only.
‡ No reliable measurements recorded.
§ Region never investigated.

starting at 17.2μ and a C-I series starting at 17.5μ. Tables V and VII give values for combination series similar to those of Table III.

If the series whose members appear in Table II arises from oscillations of a C-Cl pair of atoms, then one should expect to find a corresponding series of strong bands in the spectrum of carbon tetrachloride, CCl_4. On the contrary, investigators have repeatedly reported perfect transparency of this substance for short infra-red rays. The writer, using a cell thickness of many centimeters, has observed a few very weak bands, which correspond to C-H and C-Cl bands. The substance tested was of an ordinary commercial grade, and it is probable that the bands were due to impurities. A 15 mm cell of tetrachlorethylene, $Cl_2C{:}CCl_2$,

from a sample prepared by the Eastman Research Laboratories, showed weak bands similar to those of carbon tetrachloride. If these are due to

TABLE V

Combination bands of C-H and C-Br series.

	calc. $\nu_c \times 10^{-12}$	calc. λ	methylene bromide	bromoform
$\nu_1+\nu_1'$	64.1	4.68	‡	‡
$\nu_1+\nu_2'$	81.6	3.68	‡	‡
$\nu_1+\nu_3'$	99.1	3.015	‡	‡
$\nu_1+\nu_4'$	116.6	2.58	‡	
$\nu_1+\nu_5'$	134.1	2.25	‡	2.29
$\nu_1+\nu_6'$	151.6	1.985	.....	.....
$\nu_1+\nu_7'$	169.1	1.78	1.80	1.78
$\nu_2+\nu_1'$	109.1	2.75	‡	2.73
$\nu_2+\nu_2'$	126.6	2.37	‡	2.36
$\nu_2+\nu_3'$	144.1	2.08	2.06	2.08
$\nu_2+\nu_4'$	161.6	1.86	1.88	1.90 *
$\nu_2+\nu_5'$	179.1	1.675	1.695 †	1.67 *
$\nu_2+\nu_6'$	196.6	1.53	.....	1.55 *
$\nu_3+\nu_1'$	152.7	1.97	1.93 *	.....
$\nu_3+\nu_2'$	170.2	1.50	1.47	1.55 *
$\nu_3+\nu_3'$	187.7	1.38	1.405 *	1.40 *
$\nu_3+\nu_4'$	205.2	1.275	1.27	1.285*

* Superposed upon another band.
† Occurs as a point of inflection only.
‡ No reliable measurements recorded.

TABLE VI

Calculated and observed wave-lengths of a C-I series.

n	calc. $\nu_n \times 10^{-12}$	calc. λ	methyl iodide CH_3I	methylene iodide CH_2I_2
1	17.2	17.5	§	§
2	34.4	8.75	8.25 *	‡
3	51.6	5.83	5.8 †	‡
4	68.7	4.38	4.55 *	‡
5	85.8	3.50	3.40 *	‡
6	103.0	2.92	.....	‡
7	120.0	2.50	†	2.52†
8	137.5	2.19	2.23 *	2.15*
9	154.5	1.945	1.94	1.95
10	171.6	1.750	1.74 †	1.73†
11	189.0	1.580	1.59 †	1.63*
12	206.2	1.455	1.455	1.49
13	223.5	1.345	1.35 *	1.37*
14	240.5	1.250	.....	†
15	257.5	1.165	1.15 *	1.15*
16	275.0	1.095	1.15 *	1.15*

* Has another band superposed upon it.
† Occurs as a point of inflection only.
‡ No reliable measurements recorded.
§ Region never investigated.

the compounds themselves they possess but a small fraction of the intensity which would be expected. The anomalous effects in the

spectra of these substances may be in some way associated with the symmetry in the molecular structure.

Since there is no observable deviation from linearity in the above series the molecular forces acting must be very nearly linear. The presence of combination frequencies requires a quantum theory interpretation. This means that the first member of the series, due to an energy jump from oscillation state zero to oscillation state one, will be practically equal to the primary rate of vibration. The first member, then, of the series should be approximately expressible by

$$\nu = c/\lambda = 1/2\pi\sqrt{U/M}$$

where U is the force between the two atoms and M the reduced mass. M is determined by $1/M = 1/M_c + 1/M_x$ where M_c and M_x are the masses of the carbon and halogen atoms respectively.

TABLE VII

Combination bands of C-H and C-I series.

	calc. $\nu_c \times 10^{-12}$	calc. λ	methyl iodide	methylene iodide
$\nu_1+\nu_1'$	63.8	4.71	4.55	‡
$\nu_1+\nu_2'$	77.3	3.88	*	‡
$\nu_1+\nu_3'$	98.1	3.06	*	
$\nu_1+\nu_4'$	114.9	2.61	2.61	2.62
$\nu_1+\nu_5'$	134.0	2.27	2.23 *	2.32*
$\nu_1+\nu_6'$	149.1	2.01	.....	1.98*
$\nu_1+\nu_7'$	167.0	1.795	*	....
$\nu_2+\nu_1'$	108.5	2.76	2.77	2.72
$\nu_2+\nu_2'$	123.5	2.385	2.38	2.32*
$\nu_2+\nu_3'$	143.0	2.095	2.1	2.08
$\nu_2+\nu_4'$	159.5	1.875	1.87	1.84
$\nu_2+\nu_5'$	177.5	1.69	1.66 *	1.68*
$\nu_2+\nu_6'$	194.5	1.54	*	....
$\nu_3+\nu_1'$	152.5	1.97	1.94	1.98
$\nu_3+\nu_2'$	169.5	1.77	*	1.73†
$\nu_3+\nu_3'$	187.0	1.605	1.61 *	1.63*
$\nu_3+\nu_4'$	204.0	1.47	1.455*	1.48
$\nu_3+\nu_5'$	220.5	1.36	1.35 *	1.37*

* Superposed upon another band.
† Occurs as a point of inflection only.
‡ No reliable measurements recorded.

The value of U will be different for every chemical bond; yet the above formula should serve for a qualitative comparison of the frequencies among bonds of a similar character. Thus, it should serve for a comparison among the fundamental frequencies due to C-H, C-Cl, C-Br and C-I, for hydrogen, chlorine, bromine and iodine atoms lack one electron only in the K, M, N and O shells, respectively. The departure from constant proportionality between values of $\sqrt{M}$ and

λ_1 as given in Table VII may be regarded as a measure of the differences in the strengths of the chemical bonds among the four cases cited. The results lead to the conclusion that in this type of bond the iodine atom is held by the carbon atom more tightly than are the chlorine or bromine atoms. This need not be interpreted as in conflict with the fact that bromine and chlorine will replace iodine in the molecule, since this replacement is determined by the heat of dissociation, which in turn depends upon the distance of separation of the atoms as well as upon the bonding forces.

TABLE VIII

Bond	$\sqrt{M}/\sqrt{M_H}$	λ_1	$\sqrt{M}/\lambda_1$
C–H	0.96	6.44μ	0.149
C–Cl	3.00	16.8	0.178
C–Br	3.30	17.2	0.192
C–I	3.45	17.5	0.197

The writer is much indebted to Mr. Edward Condon of Berkeley, California, who has called his attention to an article by Born and Heisenberg[8] on the theory of polyatomic molecules and for his assistance in the interpretation of the bearing of this article upon the present paper. Born and Heisenberg assume a molecule consisting of electrons and nuclei, the nuclei being ordinarily at rest with approximately linear forces acting between them, such forces arising from the motions of the electrons. Higher energy states of the nuclei are also assumed to exist, and the evaluation of these states is obtained by a series of approximations. The first approximation leads to the conclusion that during a change from one state to another a member of a linear, or harmonic, series of frequencies should be emitted or absorbed. A second approximation shows that a linear deviation from a true harmonic relation should occur in the frequency series absorbed or emitted. It should be pointed out, however, that the characteristic frequencies assumed under this theory to occur during energy changes within the molecule are dependent in some manner upon all parts of the molecule. The theory does not deal with the isolation of a portion of the molecule, for example, a pair of atoms. The results of infra-red absorption study, however, make it very apparent that certain fields of force may be considered practically isolated within the molecule. With this interpretation it would seem that C-H series might be regarded as experimental evidence of the existence of the type of frequency series predicted by the second approximation in Born and Heisenberg's solution,

[8] Born and Heisenberg, Ann. d. Physik **74**, 1 (1924).

while the other four series might be regarded as completely expressed within the limits of experimental error by their first approximation solution.

The bands attributed in this paper to the halogens are not characteristic alone of the simple types of molecule considered here. In another paper numerous molecules of a more complicated nature, many of them containing halogen atoms, will be dealt with. It will be found that many of these bands may be identified in the more complicated spectra which these substances present.

DEPARTMENT OF PHYSICS,
UNIVERSITY OF CALIFORNIA, SOUTHERN BRANCH,
April 16, 1926.

STANDARD WAVE-LENGTHS FOR USE IN THE EXTREME ULTRA-VIOLET

By Stanley Smith and R. J. Lang

Abstract

Wave-lengths of a number of lines, chiefly of carbon, which frequently occur in the spectra of other elements have been measured in the second and third orders on plates obtained in a vacuum spectrograph with a concave grating with a radius of 6 feet ruled with 30,000 lines to the inch. The dispersion was approximatly 4.5A per mm. The carbon lines and the iron standard lines used as comparisons were obtained simultaneously by passing a condensed spark discharge between a carbon and an iron electrode. Details are given of a new method of obtaining curves to correct for (a) deviation of the spectra from normality, (b) error in the tilt of the photographic plate. These curves can be used for correcting the calculated wave-lengths obtained by interpolation between any pair of standards chosen within the range of the curves.

I. Introduction

SPECTROSCOPISTS working in the extreme ultra-violet region are well aware that at the present time the greatest obstacle to attaining a higher degree of precision in the measurement of wave-length is the lack of adequately accurate standards in this region.

The vacuum spectroscope, which has already been described in detail[1], employing a concave grating of radius 6 feet with 30,000 rulings to the inch gives a dispersion of about 4.5A per mm in the first order. This dispersion being almost four times as large as that hitherto obtained in vacuum grating work, it was thought that the instrument might well be used to measure as accurately as possible a number of well known spectral lines which may then be regarded as standards for future work in the extreme ultra-violet. The lines selected are chiefly those of carbon, since of all the lines of foreign origin found in spectra obtained from condensed sparks in vacuo, those due to carbon are by far the most frequently occurring and occur with the greatest intensity. The carbon spectrum was obtained *simultaneously* with an iron spectrum by using an electrode of each element in the spark gap. By this arrangement it was hoped to eliminate the possibility of a relative displacement between the lines of carbon and of iron as might easily occur from various causes if the spectra of the two elements were obtained by two separate exposures. Even

[1] Lang and Smith, J.O.S.A. **12**, 523 (1926).

in the case of a single exposure it has sometimes been found that the spectral lines appear doubled although it was definitely known that the focusing was extremely good. The reason for this effect is to be found in a change in the relative positions of the spark gap, slit, and grating caused by the slight adjustments to the electrodes which must necessarily be made from time to time during the exposure. It will be readily understood that the possibility of such a displacement occurring when a complete change of electrodes is made is by no means negligible.

II. Theory of Method of Measurement

In the case of a concave grating operated in a vacuum the mechanical difficulties do not permit the use of a Rowland mounting. The obvious

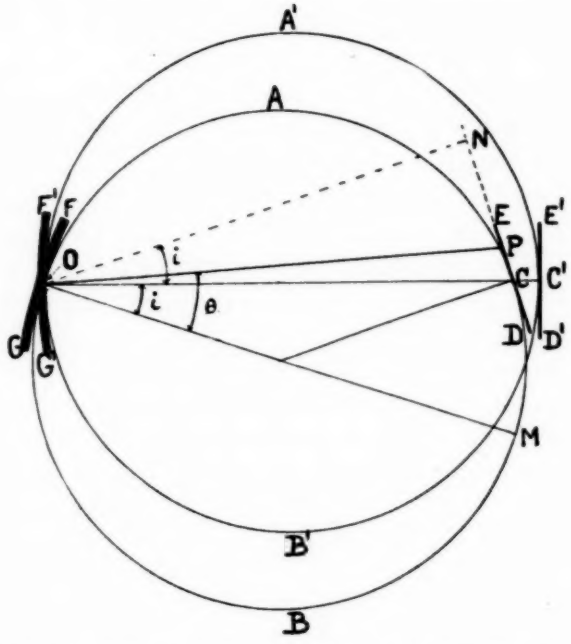

Fig. 1. Showing relative positions of grating *FG* and photographic plate *ED*.

advantages of working with normal spectra are therefore lost. The mechanical arrangement which naturally suggests itself on account of the facility of adjustment, is one in which the slit source is coincident with the center of the photographic plate and the plate (assumed to be short) is a tangent to the focal circle, the point of contact being the center of the plate. In Fig. 1 *F'G'* represents the grating, *C'* the center of curvature, and *OA'B'* the focal circle when

the angle of incidence of the light on the grating is zero. $E'C'D'$, tangent to this circle at C' represents the photographic plate whose center C' is coincident with the slit. In order to throw another region of the spectrum on the plate the grating is rotated about O through an angle i into the position FG the focal circle moving to OAB. It is now clear that on moving the center of the grating along OC' through a distance $R(1-\cos i)$, R being the radius of curvature of the grating, the center of the plate together with the slit itself will be brought on to the focal circle at C. On rotating the plate about C through the angle i the plate will touch the focal circle and the spectrum will again be in focus. The tilting of the grating and its translation along OC' are readily effected from the outside of the evacuated spectrograph as previously described.[1] The photographic plate is given a corresponding angle of tilt by interposing a brass wedge, whose angle has the given value i, between the plate and the plate holder without moving the center of the plate relative to the grating. To simplify the mechanical construction of the spectrograph the slit S actually lies about 4 cms distant from the plane of the focal circle, and C, the center of the plate, is in the corresponding position on the other side of the plane, i. e. OS is equal to OC and the plane SOC is perpendicular to the plane of the focal circle. It is assumed that although such an arrangement will alter slightly the scale of the spectrum it will not appreciably affect the relative positions of the lines in the spectrum.

The spectrum will be practically normal only for the case in which the angle of incidence is zero. For all other angles of incidence calibration curves will have to be obtained in order to correct the estimated wave-lengths for the deviation of the spectrum from normality. As flat plates were used, it was necessary to limit their lengths if uniformly good focusing over their entire lengths was desired. Consequently it was decided to photograph the spectrum from 300A to 4300A in nine sections of about 600A each, with 600, 1000, 1400, 1800, 2200, 2600, 3100, 3600 and 4000A respectively at the center of the plate. The illustrate the method employed for constructing the calibration curves for each of these regions let us select the 700-1300A region as an example.

Let P, Fig. 1, be the position of a spectral line λ whose angle of diffraction is θ, the normal to the grating being OM and N the foot of the perpendicular drawn from O on to DE produced. It is clear that

$$NP = ON\tan(2i-\theta) = R\cos^2 i\tan(2i-\theta).$$

From the relation $\sin i + \sin\theta = N\lambda$ for the first order spectrum where N is the number of lines per centimeter of the grating the value of θ corresponding to a given λ can be found and therefore the corresponding value of NP can be calculated. This was done for every 50A

TABLE I

Sample set of data illustrating how corrections for lack of normality of spectra are made.

λ	y (cms)	$n\Delta+\delta y$ (cms)	$\delta\lambda$ in A
700	0	0	0
750	1.08571	$\Delta+.00314$	$-.145$
800	2.17046	$2\Delta+.00532$	$-.246$
850	3.25437	$3\Delta+.00665$	$-.307$
900	4.33756	$4\Delta+.00727$	$-.336$
950	5.42015	$5\Delta+.00729$	$-.336$
1000	6.50227	$6\Delta+.00684$	$-.316$
1050	7.58398	$7\Delta+.00598$	$-.276$
1100	8.66538	$8\Delta+.00481$	$-.222$
1150	9.74672	$9\Delta+.00357$	$-.165$
1200	10.82799	$10\Delta+.00227$	$-.105$
1250	11.90933	$11\Delta+.00104$	$-.048$
1300	12.99086	$12\Delta+0$	0

from 700A to 1300A. The distances, y, of the lines having these values of λ from the position of 700A were then computed and are tabulated in the second column of Table I. The average dispersion between

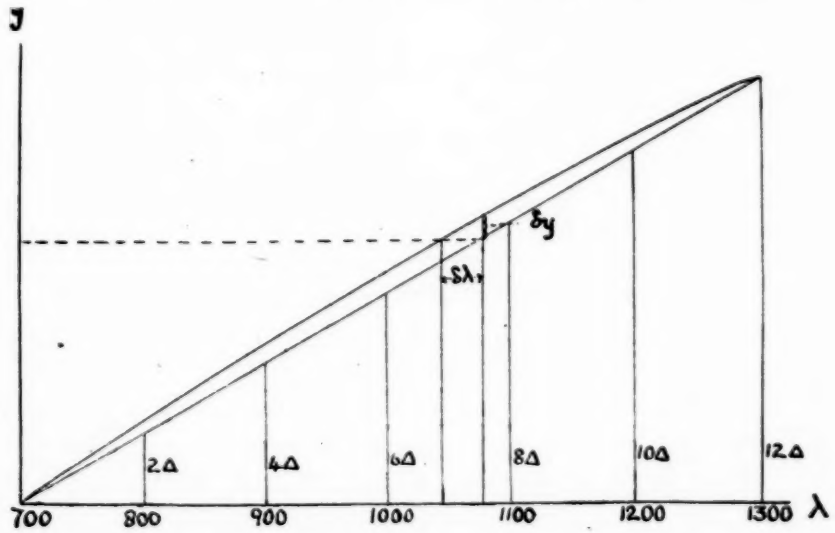

Fig. 2. Illustrating derivation of dispersion correction curve.

700A and 1300A is 1.08257 cms per 50A. Denote this quantity by Δ. Taking 700A and 1300A as standards and assuming that the spectrum is normal between these limits the values of y for 750A, 800A, 850A,

etc. would be Δ, 2Δ, 3Δ etc. But as is seen in the third column of the table the actual y's are larger than these values. It is clear from Fig. 2 that the values of λ estimated on the assumption that the spectrum is normal will be too large. The necessary correction $\delta\lambda$ for each λ calculated in the above table can easily be found by dividing δy by the slope of the dispersion curve. The values of $\delta\lambda$ thus obtained are recorded in the fourth column of the table. The calibration curves $(\delta\lambda,\lambda)$ for six settings of the grating are plotted in Fig. 3. The numbers 1, 2, 3, 4, 5 and 6 refer to cases in which the wave-lengths at the center of the plate are 600, 1000, 1400, 1800, 2200 and

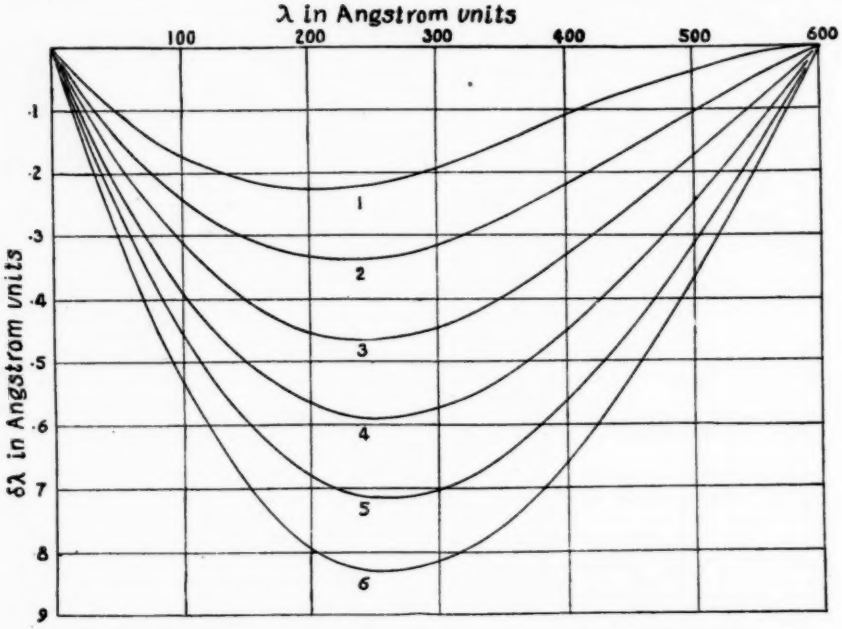

Fig. 3. Showing correction curves for abnormality of spectrum.

2600A respectively. It is interesting to note that a point of inflexion occurs near the upper limit of λ for curves 1 and 2. This arises from the fact that $dy/d\lambda$ has a minimum value at these points, giving points of inflexion in the (λ, y) curves. The values of λ at which these occur can also be found theoretically, for it may be shown that the angle of diffraction θ for such points is given by the following equation

$$\tan^2\theta+3\tan\theta/\tan 2i=2$$

For the first three curves in Fig. 3 the λ's corresponding to the values of θ obtained from this equation fall within the range of wave-lengths plotted. The practical importance of this fact is that if standards

are selected which are fairly symmetrically placed with regard to a point of inflexion and not too far from it, the spectrum between these standards will be practically normal.

Each curve can be used to correct for the deviation of the dispersion from that of a normal spectrum between *any* two standard lines lying within the range of the curve in the following way. A straight line is drawn joining the two points on the curve corresponding to the two standard λ's; the required corrections are then given by the portions of the ordinates intercepted between this straight line and the curve. The corrections obtained in this way have in a number of cases been compared with δλ calculated directly and the agreement between the two sets of values has been found to be very close. Table II

TABLE II

Comparison of wave-length corrections obtained by direct computation and by graphical means.

λ	$-\delta\lambda$ in A (computed)	$-\delta\lambda$ in A from 3700–4300 calibration curve
3800	0	0
3825	.151	.152
3850	.278	.280
3875	.382	.384
3900	.466	.467
3925	.527	.527
3950	.568	.569
3975	.588	.589
4000	.592	.592
4025	.575	.574
4050	.540	.541
4075	.489	.488
4100	.421	.421
4125	.338	.341
4150	.240	.241
4175	.126	.127
4200	0	0

shows such a comparison. The calibration curve was computed and plotted between the limits 3700A and 4300A. The intercepts of the ordinates between this curve and a straight line joining points on the curve corresponding to 3800A and 4200A are tabulated in the third column.

The effect produced by an error in the tilt of the plate must now be considered. In general such an error would alter the scale of the spectrum and would also change the relative positions of the lines. The first effect will, of course, introduce no error into the computed values of the wave-lengths if an interpolation method between standards is employed. Correction curves for the second effect i. e. the change in the relative positions of the lines, can be obtained in the

following manner. In Fig. 4, O represents the pole of the grating, AB the correct position of the plate, A and B being the positions of the two standards between which the interpolation is to be made. $A'B'$ represents the plate when the tilt exceeds the correct value, by a small angle ϕ. Let y and y' denote the distances from A and A' respectively of the same spectral line situated at P and P'. In order

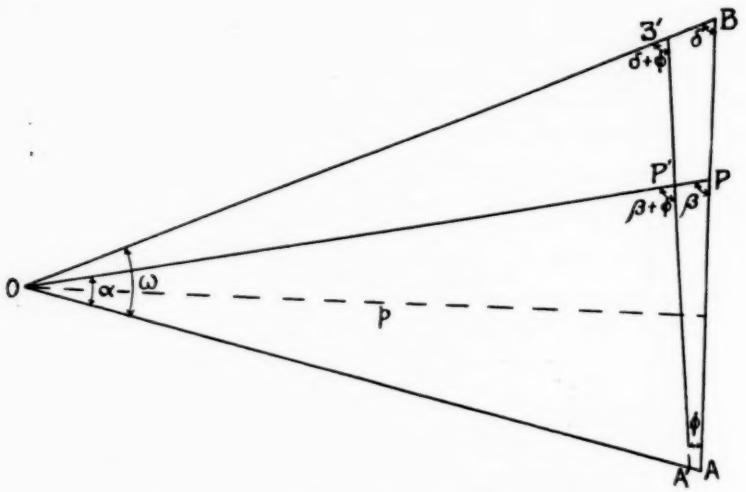

Fig. 4. Illustrating correction for error in tilt of plate.

to make y and y' comparable it is, of course, necessary to put $A'B'$ equal to AB. Using the notation indicated in Fig. 4 $y/OA = \sin\alpha/\sin\beta$ and $y'/OA' = \sin\alpha/\sin(\beta+\phi)$ also $OA/AB = \sin\delta/\sin\omega$ and $OA'/A'B' = \sin(\delta+\phi)/\sin\omega$. Remembering that $A'B' = AB$ it follows that

$$y'/y = 1+\cot\delta\tan\phi/(1+\cot\beta\tan\phi).$$

If ϕ is small this reduces to

$$y'-y = y\tan\phi(\cot\delta-\cot\beta)$$

or
$$y'-y = \delta y = y(AB-y)\tan\phi/p = \phi y(AB-y)/p$$

where p is the perpendicular distance of O from AB. If ϕ is positive, i. e. the plate is tilted more than it should be, the computed wavelengths will be too large by an amount $\delta\lambda$ where

$$\delta\lambda = \frac{\delta y}{\text{slope of dispersion curve}} = \frac{\phi y(AB-y)}{p \times \text{slope of dispersion curve}}$$

By using the values of y already computed as explained above ($\delta\lambda$,λ) curves can easily be plotted for any given values of ϕ. These curves are almost parabolic. They would, of course, be truly parabolic if the

spectrum were normal. As in the case of the curves in Fig. 3 they can in a precisely similar manner be used for *any* two standards provided these standards have wave-lengths intermediate between those for which the curves were originally constructed. In practice ϕ is not directly known but its value can be estimated very easily. Suppose that a correction curve for $\phi = 1°$ has already been plotted. Then using any two given standards the wave-lengths of a number of intermediate lines, accurate values of whose wave-lengths have previously been determined, are computed by using the dispersion correction curves in Fig. 3. On comparing the differences between the computed and known values of these wave-lengths with the corresponding $\delta\lambda$'s read off from the tilt correction curve, the actual value of ϕ can be estimated because the error $\delta\lambda$ for a given λ is directly proportional to ϕ. The corresponding correction for any wave-length within the region investigated can now be found from the correction curve for $\phi = 1°$.

III Experimental Procedure and Results

For a general description of the operation of the spectrograph reference should be made to the authors' previous paper already mentioned. Very great care was exercised in the focusing of the spectra on the plates. In the neighborhood of the position of best focus it was found that on moving the grating 1/64 inch towards or away from the photographic plate an appreciable difference in the definition of the images could be observed. Having once carefully focused the grating for one particular value of the angle of incidence i_1, the distance through which the grating had to be moved to bring the spectrum in focus for any other value i_2 of the angle to incidence was calculated from the expression $R(\cos i_1 - \cos i_2)$. In order to give the plate the necessary tilt, i, a brass wedge cut to the angle i as accurately as possible was interposed between the plate holder and the plate. In effecting this tilt the plate was always rotated about its center i. e. C in Fig. 1. A spectrum was then photographed and the wave-lengths of a number of standard lines were measured corrections being applied for the abnormality of the spectrum. An investigation of the residuals between the computed and known wave-lengths of these standards enabled the error in the angle of tilt to be estimated by using the tilt error curve as explained above. The angle of the wedge was accordingly altered until on an average the residuals attained the value zero. The plates were measured on a comparator reading to .001 mm. Ten settings were made on each line to be measured and

on each standard line used. The plate was then reversed and the process repeated. Care was taken to keep the temperature of the plate as nearly constant as possible throughout the measurements.

The mean values of the computed wave-lengths are given in the third column of Table III and the mean deviations from the mean are tabulated in the fourth column. The number of plates on which the

TABLE III

Wave-lengths of some lines of a carbon-iron spark in the far ultra-violet.

Authors				Simeon	Hopfield and Leifson	Millikan and Bowen
Number of plates	Order of spectrum	λ (IA vac.)	Mean deviation	λ (IA vac.)	λ (IA vac.)	λ (IA vac.)
7	2 and 3	1335.70	.009	1335.66	1335.75	1335.72
7	2 and 3	1334.51	.007	1334.44	1334.57	1334.54
3	2	1329.60	.010	1329.60	.....	1329.60
2	2	1329.12	.010	.....	.....	1329.14
6	2	1323.93	.015	1323.79	.....	1323.96
6	2 and 3	1247.37	.006	1247.2	.....	1247.43
3	2	1215.68	.010	1215.53	1215.68	.....
5	3	904.47	.016	.....	.....	904.48
5	3	904.17	.006	.....	.....	904.17
5	3	903.95	.012	.....	.....	903.98
5	3	903.62	.010	.....	.....	903.63
2	2	1561.46	.000	1561.32	1561.39	1561.47
2	2	1560.71	.005	1560.67	1560.46	1560.76
2	2	1560.33	.000	1560.16	.....	1560.34
2	2	1550.80	.010	1550.8	.....	1550.84
2	2	1548.22	.005	1548.3	.....	1548.26
5	2	1402.75	.018	.....	.....	.....
5	2	1393.75	.016	.....	.....	.....
5	2	1176.36	.010	.....	.....	1176.40
5	2	1175.98	.012	.....	.....	1176.05
5	2	1175.66	.016	.....	.....	1175.72
5	2	1175.25	.012	.....	.....	1175.31
5	2	1174.92	.004	.....	.....	1174.96
2	3	1037.03	.005	1036.84	1037.03	1037.03
2	3	1036.35	.000	1036.22	1036.33	1036.35
2	3	1010.38	.000	.....	.....	1010.38
2	3	1010.08	.005	1010.09	.....	1010.10
2	3	977.03	.005	.....	.....	977.02

lines were measured is stated in the first column. The values found by Simeon[2], Hopfield and Leifson[3], and Millikan and Bowen[4] for the corresponding lines are also tabulated for comparison. Included with the carbon lines are the Si IV doublet 1402A, 1393A and the first member of the Lyman series of hydrogen 1215A. It will be observed that the table is divided into two sections. The lines in the upper part of the table were measured in the 2600A region using as comparison

[2] Simeon, Proc. Roy. Soc. **102,** 484 (1922).
[3] Hopfield and Leifson, Astrophys. J. **58,** 59 (1923).
[4] Millikan and Bowen, Phil. Trans. **A 225,** 394 (1926).

lines the primary international iron arc standards λ(I. A. vac) 2740.359, 2715.223, 2563.309, 2414.044 and 2374.462. The remaining lines in the table were measured in the 3100A region. It was found that in this region primary iron standards were difficult to obtain and if they appeared on the plates at all they were extremely faint. Consequently it was necessary in some cases to use other iron lines as comparisons. The following are some of those used; λ(I. A. vac) 3228.72 3155.11, 2985.70, 2768.33 and 2344.22, the values being taken from Kayser's Handbuch der Spectroscopie Vol. 7 and reduced to λ(I. A. vac) by the tables given by Meggers and Peters.[5]

To test the accuracy of the method of measurement the same lines were measured in some cases by using different pairs of standards. The agreement between the values computed from the different sets of standards was found to be very satisfactory. The results given

TABLE IV

Comparison of wave-lengths computed using different pairs of standards.

Spectral line	using standards 2740.359 and 2374.462	using standards 2740.359 and 2563.309
Fe. Int. Std. 2715.223	2715.22	2715.22
C. second order 1335 doublet	2671.38	2671.37
	2669.02	2669.02
C. second order 1329	2659.22	2659.21
C? second order?	2658.27	2658.26
C. second order 1323	2647.87	2647.88
Fe. Int. Std. 2629.079	2629.07	2629.07

in Table IV will serve as an example. The grating used in this work was found to be so inefficient below 900A that the higher orders for lines of such wave-lengths could not be obtained on the plates. However by employing a more suitable grating it is hoped that in the near future carbon lines in the extreme ultra-violet below 900A may be measured with an accuracy which will permit of their use as standards in this region.

DEPARTMENT OF PHYSICS,
UNIVERSITY OF ALBERTA,
April 10, 1926.

[5] Meggers and Peters, Bull. Bur. Stand., No. 327 (1918).

PHOTO-IONIZATION OF A GAS BY A DISCHARGE IN THE SAME GAS[1]

By F. L. Mohler

Abstract

Method. Measurements were made in a tube containing two thermionic units electrically shielded from each other. The first served to give a discharge, the second detected ions produced by the radiation from the first by means of their effect on the space charge.

Results. Relatively little photo-ionization is produced by arc radiation, while spark excitation and soft x-radiation give a strong effect. Curves of photo-effect versus discharge voltage show critical potentials which have been interpreted as follows: Ionization of n_2 rare gas shell—Cs, 13.0; K, 19.0: Spark excitation—Cs, 18.5; K, 21.6; A, 32.2; Ne, 48.0: Double ionization—Cs, 21.5; K, 31.8; A, 34.8; Ne, 54.9: Ionization of n_1 rare gas shell—Cs, 39.0; K, 48.0; A, 39.6. The neon II spectrum is excited at 55 volts.

It was shown that photo-electric emission from the electrodes was at least ten times as great as the photo-electric emission from the gas, while the current change produced by the space charge effect was more than 2400 times the ion current in argon and caesium, the upper limit being quite indefinite.

Introduction

SINCE the first experiments by Davis and Goucher[2] numerous results have been published on the photo-electric effect of radiation from a thermionic discharge as measured by electrodes within the vacuum tube but electrically shielded from the discharge. The method has been particularly useful as a means of locating critical potentials above the first ionization potential. These experiments give no direct evidence as to whether the photo-electrons originate from the metal electrodes or from the gas surrounding them, but undoubtedly both sources contribute to the current when the discharge voltage is high.

In two recent papers,[3] there is described a sensitive method of distinguishing the photo-ionization of a gas from the electron emission from metal electrodes, and measurements are given of the photo-sensitivity of caesium vapor for monochromatic light over the range 3900A to 2500A. The vapor was contained in a two electrode thermionic tube with conditions so adjusted that the current was limited by

[1] Published by permission of the Director, Bureau of Standards, Department of Commerce.

[2] Davis and Goucher, Phys. Rev. **10**, 101 (1917).

[3] Foote and Mohler, Phys. Rev. **26**, 195–207 (1925); Mohler, Foote and Chenault, Phys. Rev. **27**, 37–50 (1926).

electron space charge. Ions produced by radiation neutralized the space charge and caused a change in thermionic current which was enormously greater than the actual ion current. The sensitivity curves showed that the photo-ionization reached a sharp maximum at the limit of the principal series but that, by secondary processes measurable ionization was produced on the red side of the limit when the exciting wave-length coincided with lines of the absorption series from $1s-4p$ to $1s-\infty p$.

The present paper deals with an application of the space charge method for measuring the photo-ionization produced in a gas by the radiation from a thermionic discharge in the same vacuum tube. The results have some bearing on the general theory of discharges in gases, but the method has been used primarily as a tool for measuring critical potentials. To locate excitation stages above the first ionization potential by electrical measurements, it is necessary to find

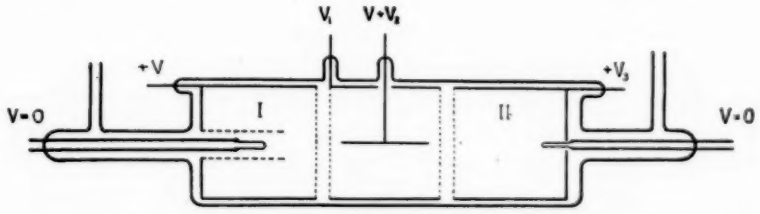

Fig. 1. Double discharge tube. Unit II detects ions produced by radiation from the discharge in I. The manner of applying potentials is indicated.

some effect which is not masked by the copious ionization and radiation produced at low voltage. Measurement of positive ions is entirely unsuited for this purpose and radiation measurements of the usual type have serious limitations. It was hoped that the photo-ionization effect would meet this requirement and the following results show that this is in fact the case. The published curves[3] show that there will be some photo-ionization by arc radiation, but I find that this light is relatively ineffective compared with radiation resulting from double ionization or soft x-ray excitation.

Apparatus and Procedure

The type of discharge tube used is illutrated in Fig. 1. It contains two thermionic units I and II, with screening electrodes between to prevent the passage of electrons and ions from one side to the other. The method of applying potentials is indicated in the diagram. Unit I gives a thermionic discharge at measured current and voltage. $V+V_2$ was usually 100 volts and V_1-6 volts. Unit II is the ion de-

tecting system for measuring the photo-ionization of gas within II by radiation from I. It is designed so that the anode almost completely incloses the fine wire cathode so as to entrap any positive ions and magnify their effect on the space charge.[4] V_3 was usually between 0.5 and 2 volts and was kept constant during each series of experiments. Either tungsten or oxide coated platinum filaments were found suitable. The latter were somewhat less sensitive but more constant than the tungsten.

The observations consisted of measurements of the change in thermionic current in II produced by a discharge in I. To measure this current change, the "dark current" through the galvanometer across II was balanced by a potentiometer circuit and the galvanometer sensitivity increased to the desired amount. Then for each setting of the potential V across I, readings were taken of the discharge current in I and of the deflection of the galvanometer across II with the discharge in I both on and off. In computing results, the difference in these galvanometer deflections divided by the discharge current in I was plotted against the potential V. The initial velocity correction to the applied potential was based on the observed value of the first ionization potential. Removal of the potential $V+V_2$ from the electrode at the middle of the tube permitted ions from the discharge to reach II, and at low pressures accurate measurements of the ionization potential could be made by use of the space charge effect. With gas pressures greater than .01 mm, it was preferable to to measure, by the Lenard method, ions reaching the screening cylinder.

Results

Caesium. The metal was distilled into the body of the tube and the tube maintained at about 160°C, giving a vapor pressure of about .02 mm. Fig. 2 shows some typical curves, taken with nearly constant detecting sensitivity, but with different discharge currents, and Table I gives some data on the curves. Mean values for the critical potentials based on 20 curves are—

$$13.0 \pm .5, 18.5 \pm 1, 21.5 \pm .5, 39.0 \pm 1 \text{ volts.}$$

Uncertainty as to the potential correction is the chief factor in the probable error 0.5. The measurements show that, with discharge currents less than 6×10^{-5}, the photo-current at a given voltage is nearly proportional to the discharge. current With larger currents, the photo-effect above 13 volts increases more nearly as the square

[4] Kingdon, Phys. Rev. **21**, 408 (1923).

of the discharge current. Curves extending over a considerable range of voltage are always distinctly concave to the voltage axis.

TABLE I

Data for curves of Fig. 2.

Curve No.	Maximum discharge current	Maximum current of photo-effect	Maximum volts
I	28×10^{-5}	5.3×10^{-7}	16
II	6×10^{-5}	4.5×10^{-7}	30
III	1.9×10^{-5}	4.8×10^{-7}	46
IV	1.3×10^{-5}	3.3×10^{-7}	46

Potassium. Relatively few curves were obtained with this vapor. The tube was at about 240°C, giving a vapor pressure of the order of .05 mm. The mean values for the critical potentials are

$$19.0\pm1,\ 23.8\pm1,\ 31.8\pm1,\ 48.4\pm1 \text{ volts},$$

the first value being based on published measurements.[5] Curves are similar to the caesium curves, except that the second point is much more pronounced in this case.

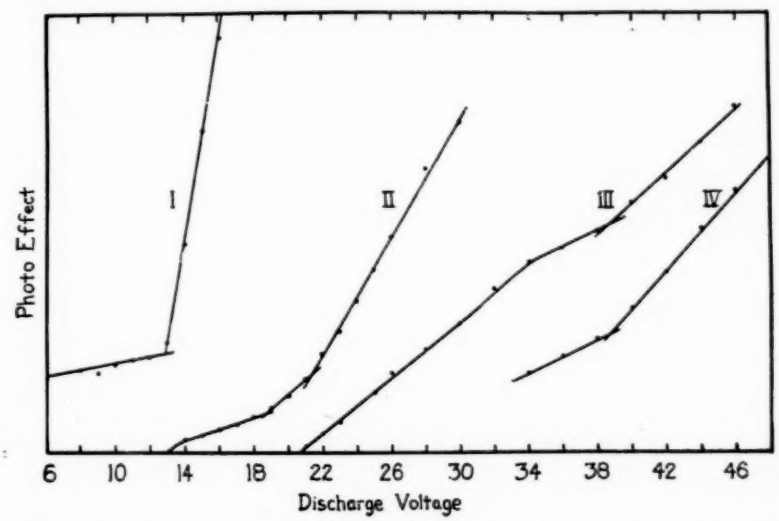

Fig. 2. Photo-ionization of caesium vapor as a function of the discharge voltage. (See Table I.)

Argon. Gas which was known to contain some nitrogen was streamed continuously from a reservoir through a fine capillary tube, hot calcium chips, a liquid air trap, the discharge tube and a second liquid air

[5] Mohler, "Critical Potentials Associated with Excitation of Alkali Spark Spectra," Sci. Paper, Bur. of Stds., No. 505, 1925.

trap. Many curves were obtained with argon in testing out various modifications in the tube design. Fig. 3 gives some typical curves

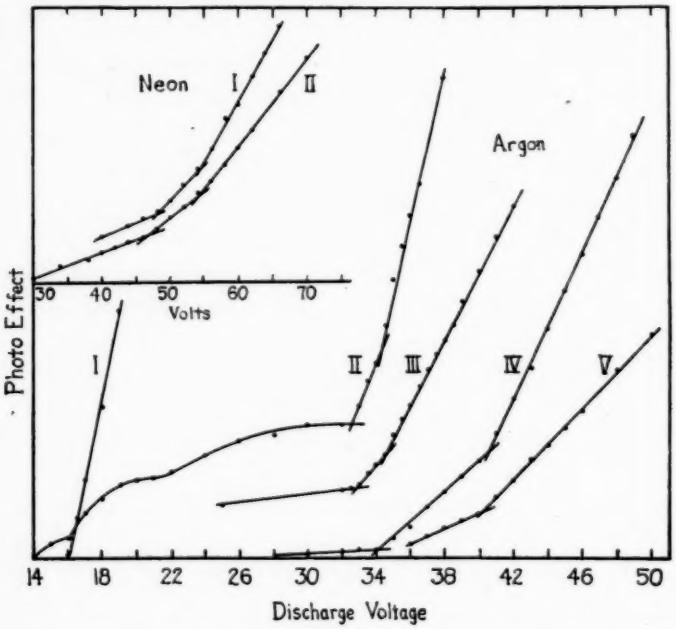

Fig. 3. Photo-ionization of neon and argon as a function of the discharge voltage. (See Table II.)

and Table II gives data relating to them. The mean values of the critical potentials are

$$32.2 \pm .2,\ 34.8 \pm .5,\ 39.6 \pm .5 \text{ volts},$$

the potentials being based on the value 15.4 for the first ionization potential.[6] The sensitivity of ion detection is not the same for the

TABLE II

Data for curves of Fig. 3

Curve No.	Pressure	Maximum discharge current	Maximum photo-current	Maximum volts
Argon I	.01	$.42\times10^{-4}$	Ion current	19
II	.01	8.5×10^{-4}	54×10^{-7}	38
III	.01	$.58\times10^{-4}$	34×10^{-7}	42
IV	.04	2.1×10^{-4}	7.6×10^{-7}	48
V	.04	4.2×10^{-4}	13.3×10^{-7}	50
Neon I	.01	$17.\times10^{-4}$	3.5×10^{-7}	70
II	.01	$18.\times10^{-4}$	2.8×10^{-7}	70

[6] Hertz and Kloppers, Zeits. f. Physik **31**, 463 (1925).

different curves. The effect below 30 volts was relatively large for high discharge currents (curve II), while increased pressure made the change in slope near 40 volts more pronounced (curves IV and V).

Neon. Gas which was known to contain a trace of helium was treated in the same way as the argon. Curves and data are included in Fig. 3 and Table II. The ion detecting sensitivity was much lower for neon than for the other gases and the changes in slope at the critical potentials were less distinct. Mean values for these potentials relative to the spectroscopic value 21.5 volts for the first ionization potential[7] are

48.0 ± 1 and 54.9 ± 1 volts.

The second points falls close to the ionization potential of the helium ion, but spectroscopic results described below show that the potential can safely be ascribed to neon. The curves showed no other critical potentials characteristic of helium.

Spectroscopic observations. A number of spectrograms of thermionic discharges were made to aid in the interpretation of the electrical measurement. A third spectrum of caesium had previously been reported[5] with an excitation potential less than 60 volts. Further photographs of the discharge show a trace of this spectrum at 40 volts with a discharge current of 10^{-2} amps, while with a current of 2×10^{-3} amps the lines were not visible below 55 volts. The spectrum is faint and the threshold potentials could not be located accurately.

Dejardin[8,9] has measured the potentials required to excite the second spectra of the rare gases but his work on neon[9] had not been published at the time my experiments were made. For that reason I have taken a series of spectrograms of the neon discharge. I used a three electrode thermionic tube with the grid and plate at the same potential and photographed the spectrum with a quartz spectrograph. Exposures were made at a series of potentials with currents of a few milli-amperes and a gas pressure of about .05 mm. The second spectrum was absent at 54 volts, distinctly visible at 55 and strongly enhanced in exposures at 58, 60 and 70 volts. The plates show about 25 of the stronger lines of the neon II spectrum[10] with no evidence of any real difference in excitation potentials of the different lines. The strong lines are all between 3700A and 3300A. Discrepancies between

[7] Lyman and Saunders, Nature **116**, 358 (1925).
[8] Dejardin, Ann. d. Physique **11**, 241 (1924).
[9] Dejardin, Comptes Rendus **182**, 452 (1926).
[10] Merton, Proc. Roy. Soc. **89A**, 447 (1913–14);
L. and E. Bloch and Dejardin, Comptes Rendus **180**, 731 (1925).

my results and those of Dejardin[9] will be considered in the following section.

Interpretation of Results

Caesium and potassium. The paper on excitation of alkali spectra[5] gives a basis for the interpretation of the present results, and the correlation is shown in Table III. There is good agreement except in

Table III

Critical potentials of alkalies.

Ref. No.	Caesium Photo-ionization	Caesium Other data[5]	Rubidium Published data[5]	Potassium Photo-ionization	Potassium Published data[5]	Interpretation
1	13.0±.5	14 ±2	16.0±.5	19 ±1	19±1	Ioniz. of n_2 rare gas shell. 2nd spectrum with high current.
2	18.5± 1		21.6±.5	23.8±1	23±1	Ioniz. + ion excitation.
3	21.5±.5	21.5±1	25.2±.1	31.8±1	28±1	Double ioniz. 2nd spectrum with low current.
4	39.0± 1			48.0±1		Ioniz. of n_1 rare gas shell. 3rd spectrum high current.
5		55 ±5				3rd spectrum low current.

Table IV

Critical potentials of rare gases.

Ref. No.	Argon Photo-ionization	Argon Published data	Neon Photo-ionization	Neon Published data	Interpretation
1		15.4[6]		21.5[7]	1st ionization potential
2	(16.8)		(26.5)		Excitation of ion.
3	(19.4)	19.0[8]	(33.4)		Ioniz. of ion. 2nd spectrum with high current.
4	32.2		48.0		Ioniz. + excitation of ion.
5	34.8	34 [8]	54.9	48 [9]	Double ioniz. 2nd spectrum with low current.
6	39.6				Ionization of n_1 shell.
7		70 [8]			Third spectrum with low current.

the case of point 3 of potassium. In all cases the new value is probably to be preferred. The manner in which the excitation of the third caseium spectrum depends on the current indicates that it is a spark spectrum.

Argon and neon. Various observers[8,11] have found that the argon II spectrum is excited near 34 volts with low currents, and near 19

[11] Horton and Davies, Proc. Roy. Soc. **102A**, 131 (1922).

volts with high currents, the difference in the potentials being about equal to the first ionization potential. This clearly indicates that the low current excitation potential measures the work of double ionization. Experiments involving electromagnetic analysis of ions[12] give a much higher value, 45 volts, for the work of double ionization. As other methods fail to show a critical potential at this point, I have interpreted my data on the basis of the spectroscopic results as shown in Table IV. Values in parentheses are ionization and excitation potentials of the ions, computed by subtracting the first ionization potential from the observed higher potentials.

The above described experiments indicate that the neon II spectrum is excited near the higher of the two observed critical potentials, and that all of the stronger lines appear within a volt or two of this potential. The recent results of Dejardin[9] are not in agreement with this. He finds one group of lines (included among the strong lines observed by the author) excited near 48 volts, while a second group (only a few faint lines observed in the present work) appear above 52 volts. For this he used a low pressure discharge concentrated by a magnetic field. With an intense discharge at high pressure the first group appeared between 28 and 30 volts. Since the serious sources or error, space charge, oscillating discharge, and multiple excitation all tend to make observed values too low, I believe that my higher value for the excitation of the first group is nearer the true value, and the neon results in Table II are interpreted on this basis. Dejardin's use of a magnetic field to concentrate the discharge would obviously increase the current density in his experiments and a multiple excitation involving the excitation stage (4) of Table IV would explain this result. My spectrograms give no conclusive evidence for or against the existence of a higher critical potential for Dejardin's second group.

Point (2) of neon can probably be interpreted as measuring the work required to raise an electron in the ion from a 2_2 orbit to a 3 quantum orbit; for the ionization potetial of a 3 quantum state in a hydrogenic ion is 6.0 volts while the ionization potential of this neon level is $33.4-26.5=6.9$ volts. The 3 quantum orbits are probably the final states for the spark lines between 3700 and 3300A. These potential values indicate that the absorption lines of the neon ion with final state 2_2 lie between 465A and 370A, while all other lines of the second spectrum will fall on the long wave-length side of 1800A. These predictions are not in conflict with published results,[13] which

[12] Barton, Phys. Rev. **25**, 469 (1925).
[13] Lyman and Saunders, Proc. Nat. Acad. Sci. **12**, 92 (1926).

mention many lines near 430A, but these unclassified lines may include spectra involving the 2_1 level as well as higher stages of ionization of the level 2_2.

The n_1 levels of the rare gas shell. Tables III and IV identify potentials of potassium and caesium and of argon, as measuring the energy levels of n_1 electrons. There are two reasons for this: first, that other possibilities seem to be excluded, and second, that the magnitudes of the observed potentials are consistent with the general scheme of atomic structure. This is shown in Fig. 4, a Moseley diagram of the beginning of the M series, which includes the observed points, together with

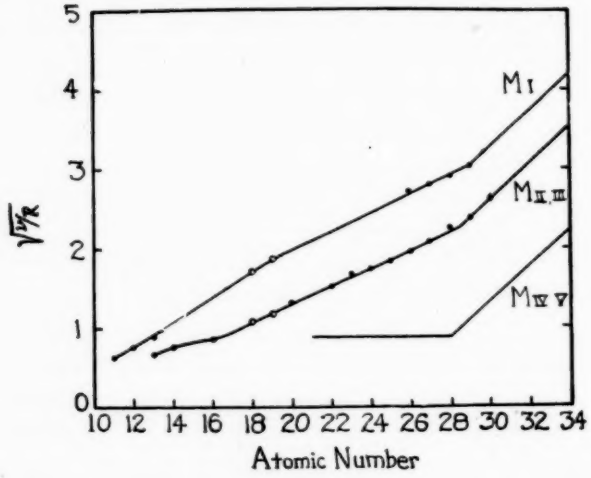

Fig. 4. The beginning of the M series. Dots give limits computed from optical and x-ray data, while circles are based on critical potential values for potassium and argon.

limits computed from optical and x-ray spectra. The 5_1 level of caesium can not be checked in this way but the screening separation of the n_2 and n_1 levels

$$\sqrt{\frac{\nu}{R}(n_1)} - \sqrt{\frac{\nu}{R}(n_2)}$$

is 0.69 for both potassium and caesium. This is definitely larger than the value 0.57 found in the x-ray range between levels of azimuth numbers 1 and 2, but agrees with the values .73 to .64 given by the computed M levels of metals of the iron group (Fig. 4).

Quantitative considerations. In the introduction, I raised the question as to whether photo-ionization contributed appreciably to the total photo-electric effect measured by the usual radiation potential method.

The space charge effect does not give an absolute measure of the photo-ionization. A partial answer to the question is given by the following experiments. The "radiation current" in II (Fig. 1), with other connections as before, but with the filament cold, measures the photo-electrons from the gas, plus photo-electrons from the small area of the cathode and the adjacent screening electrode. With potentials on II reversed, one measures the photo-electrons from the gas plus those from the large area of the cylinder II. The current in the second case was, in order of magnitude, 10 times as large as in the first case in the range of conditions here used. We conclude that, under comparable conditions, photo-electrons from the metal electrodes contribute at least nine tenths of the radiation effect as commonly measured.

The photo-electric current in case one (filament cold and potentials as in Fig. 1) is certainly greater, possibly much greater, than the photo-ionization current alone. Comparison of this current with the current change produced by the space charge effect will at least set a lower limit to the ratio of electron current change to ion current. Measurements in caesium and argon gave ratios of 3800 and 2400 respectively. I have also drawn a measured ion current from the discharge into II and measured the resulting change in thermionic current. The ratio then is much smaller, being about 300 for caesium. The reason for the difference is evident. Ions formed within the cylinder II may circulate many times around the cathode before falling into it.[4] Ions drawn into the space can go directly to the anode in spite of the small retarding field, and then the ratio is, as we should expect, less than the mobility ratio, 500, of electrons as compared with caesium ions.

The current change produced by photo-ions is known to be proportional to the radiation intensity, provided the electron current change is small compared with the dark current.[3] It follows that the effect should here be proportional to the discharge current as long as the current density in the discharge is small enough to avoid secondary effects such as collisions of electrons and ions. We have found that with the caesium such a proportionality held with currents less than 6×10^{-5} amps, but that with higher currents the photo-effect above 13 volts increased at an abnormal rate. This can be correlated with results showing high current excitation of the caesium II spectrum at this potential.[5] Similarly in argon (Fig. 2, curve II), large discharge currents gave an abnormal increase in photo-effect below 30 volts, which is probably related to ion excitation by collisions of electrons and ions.

In all cases the most conspicuous critical potential was that giving double ionization of the n_2 shell. This is probably because the strongest lines of the ion spectrum lie close to the n_2 absorption limit where the absorption coefficient of the gas is high. The radiation resulting from n_1 ionization is probably weakly absorbed, and the intensity must be relatively great. This conclusion is supported by the fact that with argon, increased pressure made the effect above the n_1 critical potential relatively large. The radiation passed through about 10 cm of gas before reaching the detecting chamber so that with the higher pressures the spark lines were reduced by absorption much more than the n_1 spectrum.

BUREAU OF STANDARDS,
DEPARTMENT OF COMMERCE,
April 27, 1926.

THE EFFECT OF RECOMBINATION ON THE PRIMARY PHOTO-ELECTRIC CURRENT FROM A CRYSTAL

By W. Howard Wise

Abstract

Taking into account recombination, mathematical expressions are derived for the primary photo-electric current to be expected from crystals both when the light is normal to the electric field and when the light is parallel and opposite to the electric field. On comparing with the experiments on rock salt it is found that recombination is sufficient to account for the drop in current with time. The decrease in current when the light is opposite to the field and most strongly absorbed, is shown to be partially accounted for by recombination. The effect of the unknown process causing the major portion of the drop is thus isolated and a more rigorous test of any theory which may be proposed to account for it made possible.

I

MANY crystals when placed in an electric field and illuminated by light of a frequency range peculiar to the crystal are found to be conducting. The experiments of Gudden and Pohl[1] on this subject show that the current so obtained is of two kinds: (1) a primary current due to photo-electrons which the light has liberated from the atoms of the crystals, (2) a secondary current representing the motion of the positive ions toward the cathode. Under suitable experimental conditions the current is entirely of the first or primary kind. In this case the positive ions accumulate in the crystal and by capturing electrons on their way to the anode materially reduce the primary current.[2] It is the purpose of this investigation to calculate, with certain idealizations, how much this recombination reduces the primary current.

The experiments are of two classes; in the first the light is perpendicular to the electric field (fig. 3); in the second the light is parallel and opposite to the electric field[3] (Fig. 6).

If the light is parallel to the electric field lateral diffusion of the electrons can have no effect on the current because the field is normal to layers of electrons of constant density.

If the light is perpendicular to the electric field the effect of lateral diffusion is to flatten out the original density distribution $e^{-\mu x}$ given

[1] Gudden and Pohl, Zeits. f. Physik **17**, 331 (1923).
[2] Gudden and Pohl, Naturwissenschaften **11**, 354 (1923).
[3] Gudden and Pohl, Phys. Zeits. **26**, 481 (1925).

by the light. Those electrons diffusing from regions of greater electron density (and consequent greater ion density) to regions of lesser electron density (and consequent lesser ion density) have a better chance of escaping recombination with some ion and reaching the anode than those electrons which do not diffuse. On the other hand those electrons which do not diffuse have a smaller chance of reaching the anode than they would have, did not some others diffuse, because they must now escape not only the ions normally in their path but also those ions which the diffusing electrons escape. The effect of diffusion is thus somewhat self-compensating and a considerable change in the distribution of electrons from this cause need not, so far as can be seen without actually taking it into account in the calculations, cause a material change in the primary current. As it is not an easy matter to take diffusion into account in calculating the current to be expected

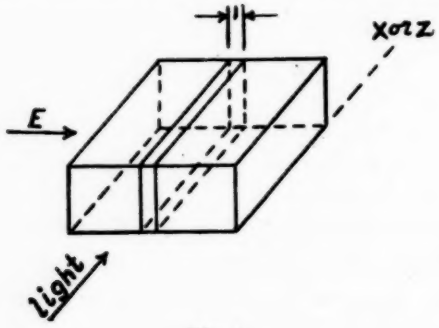

Fig. 1.

it will be shown instead, that, for the experiments to which the expression derived for the current is to be applied, diffusion does not sensibly alter an original distribution while it traverses the crystal. This is done in section II. In section III the primary current is computed for the case of a field at right angles to the incident light and in section IV it is computed for the case of a field parallel and opposite to the incident light.

II

Let free electrons be present in a crystal and be distributed according to the law $e^{-\mu x}$ which is the law by which they are photo-electrically liberated. μ is the absorption constant for the light used. Suppose now that these electrons are uniformly distributed in a unit layer under the curve $e^{-\mu x}$. The problem before us is to find out how much diffusion has flattened out this original distribution by the time the field E has pulled the unit layer over to the anode.

Because of diffusion each element of volume $e^{-\mu z}dx$ in the unit layer will in time assume the distribution ke^{-au^2} where k and a are determined by the condition

$$k\int_{-\infty}^{\infty} e^{-au^2}du = \text{area under the elementary probability curve}$$

$$= k\sqrt{\pi/a} = e^{-\mu z}dx \tag{1}$$

Since an electron can not diffuse from the surface of the crystal into the air the probability curve must be folded back at the surface of the crystal. The contribution of an element of volume $e^{-\mu z}dx$ to the electrons at any other point in the same unit layer after the redistribution is thus from two parts of the little probability curve

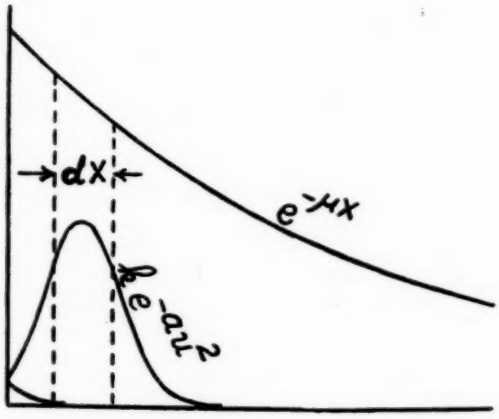

Fig. 2.

distant $2x$ apart. The number of electrons at a point z due to the diffusion of $e^{-\mu z}dx$ electrons starting from the point x is therefore

$$d\rho = ke^{-a(x-z)^2} + ke^{-a(x+z)^2}$$

But from (1) we have $k = \sqrt{a/\pi}e^{-\mu z}dx$ and consequently

$$d\rho = \sqrt{a/\pi}\left\{e^{-a(x-z)^2} + e^{-a(x+z)^2}\right\}e^{-\mu z}dx$$

The total number of electrons between z and $z+1$ is then

$$\rho = \sqrt{a/\pi}\int_0^{\infty}\left\{e^{-a(x-z)^2} + e^{-a(x+z)^2}\right\}e^{-\mu z}dx \tag{2}$$

This new distribution function ρ satisfies the differential equation

$$\frac{d^2\rho}{dz^2} = \mu^2\rho - 2\mu\sqrt{a/\pi}e^{-az^2} \tag{3}$$

The properties of ρ are not apparent from (2) but (3) shows that ρ does have the characteristics to be expected from the nature of the problem: for if $a \doteq \infty$, meaning that there is no diffusion, (3) reduces to $d^2\rho/dz^2 = \mu^2\rho$ of which the solution is $\rho = e^{-\mu z}$ which is the original distribution law; as z becomes very large (3) again reduces to $d^2\rho/dz^2 = \mu^2\rho$ with the solution $\rho = e^{-\mu z}$ which means that if the original distribution is quite uniform, as it is for large values of z, then diffusion does not affect it.

The expression (2) has yet to be put in a form suitable for computation.

$$\rho = \sqrt{a/\pi}\int_0^\infty \left\{e^{-a(x-z)^2} + e^{-a(x+z)^2}\right\} e^{-\mu x}\, dx$$

$$= e^{\mu^2/4a}\left[\cosh \mu z - \sqrt{a/\pi}\left(e^{\mu z}\int_0^{z+\mu/2a} e^{-as^2} dS - e^{-\mu z}\int_0^{z-\mu/2a} e^{-as^2} dS\right)\right] \quad (4)$$

If the electron can be looked upon as having a mean free path l then

$$a = 4^2/\pi^2 n l^2,$$

where n is the number of collisions it has made,

$\mu = el/2mv =$ mobility of the electron

$V = \mu E = eEl/2mv =$ velocity with which it proceeds through crystal,

$V/v = eEl/2mv^2 =$ ratio of forward progress to total random motion,

$n = vd/Vl = \dfrac{2d}{eEl^2} = mv^2 =$ number of collisions made in advancing a distance d.

$$\therefore a = 4^2/\pi^2 n l^2 = \frac{4^2}{\pi^2}\,\frac{eE}{4d}\,\frac{1}{\frac{1}{2}mv^2} = 3130\, E_v/Td$$

where E_v is the electric field in volts per cm and T is the absolute temperature. Let $T = 306°$; take $d = 15$ cm or half the crystal thickness; assume $E_v = 117.5$; then $a = 8100$.

As μ affects only the abscissa scale when $e^{-\mu z}$ is plotted let $\mu = 1$.

$$\rho = e^{1/32{,}400}\left[\cosh z - \frac{90}{\sqrt{\pi}}\left(e^z\int_0^{z+1/16200} e^{-as^2} ds - e^{-z}\int_0^{z-1/16200} e^{-as^2} ds\right)\right]$$

Let $90s = t$ and then if $s = z \pm 1/16200 \quad t = 90z \pm 1/180$

$$\rho = \cosh z - \frac{1}{\sqrt{\pi}}\left(e^z\int_0^{90z+1/180} e^{-t^2} dt - e^{-z}\int_0^{90z-1/180} e^{-t^2} dt\right)$$

The greatest change due to diffusion must occur at the origin $z=0$ for it is here that the slope of the curve $e^{-\mu z}$ is greatest (x positive). Placing therefore $z=0$ we calculate

$$\rho_0 = 1 - \frac{1}{\sqrt{\pi}} \int_{1/180}^{1/180} e^{-t^2} dt = 1 - .0062 = .9938 ,$$

or that the average maximum change in an ordinate, under the conditions stated is 0.6 percent or less; less because the average electron travels less than half the crystal thickness.

From these considerations it is seen to be permissible to assume in the mathematical work of deriving the expression for the primary current that the electrons move only in the direction of the electric field.

III

It is assumed that an electron reaches the anode unless it recombines with an ion and that the radiation emitted when recombination occurs does not liberate another electron before it reaches the surface of the crystal and escapes. Were this condition not completely fulfilled the effect would merely be that diffusion and the distance between ions would both appear to be greater than normal: for the disappearance of an electron in one place and its appearance in another could be looked upon as diffusion and by this process one collision with an ion has been lost.

The mean free path of the electrons, referred to ions, is taken to be $\lambda = 1/N\pi\sigma^2 b$ where N is the number of ions per cc, σ is the radius of an ion and b may be a function of the mobility of the electrons, of the field, and consequently a function of the concentration of ions but is assumed to be a constant. This point will be brought up again.

If $\lambda(s)$, the mean free path of electrons appropriate to the position s, be so defined that the chance of an electron's recombining in the distance ds is $ds/\lambda(s)$, it may readily be shown that the chance $P(s_1, s_2)$ of an electron's going from a position s_1 to a position s_2 without recombining is given by

$$P(s_1, s_2) = e^{-\int_{s_1}^{s_2} ds/\lambda(s)}$$

Then the chance that an electron liberated a distance z from the cathode at time t will go to a point distant y from the cathode and recombine in the distance dy is $P(z, y, t)\, dy/\lambda(y, t)$ provided we may

neglect the change in λ at any point during the time it takes an electron to go from z to y. If this is not permissible we must write instead that the chance is $P(z, y, t_r)dy/\lambda(y, t)$ where

$$P(z,y,t_r)=e^{-\int_z^y \frac{ds}{\lambda[s,\, t-(y-s)/\mu E]}}$$

and μ is the mobility or velocity in a unit field.

The rate at which electrons are being liberated is a function of x only, $F(x)$. Then from the element of volume $kdxdz$ there are liberated $kdxdz \cdot F(x)$ electrons per sec. of which the number recombining in the element of volume $kdxdy$ is $kdxdz \cdot F(x)P(z, y, t_r)\, dy/\lambda(y, t)$ at the time t if $t \geqq (y-z)/\mu E$.

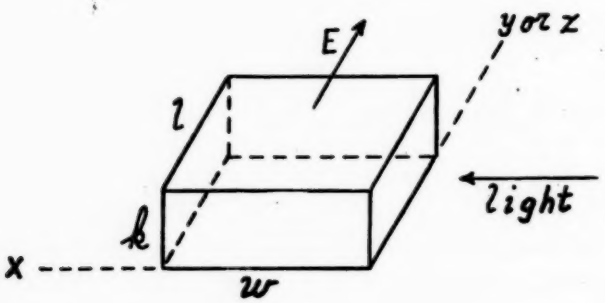

Fig. 3.

If there are n electrons per sq. cm per sec. leaving the cathode, the number of these which combine with ions in the element of volume $kdxdy$ is $kdx \cdot nP(0, y, t_r)\, dy/\lambda(y, t)$ per sec. at the time t. In the experiments to which this work is to be applied $n=0$ but it will be retained for the present.

During the time $t<l/\mu E$ the total number of liberated electrons which recombine in $kdxdy$ is

$$kdxdyF(x)\frac{1}{\lambda(y,t)}\int_{y-\mu Et}^{y} P(z,y,t_r)dz$$

per sec.

So up to the time $t=y/\mu E$ the total number of electrons recombining per sec. in $kdxdy$ is

$$kdxdy\, 1/\lambda(y,t)\left[nP(y-\mu Et,y,t_r)+F(x)\int_{y-\mu Et}^{y} P(z,y,t_r)dz\right]$$

while the number being produced per sec. is $kdxdyF(x)$. The difference must be the net rate of increase of ions which is

$$kdxdy\frac{\partial N}{\partial t}=kdxdy\frac{1}{\pi\sigma^2 b}\frac{\partial}{\partial t}\frac{1}{\lambda(y,t)}$$

and hence we have

$$\frac{1}{\pi\sigma^2 b}\frac{\partial}{\partial t}\frac{1}{\lambda}=F(x)-\frac{1}{\lambda}\left[nP(y-\mu Et,y,t_r)+F(x)\int_{y-\mu Et}^{y}P(z,y,t_r)dz\right] \qquad (1)$$

as the defining equation for $\lambda=\lambda(x, y, t)$ up to $t=y/\mu E$. The second term on the right has the lower limit $y-\mu Et$ for the integral because the chance that the $nkdx$ electrons reach the point $y-\mu Et$ is 1 if $t<y/\mu E$. If $t>y/\mu E$ we must write instead of (1)

$$\frac{1}{\pi\sigma^2 b}\frac{\partial}{\partial t}\frac{1}{\lambda}=F(x)-\frac{1}{\lambda}\left[nP(0,y,t_r)+F(x)\int_{0}^{y}P(z,y,t_r)dz\right] \qquad (1.1)$$

It is convenient to rewrite Eq. (1) as

$$A\frac{\partial}{\partial t}\frac{1}{\lambda}=1-\frac{1}{\lambda}\left[BP(y-\mu Et,y,t_r)\int_{y-\mu Et}^{y}P(z,y,t_r)dz\right]$$

where $A=[\pi\sigma^2 bF(x)]^{-1}$ and $B=n/F(x)$

$$\text{or}\qquad -A\frac{\partial}{\partial t}\log\lambda=\lambda-\left[BP(y-\mu Et,y,t_r)+\int_{y-\mu Et}^{y}P(z,y,t_r)dz\right] \qquad (1.2)$$

Now let

$$\lambda=1/\frac{\partial}{\partial s}\log v\left(s,t-\frac{y-s}{\mu E}\right)$$

under the integral signs and

$$1/\frac{\partial}{\partial y}\log v(y,t)$$

outside the integral signs where $s=y$. Since $\lambda=\infty$ if $t=0$ $v(y, 0=v_0=\text{const}$. With this change of variable Eq. (1.2) becomes

$$A\left(\frac{\partial v}{\partial t}-v\frac{\partial^2 v}{\partial y\,\partial t}/\frac{\partial v}{\partial y}\right)+v^2/\frac{\partial v}{\partial y}=Bv_0+\int_{y-\mu Et}^{y}v\left(z,t-\frac{y-z}{\mu E}\right)dz \qquad (2)$$

If we differentiate (2) with respect to y and t and then add the results we get the following differential equation

$$\frac{\partial}{\partial y}\left[A\left(\frac{\partial v}{\partial t}-v\frac{\partial^2 v}{\partial y\,\partial t}\Big/\frac{\partial v}{\partial y}\right)+v^2\Big/\frac{\partial v}{\partial y}\right]$$

$$+\frac{1}{\mu E}\frac{\partial}{\partial t}\left[A\left(\frac{\partial v}{\partial t}-v\frac{\partial^2 v}{\partial y\,\partial t}\Big/\frac{\partial v}{\partial y}\right)+v^2\Big/\frac{\partial v}{\partial y}\right]=v \qquad (3)$$

which must be solved for v if we are to know how the current rises when the light in turned on.

The current passing any point. The part of the $kdxdzF(x)$ electrons liberated per second from the element of volume $kdxdz$ that reaches the point y is

$$kdxdzF(x)\;\; P(z,y,t_r)$$

Of the n electrons passing 1 sq. cm per sec. at the point $y-\mu Et$ at the time $t=0$ the number passing 1 sq. cm per sec. at the point y at the time t is

$$nP(y-\mu Et,y,t_r)$$

up to the time $t=y/\mu E$.

Then the total number of electrons passing 1 sq. cm per sec. at time t at the point y is

$$\delta I_v/e=M=F(x)\int_{y-\mu Et}^{y} P(z,y,t_r)dz+nP(y-\mu Et,y,t_r) \qquad (4)$$

Placing now

$$\lambda=1/\frac{\partial}{\partial s}\log\, v\left(s,t-\frac{y-s}{\mu E}\right)$$

as before we get

$$M=F(x)\left[Bv_0/v+\frac{1}{v}\int_{y-\mu Et}^{y} v\left(z,t-\frac{y-z}{\mu E}\right)dz\right]$$

or

$$M=\frac{F}{v}\left[A\left(\frac{\partial v}{\partial t}-v\frac{\partial^2 v}{\partial y\,\partial t}\Big/\frac{\partial v}{\partial y}\right)+v^2\Big/\frac{\partial v}{\partial y}\right] \qquad (4.1)$$

From (3) then we have

$$\frac{\partial}{\partial y}\left(\frac{Mv}{F}\right)+\frac{1}{\mu E}\frac{\partial}{\partial t}\left(\frac{Mv}{F}\right)=v \qquad (5.0)$$

or

$$\frac{\partial^2}{\partial y^2}\left(\frac{Mv}{F}\right)-\frac{\partial v}{\partial y}=\frac{1}{\mu^2E^2}\frac{\partial^2}{\partial t^2}\left(\frac{Mv}{F}\right)-\frac{1}{\mu E}\frac{\partial v}{\partial t} \qquad (5)$$

In all the experiments of Gudden and Pohl the current leaps immediately to a maximum and then decreases. This indicates that μE is very large and consequently that the time taken for an electron to cross the crystal is small compared with the time required for the distribution of ions to change sensibly. We have then to deal with (1.1) and with (3) rewritten as

$$\frac{\partial}{\partial y}\left[A\left(\frac{\partial v}{\partial y}-v\frac{\partial^2 v}{\partial y\partial t}\Big/\frac{\partial v}{\partial y}\right)+v^2\Big/\frac{\partial v}{\partial y}\right]=v \tag{3.2}$$

or

$$A\frac{\partial^2 v}{\partial y\partial t}-v-\frac{\partial}{\partial y}\left[v\left(A\frac{\partial^2 v}{\partial y\partial t}-v\right)\Big/\frac{\partial v}{\partial y}\right]=0$$

or $\partial^2 v/\partial y\partial\tau=v$ where $\tau=t/A=\pi\sigma^2 bF(x)t$ (3.3)

Following the suggestion of (5) that t and y may enter into v in the same way, we assume $v=v[(\tau+g)(y+h)]$ and find that (3.3) reduces to the total differential equation (the other simple and most obvious assumption $v=v(\tau+y)$ does not yield a suitable form of solution): $(\tau+g)(y+h)v''+v'=v$. Letting $(\tau+g)(y+h)=-\alpha^2/4$ this becomes

$$v''+v'/\alpha+v=0$$

and therefore

$$v=J_0(\alpha)=J_0[2i\sqrt{(\tau+g)(y+h)}]$$

Using now the fact that $n=0$ and μE is large we may rewrite (2.2) in the following form

$$A\frac{\partial}{\partial t}\frac{1}{\lambda}=1-\frac{1}{\lambda}\int_0^y P(z,y,t)dz \tag{2.5}$$

or

$$\frac{\partial v}{\partial\tau}=\int_0^y v(z,\tau)dz \tag{2.6}$$

where we have used (3.3) and $1/\lambda=\partial\log v/\partial y$.

The condition

$$\lambda=1/\frac{\partial}{\partial y}\log v=\infty$$

if $t=0$ makes $g=0$ for only then will v be independent of y when $t=0$. Substituting $J_0[2i\sqrt{\tau(y+h)}]$ into (2.6) we find that $h=0$. Therefore

$$\lambda=1/\frac{\partial}{\partial y}\log J_0(2i\sqrt{\tau y})$$

Substituting (3.3) in (4.1) we find

$$\delta I_y = eF\frac{\partial v}{\partial \tau}/v = \frac{e}{\pi\sigma^2 bv}\,\frac{\partial v}{\partial t} = \frac{eyF}{v}\,\frac{\partial v}{\partial(\tau y)} = eyFv'/v$$

Hence

$$I_l = ekl\int_0^w \frac{v'(\tau l)}{v(\tau l)}F(x)dx \tag{6}$$

Wherein we have taken account of the fact that the crystal is k cm high and that the current is measured at the anode where $y=l$. The ratio v'/v may be expanded into a power series and then

$$I = ekl\int_0^w [1+a_1\tau l+a_2(\tau l)^2+a_3(\tau l)^3+\cdots]F(x)dx$$

If Q_0 ergs of energy enter 1 sq. cm. of the surface each second the energy remaining in this square beam at a depth x in the crystal is $Q_1 = Q_0 e^{-\mu x}$. Of the energy remaining in the beam when it reaches the rear face a fraction r is reflected and this fraction behaves just like the original beam. The energy at any point is thus made up of an infinite series of terms. The sum, Q, of this series is

$$Q_0(e^{-\mu x}+re^{-2\mu w}e^{\mu x})/(1-r^2e^{-2\mu w}) = Q_0 A\cosh\{\mu(x-w)+\log\sqrt{r}\}$$

where $$A = 2\sqrt{r}\,e^{-\mu w}/(1-r^2e^{-2\mu w})$$

The rate at which electrons are being liberated at the depth x is

$$F(x) = -\frac{1}{h\nu}\,\frac{dQ}{dx} = -(Q_0\mu/h\nu)A\sinh[\mu(x-w)+\log\sqrt{r}]$$

therefore

$$I = ekl\int_0^w [1+a_1(\pi\sigma^2 btl)F+a_2(\pi\sigma^2 btl)^2F^2+\cdots]Fdx$$

$$= ekl(Q_0/h\nu)A[B_1+a_1(\theta A)B_2+a_2(\theta A)^2B_3+\cdots] \tag{7}$$

where

$$\theta = \pi\sigma^2 btlQ_0\mu/h\nu \quad \text{and}$$

$$B_n = \int_0^w (-1)^n\sinh^n[\mu(x-w)+\log\sqrt{r}]\mu dx$$

If r is negligible then $F=(Q_0\mu/h\nu)e^{-\mu x}$ and (7) becomes

$$I = ekl(Q_0/h\nu)[(1-e^{-\mu w})+\tfrac{1}{2}a_1\theta(1-e^{-2\mu w})+\tfrac{1}{3}a_2\theta^2(1-e^{-3\mu w})+\cdots] \tag{7.1}$$

If most of the light is absorbed in the crystal and r is small it will be sufficiently accurate to correct for the light passing clear through by making w infinite. With w infinite (7.1) becomes

$$I = ekl(Q_0/h\nu)f(\theta) \tag{7.2}$$

where $f(\theta) = 1 + \frac{1}{2}a_1\theta + \frac{1}{3}a_2\theta^2 + \cdots = (1/\theta)\log J_0(2i\sqrt{\theta})$.

The same result could be obtained by making w infinite in (6).

$$\lim_{\theta \doteq \infty} f(\theta) = \lim_{\theta \doteq \infty} J_1(2i\sqrt{\theta})/i\sqrt{\theta}J_0(2i\sqrt{\theta}) = 0$$

The theory thus says that, ν and Q_0 being constant, the current should drop with time as shown in Fig. 4 for θ is a linear function of the time.

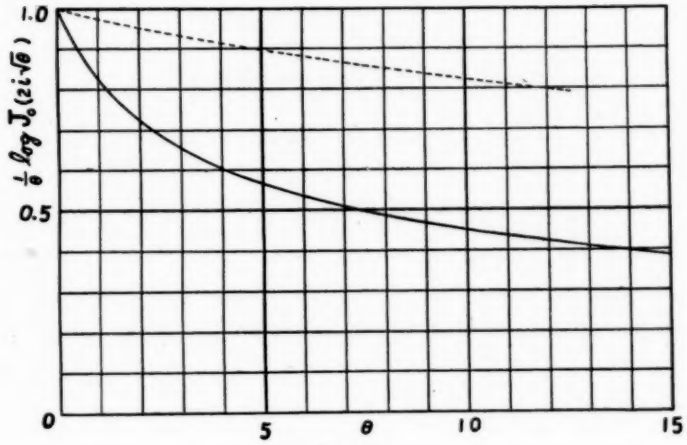

Fig. 4.

This is just what Gudden and Pohl have observed in NaCl[f]. With intense illumination they got a drop such as shown. With weak illumination they got very little drop in the same length of time and this is to be expected from the form of θ. If Q_0 is small it takes a long time for θ to become large.

If the experimental conditions were such that most of the light was absorbed in the rock salt it is permissible to compare $f(\theta)$ with the experimental curves, otherwise it would be necessary to use the more exact expression for I. As b is not known the test of the theory will consist of seeing if the constant b can be so chosen that the theoretical curve will lie along the experimental curve. The following figure shows how closely $f(\theta)$ can fit the experimental curve.

In view of the approximations introduced in deriving $f(\theta)$ and in applying it to the experiments the fit seems very good and appears to

warrant the conclusion that recombination is sufficient to account for the decrease in the current with time and that the assumption b = constant was not sensibly incorrect.

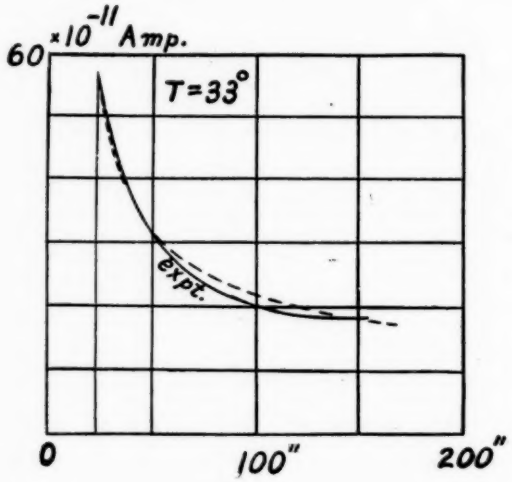

Fig. 5.

IV.

In the experiments on diamond, ZnS and HgS the light was, as shown in the accompanying figure, parallel and opposite to the electric field. The rate of production of electrons is now not a function of x but of y

$$F(y)=\frac{Q_0\mu}{h\nu}e^{-\mu(l-y)}$$

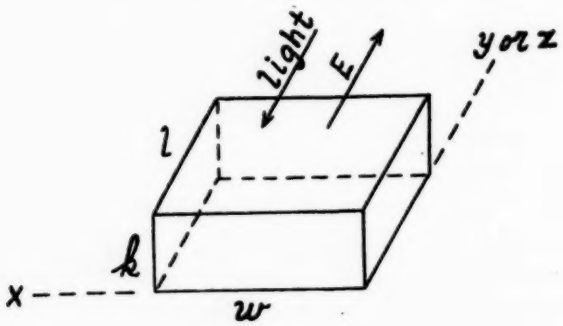

Fig. 6.

Reflection at the rear face of the crystal is neglected.

Since it was found possible and necessary to neglect the change in the density of ions while an electron is crossing the crystal, that

simplification will now be made at the start. The total number of electrons recombining in the element of volume $kdxdy$ is got by integrating $kdxdzF(z)P(z,y,t)dy/\lambda(y)$ from $z=0$ to $z=y$ and so is

$$kdxdy\frac{Q_0\mu}{h\nu}\frac{1}{\lambda(y)}\int_0^y e^{-\mu(l-z)}P(z,y,t)dz$$

per sec. The number of electrons liberated per sec. in the same element of volume is

$$kdxdy\frac{Q_0\mu}{h\nu}e^{-\mu(l-y)}$$

and taking the difference we get, as before, the net rate of production to be

$$kdxdy\frac{Q_0\mu}{h\nu}\left[e^{-\mu(l-y)}-\frac{1}{\lambda}\int_0^y e^{-\mu(l-z)}P(z,y,t)dz\right]$$

which must equal

$$kdxdy\frac{\partial N}{\partial t}=kdxdy\frac{1}{\pi\sigma^2 b}\frac{\partial}{\partial t}\frac{1}{\lambda}$$

Therefore

$$\frac{1}{\pi\sigma^2 b}\frac{\partial}{\partial t}\frac{1}{\lambda}=\frac{Q_0\mu}{h\nu}e^{-\mu l}\left[e^{\mu y}-\frac{1}{\lambda}\int_0^y e^{\mu z}P(z,y,t)dz\right] \qquad (1.0)$$

or

$$\frac{\partial}{\partial\tau}\frac{1}{\lambda}=e^{\mu y}-\frac{1}{\lambda}\int_0^y e^{\mu z}P(z,y,t)dz \qquad (1)$$

where $\tau=(\pi\sigma^2 bQ_0\mu/h\nu)e^{-\mu l}t$ defines λ as a function of t and y.

This last equation may also be written

$$-\frac{\partial}{\partial\tau}\log\lambda=\lambda e^{\mu y}-\int_0^y e^{\mu z}P(z,y,t)dz$$

Differentiating once with respect to y we have

$$-\frac{\partial^2}{\partial y\partial\tau}\log\lambda=e^{\mu y}\left(\frac{\partial\lambda}{\partial y}+\mu\lambda\right)-\left[e^{\mu y}-\frac{1}{\lambda}\int_0^y e^{\mu z}P(z,y,t)dz\right]$$

$$=e^{\mu y}\left(\frac{\partial\lambda}{\partial y}+\mu\lambda\right)-\frac{\partial}{\partial\tau}\frac{1}{\lambda}$$

Let $e^{\mu y}=\zeta$, $\dfrac{\partial}{\partial y}=\dfrac{\partial}{\partial \zeta}\dfrac{d\zeta}{dy}=\mu\zeta\dfrac{\partial}{\partial\zeta}$ and get

$$-\mu\zeta\frac{\partial^2}{\partial\zeta\partial\tau}\log\lambda=\zeta\left(\mu\zeta\frac{\partial\lambda}{\partial\zeta}+\mu\lambda\right)-\frac{\partial}{\partial\tau}\frac{1}{\lambda}$$

or

$$\frac{\partial^2}{\partial\zeta\partial\tau}\log\lambda=\frac{1}{\mu\zeta}\frac{\partial}{\partial\tau}\frac{1}{\lambda}-\left(\zeta\frac{\partial\lambda}{\partial\zeta}+\lambda\right)$$

$$=\frac{\partial}{\partial\tau}\frac{1}{\mu\zeta\lambda}-\frac{\partial}{\partial\zeta}(\zeta\lambda)$$

Placing $\lambda=e^{\xi}$, $1/\mu\zeta=\beta$, $\zeta=\alpha$ this takes the standard form

$$-\frac{\partial^2\xi}{\partial\zeta\partial\tau}=\frac{\partial}{\partial\zeta}(ae^{\xi})-\frac{\partial}{\partial\tau}(\beta e^{-\xi})$$

of which the solution is known to be $e^{\xi}=\lambda=v/u$ where v and u must satisfy the equations $\alpha v=\partial u/\partial\tau$ and $\beta u=\partial v/\partial\zeta$ or $\zeta v=\partial u/\partial\tau$ and $u/\mu\zeta=\partial v/\partial\zeta$, which can be combined into the one equation

$$v=\mu\frac{\partial^2 v}{\partial\zeta\partial\tau}\quad\text{or}\quad v=\frac{\partial^2 v}{\partial\zeta\partial\tau_1}$$

where $\tau_1=\tau/\mu$.

If we place $e^{\mu y}=\zeta$ in the original integral equation (1) it becomes

$$-\frac{\partial}{\partial\tau}\log\lambda=\mu\zeta-\frac{1}{\mu}\int_1^{\zeta}e^{-\int_{z_1}^{\zeta}\frac{d\zeta}{\mu\zeta\lambda}}\,dz_1$$

Now

$$\lambda=v/u=v/\mu\zeta\frac{\partial v}{\partial\zeta}\quad\text{or}\quad 1/\mu\zeta\lambda=\partial\log v/\partial\zeta$$

whence by substitution

$$\frac{v}{\mu}\left(\frac{\partial v}{\partial\zeta}\right)^{-1}-\frac{1}{v}\frac{\partial v}{\partial\tau}=\frac{v}{\mu}\left(\frac{\partial v}{\partial\zeta}\right)^{-1}-\frac{1}{\mu v}\int_1^{\zeta}v(\tau,z_1)dz_1$$

or

$$\frac{\partial v}{\partial\tau_1}=\int_1^{\zeta}v(\tau,z_1)dz_1$$

We need then a solution of $v=\dfrac{\partial^2 v}{\partial\zeta\partial\tau_1}$ that satisfies the conditions

$$\frac{\partial v}{\partial\tau_1}=\int_1^t v(\tau,z_1)dz_1 \text{ and } \lambda=\infty \text{ if } t=0$$

It has already been found that a solution of $v=\dfrac{\partial^2 v}{\partial\zeta\partial\tau_1}$ is

$$v=J_0(2i\sqrt{(\tau_1+g)(\zeta+h)})$$
$$=1+\frac{1}{(1!)^{-2}}(\tau_1+g)(\zeta+h)+\frac{1}{(2!)^{-2}}(\tau_1+g)^2(\zeta+h)^2+\cdots$$

Obviously the second condition is satisfied by taking $g=0$ and the first by taking $h=-1$, we then have

$$\lambda=1/\mu\zeta\log J_0(2i\sqrt{(\zeta-1)\tau_1})$$
$$I=\text{current}=ek\int_0^w dx\int_0^l\frac{\partial N}{\partial t}dy=ekw\int_1^{e^{\mu l}}\frac{\partial N}{\partial t}\frac{d\zeta}{\mu\zeta}$$

But $\dfrac{\partial N}{\partial t}=\dfrac{1}{\pi\sigma^2 b}\dfrac{\partial}{\partial t}\dfrac{1}{\lambda}=\dfrac{1}{\pi\sigma^2 b}\dfrac{\partial}{\partial t}\left[\mu\zeta\dfrac{\partial}{\partial\zeta}\log J_0(2i\sqrt{(\zeta-1)\tau_1})\right]$

therefore

$$I=\frac{ekw}{\pi\sigma^2 b}\frac{\partial}{\partial t}\int_1^{e^{\mu l}}\frac{\partial}{\partial\zeta}\log J_0(2i\sqrt{(\zeta-1)\tau_1})d\zeta$$
$$=\frac{ekw}{\pi\sigma^2 b}\frac{\partial}{\partial t}\log J_0(2i\sqrt{(e^{\mu l}-1)\tau_1})$$
$$=ekw\frac{Q_0}{h\nu}(1-e^{-\mu l})\frac{d}{d\theta_1}\log J_0(2i\sqrt{\theta_1}) \qquad (2)$$

where

$$\theta_1=(1-e^{-\mu l})\pi\sigma^2 btQ_0/h\nu$$

or

$$I=ekw\frac{Q_0}{h\nu}(1-e^{-\mu l})\frac{J_0(2i\sqrt{\theta_1})}{i\sqrt{\theta_1}J_0(2i\sqrt{\theta_1})} \qquad (2.1)$$

$$\lim_{t=\infty} I=\lim_{\theta_1=\infty} I=0$$

This shows how recombination should make the current drop with time when the light is parallel and opposite to the electric field.

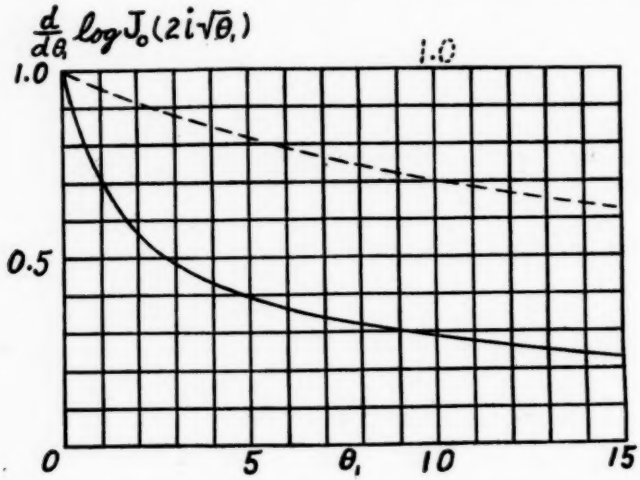

Fig. 7.

The quantity of electricity passing to the anode between the times $t=0$ and $t=t$ is

$$C=\int_0^t I\,dt=\int_0^t \frac{ekw}{\pi\sigma^2 b}\frac{\partial}{\partial t}\log J_0\left(2i\sqrt{(e^{\mu l}-1)\tau_1}\right)dt$$

$$=(ekw/\pi\sigma^2 b)\log J_0\left(2i\sqrt{(1-e^{-\mu l})\pi\sigma^2 b t Q_0/h\nu}\right)$$

$$=ekw(Q_0/h\nu)(1-e^{-\mu l})t(1/\theta_1)\log J_0\left(2i\sqrt{\theta_1}\right) \qquad (3)$$

For short observation periods (t small) the quantity c is thus seen to be proportional to t for $f(0)=1$. This is in agreement with the measurements. of Gudden and Pohl.[1]

If recombination is neglected, i. e. if $f(\theta_1)$ is made equal to one, $C=ekwQ_0t/h\nu$ which is a straight line when plotted aginst $1/\nu$. The factor $(1-e^{-\mu l})$ is left off to correct for the light that goes clear through and is lost. It is this C which Gudden and Pohl measured in their experiments on diamond, HgS, and ZnS.

The dotted curve in Fig. 8 gives the results of the experiments on ZnS in terms of C/Q_0. The dashed straight line is the C/Q_0 which would have been obtained had every $h\nu$ liberated one electron which also reached the anode. It was located by multiplying the ordinate at $405\mu\mu$ by 7/6.55. Neglecting recombination the experimental value, of h is here 7×10^{-27} instead of 6.55×10^{-27}. The difference is said to

be within the experimental error. The full curve is the C/Q_0 given by Eq. (3). It was calculated with the aid of the curves given by Gudden and Pohl[1] for μ in ZnS, taking $l = .6$mm and so choosing b as to make the two curves coincide at $\lambda = 400\mu\mu$. It represents then the "Ausbeute" to be expected if recombination were the only phenomenon tending to reduce the current, and provided the phenomenon other than recombination which causes the large drop at $350\mu\mu$ is inoperative at and beyond $400\mu\mu$. Judging from the shape of the dotted curve this is the case.

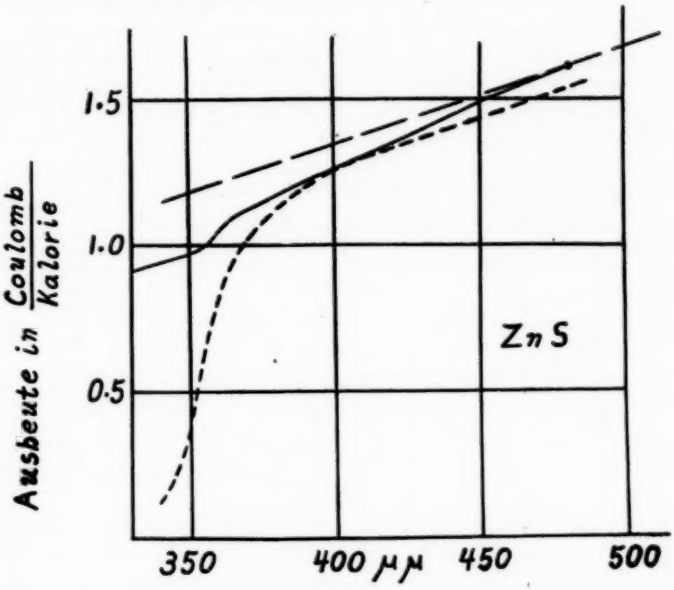

Fig. 8.

The peculiar drop is such as would be caused by a rapid increase in b between 400 and $340\mu\mu$, this does not seem at all likely. If it is caused by initial recombination or some other reason amounting to the same thing it is equivalent to a decrease in Q_0, and we must have $Q_0 = Q_0(\nu)$. This does not affect the validity of equations (2) and (3) because the integrations were only with respect to space and time.

The effect of the unknown process causing the peculiar drop in current when the light is most strongly absorbed is thus seen to be less than it would seem to be were recombination neglected. By determining b where the effect is inappreciable we see how big the effect is at the shorter wave-lengths.

NORMAN BRIDGE LABORATORY OF PHYSICS,
CALIFORNIA INSTITUTE OF TECHNOLOGY,
March 8, 1926.

See page 1331.

SMALL-SHOT EFFECT AND FLICKER EFFECT

By W. Schottky

Abstract

The Flicker Effect.—J. B. Johnson observed, under certain conditions (oxide coated and tungsten filaments, low frequencies, electron currents high but not high enough for space charge effects), voltage fluctuations across connected resonant circuits which were much larger than the theory of the small-shot effect would lead one to expect. Analyzing Johnson's curves, it is found that this effect increases as the square of the electron current i_0 instead of as the first power as in the case of the small-shot effect. This fact supports Johnson's hypothesis that the effect is independent of the small-shot effect and that it should be attributed to fluctuations in the properties of the surface (flickering) resulting in fluctuations in the electron current. The *trend with the natural frequency* of the connected circuit is likewise different from that observed in the small-shot effect. This can hardly be due to a statistical cause, and one must furthermore assume that there is a time element involved in the elementary process underlying the flicker effect. The *elementary atomic process* underlying the flicker effect is the appearance of an individual foreign atom or molecule in the surface of the cathode, changing the ability of the surface to emit electrons so long as the foreign atom remains. The *influence exerted upon the current by foreign atoms* in the surface may be calculated with sufficient approximation from the electrical image theory and Langmuir's doublet theory. The effect is proportional to the current density, and of such magnitude as to indicate that each foreign atom exerts its doublet effect uniformly over the surface. From the assumptions that the elementary atomic processes are independent of one another and that the length of stay of the foreign atoms in the surface conforms to statistical laws, the *frequency distribution* of the flicker effect is derived and compared with Johnson's experiments, whence it is possible to determine the length of stay of the foreign atom in the surface. The total number of foreign atoms in the surface of an oxide coated filament is computed from Johnson's measurements as being about 1/3 of all the atoms present in the surface; while the average length of stay is estimated from the curves to be about .001 second. The number of foreign atoms appearing per unit time on the surface is some 200 times as great as the number of atoms of residual gas striking the surface per unit time, from which it is inferred that the essential cause of the flicker effect with oxide cathodes lies in a continual exchange of positions by the components of the oxide. For tungsten filaments the mean length of stay is greater than 1/20 second; the number of foreign atoms appearing in the surface per unit time is some 20,000 times smaller than with oxide filaments, so that in this case it would be possible to ascribe the flicker effect to residual gas atoms striking the tungsten surface and remaining on it a longer or shorter time. The *variation of the flicker effect with the square of the total current* follows from the assumption that the current change due to one foreign atom is proportional to the total current. From this assumption also follows the relative independence upon *temperature*. A value is given for the *mean square voltage fluctuation* produced by the effect in terms of the impedance of the connected

circuit, and formulas are given for circuits of various kinds. Measurements with two circuits, one being resonant and the other a pure resistance should provide a definite check of the calculated length of stay of the foreign atoms.

INTRODUCTION

THE problem of the small-shot effect in thermionic tubes has, since the first discussion by the author[1] in 1918, made several important advances. The subsequent contributions[2] have had to do partly with correcting and simplifying the calculations and with an analysis of the fundamental basis of the problem, and partly with most gratifying additions to C. A. Hartmann's original experimental results,[3] made with improved methods of measurement and over a wider range of conditions. This later work[4] has led to the discovery of new effects and to and analysis of their significance. The authors of these papers have initiated private discussions of the problem by very kindly sending me their experimental results by letter or manuscript, and since their work has appeared in the PHYSICAL REVIEW I wish to present here the results of some new considerations initiated particularly by the research of J. B. Johnson.

The measurements in the radio frequency range, made by A. W. Hull and N. H. Williams with great skill and precision, show a surprisingly accurate agreement with the original theory (numerically corrected), so that the most probable value of the charge on the electron derived from the results comes within 1 percent of the accepted value, with a mean deviation of 2 percent. Under other conditions, however, in their work and in that of Johnson, certain new effects appeared which require us to revise and supplement the meagre hypotheses of the original theory. There was found, for instance, a remarkable and hitherto not entirely explained deviation from the calculated mean square fluctuation when measurements were made while the thermionic current was limited by space charge. Hull and Williams report that in the space charge region, at radio frequencies, the mean square fluctuation falls to 1/5 of the value calculated from the theory. A similar observation is made by Johnson at 1500 periods per second, where the

[1] W. Schottky, Ann. d. Phys. **57**, 541–567 (1918).
[2] J. B. Johnson, Ann. d. Phys. **67**, 154–156 (1922).
W. Schottky, Ann. d. Phys. **68**, 157–176 (1922);
R. Fürth, Phys. Zeits. **23**, 354–362 (1922);
T. C. Fry, J. Frankl. Inst. **199**, 203–220 (1925);
N. Campbell, Phil. Mag. **50**, 81–86 (1925).
[3] C. A. Hartmann, Ann. d. Phys. **65**, 51–81 (1921).
[4] A. W. Hull and N. H. Williams, Phys. Rev. **25**, 147–173 (1925);
J. B. Johnson, Phys. Rev. **26**, 71–85 (1925).

measurements give 1/3 the expected value. These estimates refer to tubes containing grids, the grid being held at a small negative potential. In the case of two-electrode tubes the suppression of the fluctuations is of quite a different magnitude. Johnson finds in one instance a reduction of the small-shot effect by a factor of fifty.[5] This remarkable behavior has not yet been satisfactorily accounted for, although the most direct hint has been given by Norman Campbell[2] when he suggests that in the space charge region "electrons tend to follow each other at regular intervals." In this connection a fact concerning macroscopic flow of electrons should be emphasized. It is well known that an increase or decrease in the cathode temperature, and therefore in the primary emission, causes but little variation in the space-charge-limited current. Perhaps the tendency to chaotic increase and decrease in number of electrons which causes the small-shot effect may be regarded as simply the equivalent of fluctuations in the emission, so that the space-charge-limited current reproduces these fluctuations in the same reduced measure as those caused by variation in the cathode temperature.

It is not the purpose of this article to deal further with this interesting question. Neither have I much to contribute to the neat experiments of Hull and Williams which seek to reveal the character of secondary emission through measurements on the small-shot effect.[6] I am rather concerned with the explanation of a third fundamental effect, discovered by J. B. Johnson in the region of low frequencies and large temperature-limited electron currents. This effect manifests itself as a hundred fold to a thousand fold increase in the value of the small-shot effect measurements when the circuit associated with the tube is of low natural frequency. Johnson has found this effect both with tungsten filaments and with oxide coated filaments. He has investigated its relation to the frequency and to the emission current, and has proved that for a given tube the effect[7] depends upon these two variables alone. He shows that the divergence of this effect from the small-shot effect is the greater the greater the specific emission from the filament and the lower the frequency. The independent character of this effect leads him to think that it is not caused by the atomic structure of electricity,

[5] This reduction is not the result of the lowering of resistance of the tube in the space charge region, a resistance which makes for high damping of the resonant circuit. This effect is taken into account in the computation. We may assume also that the authors considered sufficiently the variation of amplification with reference in the cases of high damping where contribution to the total effect are made from a considerable frequency range.

[6] See also N. Campbell, l.c.[2]

[7] Or rather on the ratio of the observed to the calculated effect.

but rather by fluctuations in the properties of the cathode surface, resulting in greater irregularities than those associated with the small-shot effect. If we had to do with emission of light instead of electrons, we would speak of a chaotic variation of light intensity taking place over the surface of the cathode, a phenomenon which we should describe by the word "flicker." If, as I shall endeavor to further confirm, Johnson's explanation of the phenomenon is the correct one, then we may use the analogy and call the new effect the "flicker effect."

Variation of Flicker Effect with Current

Let us attempt, with the aid of Johnson's results, to differentiate more clearly between the two effects. Fig. 1 reproduces the observa-

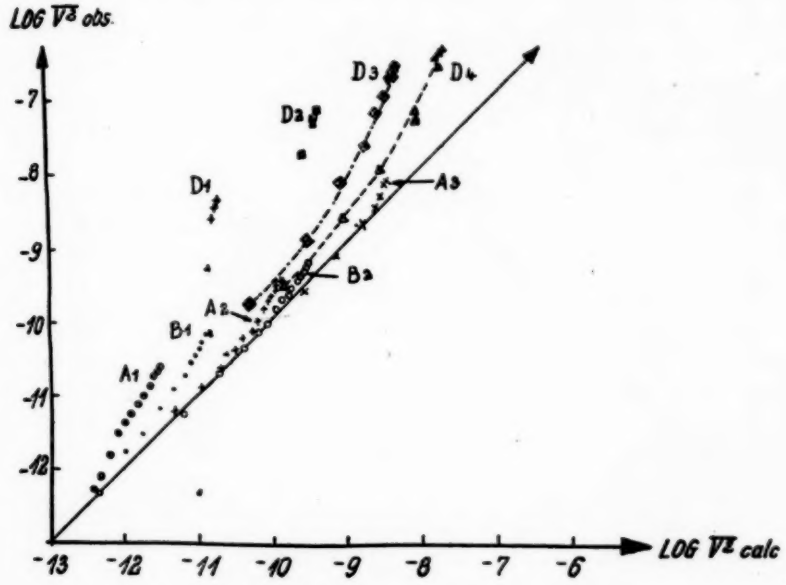

Fig. 1. Reproduction of observations by Johnson

tions collected by Johnson in his Fig. 10.[4] The letters $A-D$ signify different series of measurements with different inductances in the measuring circuit. The natural frequency of the circuit was lowest for the series D, and highest for A_3, the frequency range being from 160 to 33,000 radians per second. The current emission from the oxide coated filament ranged from .1 to 5 milli-amperes. The abcissa are the mean square voltage fluctuations at the terminals of the resonant circuit, as calculated from the current and the circuit constants by the formula for the small-shot effect; the ordinates are the corresponding observed values.

We see that the lower part of the curve has a tendency to follow the theoretical line $\log \overline{V^2}_{obs} = \log \overline{V^2}_{calc}$. We conclude, so far as the observations go, that at every frequency of the resonant circuit there is a region of sufficiently low current in which the small-shot effect contributes by far the most to the fluctuations. This result, even though further confirmation is desired, seems to me to indicate positively that the theory of the small-shot effect holds also in the range of low frequencies provided the rate of emission is low enough.

Let us examine the deviation from this simple relation which sets in at higher values of the emission current. As $\overline{V^2}_{calc}$ increases,

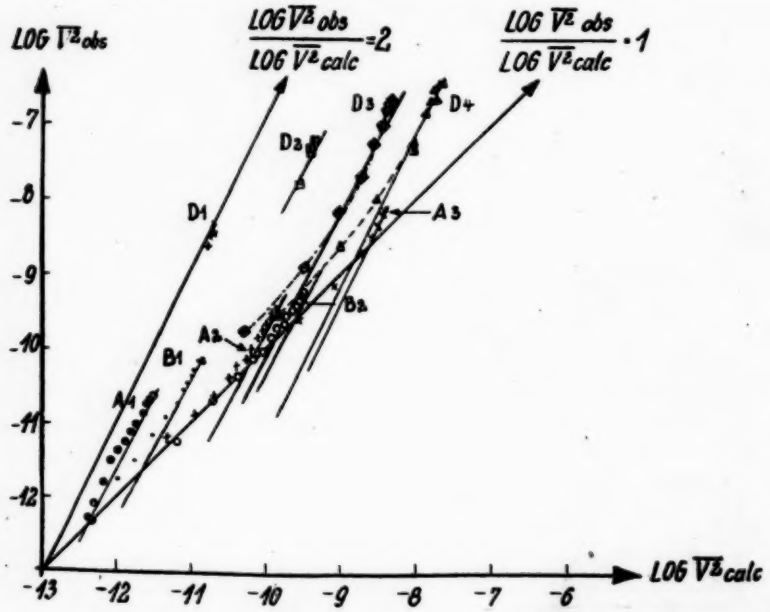

Fig. 2.

that is, as the current becomes larger, all of the observational curves depart upwards from the theoretical curve based on the theory for the small-shot effect. The nature of this departure I have tried to show somewhat roughly in Fig. 2. It seems not to conflict with Johnson's measurements to suppose that as i_0 increases the curves again approach the slope of straight lines with twice their initial slope. This means, however, since the scales are logarithmic, that at the higher values of $\overline{V^2}_{calc}$ the observed quantity $\overline{V^2}_{obs}$ becomes proportional to the square of $\overline{V^2}_{calc}$, and that therefore in this region where the small-shot effect contributes little the *observed mean square voltage fluctuations become proportional to the square of the emission current.*

If this law is found to hold, it will give strong support to Johnson's belief that we here have a new effect which is independent of the small-shot effect. It may readily be supposed that the curves of Fig. 1 result from the superposition of two effects, one proportional to the first power and the other to the square of the space current. If this is so, the magnitude of the flicker effect may be obtained either by subtracting $\overline{V^2}_{calc}$ from the observed curves, or by working in the region where the contribution of the small-shot effect to the fluctuations is negligible and where the proportionality with i_0^2 holds.

Interpretation of the Flicker Effect: Frequency Variation

Is the proportionality of the flicker effect to i_0^2 to be expected if the origin of the effect is what Johnson assumes? If, in accordance with this conception, the fluctuations are caused by spontaneous changes in the cathode surface which alter the emission, then clearly the proportionality with i_0^2 must hold. We have only to suppose that as i_0

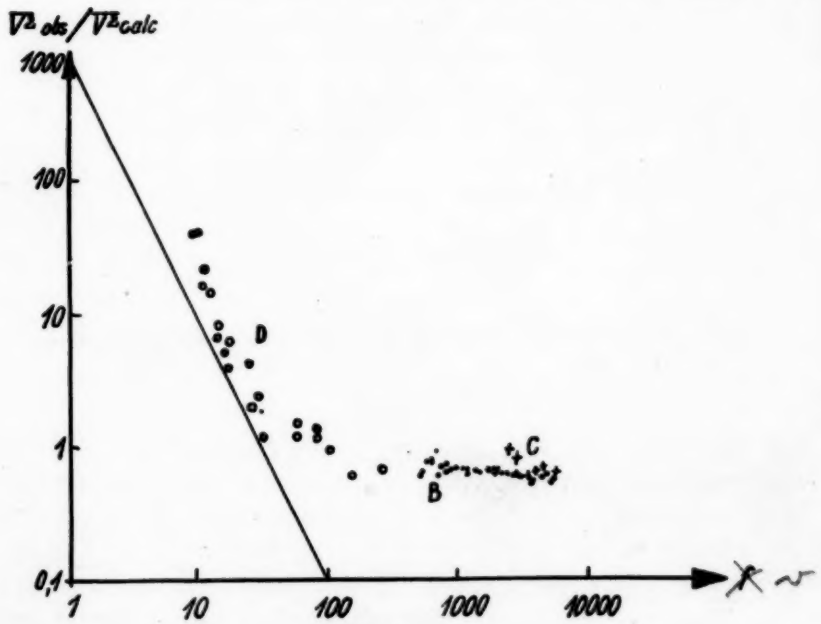

Fig. 3.

varies, the character of the surface fluctuations does not change; and that the absolute value of the corresponding fluctuations in the emission current remains proportional to i_0, or, in other words, that alteration in the surface condition is always accompanied by the same relative

change in emission. The second assumption agrees completely with all that we know about variation of electron emission. It is substantially correct for all the possible sources of variation named by Johnson, such as evaporation, diffusion, chemical action, structural changes, bombardment by gas ions, etc. Less certain is the first assumption, that regarding the invariant character of the surface changes as i_0 varies. I shall return to this point later in the discussion of the theory.

It was the dependence of the observed effect upon frequency which suggested to Johnson more definite conclusions regarding the origin of the spontaneous perturbation in the emission from the surface. This frequency variation is shown, to the same logarithmic scale as

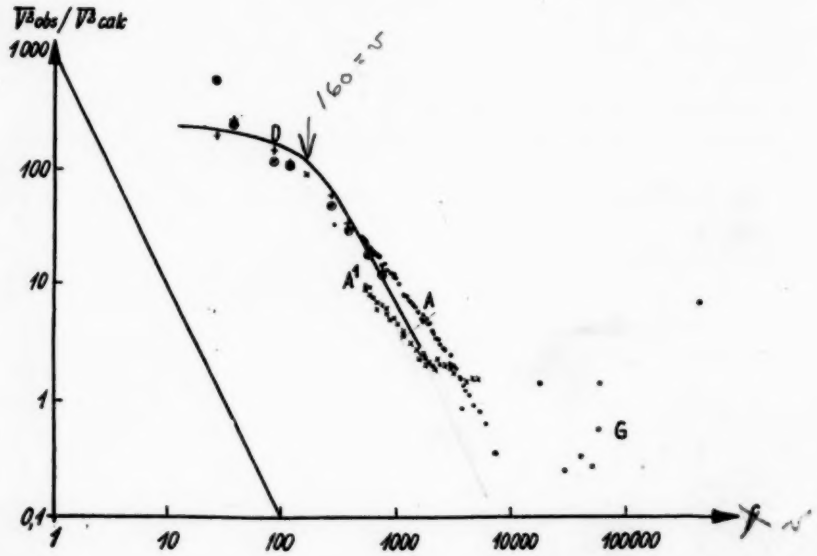

Fig. 4.

before, in Figs. 3 and 4, taken from Johnson's paper. Fig. 3 corresponds to a tungsten filament, Fig. 4 to an oxide coated one, and all observations were made at an emission of 5 milli-amperes. (The meaning of the solid line drawn in Fig. 4 will be explained later). It is to be observed that in the region where the flicker effect predominates, where $\overline{V^2}_{obs}/\overline{V^2}_{calc} >> 1$, the curves rise rapidly with decreasing frequency. The rate of rise seems to be given approximately by the straight lines in the figures, drawn with the slope $-1/\nu^2$ where ν is the frequency. This rapid rise of the flicker effect with decreasing frequency and increasing period of the circuit, as well as the high absolute value of the observed fluctuation, leads Johnson to suppose that we are dealing

with a phenomenon which is not a result of the emission of individual electrons, but which is rather of a more intensive and extensive nature, affecting at once the emission of a great number of electrons.[8] Whence, however, the rapid rise of the effect with the period of the circuit? Johnson sees the reason simply in the fact that fluctuations having greater intensity or area also demand a longer duration than feeble or less extensive ones. Illuminating as this argument is, it requires a little closer scrutiny. We may ask, for instance, why this argument cannot similarly be used for the small-shot effect, in which also there is greater opportunity for large deviations from the average during long time intervals than in a very short time. Apparently some explanation other than the above must be found for the frequency variation of the flicker effect. Indeed, there is a difference between the two phenomena deducible directly from Johnson's interpretation. In the small-shot effect the number of transferred individual charges obeys the laws of probability. In the flicker effect, on the other hand, the primary variations assumed by Johnson depend not upon the number of charges but upon *the condition of a small surface region during the time in which it emits a certain increased or decreased current.* The number of charges transferred in consequence of this condition depends furthermore upon the duration of the condition. In general, any characteristic of the phenomenon having the dimension of time, and being therefore in some way relatable to the natural period of the resonant circuit, will give rise to a frequency variation, in contrast with the small-shot effect which involves no such time constant.

This general inquiry could perhaps be pursued even a little further. If the above characteristic time is large compared to the period of the

[8] This hypothesis, by which I attempted to explain Hartmann's results, I had abandoned even before the appearance of Johnson's article. Numerical calculations based on the heat conduction constant for tungsten convinced me that any such cooling is much too evanescent to influence the electron emission. In a letter to Dr. Hull on this subject in May, 1925, I also took exception to the statements made by Hull and Williams regarding the apparent capacity effect associated with the electron current, discovered by Mr. Hartmann. We concluded that the effect was caused by a lag in the establishment of temperature equilibrium as the space current was altered. Hull and Williams cite their own results in refutation of the existence of such an effect, the capacity C_i being supposed by them to represent constant capacity shunted across the terminals. This supposition, suggested no doubt by Hartmann's notation, is not in agreement with our explanation. The thermal lag theory demands that the effect should vanish at high frequencies in agreement with Hull's observations. Dr. Johnson, also, has sent me some results of measurements upon the tubes he used (oxide coated filaments). These tend to show a capacity effect at low frequencies decreasing toward higher frequencies. They also show remarkable hysteresis phenomena. These effects, easily to be derived from the data of emission and heat conduction, may be worthy of further experiments.

circuit then the disposition of the surface to emit a positive or negative current increment is very ineffectually transmitted to the resonant circuit, since only the more or less abrupt beginning or end of the current increment contributes much to the induction of oscillating current in the circuit. The action has an analogy in the interruption of an alternating current at time intervals that are great compared with the period of the circuit, the residual direct current being very small. The effective part of the current increments may easily be shown to be proportional to the period τ of the resonant circuit when τ is small compared with the duration of the current increment. Consequently, the mean square voltage amplitude at the terminals of the circuit will show a variation with τ^2, in contrast with such phenomena as the small-shot effect which do not have their origin in a characteristic time constant that is large compared with the period of the circuit. This seems to furnish a plausible explanation for the frequency variation observed by Johnson.

The same arguments lead to yet another conclusion which is not so directly evident from the data in Figs. 3 and 4. When the period τ approaches and eventually exceeds the assumed characteristic time constant, the cause of the increase of the observed effect with rising period τ gradually disappears, and the variations in the state of the surface result merely in increments to the electron current. This condition seems to be quite analogous to that producing the small-shot effect, except that the quantity of charge emitted as the result of a single surface fluctuation may be considerably greater than that of one electron. We may therefore at sufficiently low frequencies expect the frequency curve again to bend over and approach a horizontal course toward zero frequency. Perhaps it is bold to surmise evidence for such an inflection toward the horizontal in the series of points *D* of Fig. 4. If further experiments should confirm this surmise, such curves would give directly a measure of the charge associated with the individual fluctuations. From Fig. 4 we should expect that groups of 100 to 1000 electrons are involved, corresponding to the 100 to 1000 fold increase in the observed effect over the small-shot effect. Furthermore, if the shape of the solid curve should turn out to be correct, then the value of the period τ at which the curve bends toward the horizontal would give directly the value of the assumed time constant. Judging from Fig. 4 one estimates this time constant to be $1/2\pi \times 1/100$ sec.[9]

[9] We evidently must consider not the whole period but only such a fraction as $\tau/2\pi$ over which the phase is roughly constant.

Fundamentals of the Flicker Effect

After what has already been said about the small-shot effect it is hardly possible to suppose that the time constant which is characteristic of this effect can have any connection with the spatial or secular *statistics* of the process; in other words, it can not be something which concerns simultaneously a large number of independent invididual events. Seemingly, we must search for a *time constant which is defined by a single event or process, independent of other elementary fluctuation events*. If this is so, what type of elementary independent events might compose the surface perturbation which manifests itself as flicker effect?

Almost all the phenomena named by Johnson involve the appearance of foreign atoms on the surface.[10] The far-reaching effects of foreign atoms in the surface of an electron emitter have been worked out quantitatively, particularly by Langmuir. We know that in certain circumstances it is possible for a single layer of atoms to raise or lower the emission a thousand fold. It seems plausible to suppose, therefore, that the origin of the flicker effect discovered by Johnson lies in *fluctuations in the surface layer of foreign atoms*. These atoms reach the surface by diffusion from within, or by deposit from the remanent gas of the tube. With compound materials such as barium oxide the surface may be changed also by partial evaporation of one component or by spontaneous rearrangements of both.[11] These processes probably consist of the advent or departure at the surface of a single atom or a small group of atoms in the molecular condition. The presence of a few foreign atoms thus furnishes a certainly permissible and for a first calculation sufficient basis, in the assumption that the *coming or going of separate foreign atoms or molecules may be regarded as elementary* events which are independent of one another.

We have thus, as in the case of the small-shot effect, arrived at the *atomic nature of matter* as the ultimate cause of the observed fluctuation. It is a short step to give a definite interpretation to the time constant characteristic of the elementary processes. Presumably we have to do with the duration τ' of the existence of an individual atom or molecule in the surface, for the change in emissivity caused by a single

[10] The direct contribution to the current from ion bombardment and from secondary electrons is clearly of little moment, and the same is true of the temperature effect. It is therefore only the capture of gas ions on the surface that matters. The effect of recrystallation I think is negligible.

[11] On the other hand, the evaporation of an atom from a pure substance, such as a tungsten atom from a tungsten filament, can have little influence on the emissivity at that particular place.

foreign particle would probably be co-extensive with the presence of the particle in the surface. The particle would give rise to a steady change γ in the average current, and this process is identical with the one with which we attempted to explain the variation of the flicker effect with the frequency.

For the determination of γ we shall temporarily assume only the general relation

$$\gamma = F i_0 ,$$

where i_0 is the space current and F is a very small numerical factor, of the order of magnitude 10^{-16}. The determination of F with the aid of Langmuir's extension to the electrical image theory will be considered after the discussion of the fluctuation processes. Suffice it to say that F is the same for all foreign atoms of the same type, and is therefore constant for definite values of τ' and i_0.

If different types of foreign atoms are present in the surface, then the typical elementary currents and factors must be considered separately:

$$\gamma_1 = F_1 i_0 , \quad \gamma_2 = F_2 i_0 , \text{ etc} .$$

This generalization will be omitted, however, and the presence of only one type of foreign atoms will be postulated.

Mathematical Treatment of the Fluctuation

The procedure proposed in the following is closely related to that originally used in calculating the small-shot effect. We make a Fourier analysis or spectral resolution of the current fluctuations and we ascertain the action upon a connected current circuit by summing the actions of their various harmonic components upon it. This procedure, though it is perhaps not mathematically the simplest and perhaps will later be replaced by a more elegant one (as in the case of the small-shot effect), has the advantage of greater generality and in addition makes it possible to carry out an entirely separate investigation of the fluctuation process itself and of its action upon the circuits. For the engineer this method is convenient in that the only properties of a connected circuit which enter into the calculation are its directly measurable impedance values (within certain frequency ranges). Finally as regards T. C. Fry's objection[2] that unordered processes of this type admit of no Fourier resolution and possess no definite spectrum, I may say that we are not concerned with the individual Fourier coefficients but with their root mean square values within small frequency ranges; and these mean values have a definite physical meaning

as I emphasized in speaking of the small-shot effect[1] and as we shall see similarly in dealing with the flicker effect.[12]

Fig. 5 represents the electrical connections of the experimental tube and circuit, all batteries being omitted. Let R represent the impedance of the tube and Z' the impedance of the connected circuit (both of these impedances will in general be complex) and represent

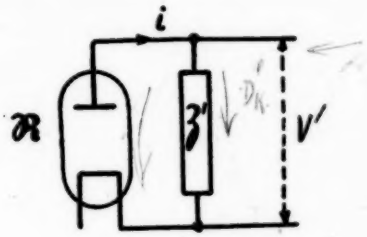

Fig. 5.

by D_k the amplitude of the current flowing in Z'; and by V' the voltage amplitude across the ends of Z' (which in general has a phase displacement relative to D_k). Then we have

$$V' = D_k Z'. \tag{2}$$

Now we introduce the primary current in the tube of amplitude A_k, whose phase is generally shifted with respect to D_k. This is by definition the current which would flow in the tube under the action of any forces producing alternating current if the tube were short-circuited so that there were no reactions upon the current flowing through it. This amplitude we can take as real, referring all phases to that of the primary current. We then evidently have

$$A_k = D_k + V'/R\ ; \tag{3}$$

from (2) and (3), we have

$$\begin{aligned} A_k &= V'(1/R+1/Z') \\ V'^2 &= A_k^2 \frac{1}{(1/R+1/Z')^2} \quad \text{or} \\ V'^2 &= A_k^2 Z^2, \end{aligned} \tag{4}$$

in which Z represents the combination resistance of the circuit composed of the tube plus the connected circuit, each measured from the two electrodes of the tube. This procedure eliminates the problem

[12] Certain changes in the previously published argument indicated by the substitution of the symbols a and c instead of A_k and C_k are due to detailed explanations and criticisms in letters from Dr. Fry, for which I am deeply grateful.

as to whether the tube capacity should be considered as belonging to the tube or to the external circuit.

The mean value over time of the square of the voltage is $\frac{1}{2}V'^2 = \frac{1}{2}A_k^2 \times Z^2$, in which the symbols V' and Z now signify the *absolute values* of the quantities previously designated. Suppose now that there is a very great or infinite number of partial current amplitudes A_k and B_k which correspond to various independent frequencies as in a Fourier analysis: then at the ends of the tube there will be a resultant fluctuation of voltage of which the root mean square value is obtained by simple addition of the root mean square values of the components. Representing by V the momentary value of the voltage fluctuation at the terminals of the tube (apart from constant voltage differences) we have

$$\overline{V^2} = \frac{1}{2}\sum_1^\infty A_k^2 Z^2 + \frac{1}{2}\sum_1^\infty B_k^2 Z^2. \tag{5}$$

In this equation A_k, B_k and Z are in general functions of frequency which must be known in order to determine $\overline{V^2}$. We suppose this function already known for Z by calculation or measurement. A_k and B_k remain to be determined.

It follows at once that if the readings of the measuring apparatus are not proportional to V'^2 for every frequency, we have to deal with a quantity

$$\overline{V_e^2} = \frac{1}{2}\sum \beta^2 (A_k^2 + B_k^2) Z^2 \tag{6}$$

in which β stands for the coefficient by which V' must be multiplied to give the observed reading and may depend on the electrical connections and on the properties of the measuring instrument and must be known as a function of frequency.[13]

Spectrum of the Flicker Effect

For calculating the equations (5) and (6) we select a frequency interval so small that Z and β can be regarded constant for this range. This interval, however, must not be regarded as infinitely small but as containing many Fourier components, which is possible because we take the fundamental period T of the Fourier analysis as very large

[13] This fact, which I have called attention to before (Ann. d. Physik 68, 169 (1922)), was used by Hull and Williams in reducing their measurements. This reference contains also the generalization of the small-shot effect formula which was later introduced by Fry and used by Johnson.

and continue to employ the representation by sums merely for the sake of simplicity. Now we identify the partial amplitudes A_k and B_k with those designated by the same symbols in the Fourier series

$$j = \sum_{k=1}^{\infty} A_k \cos \omega_k t + \sum_{k=1}^{\infty} B_k \sin \omega_k t$$

in which j stands for the primary fluctuation current of the flicker effect, that is to say, the primary current minus its constant component. Then the quantity $\sum_{\omega}^{\omega+\Delta\omega} (A_k^2 + B_k^2)$ is the sum to be taken for any number of terms and can be written $(\overline{A_k^2} + \overline{B_k^2})\Delta k$, in which the overlined symbols are the mean values of A_k^2 and B_k^2. Consequently we are concerned, as we should be, only with the mean square values of the amplitudes of enormously many components. Considering the unordered character of the process, we naturally have $A_k^2 = B_k^2$ and therefore we may now write Eq. (5) or (6):

$$\overline{V^2} = \sum_{k=1}^{\infty} \overline{A_k^2}\, Z^2\, \Delta k \tag{7}$$

in which

$$\overline{A_k^2} = \frac{4}{T^2} \int_0^T (j \cos \omega_k t dt)^2 ,$$

T being the duration of the chosen Fourier period. In calculating the small-shot effect it was shown that the mean square value of the above integral in that case has the value

$$\tfrac{1}{2} T e i_0$$

so that

$$\overline{A_k^2} = \frac{2}{T} e i_0 \text{ and } \overline{A_k^2}\ \Delta k = T \cdot \Delta v \cdot \frac{2}{T} e i_0 = 2 e i_0 \Delta v$$

Hence, in going over to Fourier integrals it is permissible to represent the spectrum by an expression $a^2 dv$, wherein $a^2 = 2ei_1$ represents the sum of the mean square values of the current amplitudes belonging to the cosine vibrations per unit of frequency change, and an equally large value is obtained for the sine vibrations.

Consequently $c^2 (= 4ei_0)$ is in the case of the small-shot effect the square of the average effective amplitude of the small-shot current per unit of frequency. This quantity (which corresponds to the coefficient introduced by Planck into the radiation formula) is independent of frequency, that is to say, the spectrum of the small-shot effect shows, for all periods which are not smaller than the time of transit of an elec-

tron, a perfectly uniform distribution over all frequencies affected.[14] We now have the task of determining the corresponding spectrum distribution $\overline{A_k^2}$, a^2 or c^2 for the flicker effect and we know already from the *measurements* that this distribution cannot be independent of frequency.

First of all we calculate the value of A_k^2 for a single value of k,

$$A_k^2 = \frac{4}{T^2}\left(\int_0^T j \cos \omega_k t dt\right)^2 .$$

In calculating the squared integral, which can be written

$$\int_0^T \int_0^T j\, dt\, j'\, dt' \cos \omega_k t \cos \omega_k t' ,$$

we first select a time element dt corresponding to a time t_1'. The contribution of this time element is

$$\cos \omega_k t_1\, dt \int_0^T j(t_1) \cdot j(t') \cos \omega_k t'\, dt' .$$

In accordance with the previous discussion, j may be expressed by

$$j = n\gamma = (N - N_0)\gamma .^{15} \qquad (9)$$

In this equation N represents the number of foreign atoms or molecules on the surface of the cathode at the time in question; N_0 represents the time average of N, and n represents the momentary deviation from the time average. Eq. (9) will according to our assumptions always be valid when the fluctuations in number of foreign molecules on a spot of the surface are on the average so small that the partial value of the emission current flowing out of this spot fluctuates relatively little. Later we shall be able to prove this more convincingly.

[14] This result seems to contradict the solution given in my first paper, according to which the mean square of the fluctuation current flowing during period τ should depend upon τ according to $\overline{j_\tau^2} = ei_0/\tau$. However, c^2 is a quantity measured per unit change of frequency. If we form the equation

$$c^2 \Delta\nu = (c^2/\tau)(\Delta\tau/\tau)$$

we recognize that $\overline{j_\tau^2}$ is proportional to the integral for the squares of the amplitudes for a constant fraction $\Delta\tau/\tau$ of the period in question. Closer agreement cannot be demanded under the circumstances.

[15] The assumption contained in this substitution, that the current due to a foreign atom during the sojourn of the atom in the surface is constant in time, naturally does not include the small-shot effect. However, it will be possible to calculate the two effects independently.

Using Eq. (9), the integral which must be computed assumes the form

$$\gamma^2 \int_0^T n(t_1)n(t') \cos \omega_s t' \, dt' \, . \tag{10}$$

In the second integration the variable t runs through all values from 0 to t for a given time t_1. Since however, many cases will occur in which n is numerically equal to $n(t_1)$ we need not calculate any individual value but only the mean value of the integrand for a given difference between the times t_1 and t'. First therefore, we are concerned with the mean value $\overline{n_1 n'}$ for a given value of the quantity $t'-t_1$. If this quantity is 0 we have $n'=n_1$. As the difference between t_1 and t' becomes greater however, the less becomes the coherence of n_2 and n' and for somewhat larger values of time n' can quite as well have the same as the opposite sign to n_1; consequently, we need take account only of residual effects.

Now in order to make an exact calculation of the quantity $\overline{n_1 n'}$ for any arbitrary value of $t'-t_1$, at many repetitions of the "instants t_1" (so we shall designate the times at which $n=n(t_1)$) we must introduce the probable time of sojourn of the foreign molecules in the surface. If we represent by $1/\alpha=\tau'$ the average time of sojourn of the molecules in the surface, it follows from the definition that out of N_1 molecules present at a given time, the number present at a time Δt later will be $N_1 e^{-\alpha \Delta t}$. The molecules which are not present at both the beginning and the end of the interval have no particular relation to one another. They can influence the numbers n_1 and n' either in the same sense or in opposite senses. Consequently, so far as I can see, we need only consider the foreign molecules which are present at both the beginning and the end of the interval, when computing $\overline{n_1 n'}$. We obtain

$$n_1 n' = (N_1 - N_0)\,(N' - N_1) \, .$$

If we take the average over many "instants t_1," holding n_1 and Δt constant we have

$$\overline{n_1 n'} = (N_1 - N_0)\,(N' - N_0) = (N_1 - N_0)\,(N_1 \epsilon^{-\alpha \Delta t} - N_0) \, .$$

Introducing the relation $N_1 = N_0 + n_1$ we get

$$\overline{n_1 n'} = n_1^2 \epsilon^{-\alpha \Delta t} + (1 - \epsilon^{-\alpha \Delta t}) n_1 N_0 , \tag{11}$$

since $\bar{n}$ is equal to 0 by definition. Inserting this result into Eq. (10) and making the substitution

$$\cos \omega_k t' = \cos \omega_k t_1 \cos \omega_k \Delta t \pm \sin \omega_k t_1 \sin \omega_k \Delta t$$

the integral takes the form

$$\gamma^2 n_1^2 \cos \omega_k t_1 \int_0^T \cos \omega_k \Delta t \, \epsilon^{-\alpha \Delta t} dt' \pm \gamma^2 n_1^2 \sin^2 \omega_k t_1 \int_0^T \sin \omega_k \Delta t \epsilon^{-\alpha \Delta t} dt' \tag{12}$$

plus an expression dependent on $n_1 N_0$ which will later be seen to vanish. In the two integrations of Eq. (12), we may extend the integration from $-\infty$ to $+\infty$ for any value of t_1 without perceptible error, since the integrand of t_1 soon becomes immeasurably small in both directions and since the "instants t_1" which lie near the times 0 and T play no part if T is made sufficiently great. Integrating both integrals from $-\infty$ to t_1 and setting $dt' = d(\Delta t)$, we get for the first integral

$$-\int_{-\infty}^{\Delta t = 0} \cos \omega_k \Delta t \, \epsilon^{-\alpha \Delta t} d(\Delta t) = \frac{\alpha}{\alpha^2 + \omega_k^2}.$$

Carrying the integration on to $+\infty$ we double this value. The value of the sine integral is the sum of pairs of equal and opposite terms, and vanishes. Consequently the expression (12) becomes simply equal to

$$\gamma^2 n_1^2 \cos \omega_k t_1 \frac{\alpha}{\alpha^2 + \omega_k^2}.$$

If we make $t_1 = t$ and integrate over t (Eq. (8)) we obtain:

$$-\int_0^T \cos^2 \omega_k t \, n^2 \frac{\gamma^2 \alpha}{\alpha^2 + \omega_k^2} dt = \overline{n^2} \frac{\gamma^2 \alpha}{\alpha^2 + \omega_k^2} \cdot T/2 \tag{13}$$

since a mean value of each $\overline{n^2}$ for a given value of the cosine can be set equal to the general mean value, and the integral of the square of the cosine gives a value $T/2$.

Since the term in Eq. (11) which is proportional to $n_1 N_0$ contributes nothing to the integral (8) in the corresponding calculation, it follows that in the averaging corresponding to Eq. (13), the mean value of $\bar{n}$ occurs, and this by definition is zero. However, we cannot make this assertion for any *particular term* A_k^2 of the Fourier resolution any more than we could for the small-shot effect (*loc. cit.* [1], p. 559), as it might perfectly well happen that the quantities n have incidental coherence with the cosine function. It is probable, therefore, that a Fourier reso-

lution for the individual coefficients does not lead to definite results but since we are concerned only with the mean values of A_k^2 over very many or infinitely many values of k, I regard the above calculation which gives the summary and definite result as justified. I hope that from the preceding it will be possible some time to deduce the results which follow in a much simpler manner.

Substituting (13) in the equation for A_k^2 and keeping in mind that this symbol stands for a mean value derived from many values of k, we have

$$\overline{A_k^2}=\frac{2}{T}\,\overline{n^2}\,\frac{\gamma^2\alpha}{\alpha^2+\omega_k^2}\,. \tag{14}$$

If we form the equation

$$A_k^2\Delta k=A_k^2T\Delta\nu\,,$$

we obtain from (14)

$$A_k^2\Delta k=2\overline{n^2}\gamma^2\frac{\alpha}{\alpha^2+\omega_k^2}$$

in which the symbol ω_k stands for a mean value of the different values of k falling within the interval $\Delta\nu$. Passing to the limiting case of the interval by putting $T=\infty$, and writing $d\nu$ for $\Delta\nu$ and $\omega=2\pi\nu$ for ω_k, then we obtain the spectrum distribution of the flicker effect in the form

$$a^2d\nu=2\overline{n^2}\gamma^2\frac{\alpha}{\alpha^2+\omega^2}d\nu\,.$$

Up to the present we have considered only the cosine function of the Fourier analysis. The sine functions naturally give the same amount so that we finally obtain the total value per unit of frequency change of the average Fourier coefficient:

$$c^2=4\overline{n^2}\gamma^2\frac{\alpha}{\alpha^2+\omega^2}\,. \tag{15}$$

Discussion

Trend with frequency. In order to remain in contact with the experiments, we must first say something about the ratio of c^2 to the magnitudes observed by Johnson. Johnson referred all measurements to the formula for the small-shot effect after he had established that the constants of the resonant circuit enter into the present effect in the same

manner as into that; he plotted the quantity $\overline{V^2}_{obs}/\overline{V^2}_{calc}$ which according to the theory is given by

$$\overline{V^2_{obs}}/\overline{V^2_{calc}}=(\overline{V_F^2}+\overline{V_S^2})/\overline{V_F^2}=\overline{V_F^2}/V_S^2+1 \tag{16}$$

and in which V_F stands for the contribution made by the flicker effect V_S for that of the small-shot effect.

Now in the following section we shall see that in sufficiently selective circuits such as were used in the principal experiments of Johnson, the following equality holds:

$$\overline{V_F^2}/\overline{V_S^2}=\overline{c_F^2}/\overline{c_S^2}$$

in which c_F and c_S stand for the amplitudes of the natural frequencies of the resonant circuit in the two cases. On account of (16) we may write

$$c_F^2/c_S^2=\overline{V^2_{obs}}/\overline{V^2_{calc}}-1 \tag{16a}$$

and since we know the quantity $c_S^2=4ei_0$, the curves obtained by Johnson give the absolute value of c_F almost directly. Dropping the subscript F, we have

$$c^2=4ei_0\left(\overline{V^2_{obs}}/\overline{V^2_{calc}}-1\right) \tag{17}$$

in which the second term on the right hand side may be omitted when $\overline{V^2}_{obs}$ is large compared to $\overline{V^2}_{calc}$.

Let us now turn back to the theoretical statements about c^2 and discuss the trend with frequency to be expected according to the theory. In Eq. (15), $\overline{n^2}$ is independent of the frequency and so also are γ and α. We find thus that, in contrast to the small-shot effect in which the corresponding expression c^2 had the value $4ei_0$, *the spectrum of the flicker effect depends on the frequency*; obviously, so long as the frequency ω is large as compared to the previously defined quantity $\alpha=1/\tau'$, the quantity c^2 is proportional to $1/\omega^2$. If, however, the frequency is equal to or less than $1/\tau'$ the trend with frequency is no longer of this type; and near zero frequency the expression becomes independent of frequency:

$$c^2_{\omega=0}=4\overline{n^2}\gamma/\alpha$$

Consequently, we have

$$\frac{c^2}{c^2_{\omega=0}}=\frac{1}{1+\omega^2/\alpha^2} \tag{18}$$

and we see directly that it is possible to determine the quantity α by measurements of c^2 at two or more values of frequency, for instance

by a measurement near zero frequency and at a frequency $\omega > \alpha$. The relation is

$$\alpha^2 = \omega^2 \frac{c^2}{(c^2_{\omega=0} - c^2)}$$

The relative trend with frequency as given by (16) is shown in Figs. 6a and 6b, once in linear and once in double logarithmic coordinates.

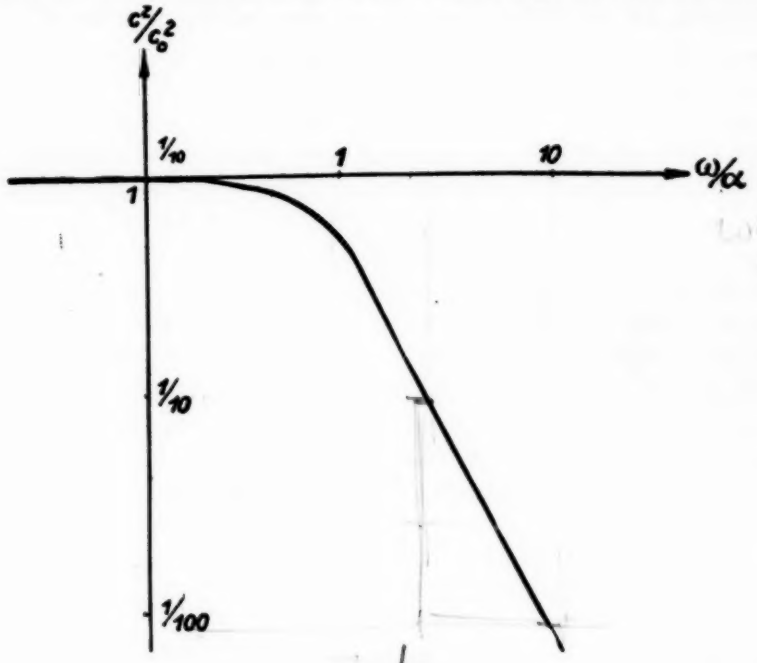

Fig. 6a

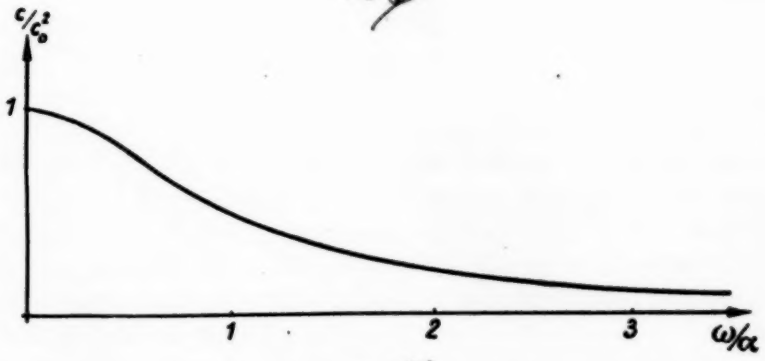

Fig. 6b

Let us compare this theoretical curve 6b with the observations by Johnson, plotted on the same scale. In Fig. 3 one observes only an

increase of the quantity $\overline{V^2}_{obs}/\overline{V^2}_{calc}$ at low frequencies which seems to be even more rapid the lower the frequency. The more extensive measurements shown in Fig. 4 made upon oxide coated filaments, give indications that we have both a trend roughly proportional to $1/\omega^2$ and at very low frequencies also a bending similar to that in Fig. 6b. Since in the experiments i_0 was kept constant and the second term on the right hand side of Eq. (17) is negligible almost throughout, the curves for $\overline{V^2}_{obs}/\overline{V^2}_{calc}$ plotted logarithmically as functions of frequency have the same shape as the curve for $c^2/c^2{}_{\omega=0}$ in Fig. 6. I have tried to draw this curve into Fig. 4 as closely as possible to the points. The agreement is clearly not very good and yet it is good enough to encourage more exact measurements as a test. If one should take the continuous curve as a sufficiently exact plot of the observations, the frequency $\omega=\alpha$ would lie somewhere near the place indicated by the arrow in Fig. 4, at the frequency of about 160. We should then infer that $\alpha=2\pi\cdot 160=1000$ and that the average time of sojourn of the foreign atoms in the surface of the oxide coated filament used by Johnson is about $\tau=.001$ sec. We do not need to emphasize that this instance is given only as an example of the kind of conclusions to be drawn without claiming the reality of the processes discussed before repetition and extensions of the measurements have been carried out.

The dependence on current. Since it has been assumed that the various foreign atoms in the surface are independent of one another, we have, according to the well-known law of fluctuations

$$\overline{n^2}=N_0\,. \tag{19}$$

For γ we substitute the value Fi_0 from Eq. (1). According to Eq. (15) we then obtain

$$c^2=4N_0F^2\frac{\alpha}{\alpha^2+\omega^2}i_0^2\,. \tag{20}$$

Because of the relation between c^2 and V^2 of Eq. (16) (omitting the -1), this relation gives the quadric law of variation with current displayed by the flicker effect and recorded graphically in Fig. 2. It is being assumed that N_0, F and α may be regarded as sufficiently independent of temperature. Although i_0 depends on it, the variation of i_0 with temperature is so rapid that it would be permissible to regard these quantities as sufficiently independent of temperature even though they varied as the first or second power of T or its reciprocal. We may regard this assumption as permissible for the time interval represented by $1/\alpha$ and, according to a theory yet to be given, for the factor F.

It is, however, questionable whether the number of foreign atoms per unit area above designated by N_0 does not vary as rapidly with temperature as does i_0. Here we may introduce instead of N_0 the symbol $Q_0 = N_0/\tau' = N_0\alpha$, representing the number of foreign molecules arriving per second in the surface. If this quantity is determined primarily by appearance of atoms coming from the gas, its variation with temperature will be small. With certain diffusion processes from the interior of the wire, on the other hand, we may expect rapid changes with temperature for N_0 and hence variations from the i_0^2 law. So long as variation of this sort has not been observed, it seems permissible to suppose that the flicker effect is not to be attributed to processes varying for example with the temperature proportionally to $e^{-B/T}$, where B is some quantity larger than the constant b of thermionic emission. For instance, if the i_0^2 law should be found valid for tungsten, (unfortunately we have no measurements with current variation in the region of the flicker effect) it would be possible to exclude from among Johnson's suppositions, the conceptions of diffusing thorium atoms into the surface, the normal evaporation of these atoms and the reduction of thoria, since these three effects, according to Langmuir's[16] beautiful investigations, vary in the aforesaid manner, with the value of B larger than the thermionic constant.

Finally it is to be noted that upon introducing Q_0, Eq. (20) takes the form

$$c^2 = 4Q_0F^2\frac{1}{\alpha^2+\omega^2}i_0^2 \,. \tag{21}$$

Accordingly, in the frequency region where $\omega >> \alpha$ and where $1/\omega^2$ gives the frequency variation, the magnitude of c^2 for any particular frequency and current is influenced only by the factor F and the rate at which new foreign particles appear in the surface. One can even conclude that this will happen when there are two or more kinds of foreign molecules; the effect will then be determined by the several values of Q, each obtained by a corresponding factor F.

Influence of the effect on a connected circuit. Substituting in Eq. (7) the expression $\overline{A_k^2}\Delta k$ by $\frac{1}{2}c^2 d\nu$ and integrating over the complete frequency range, we obtain for the time average of the square of the voltage fluctuation in a circuit connected as in Fig. 5, the equation

$$\overline{V^2} = \int_0^\infty \tfrac{1}{2}c^2 Z^2 d\nu$$

[16] I. Langmuir, Phys. Rev. **22**, 357, 389 (1923).

in which Z signifies the absolute value of the combined impedance of the tube and circuit. Introducing expression (21) for c^2 and writing $d\omega/2\pi$ for dv we get

$$\overline{V^2} = 1/\pi \cdot Q_0 F^2 i_0^2 \int_0^\infty \frac{Z^2 d\omega}{\alpha^2+\omega^2} . \tag{22}$$

We will consider three special cases.

1—Constant ohmic resistance outside to be designated by R_a; constant ohmic resistance in the tube to be designated by R_i, V here to be written as V_1. The impedance Z, which is the sum of R_a and R_i connected in parallel, is constant, and integrating (22) we get

$$\overline{V_1^2} = \frac{1}{2}\frac{Q_0}{\alpha} F^2 i_0^2 Z^2 = \frac{1}{2} N_0 F^2 i_0^2 Z^2 = \frac{1}{2} N_0 \gamma^2 Z^2 . \tag{23}$$

This result differs from that for the small-shot effect where even in the case of a pure ohmic resistance we do not get a result independent of residual natural oscillations, but on the contrary we should get infinitely great values of $\overline{V_1^2}$ when the natural frequency is infinite, no matter how great the damping.[17]

When $R_a >> R_i$

$$\overline{V_1^2} = \tfrac{1}{2} N_0 \gamma^2 R_a ; \tag{23a}$$

when $R_a = R_i$ then

$$\overline{V_1^2} = \tfrac{1}{4} N_0 \gamma^2 R_i ; \tag{23b}$$

and obviously $\overline{V_1^2} = 0$ when $R_a = 0$. Naturally, in actual measurements we must take care to separate the fluctuations of voltage from the steady voltage and to shunt out by a capacity any high frequency natural oscillation which might exceed the small-shot effect. This capacity would not influence the measurements on the flicker effect.

2—Resonant circuit with very small damping. In this case the ordinary procedure in dealing with circuits leads to an expression for the impedance:[18]

$$Z^2 = \omega_0^2 L_1^2 \frac{x^2+r^2}{(1+R/R_1-x^2)^2+r_1^2 x^2}$$

[17] Naturally the rapid decline of amplification with increasing frequency prevents anything of this sort being observed. This case might, however, be of some influence with particular experimental arrangements. One must assume that even in the small-shot effect some kind of critical time exists beyond which the effect declines as the square of the period.

[18] In evaluating the small-shot effect Hull and Williams (l.c.) used an expression for $\overline{v_k^2}$ obtained by ignoring r^2 and R/R_1 in the above equation for Z, which in that case is quite permissible. In the expression I gave in 1922 (l.c.) I ignored the second but took account of the first of these quantities. Fry (l.c.) was the first to carry through a calculation in which account was taken of both of these quantities, using the complete expression for Z.

in which R stands for the series resistance and R_1 for the total shunted resistance of the resonant circuit, ω_0 for the natural frequency of the circuit, r for the ratio $R/\omega_0 L$, $(\omega_0^2 LC=1)$, r_1 for the expression $R/\omega_0 L + \omega_0 L/R_1$ and $x=\omega/\omega_0$. The mean square of the voltage fluctuation V across the terminals of the resonant circuit is found by Eq. (22) in the case of the flicker effect to be:

$$\overline{V^2}=\frac{1}{\pi}Q_0F^2i_0^2\omega_0L^2\int_0^\infty \frac{1}{x^2+\alpha^2/\omega_0^2}\,\frac{(x^2+r^2)dx}{(1+R/R_1-x^2)^2+r_1^2x^2}. \qquad (24)$$

If now r_1, r^2 and R/R_1 are very small compared with unity we can set $x=1$ in the first factor of the integral and reduce the second to the expression[19]

$$\int_0^\infty \frac{x^2}{(1-x^2)^2+r_1^2x^2}=\pi/2r_1\,.$$

If for the special case we write $\overline{V_2^2}$ instead of $\overline{V^2}$ we get

$$\overline{V_2^2}=\tfrac{1}{2}Q_0F^2I_0^2\frac{\omega_0L^2}{r_1}\,\frac{1}{1+(\alpha/\omega_0)^2}$$

which by (21) becomes

$$\overline{V_2^2}=\frac{c^2}{8}\,\frac{\omega^3{}_0\,L^2}{r_1} \qquad (25)$$

in which c stands for the specific Fourier amplitude at the natural frequency ω_0 of the resonant circuit. Naturally this expression is the same as that arrived at for the small-shot effect, the amplitude c being in that case the same for all frequencies. Subject to the assumptions, therefore, we may write $\overline{V_F^2}/\overline{V_S^2}=C_F^2/C_S^2$.

Combining Eqs. (21), (23) and (25) we get an expression involving α of the form

$$\alpha+\frac{\omega_0^2}{\alpha}=\overline{V_1^2}/\overline{V_2^2}\,\frac{\omega^3{}_0\,L^2}{\gamma_1}\,\frac{1}{Z^2}\,. \qquad (26)$$

The quantities c and ω_0 refer to the natural frequency of the circuit for Case 2, and Z is to be found from the circuit constants for Case 1. By means of this equation we are enabled to determine α by one measurement with pure resistance and one measurement with a resonant circuit connected to the tube.

[19] W. Schottky, Ann. d. Phys. **68**, 157 (1922).

3—General form of resonant circuit. If the simplifying assumptions made in Case 2 are dropped, the integral in Eq. (24) must be calculated as it stands. We introduce the following symbols: $\alpha/\omega_0=s$;

$$x^2/(1+R/R_1)=x'^2;\ r^2/(1+R/R_1)=r'^2;\ r_1^2/(1+R/R_1)=r'_1{}^2;$$
$$s^2/(1+R/R_1)=s'^2.$$

Then the integral in (24) is equal to

$$1/s'^2\cdot 1/(1+R/R_1)^{3/2}\cdot\int_0^\infty \frac{1}{x'^2/s'^2+1}\cdot\frac{r'^2+x'^2}{(1-x'^2)^2+r'_1{}^2x'^2}dx'.$$

This integral may be reduced to the integrals S_1 and S_2 used in the simplified solution for the small-shot effect by suitable transformations; its value becomes

$$\frac{1}{(1+R/R_1)^{3/2}}\,\frac{\pi}{2r_1'}\,\frac{1+r'^2(1+r'_1/s')}{s'^2+r_1's'+1}.$$

We thus obtain from (24) after further transformation the value

$$\overline{V^2}=\tfrac{1}{2}Q_0F^2i_0^2\,\omega_0L^2/r_1\frac{1+r^2(1+r_1/s)}{(1+R/R_1)\,(1+R/R_1+r_1s+s^2)}.$$

Calculation of the basic factor F from the image theory. Since c^2 and α can be determined from the measurements, it should be possible, if our theory is right, to make an experimental determination of $N_0F^2i_0^2=N_0\gamma^2$ (in Eq. (21) or of $(N_0/\alpha)F^2i_0^2=Q_0F^2i_0^2=Q_0\gamma^2$. It would, however, not be possible by measurements on the flicker effect to separate the two components Q_0 and F or N_0 and F. An interesting question arises, whether one of these factors N_0 or Q_0 or F or γ, can be determined in any other way so that the other could thereupon be ascertained by measurements on the fluctuations. We will attack this problem by attempting to determine F theoretically and then, using the values of N_0F^2 determined from Johnson's measurements, to determine N_0 and Q_0; whence we shall be able to make more exact deductions as to the process underlying the flicker effect.

Space permits only an approximate statement of the theory. The essential points are as follows. The action of a single foreign atom on the surface is calculated by means of Langmuir's theory[16] from the doublet effect which it produces in the surface, every foreign atom in the surface being more or less strongly polarized. The determining factor is the increment in local potential created by the atom at the image threshold where the distance, h, from the surface is 10^{-5} cm.

At any point within this threshold distance (Fig. 7) the foreign atoms of a certain area act together; the foreign atoms which lie outside of a circle of area approximately equal to πh^2, directly underneath the point in question, produce only a constant contribution to the effect at the point, while the spatial and temporal irregularities in the distribution of the foreign atoms are without effect except within the area of the circle. We represent by g the electrical moment of the average double layer for the circular area σ in question (note that this is subject to fluctuation), by g_0 the average value of electrical moment for the entire surface and by y the difference between g and g_0. The effect of the foreign atoms upon the potential at the point P is made up of two parts; first the constant part contemplated in the ordinary Langmuir theory, dependent on the value g_0 for uniform distribution of atoms over the entire

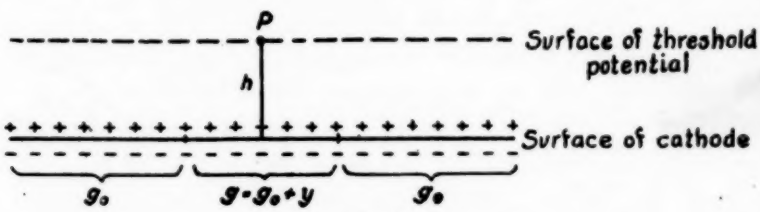

Fig. 7.

surface; and second, a contribution y to be regarded as coming from an additional uniform distribution of atoms over the circular area σ. We will now consider this second contribution. The effect of the additional layer (σy) upon the potential in P is to be calculated approximately from the potential drop which the layer y would produce if infinitely extended (approximation 1). Representing by δ the extra potential measured in electrostatic units produced at P by the layer we have $\delta = 4\pi y$.

Accordingly the effect of a *single* additional foreign atom arriving in the circular area and having the moment p, consists in producing a potential change $\theta = 4\pi p/\sigma$ in the neighborhood of P. This effect will extend nearly uniformly over a surface of the area of the aforesaid circle drawn around the foreign atom as center. A change in the potential at the potential threshold along the surface σ produces an alteration of the current σi flowing out through this surface (i = average momentary current density in the area σ) by the factor $\epsilon^{e\theta/kT}$; or when $e\theta$ is much less than kT as is always the case for one single foreign atom, a change by the ratio $1 + e\theta/kT$. The additional current is then given by

$$\gamma = \sigma i \, e\theta/kT = ie \, 4\pi p/kT \, . \qquad (27)$$

If we wish to relate γ not to the local current density i, but to the average current density i_{00} determined from the measured electron current i_0 divided by the cathode area, we must know the relation between i and i_{00}; according to the preceding equation this is

$$i = i_{00}\epsilon^{e\delta/kT} = i_{00}\epsilon^{4\pi ey/kT}.$$

The larger the area σ the smaller is the deviation of the average electrical moment g from the value g_0, in other words the smaller is y. We assume (approximation 2) that the relative change of the electron current flowing out in the vicinity of P due to the spatial change in potential along the surface at the potential threshold is small compared to unity.[20] We can then set $i = i_{00}$ with sufficient approximation and obtain from (27) the equation

$$\gamma = i_{00}e4\pi/kT$$

which signifies that (subject to our assumptions) γ *becomes independent of the magnitude of the region in question*, that is, of the critical distance h and therefore *of the field strength*. Consequently our factor F, to be designated by f when referred to the current i_{00}, becomes

$$f = \sigma e\theta/kT = 4\pi pe/kT \cdot \tag{28}$$

The quantity p may be determined from known data with sufficient accuracy in such cases as those Langmuir's theory covers. Let N_1 be the number of foreign atoms per unit area when the surface is filled with foreign atoms;[21] let $\Delta\varphi$ represent the change of potential at the threshold produced by this number of atoms. Any smaller number $n = \theta_1 N_1$ of foreign atoms will produce a smaller change of potential $\theta_1\Delta\varphi$ in the same area. Considering once more an area σ containing σN atoms we find that when an additional foreign atom arrives at this surface the change in θ, equals $1/\sigma N_1$, independent of the value of n; the corresponding change in potential at P is given by

$$\theta = \Delta\varphi/\sigma N_1 \, . \tag{29}$$

Since $\theta = 4\pi p/\sigma$,
we have

$$4\pi p = \Delta\varphi/N_1 \, ,$$

[20] This assumption is the more justified the larger the area σ and the distance h, in other words the smaller the applied field strength. The investigation of the fluctuation effects, both secular and spatial, at extremely high field strength requires particular consideration for which the foregoing serves as a preparation.

[21] In the case of thorium atoms of tungsten, Langmuir assumes this number equal to about one half the number of tungsten atoms in the surface, $N_1 = 7.6 \times 10^{14}$.

and equation (28) becomes

$$f = e\Delta\varphi / N_1 kT \,. \tag{30}$$

The quantity $e\Delta\varphi/k$ is equal to the difference Δb between the exponential constants of the clean and the completely covered metal. This quantity is positive or negative according as the foreign atoms favor or hinder the outflow of electrons (examples are thorium and oxygen atoms on tungsten). It may be calculated from the saturation current I_0 of the clean metal and I_1 of the covered metal by means of the equation

$$\Delta b = e\Delta\varphi/k = T(\log I_1 - \log I_0) \,.$$

Its order of magnitude is $\pm 10{,}000$ to $20{,}000$. We have thus obtained a value for

$$f = \Delta b / N_1 T \,^{22} \tag{31}$$

which is of the order of magnitude

$$\frac{15000}{7.6\times 10^{14}} \frac{1}{T}$$

or roughly $\pm 2\times 10^{-14}$. For γ, with current densities of about 0.1 ampere per square centimeter, we obtain a magnitude of about 2×10^{-15} amp. or 10^4 electrons per second.

Computation from the flicker effect of the number of foreign atoms in the surface. The following computation is meant to serve only as an example and to test the theory so far as order of magnitude goes. According to (17) and (20) we have

$$4N_0 F^2 \frac{\alpha}{\alpha^2+\omega^2} i_0^2 = 4ei_0\left(\overline{V^2}_{obs} - \overline{V^2}_{calc} - 1\right).$$

We introduce the following symbols for the above quantities when referred to unit area: $fi_{00} = Fi_0 = \gamma$; $i_{00} = i_0/S$ (S is the total surface); $N_{00} = N_0/S$ (N_0 is the number of foreign atoms per unit area). We get

$$N_{00} f^2 i_{00} \cdot \frac{\alpha}{\alpha^2+\omega^2} = e\left(\overline{V^2}_{obs}/\overline{V^2}_{calc} - 1\right) .^{23}$$

[22] We observe that the same expression for f would be obtained if the effect of each individual foreign atom were calculated as if its electrical moment were distributed uniformly over the surface.

[23] In this equation let me point out incidentally that both sides in a certain sense signify the "elementary electrical quantum of the flicker effect." In case the second term (-1) can be neglected these expressions are identical with that designated by Johnson as e'.

It follows that

$$N_{00}f^2=\frac{\alpha^2+\omega^2}{\alpha}\cdot\frac{e}{i_{00}}(\overline{V^2}_{obs}/\overline{V^2}_{calc})-1). \tag{32}$$

Let us calculate the right-hand member of this equation for *oxide coated filament* using the point on the curve in Fig. 4 indicated by the arrow, at which point we assume $\alpha=\omega=1000$. For this point the ratio between $\overline{V^2}_{obs}$ and $\overline{V^2}_{calc}$ is about 100, so that the second term in the parentheses (-1) may be neglected. The current i_{00} may be estimated at about 0.3 amp/cm² while the electronic charge, e, is 1.56×10^{-19} coulomb. We have, therefore,

$$N_{00}f^2=2000\times1/0.3\times1.56\times10^{-19}\times100=10^{-13}.$$

Assuming $f\doteq2.10^{-14}$ we obtain $N_{00}=10^{-13}\times10^{28}/4=2.5\times10^{14}$. Since as we have seen N_1 is of the order of magnitude 7.5×10^{14} when the surface is completely covered, it follows that,

$$\theta_1=N_{00}/N_1=1/3\ ,$$

that is to say, the flicker effect of oxide coated filaments is due to foreign atoms the number of which is of the same order of magnitude as the number of atoms of the underlying metal in the surface.

In this calculation the factor which is most uncertain is the value for α, that deduced from the mere indication of saturation in Johnson's curve. It is therefore important to be able, without knowing the value of α to calculate the number of foreign atoms Q_{00} which strike unit area per second from measurements made in the region where $\overline{V^2}_{obs}/\overline{V^2}_{calc}$ varies approximately as $1/\omega^2$. Since $N_{c0}\alpha=q_0$, it follows from (32) that

$$Q_{00}f^2=(\alpha^2+\omega^2)e/i_{00}\cdot(\overline{V^2}_{obs}/\overline{V^2}_{calc}-1)\ , \tag{32'}$$

and in the region in question α^2 is negligible in comparison with ω^2. At the frequency 1000, $(\omega=6300)$ the value of $\overline{V^2}_{obs}/\overline{V^2}_{calc}$ given by the curve in Fig. 4 is about 7. Hence $Q_{00}f^2=(6300)^2\times1/0.3\times1.56\times10^{-19}\times6=1.2\times10^{-10}$ and with the foregoing value of f we find $Q_{00}=3.5\times10^{17}$.

Suppose a gas in which Q_{00} atoms pass through unit area per unit time; the pressure of the gas would be

$$p=8.75\times10^{-21}\sqrt{T/1000}\ \sqrt{14}\,Q_{00} \tag{33}$$

in millimeters of mercury. Taking the above value of Q_{00} and assuming $T=1300$, $M=32$ (oxygen), we get the value 2×10^{-2} for the pressure. Now the pressure in ordinary tubes is 10^{-4} mm or lower. Since the quantities which enter into the calculation can scarcely be thought

uncertain by as much as a factor of 100 (f is least accurately known), we may conclude from the theory as given, that the flicker effect is not due to collisions of molecules of the gas with the surface of the filament, but results from some other and much more frequently occurring process. From the number of atoms per unit area which we have computed it seems natural to imagine that the ions of both kinds which form the oxide are continually exchanging their places in the surface; but any uniform sequence is not to be thought of, and the occurrence of metal and oxygen ions in the surface are to be considered as independent events. Johnson observed that foreign gases admitted to the tube did not affect the phenomenon very much, which may be taken to support the foregoing conclusion.

In the experiment with a *tungsten filament* (Fig. 3) it is necessary to assume a value for α at least 50 times smaller than with the oxide coated filament, that is, a value less than 20. Considering how uncertain the actual value of α is, we can do no more than calculate Q_{00} approximately from Eq. (32′) neglecting α^2 in comparison to ω^2. At the frequency of 10 cycles per second ($\omega=63$) the quantity $\overline{V^2}_{obs}/\overline{V^2}_{calc}-1$ is equal to about 15. The current i_{00} is probably about 0.1 amp/cm.[2] Using the same value of f as before, we get

$$Q_{00}=10^{28}/4\times 63^2\times 1/0.1\times 1.56\times 10^{-19}\times 15=2.10^{13},$$

which value is about 20,000 times smaller than that for the oxide coated filament. Were atoms of residual gas responsible for this, the pressure need only be 10^{-6} mm Hg. This is about the lowest limit of residual gas pressure in ordinary tubes. The impact and gradual absorption of gas atoms on the surface may therefore easily account for the effect with tungsten. A repetition with tungsten filaments of the experiments made by Johnson upon the effect of gas upon oxide coated filaments would either confirm or confute this interpretation.

Taking a value greater than 1/20 second for τ' together with the calculated value of Q_{00} we get a value greater than 10^{12} for the number of foreign atoms per unit area, or the relative covering θ_1 is more than 1/750. A more accurate value can be obtained by means of this theory only after extending the measurements in the direction of lower frevencies or using a pure resistance in place of the resonant circuit.

Physikalisches Institut der Universität Rostock, Germany.
November 30, 1925.*

* Received April 5, 1926.

FLOW OF IONS THROUGH A SMALL ORIFICE IN A CHARGED PLATE

By Lewi Tonks, Harold M. Mott-Smith, Jr., and Irving Langmuir

Abstract

Measurements of ion and electron current densities and temperatures in a low pressure arc may be made with a collector which is screened by a close parallel electrode pierced with uniform circular holes. *The electrostatic potential distribution in the neighborhood of a pierced electrode*, pierced with either slit or hole, has been worked out. *The volt-ampere characteristic for random electrons* is exponential for the higher retarding voltages and the exponent gives a temperature slightly too high. When the anode drop is known the current density of electrons can be calculated. *The volt-ampere characteristic for positive ions* is linear for small accelerating voltages. For small retarding voltages the characteristic is not a pure exponential. The characteristic gives anode drop, ion current density, "transverse" ion temperature and "longitudinal" ion temperature. The limitations and possible errors are discussed.

IN ORDER to separate the ionic and electronic parts of the electric current to an electrode immersed in an electric discharge in a gas, A. F. Dittmer suggested allowing these carriers to pass through small holes in a plane electrode and collecting them on a second electrode parallel to and behind the first, keeping the gas pressure low enough so that no collisions occurred between the sheath edge, A, and the second electrode, C, cf. Fig. 4. By adjusting the potentials on these electrodes it can be so arranged that either ions alone or electrons alone reach electrode C. The necessary variation in electrode potentials has a negligible effect on the discharge because of the presence of the sheath before the pierced electrode B. The thickness of this sheath must be greater than the hole diameter to prevent the discharge from penetrating through the hole. Other conditions, also, must be fulfilled, as will appear when the different cases are analyzed.

The carriers, which it is desired to keep from reaching C, can be prevented from doing so either by the field between B and C, or by the field between sheath edge and B. Thus there are two fundamental potential arrangements; in the first the carriers to be collected on C are initially retarded then accelerated, in the second they are initially accelerated then retarded.

The first arrangement is unsuited to measurements on positive ions (hereafter called simply ions) because it requires that B be made positive with respect to the anode. This situation cannot usually be realized for it is the most positive electrode of any considerable size which acts

as anode in the discharge. The second arrangement, on the other hand, is unsuited to measurements on electrons. They should be collected in an accelerating field because of electron reflection. On account of this specific application of each arrangement, we shall hereafter speak of positive and negative voltages, rather than accelerating and retarding voltages.

The present paper treats first, the measurement of the current density in a high velocity beam of electrons; second, the volt-ampere characte.istic of electrons having a Maxwellian distribution of velocities in the discharge; and third, the volt-ampere characteristic of ions having Maxwellian and other velocity distributions in the discharge. Preliminary to this, the equations for the electric potential field in the neighborhood of both a slit and a circular hole in an infinite charged plane are derived, and the transverse velocity and displacement acquired by a fast electron (ion) in traversing such a field are calculated.

I. The Electrostatic Field about a Slit

The potential distribution about a slit in an infinite plane charged electrode[1] is found by applying a Schwartz transformation[2] to the polygon $ABC \cdots H$ of Fig. 1. Proceeding to the limit by allowing

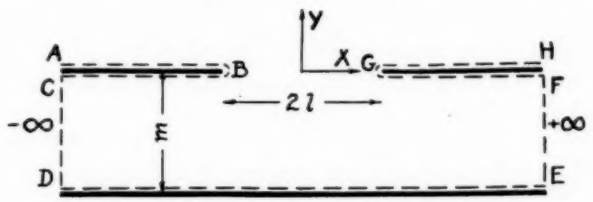

Fig. 1.

m to approach ∞ as $\partial V/\partial y$ at $y=+\infty$ remains finite and equal to $-E$, the potential V near a slit is found to be given by the parametric equations:

$$x=-\frac{U}{E}-\frac{El^2}{4}\frac{U}{U^2+V^2} \tag{1}$$

$$y=-\frac{V}{E}+\frac{El^2}{4}\frac{V}{U^2+V^2},\quad V\geqq 0 \tag{2}$$

[1] The hydrodynamic case corresponding to this problem and also to the problem of the hole in a plate has been treated by Lamb, Hydrodynamics, 3rd edition, p. 77 and p. 137 respectively, but it has been thought worth while to sketch derivations of the potential using more usual coordinate systems.

[2] Jeans, Electricity and Magnetism, 2nd edition, p. 271.

and the boundary conditions of the field reduce to those shown in Fig. 2. To realize the general case where $\partial V/\partial y$ is different from zero on both sides of the electrode, it is only necessary to superpose a uniform electric field parallel to the y-axis modifying U and V in Eqs. (1) and (2) in such a way as to retain their conjugate properties.

U, the parameter, and function conjugate to V, has a very simple physical meaning. Keeping U constant and taking V as parameter in Eqs. (1) and (2) (or these equations modified as contemplated above) gives the lines of electric force just as $V=$constant gives the equipotentials, and the value of U associated with a line of force is proportional to the total charge (per unit length) between the foot of that line of force and the foot of the line of force for which $U=0$. Along any line $x=$constant, in Fig. 2, the change in U between any

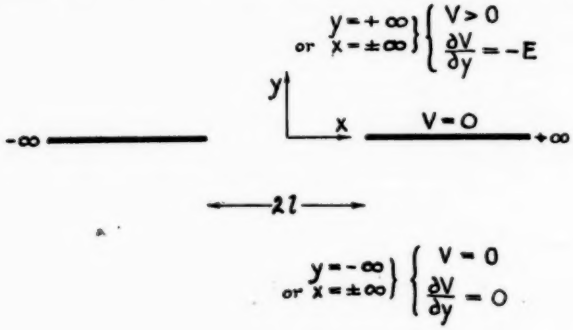

Fig. 2.

two fixed points, as given by Eqs. (1) and (2), is the same as the change in U, given by these equations modified to include the superposed uniform field. Therefore, Eqs. (1) and (2), rather than the more complicated modifications, can be used for the general case whenever, as in the next section, changes in U along a line parallel to the y-axis are involved.

The equipotentials given by Eqs. (1) and (2) are sufficiently plane when y is somewhat greater than zero for these equations to be good approximations even when the parallel electrode, C, is near. For instance, Eq. (2) shows that the equipotential $V=-6lE$ lies at $y=6l$ at some distance from the slit (x large, U large,) and lies at $y=6l(1-1/144)$ at $x=0$. In terms of potential, the potential of a conducting plane at $y=6l$ is too low at $x=0$ by $El/24$. When y is somewhat less than zero, the electric field is so weak and the potential is so nearly zero that the plane equipotential, A, may also be used there without altering the field for our purpose.

II. Transverse Velocity Acquired by a Charged Particle Passing Through the Slit

A particle of charge ϵ and mass m moving with high velocity parallel to the y-axis is subject to a transverse acceleration due to the non-uniformity of the field.

This acceleration is

$$\frac{d^2x}{dt^2} = -\frac{\epsilon}{m}\left(\frac{\partial V}{\partial x}\right)_{x=x'}$$

where V is the potential in the field and x' is the distance of the particle path from the center line of the slit. Now the discussion above shows that such non-uniformity is quite local, so that the particle acquires the same transverse velocity in traveling from $y=-\infty$ to some point near electrode B as in going from electrode A, the sheath edge of Fig. 4, to the same point. Hence the transverse velocity acquired will be

$$\dot{x} = -\frac{\epsilon}{m}\int_{-\infty}^{t_1}\frac{\partial V}{\partial x}dt = -\frac{\epsilon}{m}\int_{-\infty}^{y}\frac{1}{\dot{y}}\frac{\partial V}{\partial x}dy \tag{3}$$

If $\dot{y}$ is large it changes but slightly in the neighborhood of the slit, so $\dot{y}$ will be supposed constant and

$$\dot{x} = -\frac{\epsilon}{m\dot{y}}\int_{-\infty}^{y}\frac{\partial V}{\partial x}dy = \frac{\epsilon}{m\dot{y}}\int_{-\infty}^{y}\frac{\partial U}{\partial y}dy = \frac{\epsilon}{m\dot{y}}\Big|U\Big|_{-\infty}^{y} \tag{4}$$

where U is the function conjugate to V.

Eqs. (1) and (2) are applicable, as has been remarked above. From them

$$U = -Ex', \text{ when } y=+\infty,\ x=x'$$
$$U = 0, \text{ when } y=-\infty$$

Accordingly the total transverse velocity acquired in passing from electrode A to electrode C ($y=-\infty$ to $y=+\infty$) is

$$\dot{x}_f = -\epsilon Ex'/m\dot{y} \tag{5A}$$

Now E is the electric field in the simple case corresponding to Eqs. (1) and (2). It is equal to the difference of the actual fields on the two sides of B so that

$$\dot{x}_f = \frac{\epsilon(E_1+E_2)x'}{m\dot{y}} \tag{5B}$$

where E_1 and E_2 are the two fields, each being counted positive when directed towards B. Expressing velocities as potentials and using the mean field strength $\bar{E}=\frac{1}{2}(E_1+E_2)$

$$V_x V_y=\bar{E}^2 x'^2 \tag{6}$$

One conclusion from the preceding is that the particle has acquired one-half its transverse velocity when it reaches the plane of B. This is obviously true for a symmetrical arrangement of voltages; any unsymmetrical arrangement can be realized by superposition of a uniform field, hence it holds also for any other arrangement. In general, however, this conclusion is not valid if the slit has finite thickness.

On the other hand, it is true that $\dot{x}_f$ is given by Eq. (5B) no matter what the thickness of electrode B and what the shape of the sides of the slit so long as the slit's cross-section is constant. This follows immediately from the fact that U at A and C does not depend on the shape of the slit. Of course there is the difficulty of assigning an origin of coordinates when the slit is unsymmetrical.

A further integration of Eq. (4) would give the lateral displacement of the particle. Inasmuch as the calculation for the case of the hole is simpler and the displacement in the present case is of no interest here, that result is not calculated.

III. The Electrostatic Field about a Hole[1]

The problem is to find the potential distribution due to an infinite conducting plane with a circular hole of radius a charged to potential

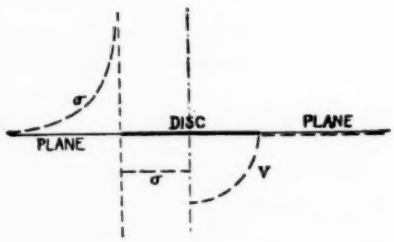

Fig. 3.

$+V$ and placed symmetrically between two parallel infinite grounded plates at a great distance away.

The limiting value of surface charge density on the central plate far from the hole is taken to be σ_0; then the uniform density on each grounded plate is $-\frac{1}{2}\sigma_0$. A uniform density $-\sigma_0$ is then superimposed over the central plane and hole in addition to the charge already existing, and to compensate for this $-\frac{1}{2}\sigma_0$ is removed from

each distant grounded plate. The central conducting plane is thereby brought to zero potential, and the problem is changed to: An infinite grounded conducting plane has a circular hole in which is placed a disk charged with a uniform density of negative electricity. Find the potential distribution.

The general nature of the distributions of potential V and charge σ are indicated in Fig. 3. It can be proved by direct substitution that a solution of Laplace's equation in cylindrical coordinates is

$$V(r,z)=\int_0^\infty e^{-uz}du\int_0^\infty f(s)J_0(ur)J_0(us)sds$$

where $f(s)$ is arbitrary. V vanishes for $z=+\infty$, and for $z=0$ is

$$V(r,0)=\int_0^\infty udu\int_0^\infty f(s)J_0(ur)J_0(us)sds=f(r)$$

The last equation is a consequence of the *Fourier-Bessel integral formula* analogous to the Fourier integral in the case of circular functions. Thus $f(r)$ is simply the potential distribution in the plane $z=0$. Taking the hole to be of unit radius, for convenience, $f(s)=0$ for $s>1$, and

$$V(r,z)=\int_0^\infty e^{-uz}du\int_0^1 f(s)J_0(ur)J_0(us)sds \tag{7}$$

Applying Gauss' theorem at the disk,

$$\left(\frac{\partial V}{\partial z}\right)_{z=0}=2\pi\sigma \tag{8}$$

to Eq. (7) gives an integral equation to determine $f(s)$. The shape of the curve for V in Fig. 3 suggested the solution

$$f(s)=A\sqrt{1-s^2} \tag{9}$$

This is tried in the equation and found to satisfy it,[3] giving for A the value $-4\sigma_0$. Hence the potential distribution in the plane $z=0$ is given by

$$f(r)=V(r,0)=-4\sigma_0\sqrt{1-r^2},\quad 0\leqq r\leqq 1$$

[3] Invaluable reduction formulae are found in Watson, "A Treatise on the Theory of Bessle Functions," pp. 373, 54, and 405, Nos. 2 and 7.

The potential distribution for the modified problem is found by putting this in Eq. (7) and reducing slightly

$$V(r,z)=-4\sigma_0\int_0^\infty \frac{e^{-uz}}{u}\left(\frac{\sin u}{u}-\cos u\right)J_0(ur)du,\quad z\geqq 0$$

The potential distribution for the original problem involving the hole of radius a is then easily seen to be

$$V(r,z)=V_0-\sigma_0\left[2\pi z+2a\int_0^\infty \frac{e^{-uz/a}}{u}\left(\frac{\sin u}{u}-\cos u\right)J_0(ur/a)du\right],z\geqq 0 \quad (10)$$

where V_0 is the potential of the plate with the hole.

The equipotential surfaces given by this equation are more nearly plane than those for the slit. On the axis of the hole Eq. (10) reduces to

$$V(0,z)=V_0-\sigma_0\left[2\pi z+4a\left(1-\frac{z}{a}\cot^{-1}\frac{z}{a}\right)\right]$$

so that the equipotential

$$V=V_1-2\pi\sigma_0 z_1\,,$$

which lies at $z=z_1$ at a distance from the hole, lies at

$$z=z_1\left[1-\frac{2}{\pi}\,\frac{a}{z_1}\left(1-\frac{z_1}{a}\cot^{-1}\frac{z_1}{a}\right)\right]$$

$$=z_1\left(1-\frac{2}{3\pi}\,\frac{a^3}{z_1^3}\right)$$

at the axis. Thus the surface at $z_1=3a$ only decreases its distance from the plane of B by 0.8 percent.

IV. Transverse Velocity Acquired by a Charged Particle Passing through the Hole

The expression for the transverse velocity can be written immediately from inspection of Eq. (3)

$$\dot{r}=-\frac{\epsilon}{m\dot{z}}\int_{-\infty}^{\infty}\frac{\partial V}{\partial r}dz=-\frac{2\epsilon}{m\dot{z}}\int_0^\infty\frac{\partial V}{\partial r}dz$$

Evaluating this[4] and introducing $\bar{E}$ gives the same results as in section II, namely

$$\dot{r}_f=-\epsilon Er'/m\dot{z} \text{ or } V_rV_z=\bar{E}^2r'^2 \quad (11)$$

[4] Watson, p. 405, No. 3, used twice, once integrated with respect to b.

The similarity between this case and the slit case extends further. Here as there the particle acquires one-half its transverse velocity in reaching the plane of B in the ideal case of zero thickness of B. Here also the total transverse velocity acquired is independent of the electrode thickness and the hole shape as long as the hole has circular symmetry. This follows from the existence of a "current function" which has been defined by Stokes for three dimensional problems concerning configurations having axial symmetry. This function is analogous to the function U conjugate to the potential V in two dimensional problems.

V. Measurement of the Current Density in a Beam of High Velocity Electrons

Under certain conditions the electrons which leave the incandescent tungsten cathode in a low pressure arc travel with nearly equal velocities in straight lines radially from the filament. One way of collecting these without at the same time collecting the random low velocity electrons and without introducing reflection errors is by using the present double electrode scheme. The potential requirements here are that a low negative voltage V_B be put on B, and a low positive voltage V_C be put on C. These potentials are relative to the sheath edge which serves as electrode A, V_B must be sufficient to repel all low velocity electrons, V_C must be sufficient to repel all positive ions, and the electrons must be moving parallel to the hole axis.

All the fast electrons which are headed for the hole pass through it and reach C. In addition some electrons which are directed toward B just outside the hole are displaced inward so that they penetrate the hole. The decrease in radial distance which enables an electron to graze the edge of the hole can be calculated readily on the assumption that B is infinitely thin and with the approximation that the transverse field is the same along the straight line path $r=a$ as along the actual path. Thus the displacement at the hole is given by

$$\Delta r' = -\frac{\epsilon}{m\dot{z}^2}\int_{\infty}^{0}\int_{\infty}^{z}\left(\frac{\partial V}{\partial r}\right)_{r=a} dzdz$$

evaluating this[5] it is found that

$$\frac{\Delta r'}{a} = \frac{\sqrt{2}}{3\pi}\,\frac{a\epsilon\bar{E}}{m\dot{z}} = \frac{\sqrt{2}}{6\pi}\,\frac{a\bar{E}}{V_D - V_B} = .075\frac{a\bar{E}}{V_D - V_B} \qquad (12)$$

[5] Watson, pp. 54 and 403, No. 2.

where V_D is the potential, intrinsically negative for electrons, necessary to reduce the drift velocity $\dot{z}$ to zero. The difference $V_D - V_B$ is used instead of V_D because it is the value of $\dot{z}$ at the hole which is significant. The effective area of the hole is then fractionally greater than the true area by

$$\Delta A/A = -2\,\Delta r'/a = 0.15\,a\bar{E}/(V_B - V_D) \tag{13}$$

It is to be noted that whereas the field, E_2, between B and C is given by $(V_C - V_B)/\delta$, where δ is the electrode separation, the field, E_1 on the sheath side of B is more nearly $-4V_B/3\sigma$, σ being the sheath thickness, on account of the space charge there. Accordingly

$$\bar{E} = \tfrac{1}{2}\left(-\frac{4}{3}\,\frac{V_B}{\sigma} + \frac{V_C - V_B}{\delta}\right) \tag{14}$$

As an example, consider the following case: hole radius, $a = 0.0125$ cm; sheath thickness $\sigma = 0.0375$ cm; electrode separation $\delta = 0.075$ cm; $V_B = -10$ v.; $V_C = +10$ v. Then $E_1 = 356$, $E_2 = 267$ and $a\bar{E} = 3.9$ v.

Calculating $\Delta A/A$ in percent for various values of V_D the following is found:

V_D :	-100	-50	-30	-20
$\Delta A/A$:	0.0065	0.015	0.029	0.059

The true electron current density in the beam is found by dividing the current to C by $A(1+\Delta A/A)$.

If the hole has appreciable thickness the side of B with the stronger longitudinal field has the stronger transverse field, and, therefore, contributes the major part of the transverse velocity. In the present example, the sheath-side field is the stronger on account of the space charge there. Accordingly $\Delta A/A$ as calculated is too small.

Electrode B collects all the ions which strike it but reflects some of the electrons. The ion component can be determined by the method of section VIII and in other ways. Thus it becomes possible by comparing the electron current densities to B and C to determine the reflection coefficient of B for electrons of different voltages in the presence of gas and ion bombardment.

VI. Measurements on the Random Electrons in an Arc

The random electrons, having, presumably, a Maxwellian distribution of velocities, can be investigated in the absence of drift electrons with essentially the same potential arrangement as in the previous case. When the electric fields on the two sides of B are equal,

the surface of minimum potential (m.p.s.), which caps the hole, becomes plane and the potential at any point on it is given by

$$V = V_B + (2\overline{E}/\pi)\sqrt{a^2 - r^2} \tag{15}$$

A general theorem pertaining to Maxwellian distributions, which is discussed in a forthcoming paper by Langmuir and Mott-Smith, Jr., applies here in all cases where $V<0$ over the minimum potential surface. In this case, the entire hole constitutes a collector which repels electrons, and there will be no "interior orbits" for the electrons between sheath edge and B. Accordingly the electrons in the plane m.p.s. have a Maxwellian distribution of velocities and a density which varies according to Boltzmann's equation. The current, therefore, which flows through the hole is

$$i_C = I_- \int_0^a e^{-\epsilon V/kT} 2\pi r dr$$

Using (15) to integrate and then (14) together with the substitutions

$$\eta_1 = -\epsilon V_B/kT,\ \eta_2 = -\epsilon(V_C - V_B)/kT$$

$$\nu = \frac{a}{\pi}\left(-\frac{4\eta_1}{3\sigma} + \frac{\eta_2}{\delta}\right),\ \Phi(\nu) = \frac{2}{\nu^2}[1 + e^{\nu}(\nu - 1)]$$

we obtain

$$i_C = \pi a^2 I_- e^{\eta_1} \Phi(\nu) \tag{16}$$

Since electrons are involved ϵ is negative. Besides, it has been assumed that V_B is negative and V_C positive. Hence η_2 and ν are always positive, and η_1 negative.

From the form of Eq. (16) it is seen that $\Phi(\nu)$ is the ratio of the currents per unit area to the hole and to electrode B (assuming no reflection), and since $\ln\Phi$ is an almost linear function of ν whose derivative changes only from 2/3 at $\nu=0$ to 1 at $\nu=\infty$ it follows that the slope of the ln i_c against V_B (η_2 constant) characteristic will differ from its usual value in other cases, namely, ϵ/kT, by a nearly constant amount. It will correspond to a higher temperature.

When V_C is made rather large so that ν is large, the equation of the characteristic is

$$i_C = \frac{2\pi^2 a I_-}{-4\eta_1/3\sigma + \eta_2/\delta} e^{a\eta_2/\pi\delta}\, e^{\eta_1(1 - 4a/3\pi\delta)} \tag{17}$$[6]

[6] See the discussion following Eq. (23) for a necessary modification to this equation.

which shows that for η_2 constant, ln i_e is nearly a linear function of η_1 whose slope is

$$\frac{d\ln i_C}{d\eta_1}=1-\frac{4a}{3\pi}\frac{d}{d\eta_1}(\eta_1/\sigma), \text{ nearly.}$$

Since σ is proportional to $\eta_1^{3/4}$ this becomes

$$d\ln i_C/d\eta_1=1-a/3\pi\sigma, \text{ nearly.} \tag{18}$$

Consequently the temperature determined from this slope is slightly greater than the true electron temperature in the ratio $1 : 1-a/3\pi\sigma$. Practically, η_1 and η_2 cannot be made very small because of incalculable changes in the sheath field, but it is instructive to consider the case. Eq. (16) becomes

$$i_C=\pi a^2 I_- e^{\eta_1}\left[1+\frac{2a}{3\pi}\left(-\frac{4\eta_1}{3\sigma}+\frac{\eta_2}{\delta}\right)\right] \tag{19}$$

and

$$d\ln i_C/d\eta_1=1-2a/9\pi\sigma, \text{ nearly,} \tag{20}$$

giving again a temperature slightly greater than the true one, now in the ratio of $1 : 1-2a/9\pi\sigma$. Accordingly the slope of the characteristic consists of a constant corresponding to the true temperature less a correction term which is small (not over 3.5 percent since σ must not be less than $3a$) and inversely proportional to the three-fourths power of V_B.

If now the sheath edge potential and the positive ion current density are known (from measurements on the positive ion current which will be discussed below in section VIII, for instance) so that V_B and V_C are known, and σ can be calculated, everything but I_- in Eq. (17) is known and the electron current density can be found.

Three factors affecting this method and introducing certain corrections must be treated in greater detail. They are, first, the effect of the random ion velocities on the electric field and sheath thickness; second the condition that the fields on the two sides of B should be equal, and third, the condition that the potential everywhere over the hole shall be less than zero.

The presence of initial velocities among the ions changes the space charge equation[7] to

$$I_+=5.44\times10^{-8}(-V_B)^{3/2}(1+\mu)/\sqrt{M}\sigma^2 \tag{21}$$

[7] Langmuir, Phys. Rev. 21, 419 (1923), Eq. (17).

where M is the molecular weight of the ion, and

$$\mu = 0.0247\sqrt{-T_+/V_B} \tag{22}$$

T_+ being the positive ion "temperature." From this it is found that

$$E_1 = -\frac{4}{3}\frac{V_B}{\sigma}\frac{1+\mu}{1+\frac{3}{8}\mu} \tag{23}$$

Thus Eqs. (17), (18), (19), and (20) should be modified by replacing $1/\sigma$ by

$$\frac{1}{\sigma}\frac{1+\mu}{1+\frac{3}{8}\mu}$$

For σ, Eq. (21) gives

$$\sigma = 7.37\times10^{-4}(-V_B)^{3/4}\sqrt{1+\mu}/M^{1/4}I_+^{1/2} \tag{24}$$

The condition that $E_1 = E_2$ is seen to be

$$-\frac{4}{3}\frac{V_B}{\sigma}\frac{1+\mu}{1+\frac{3}{8}\mu} = \frac{V_C - V_B}{\delta} \tag{25}$$

and using (24) it becomes

$$\frac{V_C - V_B}{\delta} = \frac{4}{3}\frac{M^{1/4}I_+^{1/2}(-V_B)^{1/4}}{7.37\times10^{-4}}\frac{\sqrt{1+\mu}}{1+\frac{3}{8}\mu} \tag{26}$$

The theory has been worked out on the basis of keeping $V_C - V_B$ constant, so that if a run includes an N-fold variation of V_B and (26) holds for some mean value of V_B then (26) will be out each way by the factor $N^{1/8}$ at the extremes. This results in a bulging of the m.p.s. so that its center lies at a distance z_0 from the plane of B given by the equations

$$\gamma = \frac{2}{\pi}\left(\frac{z_0/a}{1+z_0^2/a^2} + \tan^{-1}(z_0/a)\right), \quad E_2/E_1 = (1+\gamma)/(1-\gamma) \tag{27}$$

or approximately by

$$E_2/E_1 = \frac{1+1.274z_0/a - 1.70z_0^3/a^3}{1-1.274z_0/a} \tag{28}$$

which makes E_2/E_1 5 percent too large for $z_0 = .4a$ and 8 percent too large for $z_0 = -.4a$. The potential at the center of the m.p.s. is

$$V = V_B + 2a\bar{E}/\pi(1+z_0^2/a^2) \tag{29}$$

A permissible error of 1 percent in V allows an error of at least 1 percent in the second term of the right member. This in turn allows z_0/a to be as great as 0.1 and E_2/E_1 to be 1.29 by (28). But this is $N^{1/8}$, so that V_B may have a $(1.29)^8 = 7.7$-fold variation when properly chosen without exceeding the 1 percent limit set above.

Finally, the condition that the center of the m.p.s. shall be negative is given by Eq. (15).

$$\frac{\eta_2}{-\eta_1} = \frac{V_C - V_B}{-V_B} \leqq \frac{1 - 4a/3\pi\sigma}{a/\pi\delta} = \frac{\pi\delta}{a}, \text{ nearly},$$

the effect of initial ion velocities being neglected. Inspection shows that when condition (25) is satisfied this condition is satisfied also since $\sigma/a \geqq 3$.

VII. Measurements on Positive Ions: Calculation of the Volt-Ampere Characteristic of Ions Collected on C

It was noted in the preliminary remarks that to make measurements on the ions V_B must be sufficiently negative to keep any electrons

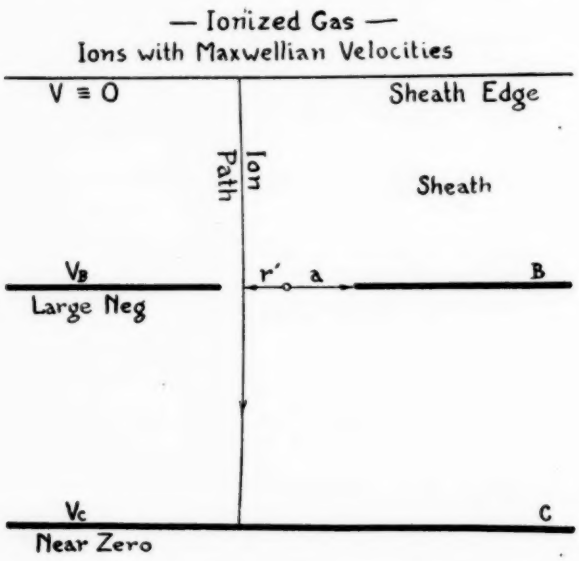

Fig. 4.

from reaching C. The situation as regards the ions is illustrated in Fig. 4 and may be described as follows: An ion of a certain u, v, w velocity class (u perpendicular to the electrodes, v and w parallel to them) leaves the ionized gas, is accelerated by B, is given an added

transverse velocity by the hole, and is then retarded by C so that it may not reach C. The v velocity axis is chosen in the sense and direction of the radius vector, r, from the center of the hole to the point at which the ion path cuts the plane of the hole. The transverse velocity $\dot{r}$ acquired by the ion increases its "transverse energy" by $\frac{1}{2}(\dot{r}^2+2\dot{r}v)$ and decreases its "longitudinal energy" by the same amount, Hence only when

$$\tfrac{1}{2}u^2-\tfrac{1}{2}\dot{r}^2-\dot{r}v \geqq \epsilon V_C/m \tag{30}$$

is the ion able to reach C, V_C being the retarding voltage on C. From Eq. (11)

$$\dot{r}_f = nr', \quad n=-\epsilon E/m\dot{z}, \text{ a constant}$$

so that the relation (30) can be written

$$\tfrac{1}{2}n^2r'^2+nr'v-(\tfrac{1}{2}u^2-\epsilon V_C/m)\leqq 0 \tag{31}$$

The two roots r_1, r_2 $(r_1<r_2)$ of the equality partially fix the respective radial limits ρ_1 and ρ_2 between which an ion of a certain velocity class in a certain retarding field (V_C) must pass in order to be collected. But besides the mathematical relations

$$\rho_1=r_1, \quad \rho_2=r_2 \tag{32A}$$

there are the additional dominant physical limitations on ρ_1 and ρ_2

$$0\leqq\rho_1\leqq\rho_2\leqq a \tag{32B}$$

Now the effective area of the hole for (u, v, w) ions is

$$\pi(\rho_2^2-\rho_1^2)$$

Accordingly the current of (u, v, w) ions is

$$i_{u,v,w}=2h'h''m^2I_+(\rho_2^2-\rho_1^2)u\exp[-h'mu^2-h''m(v^2+w^2)]du\,dv\,dw \tag{33}$$

the u velocity distribution being characterized by a different temperature from the v and w velocity distribution because in the body of the discharge there is a small electric field perpendicular to the electrodes which makes the longitudinal components of velocity greater. The relation between the h's and temperature are given below Eq. (36B).

Denoting the sum of $(\rho_2^2-\rho_1^2)$ for a positive and an equal negative value of v by A, and using the variable

$$\bar{u}^2=u^2-2\epsilon V_C/m$$

($\bar{u}$ being the final u velocity before impact on C of an ion passing through the middle of the hole), (33) becomes

$$i_{u,v}=2\sqrt{\pi h''m}h'mI_+e^{-2N'\epsilon V_C/m}A\bar{u}\exp(-h'm\bar{u}^2-h''mv^2)d\bar{u}dv \qquad (34)$$

after integration for all values of w. The limitations on ρ_1 and ρ_2 imposed by (31), 32A), (32B) necessitate breaking up the $\bar{u}$, v plane into several sections for the integration of (34) as shown in Fig. 5.

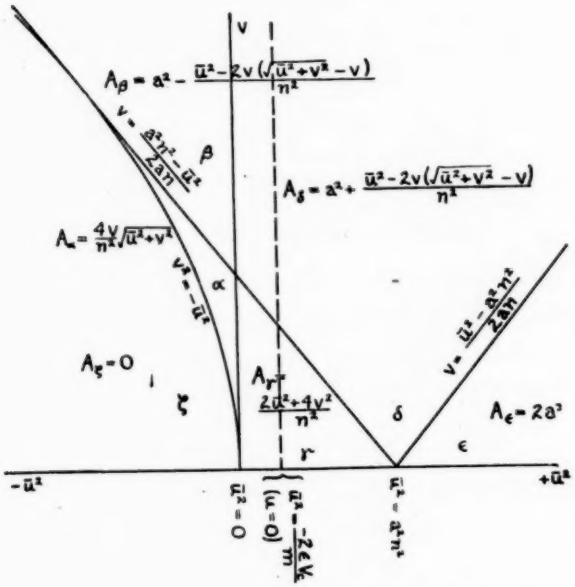

Fig. 5.

The values of the A's there given are the values appropriate to a hole all points of which are at the same potential. This is not true of the actual situation, the potential in the hole being variable and given by Eq. (15), Within the mathematical limitations of the present theory, it is sufficient, except in Eq. (39B), to write

$$A_\alpha=4\Theta\frac{v}{n^2}\sqrt{\bar{u}^2+v^2}, \quad A_\gamma=2\Theta\frac{\bar{u}^2+2v^2}{n^2}$$

where
$$\Theta=1+2a\bar{E}/\pi V_B=1-\frac{2}{\pi}\sqrt{V_t/-V_B}\,. \qquad (35)$$

The integration limits are 0 and $+\infty$ for v and $-2\epsilon V_C/m$ and $+\infty$ for $\bar{u}^2$. For accelerating potentials, $V_C<0$, that is, the lower $\bar{u}^2$ limit lies to the right of the v-axis as indicated by the dotted line, while for

retarding potentials, $V_C>0$, that is, the lower $\bar{u}^2$ limit lies to the left of the v-axis. Practically, as long as $2\epsilon V_C/m$ is considerably less than a^2n^2 and $h'm\ a^2n^2>>1$, the integration may be simplified by taking $A_\beta=A_\alpha$ and $A_\delta=A_\epsilon=A_\gamma$.

The integration then gives

$$i=-\theta\frac{i_C}{V_t}(V_C+V'+V'') \qquad \text{for } -V_t<<V_C\leqq 0 \quad (36A)^8$$

$$i=-\theta\frac{i_C}{V_t(V'-V'')}\left(V'^2\exp\frac{V_C}{V'}-V''^2\exp\frac{V_C}{V''}\right) \text{ for } V_t>>V_C\geqq 0 \quad (36B)^8$$

Here $i_c=\pi a^2I_+$, is the constant ion current when all ions are collected; $V_t=m(na)^2/2\epsilon$ is the voltage equivalent to the transverse velocity acquired by an ion grazing the edge of the hole; $V'=-1/2h'\epsilon=-kT'/\epsilon$ is the reciprocal of the slope of the semi-log plot (base e) corresponding to the temperature T' of the longitudinal velocity distribution; and $V''=-1/2h''\epsilon=-kT''/\epsilon$ is the same for the transverse velocity distribution.

The behavior of i for values of V_C less (more accelerating) than those covered in (36A) is very complicated except when $V''=0$ and therefore the general case will not be dealt with.

When transverse and longitudinal temperatures are equal (36B) reduces to

$$i=-\theta\frac{i_C}{V_t}(2V'-V_C)\exp\frac{V_C}{V'},$$

$$\text{for } V'=V'',\ V_t>>-V',\ V_t>>V_C\geqq 0 \qquad (37)^8$$

the equation of a curve on a semi-log plot which has half the slope at $V_C=0$ that it has at $V_C=\infty$ and only approximates to a straight line of slope $1/V'$ for large values of V_C.

When the transverse temperature is zero, $V''=0$ and the Eq. (36*B*) gives a straight semi-log plot of slope $1/V'$. In this case it can also be shown that

$$i=i_C \qquad \text{for } V_C\leqq -V_t \qquad (38A)$$

$$i=-\theta\frac{i_C}{V_t}\left\{V_C+V'\left[1-\exp\frac{V_C+V_t}{V'}\right]\right\} \text{ for } V_t>>-V',\ V_t<V_C<0 \quad (38B)$$

[8] See section IX, §§B and C.

When both transverse and longitudinal temperatures are zero but the ions have a longitudinal drift velocity corresponding to V_D volts the equations for the volt-ampere characteristic become

$$i = i_C \qquad \text{for } V_C \leqq V_D - V_t \tag{39A}$$

$$i = -\theta' \frac{i_C}{V_t}(V_C - V_D) \qquad \text{for } V_D - V_t \leqq V_C \leqq V_D \tag{39B}$$[8]

$$i = 0 \qquad \text{for } V_C \geqq V_D \tag{39C}$$

Here θ' is similar to θ except first, that the value of $\bar{E}$ to be used in it is that corresponding to $V_C = V_D$ instead of $V_C = 0$, and second that when V_C leaves the neighborhood of V_D and approaches $V_D - V_t$, θ' increases and approaches 1.

VIII. Measurements on Positive Ions: Interpretation of Experimental Curves

A. The potential of the discharge with respect to the anode. The voltage readings, E_C, do not give the position of $V_C = 0$ for they measure potential from the anode which is a few volts negative with respect to the discharge itself. It follows that the reading on the E_C scale of the line $V_C = 0$ is the potential of the discharge with respect to the anode. Now, Eq. (36A) shows that if a linear plot be made of the volt-ampere characteristic, a portion of it up to $V_C = 0$ will be straight. The curves of Fig. 6[9] obtained by Mr. C. G. Found using a mercury vapor arc in a tube built by Mr. A. F. Dittmer show this well. Unfortunately the deviation from a straight line is so slow at small positive values of V_C that the actual position of $V_C = 0$ cannot be found by simple inspection of the curve.

A method for finding the point $V_C = 0$ is to plot a certain root of the deviations from the straight line, against E_C. The straight line drawn through the resulting set of points cuts the E_C-axis at $V_C = 0$. The root to be used varies from the square root for $V''/V' = 0$ to the 2.7th root for $.2 \leqq V''/V' \leqq 1$ and this results in an uncertainty in the value of the discharge potential.

As an example, consider the curves of Fig. 6. Both the square root and 2.7th root of the deviations are plotted as crosses, the intersections of the straight lines through these with the axis are marked,

[9] These curves were made before any of the present theory had been developed and no particular precautions in regard to the shape or uniformity of the holes in electrode *B*, to the measurement of the distance between *B* and *C*, or to the accurate measurement of the small ion currents at the higher retarding voltages were made. Experiments in which these precautions are being observed are under way.

and it is noted that the uncertainty is about 0.1 volt. For curve A, E_C, at $V_C=0$, lies between 3.6 and 3.7, while for curve B, E_C at $V_C=0$, lies between 3.7 and 3.8 volts.

B. The fundamental transverse voltage, V_t. The slope of the linear portions of the characteristics in Fig. 6 is $-\theta i_c/V_t$. Since i_c is known

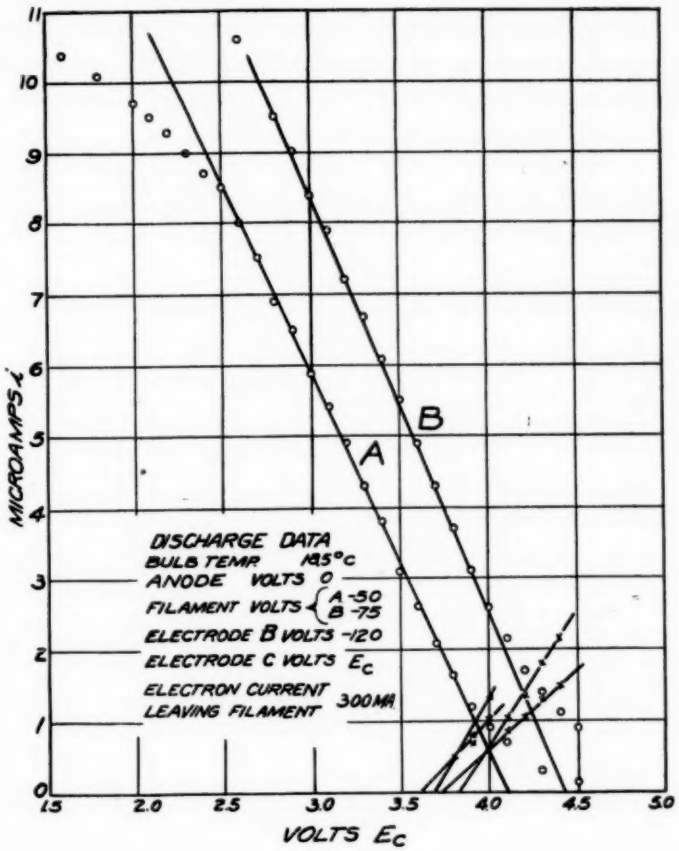

Fig. 6.

in each case, V_t can be calculated by using Eq. (35) and is found to be 1.9 and 2.2 volts respectively for curves A and B.

An independent calculation of V_t can be made using Eq. (11), $\bar{E}$ being calculated by Eq. (14) with $V_C=0$. The distance between B and C was not, unfortunately, accurately known, but lay between 0.1 and 0.2 cm and was estimated at 0.15 cm for the field strength calculation. On this basis it was found that:

For curve A; V_t (calc) = 2.4 v., V_t (from curve) = 1.9 v.
For curve B; V_t (calc) = 2.65 v., V_t (from curve) = 2.2 v.

a satisfactory agreement in view of the uncertainty of hole and size and electrode distance.

C. The voltage V′ corresponding to the "longitudinal temperature," $T' = -11{,}600\ V'$. Eq. (36B) shows that when a semi-log plot of the volt-ampere characteristic becomes straight at positive values of V_c, then the reciprocal of the slope is V'. The experimental difficulty is encountered that the determination of this quantity depends on the smaller and, therefore, usually the less accurate current measure-

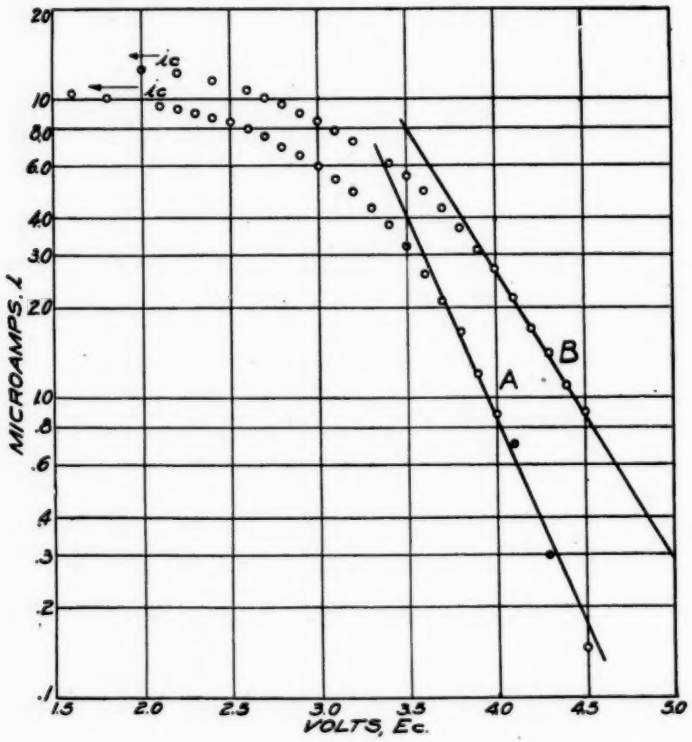

Fig. 7.

ments. This trouble appears in Fig. 7, the semi-log plot of the observations already shown in Fig. 6. Using the straight lines drawn here as the best approximation:

For curve A; $V' = -0.32$ v., $T' = 3360°\text{K}$

For curve B; $V' = -0.45$ v., $T' = 5200°\text{K}$.

D. *The voltage V″ corresponding to the "transverse temperature,"* $T'' = -11{,}600\ V''$. Eq. (36A) shows that the intercept of the E_c-axis in Fig. 6, which is terminated by $V_c = 0$ at one end, and at the other by the intersection of the straight line plot continued is the quantity

$-(V'+V'')$. This relation may be used to calculate V''. Assuming that the value of E_C corresponding to $V_C=0$ is, for curve A, 3.6 v. and, for curve B, 3.7 v., and noting that curve A intersects the E_C axis at 4.1 v. and curve B at 4.4 v., we have

For curve A; $V''=-0.18$ V., $T''=2100°$K
For curve B; $V''=-0.25$ V., $T''=2900°$K.

Even if the other values of E_C, namely 3.7 and 3.8 v. had been used, the ratio V''/V' would still have exceeded 0.2, showing that 2.7 was the correct root of the deviations and that the proper values for E_C were used above.

A further approximation to V'' can be made using (36B) by solving it for the V'' which appears in the denominator, using an approximate value of V'' in the term involving the exponential and using a value of i at which the second exponential term is relatively small. Thus for curve B at $E_C=4.4$ v., $i=1.1\mu$a., it is found that $V''=-0.24$. Accordingly $T''=2800°$K and $T''/T'=V''/V'=.53$.

E. *The decrease in i when $V_C \leqq -V_t$.* Eqs. (38) show that when $V''=0$, i is constant up to $-V_t$. But the existence of initial transverse velocities results in some ions being cut off prematurely so that a decrease in i at $-V_t$ indicates a transverse temperature different from zero. In the present case part of the decrease must be ascribed to non-uniform hole size which affects the characteristic shape most vitally in this region. Accordingly this portion of the present characteristics is unsuited to interpretation. Even in the ideal case, however, the theoretical equation for the current is very complicated in this region and also subject to errors listed in section IX, §§B and C, so that any quantitative interpretation appears impossible.

IX. Measurements on Positive Ions: Errors and Experimental Precautions

A. *The condition $V_t >> -V'$ of Eqs.* (36) *and* (37). The necessity for simplifying the integration of the ion distribution equation led to this condition. By taking $A_s=A_e=0$ an upper limit to the error is found to be about 4 percent for $V_t=-5V'$, but the actual situation is much more favorable than this. Probably the best criterion of the fulfillment of this condition is the straightness of the linear plot, Fig. 6.

B. *Effect of ion paths not parallel to hole axis.* The ions which go through the hole follow paths which deviate appreciably from parallelism with the hole axis. Insofar as this arises from the "transverse temperature," it is small, about $\sqrt{V''/V_B}$ or 0.045 radians in the case of curve B, and its effect is negligible.

The non-parallelism which arises from the acquired transverse velocity itself is only slightly larger, but its effect is not negligible. It results in a change in the effective area of the hole, which can be calculated from Eq. (13). $V_D = -V'$ may be neglected so that $\Delta A/A = .15\ a\bar{E}/V_B = -.022$ for curve B. That is, the effective area of the hole is 2 percent less than its true area. But cases in which this error is appreciable may arise. An examination of the integration leading to Eqs. (36A) and (36B) reveals that the hole size is not involved. This quantity enters only when the final substitutions listed under (36B) are introduced. Accordingly the difficulty can be readily analyzed by more exact definition. Retaining the definition of i_e as the total ion current through the hole it becomes necessary to append the factor $1+\Delta A/A$ to the mathematical expression for i_e which follows Eq. (36B). This introduces a correction coefficient of $1-\Delta A/A$ which is to be applied to the right members of Eqs. (36A), (36B), (37), (38B), and (39B). The values of V_t (from curve) of section 8B are thus 2 per cent low. *None of the other calculations based on the experimental curves is, however, affected by the non-parallelism of the ion path and the axis of the hole.*

C. *Thickness of the hole.* In sections II and IV it was concluded that neither the depth of the orifice nor its shape, provided it was of the proper symmetry, has any effect on the transverse velocity acquired by an ion whose path is perpendicular to B. The path is not perpendicular to B primarily on account of acquired transverse velocity, so if the hole is cylindrical and has appreciable depth the radial distance at which the ion enters it is less than the radial distance at which the ion leaves it. Such an ion acquires a maximum transverse velocity when it grazes the edge of the hole as it leaves. The radius appropriate for calculating this velocity is the mean of the radius of entrance and the radius of the hole itself. This mean radius is seen to be $a-\frac{1}{4}t\sqrt{-V_t/V_B}$ [or $a(1+t\bar{E}/4V_B)$ by Eq. (11)]. Here again the hole size is involved, and the reasoning of §B applies. But since here the maximum acquired transverse velocity is not directly observed, the mathematical definition of V_t as it appears below Eq. (36B) will be retained. Accordingly no change has to be made in the equations because of this change in effective radius. There is, however, an accompanying decrease in the effective hole area which allows ions to pass. The complete fractional increase (algebraic) in area is by Eqs. (13) and (11)

$$\Delta A/A - t/a\sqrt{V_t/-V_B} \text{ or } -\sqrt{V_t/-V_B}(0.15+t/a) \qquad (40)$$

where t is the depth of the cylindrical part of the hole. In the new experiments which are contemplated it is planned to make the holes conical so as to reduce t to zero.

The initial transverse velocities of the ions also cause the ion paths to deviate from the perpendicular, the effect here being to reduce the effective area of the hole for ions having $v>0$ and leave it unchanged for ions having $v<0$. As this only involves one half the ions, and as $V_t >> -V''$, any error from this cause is quite small compared with those already dealt with.

D. *Equivalence of mathematical and physical equipotentials.* In order that the mathematical solution of the field about a hole (slit) should correspond to the physical conditions it has been pointed out in section 3 (section 1) that the distances, sheath edge to electrode B and electrode B to electrode C, should be at least 3 radii (3 slit widths).

E. *Return of ions through the hole.* Any ions which are not collected by C and re-enter the sheath through the hole in B increase the space chatge there and decrease the primary ion current. As the space charge conrribution of the returned ions relative to the space charge contribution of the primary ions at any point is equal to the density of returned ions relative to that of primary ions at that point, an estimate of this error is easily made. Neglecting the initial transverse velocities of the ions for the moment, that is, assuming that all ion paths in the sheath are perpendicular to B, the transverse velocity acquired by an ion in passing through the hole at a distance r' from the center corresponds to an angular deflection of the path at B of $\sqrt{V_r/-V_B}$ radians, V_r being the acquired transverse voltage. The distance traveled before the ion reaches B again is 2δ (δ being the electrode separation) and consequently the lateral displacement of the ion when it again reaches the plane of B is $\Delta_1 r = 2 \cdot 2\delta\sqrt{V_r/-V_B}$, assuming that it follows a parabolic path.

The density of returning ions relative to outgoing ions is then $r'^2/(r'+\Delta_1 r)^2$ at B, and this can be evaluated using the above equation together with Eq. (11) and calculating $\bar{E}$ as in section VI, §B. Since, however, the returning ions contribute most effectively to the space charge when they are near the sheath edge the calculation of their radial distances must be carried one step further, that is, into the sheath once more, noting, of course, that in repassing the hole the ions acquire additional transverse velocity. To calculate the relative space charge contribution of these ions their relative density one quarter of the distance from sheath edge to electrode B was selected as a fair average value. As these ions have insufficient longitudinal energy to penetrate the sheath edge they are reflected from it and make a second

space charge contribution as they return to B which must also be added. The computation shows that the relative space charge contribution is a function only of the ratio of electrode separation, δ, to sheath thickness, σ. It has a maximum value amounting to 0.7 per cent when $\delta/\sigma = 0.7$ and drops to 0.35 per cent when δ/σ equals either 0.2 or 2.5.

Turning now to the effect of the presence of random initial transverse velocities it is seen that this has the general tendency to decrease the returned ion density, and therefore to decrease the error. Under all circumstances, then, the return of ions through the hole may be neglected.

F. *Limiting of ion current to C by space charge.* With an electrode separation greater than the sheath thickness it is evident that if B were perfectly transparent to ions, then theoretically no ions could reach C on account of space charge. Experimentally, however, there is only a narrow beam of ions flowing through a space devoid of charge, and this beam tends to diffuse on account of initial and acquired transverse velocities. It is evident that the thinner the beam is in the sheath, the greater the separation δ of the electrodes relative to the sheath thickness, σ, may be. The condition that space charge limitation shall not set in may, therefore, be roughly expressed as $\delta/\sigma \leqq \kappa\sigma/a$ or $\delta a/\sigma^2 \leqq \kappa$, where κ is a constant. In the present case $\delta/\sigma = 2$, $\sigma/a = 6$, hence $\delta a/\sigma^2 = 1/3$. Taking this as the maximum advisable value the condition above becomes

$$a\delta/\sigma^2 \leqq 1/3 \tag{41}$$

G. *Reduction of potential at the center of the hole by space charge.* If no non-uniformity is introduced into the space charge distribution in front of B by the hole, this charge gives no transverse field and cannot, therefore, change the potential at the hole center except insofar as the field E_1 is affected, a factor already dealt with in Eq. (14). But the ions which have passed through B have a non-uniform distribution and may affect the potential. Assuming, (1) a uniform field between B and C to calculate the ion velocities, (2) that the ions form a cylindrical beam behind B, and (3) that the density of ions returning from C is negligible, it is found that the change in potential sought amounts to only a few millivolts in the case of curve B. Accordingly it is most unlikely that this factor would ever become appreciable.

H. *Effect of ion repulsion.* On account of the concentration of charge in the beam, any ion which is not on the beam's center line is subject to a transverse repulsive force which tends to diffuse the beam still

more and by increasing transverse velocities, reduce longitudinal ones. No really satisfactory estimate of the magnitude of this effect has been made on account of numerous complicating factors. But in order to understand the situation better, a calculation based on certain simplifying assumptions has been made. It is easily seen that the only class of ions which is of interest is that composed of ions which just reach the plate at some fixed collector voltage. Assuming that the beam suffers no diffusion such as dealt with in §E, those ions of this class will be most affected which travel along the outside of the beam. We consider these ions only. The predominating part of the repulsion velocity acquired by such an ion will be acquired while the ion is moving either most slowly or in the vicinity of the densest space charge. Both conditions occur at the same place, namely, in the vicinity of the collector. On this basis the following assumptions were made: (1) the ion beam is bounded by the right circular cylinder which has the hole for a base, as already mentioned above, (2) an ion acquires a negligible repulsion velocity until it is within a distance of the collector of the same order as the radius of the beam (hole), (3) on account of the electrical image of the beam in the collector, the charge effective in repulsion is that in a cylinder cut from the beam which is bounded by the planes $x=x_i/4$, $x=7x_i/4$ and of diameter $3x_i/2$, x being distance from the collector, and x_i being the x of the ion, (4) the repulsive force exerted by this charge is that of a sphere of uniform charge density, of the same total charge as the cylinder, of the same diameter as the cylinder, which is tangent to the cylindrical beam boundary at the ion, i.e., x_i, (5) the charge density in the beam is given by the space charge equation treating the collector as a plane cathode and using the current density to electrode B.

Then for mercury ions it is found that the voltage corresponding to the repulsion velocity is

$$V_R''=8.43\times10^3 I_+^{2/3}a^{4/3} \tag{42}$$

For curve B, Fig. 7, $I_+=8\times10^{-4}$ amps/cm^2, $a=0.0125$ cm. Hence $V_R''=0.21$ v.

Contrary to assumption (3) the repulsion velocity acquired by the ion in travelling from $x_i=3a$ to $x_i=a$ is not negligible, though less than this. Assuming the charge between $x=a$ and $x=3a$ (as given by the space charge equation) to be redistributed uniformly throughout a sphere of radius a which is always tangent to the beam boundary at the ion as the ion travels from $3a$ to a, it is found that

$$V_R'=3.88\times10^3 I^{2/3}a^{4/3} \tag{43}$$

whence $V_R' = 0.097$ v., and the total repulsion voltage is

$$V_R = (\sqrt{V_{R_t}} + \sqrt{V_R''})^2 = 0.59.$$

This is very large compared, for instance, with V'' which is 0.24 for this curve. A re-examination of the assumptions shows that (1) is certainly not fulfilled and (5) is open to doubt. It is not unreasonable, however, to suppose that the actual space charge, including ions returning to B, if confined as contemplated in assumption (1), would be near enough on the average to that given by assumption (5). Accordingly, attention must be confined to (1). The considerations of §E show that three quarters of the way from B to C only a fraction, λ, say, of the ions lie within the cylindrical boundary of assumption (1). Accordingly, the actual force exerted on the ion by the charge inside the cylinder is certainly less than λ times the calculated force. λ is given by the approximate formula $\lambda = .29\sigma/\delta$, in the range $1.4 < \delta/\sigma < 4.0$. But the repulsive force of ions outside the cylinder balances a portion of this force, say $\sqrt{\lambda}$. Thus the actual force is $\lambda^{3/2}$ of the calculated force, and hence the repulsion voltage is λ^3 or $0.024\,(\sigma/\delta)^3$ of that calculated. In the present case V_R becomes $0.59 \times 0.003 = 0.002$. This, if correct, is small enough compared with V'' to be neglected, but the uncertainty involved demands that an experiment with ions or electrons of known temperature be done. With the above corrections the repulsion voltage in terms of the molecular weight, M, of the ion becomes

$$V_R = 99 M^{1/3} I_+^{2/3} a^{4/3} (\sigma/\delta)^3 \tag{44}$$

Summarizing the factors which vitally affect the interpretation of an experimental curve in the form of conditions to be satisfied, we have, from the paragraphs noted[1]

A. $$V_t >> -V' \quad \text{(Validity of integration)} \tag{45}$$

F. $$\frac{\delta}{a} \leqq \frac{1.82 \times 10^{-8} V_B^{3/2}}{M a^2 I_+} \quad \text{(Space change limitation)} \tag{46}$$

H. $$\left.\begin{matrix} -V'' \\ -V' \end{matrix}\right\} >> 99 M^{1/3} I_+^{2/3} a^{4/3} (\sigma/\delta)^3 \quad \text{(Ion repulsion)} \tag{44}$$

RESEARCH LABORATORY,
GENERAL ELECTRIC COMPANY,
SCHENECTADY, NEW YORK.
March 11, 1926.

MOBILITY OF THE IONS IN THE CORONA DISCHARGE

By W. M. Young

Abstract

The mobility of the ions generated in the d.c. corona discharge have been directly measured. Gas, moving with a uniform velocity, was ionized in a cylindrical corona tube and then passed into an ion chamber consisting of a hollow cylinder with electrodes along the axis. The ion current to the last electrode, when plotted as a function of the cylinder potential, exhibited maxima which indicated the presence of groups of ions. Calculation revealed a large number of groups whose mobilities, for oxygen, nitrogen, and carbon dioxide, were all less than .716 cm/sec per volt/cm, ranging down to 10^{-5} cm/sec per volt/cm. Nearly all mobilities were found below 10^{-2}, the ions apparently being generated in equal numbers, except now and then a greater number of a certain mobility were formed. The fact that the ions all possessed small mobilities seems to indicate that J. Kunz made the correct assumptions when he calculated the average value from the experimental determination of the pressure increase in the d.c. corona.

Introduction

VARIOUS pressure effects have been observed and measured for the a.c. and d.c. corona, among which is a pressure increase in the d.c. corona which appears about 1.5 seconds after the discharge is applied and which may easily amount to 3 cm of water. This pressure has been ascribed to the presence of ions of small mobility. The generation of these ions and the continual repulsion of them from the wire of a cylindrical corona tube necessarily cause an "ionic expansion" of the gas. The pressure observed, then, is due to these ions striking the walls of the corona tube.

J. Kunz,[1] from the experimental determination of such pressure increases in different gases has calculated the average mobility of the ions, his results for the gases H_2, N_2, CO_2, and O_2 being respectively: 15.1, 5.05, 1.61, and 0.23×10^{-3} (cm/sec per volt/cm). This, however, gave no information as to whether more than one type of ion was present. O. Blackwood[2] and P. J. Nolan[3] have studied the ionization produced by water spray and Erikson[4] that produced by radioactive materials. Contradictory results have been obtained on the question of whether or not groups of ions were formed. It is the purpose of

[1] J. Kunz, Phys. Rev. **19**, 169(1922).
[2] O. Blackwood, Phys. Rev. **16**, 85 (1920).
[3] P. J. Nolan, Phys. Rev. **18**, 185 (1921).
[4] H. A. Erikson, Phys. Rev. **21**, 720 (1923).

these experiments to determine the mobility of the ions formed in the corona discharge and to find out whether or not ions exist of the low mobility which Kunz has assumed in his explanation of the corona pressure.

Method

Gas free from moisture and dust was passed at a uniform rate through a short corona tube, the central wire of which was positive. The gas there ionized was passed into a tube maintained at some positive potential. The positive ions were driven toward the axis of the tube and the charge on some removed by an electrode connected to earth. The current due to other ions was measured by a quadrant electrometer connected to a second electrode. By varying the cylinder potential it was possible to obtain the electrometer current as a function of that potential and the graph of the results showed maxima which indicated the ionic

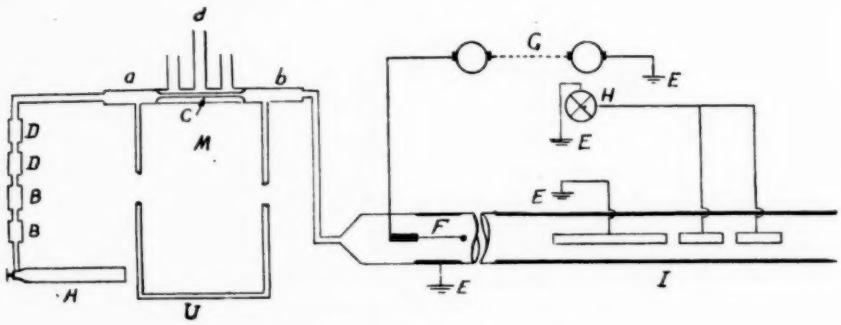

Fig. 1. Arrangement of apparatus.

mobility of certain groups. The curves contained maxima of varying magnitude. If but one mobility was present, only one maximum would be formed, but if two groups of ions existed the resulting curve would show a maximum for each group. It was not necessary to know the absolute value of the electrometer current as the mobility was determined by an equation which required only that the current reach a maximum or peak value.

Apparatus

The gas from commercial steel tanks *A* (Fig. 1) was passed through two tubes of $CaCl_2$ *B*, and two of P_2O_5 *D*, to remove moisture. Glass wool was used to remove dust particles. The gas flow was measured by a gas meter *M*, constructed on the Venturi principle, consisting of two tubes *a* and *b* of 1.3 cm internal diameter. The capillary tube *c* of 2 mm internal diameter, was surrounded by a water jacket so that

constant temperature could be maintained and measured by a thermometer at *d*. The use of the water jacket was not imperative, however, as the capillary temperature varied at most by 3°C and since the capillary was made of Pyrex glass, little change in tube diameter resulted. The *U* tube was half filled with Stanolax, a light oil practically non-volatile at room temperature. The capillary was calibrated by means of a standard gas-meter. Two capillaries were used for the various gas flows, one of diameter 1 mm and the other of diameter 2 mm. In using the gas-meter care was exercised to maintain gas velocities through the capillaries which were below the critical velocity at which turbulent flow began. The gas-meter was calibrated with air, therefore in using it for nitrogen, oxygen, and carbon dioxide it was necessary to introduce correction factors in accordance with Reynold's equation.

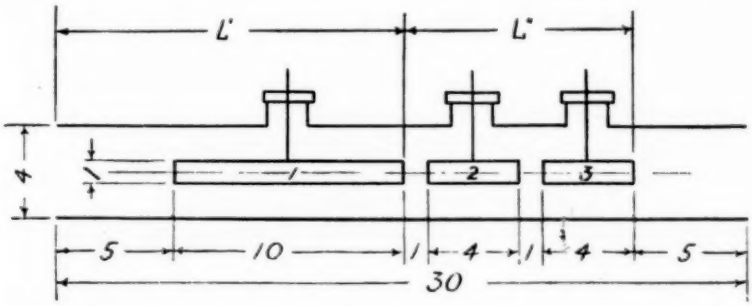

Fig. 2. Details of small ion chamber. All dimensions are in cm. The electrodes are brass tubes with closed ends.

It was desirable to have the ions generated in a small volume so that all would have approximately the same age. To this end a short corona tube *F* was used which had a length of 4 cm and internal diameter of 4.1 cm. The corona wire was always of brass, .4 mm in diameter, and had an exposed length of 4 cm. A ball of sealing wax on one end prevented the formation of a point discharge. The remaining length of corona wire was encased in hard rubber so that only the vertical portion of the lead-in wire (2 mm in diameter) and the corona wire actually within the corona tube were exposed. Corona wire and ion chamber were placed close to each other and arranged so that the gas flow through them would be in stream lines, and as uniform as possible.

A shunted D'Arsonval galvanometer was placed in the low voltage side of the corona circuit to indicate the corona current. The potential for the corona discharge was furnished by 38 d. c. shunt generators *G* of .25 kw capacity, rated at 500 volts each, connected in series. Their

field currents were so controlled that the corona potential could be established and maintained at any value.

A preliminary experiment suggested the use of the Zeleny method; accordingly two ion chambers were built which differed only in dimensions. Fig. 2 illustrates the form of the chamber. The insulators were constructed of a sulfur plug 1 cm in diameter and 1.5 cm high, separated from a hard rubber plug 1.5 cm in diameter and 1.5 cm high, by a tinfoil guard-ring connected to earth. They were supported in brass collars in the long tube. The brass rods, 2 mm in diameter, passing through the insulators were fastened by taper joints to the electrodes and served as electrode supports and connecting wires.

The second ion chamber had a total length of 112 cm and an internal diameter of 4.8 cm. The electrodes were 50, 25, and 25 cm in length respectively, and of 2 cm diameter. They were spaced 1 cm apart and 5 cm from the ends of the tube. In future work the left ends of the electrodes will be so shaped that stream line flow of the gas is preserved. With square ends on the electrodes there is a chance for turbulence.

If uniform gas velocity across the tube be assumed, then for the Zeleny apparatus the mobility K of the ions is given by

$$K = Q\log_e(b/a)/2\pi E'(L'+L'') \quad (1)$$

$$= Q\log_e(b/a)/2\pi E''L' \quad (2)$$

where Q is the quantity of gas passing any cross section per second, b and a are the radii of cylinder and electrode respectively. L' is measured from the left end of the cylinder to the right end of electrode 1, and L'' is measured from the right end of 1 to the right end of 3. E' and E'' are the voltages necessary to produce maximum ion current to $(L'+L'')$ and L' respectively. Only equation (1) was used in these measurements.

The positive potential for the cylinder of the ion chamber was furnished by flashlight and "B" batteries. To exclude electrostatic effects, the ion chamber was inclosed in a metal box and the wire leading from the ion chamber to the electrometer in a shielded glass tube. It was also necessary to shield the quadrant electrometer by a metal box, which also served to retain a rather dry atmosphere about the instrument, calcium chloride being placed in the box.

In making the measurements electrode 1 was connected to earth, 2 and 3 were connected to the electrometer. The potential necessary to cause maximum current to 2 and 3, then, was the same as that required to give a constant current to $(L'+L'')$. For one group of ions the curve between electrometer current and cylinder potential would increase to a maximum and then decrease to zero as the cylinder po-

tential increased. If two groups of ions were present two maxima would exist etc.

Several curves were taken with air merely to ascertain the form of the curve to be expected and to adjust the apparatus, but no curves are here reproduced. Suffice it to say, however, that an extremely large number of maxima were obtained in these rough measurements.

In all cases of the pure gases, every curve taken was duplicated two or three times so that the existence of the maxima was definitely established. The mobilities listed below are labeled S (strong), F (fair), W (weak). Only such mobilities are listed as were well defined on at least two curves.

The electrometer deflection due to the ion current in the ion chamber was generally small, of the order of 10^{-2} mm per second except for a small region of the nitrogen curves where it mounted up as high as 14 or 16 mm per second. It was practically impossible to repeat any curve point for point. Even if two curves were taken consecutively it was generally found that all deflection velocities would be increased or decreased. This was not due to leakage over the insulators in the ion chamber because the electrometer was tested before and after taking a set of readings, for insulation leakage, and in all cases this leakage was negligible, either zero or about .1 mm in 60 seconds. Calcium chloride was frequently used to produce a dry atmosphere within the ion chamber shield but it was found that the guard sleeve and sulfur plug were sufficiently effective in preventing leakage.

Results and Discussion

Oxygen. The whole of the region investigated is shown in Fig. 3, curves (1) and (2). It will be noted that in all cases the ion current is small, and seems to attain a certain average value above which the maxima stand out. In some cases scattered points will be noticed. The maxima have been drawn conservatively, none being indicated unless it occurred very pronouncedly on at least one other curve. In some cases a maximum has been indicated even if it occurred faintly, but in these cases it has been considered because of the fact that it occurred on nearly all curves taken in that region. It must be borne in mind that these curves were not taken on the same day or on consecutive days or with the same ion chamber; curve (1) was taken with the small ion chamber and curve (2) with the large ion chamber, (1) representing the region from 0 to about 2 volts on curve (2). This, coupled with the fact that the corona discharge is not an invariant discharge, may explain the shift of the average value of ion current.

A large quantity of ozone is found in the corona in oxygen, hence a considerable quantity of the energy passing through the corona tube was used in its formation. Since the corona current was kept constant

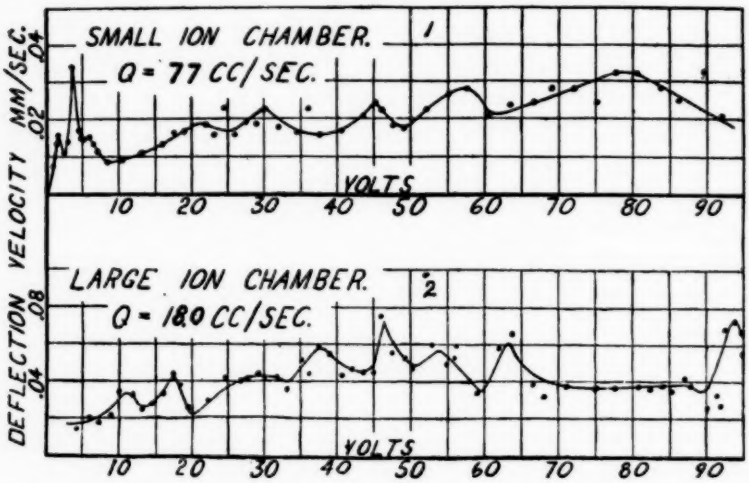

Fig. 3. Ion current in oxygen. Curve 1 represents the portion of curve 2 between 0 and 2 volts.

for all curves, this may be one reason for the small average value of the ion current.

The values of ion chamber potential, electrode length, and quantity of gas flowing per second are given below for the first seven points or mobilities secured for oxygen.

TABLE I

Sample set of data for the mobility of oxygen.

Cylinder potential E	Electrode length L	Gas per sec Q	Mobility K	Cylinder potential E	Electrode length L	Gas per sec Q	Mobility K
.75	25	76	.91	30	25	77	.023
.75	25	77	.92	29	25	76	.023
.75	25	78	.94	2.8	107	52.5	.025
			Ave. .92				Ave. .024
1.2	25	76	.57	45	25	77	.015
1.3	25	78	.54	45	25	76	.015
				67.5	25	120	.016
			Ave. .55				
2.85	25	76	.23				Ave. .015
3.00	25	78	.23	57.1	25	76	.012
3.5	25	79	.20	54.7	25	74	.012
				54.7	25	77.5	.012
			Ave. .23	54.7	25	76	.012
22.5	25	77	.031				
20.5	25	76	.033				Ave. .012
			Ave. .032				

Table II gives all the mobilities found, the number of times found, the number of curves taken over that region, and the strength of the peak in the curve.

TABLE II

Mobilities in Oxygen

Mobility cm/sec/volt/cm	Times repeated	Curves covering region		Mobility cm/sec/volt/cm	Times repeated	Curves covering region	
1.2×10^{-1}	3	3	W	3.8×10^{-3}	3	3	W
5.5 "	2	3	S	1.9 "	4	5	F
2.3 "	3	3	S	1.2 "	4	4	W
3.2×10^{-2}	2	3	W	9.4×10^{-4}	4	5	F
2.4 "	3	3	W	6.6 "	4	5	F
1.5 "	3	3	F	5.3 "	4	5	F
1.2 "	4	4	F	4.5 "	4	5	F
8.6×10^{-3}	3	4	S	3.9 "	4	5	W
6.6 "	3	4	W	2.8 "	3	5	S
5.4 "	2	3	F	2.1 "	1	1	S
4.6 "	2	3	S	1.8 "	1	1	S

In the case of oxygen as in the case of the other gases, the ion current was never brought to zero, in fact it showed no signs of going to zero even when the potential on the ion chamber cylinder was increased

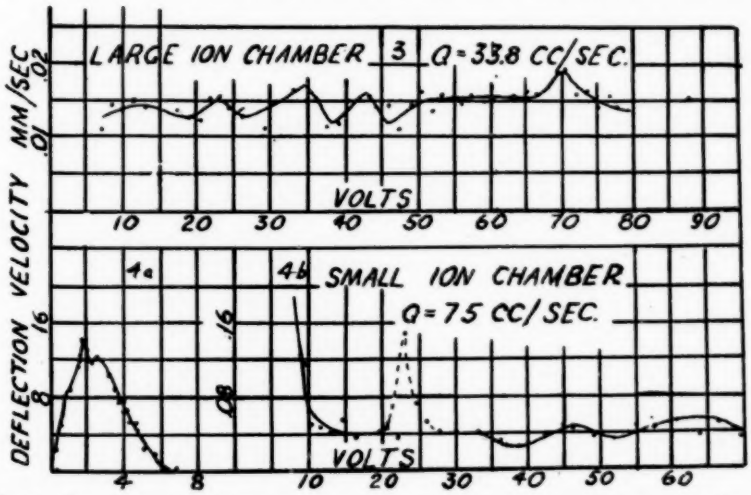

Fig. 4. Ion current in nitrogen. Curve 4*a* represents the region from 0 to 7 volts of 4*b*, and 4*b* in turn represents the region from 0 to 8 volts of 3. Apparently there is a maximum at *A* in 4*b* but it was not considered as it was not found on any other curves.

nearly 100 volts beyond that required to produce the minimum mobility listed. Hence, it may very well be that many more groups of ions are formed of exceedingly low mobility.

Nitrogen. This gas is unique among those used in that it gave a very high ion current in one small region, becoming 350 times as large as

the oxygen average. Mobilities calculated in this region were from .72 to .25 cm/sec per volt/cm. In all other regions the ion current was of the same order of magnitude as was found in the case of oxygen and the same characteristics may be here observed as were pointed out above, namely, a rather marked average ion current with now and then a maximum rising up. These curves were taken on different dates, but still have the same characteristics. The results are presented in Table III.

TABLE III

Mobilities in Nitrogen

Mobility cm/sec/volt/cm	Times repeated	Curves covering region		Mobility cm/sec/volt/cm	Times repeated	Curves covering region	
7.1×10^{-1}	2	2	S	2.1×10^{-3}	2	3	F
3.7 "	2	2	S	1.4 "	2	3	S
2.5 "	4	4	S	1.0 "	4	4	S
1.0×10^{-2}	2	2	W	6.6×10^{-4}	4	4	S
5.5×10^{-3}	3	3	F	3.8 "	3	3	S
3.8 "	4	4	W	2.9 "	1	1	F

Carbon Dioxide. In the case of carbon dioxide, one curve is shown for each part of the region investigated. It will be noticed that the curves rise continually for a considerable period and then seem to take on a slow decline. There are always these points of maximum ion current superimposed on a seemingly steadily and slowly changing ion current. The average of this slowly changing current is two or three times as great as in the case of oxygen and nitrogen. Because of the difference in Q, the quantity of gas per second, and the difference in size of the ion chambers, curve 5 represents the region from 0 to 3 volts of curve 6.

TABLE IV

Mobilities in carbon dioxide

Mobility cm/sec/volt/cm	Times repeated	Curves covering region		Mobility cm/sec/volt/cm	Times repeated	Curves covering region	
4.1×10^{-1}	4	4	S	7.9×10^{-4}	3	5	W
1.8 "	3	4	S	4.7 "	5	5	S
2.6×10^{-2}	4	4	S	2.8 "	4	5	S
1.0 "	5	5	S	2.3 "	4	5	S
5.8×10^{-3}	2	3	F	2.1 "	4	4	W
5.1 "	2	4	S	1.9×10^{-4}	4	4	F
3.7 "	2	3	S	1.7 "	4	4	S
2.6 "	5	5	S	1.4 "	3	3	S
1.0 "	4	4	S	1.0 "	2	2	S

Curves 6, 7a, and 7b, show the same region so that the maxima of the same number give the same mobility, and they illustrate well the variation in the shape of the curves for consecutive curves. The maximum

(a) of curve 5, is, of course, not determined by the points plotted but other curves covering the same region showed very clearly that the maximum existed. Therefore it is reproduced in order that the data may be complete.

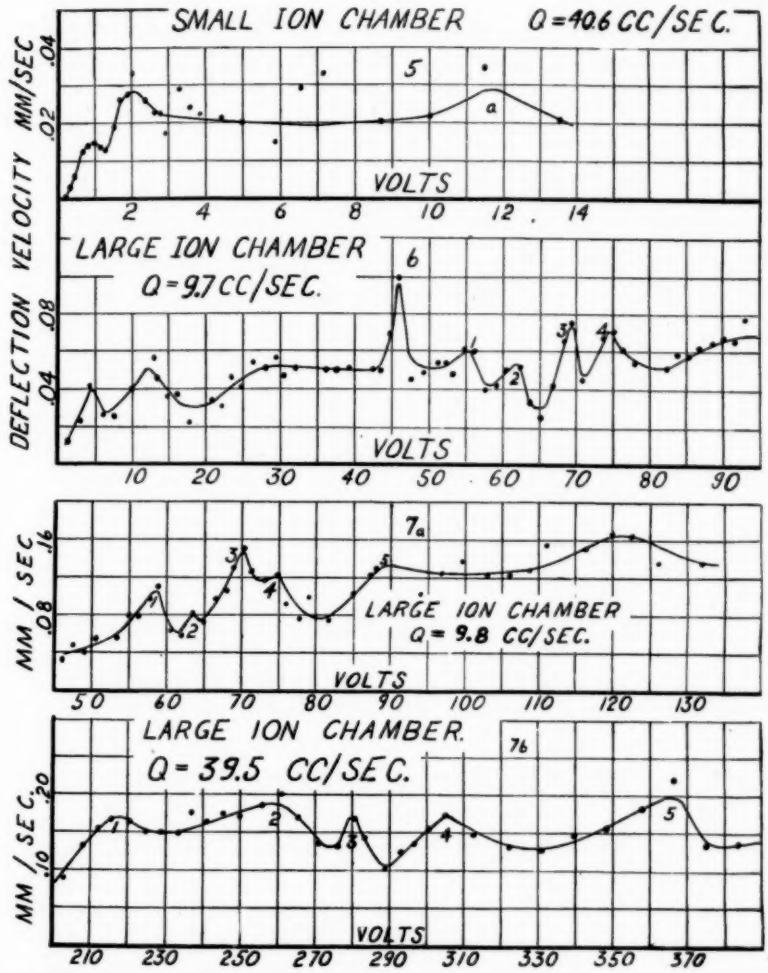

Fig. 5. Ion curve in carbon dioxide. Curves 6, 7*a* and 7*b* represent in part the same region and the numbered maxima on the three curves correspond, giving the same value of mobility.

The maxima were chosen very carefully and regions of severe scattering of points were not considered except as a maximum, well defined, was noted in another curve. The table of mobilities of the ions of carbon dioxide, is presented in Table IV.

Hydrogen was not used because of the instability of the discharge, it readily going over into the arc.

Discussion. Much progress has recently been made in enlarging the theoretical and experimental knowledge of the ions formed in the various gases by different methods, especially by L. B. Loeb, H. A. Erikson, and H. B. Wahlin. The problem is however hardly solved as there still remain contradictory statements in recent papers by Erikson,[5] who worked at atmospheric pressure, and Wahlin,[6] who used low pressures, regarding the influence of the mass and charge of the ion on its mobility. If it be tentatively assumed with Wahlin that the mass is the governing factor in the mobility, then it is possible to pick out mobilities in the above tables where the ratio of the mobilities is approximately equal to the inverse ratio of the square root of the molecular weight of the gases used. In the case of carbon dioxide, mobilities of carbon monoxide ions, corresponding to the mobilities of the nitrogen ions, and mobilities corresponding to those of oxygen ions would be expected. Several such cases were found. However if ions may acquire different charges then one might pick out mobilities in the different gases which are due to ions having two or three charges.

None of these figures is here given because the existence of such ions is not yet proved. It is indeed possible that all these mobilities may be attributed to metallic particles, atoms, or clusters of metallic molecules that are charged and that are formed by the disintegration of the corona wire by the discharge.

Attention is called to the fact that, of the mobilities given under the respective gases, some are above, some below the average value calculated by Kunz from the pressure increase. This is to be expected. The values of Kunz can only be checked by knowing the number of ions of each mobility which are formed, and by finding what pressure this totality of ions would create in the corona tube under the influence of the potential difference there present. The mobilities were not all found in the investigation as the curves were never brought back to zero, however all mobilities found are of the small value Kunz assumed.

A glance at the curves would seem to suggest that some of the peaks are drawn with greater sharpness than the method can give. It must be remembered, however, that the Zeleny method is one of high resolving power and further that the ordinates of the curves are arbitrary units and are exaggerated to show the form of the curves. Further

[5] H. A. Erikson, Phys. Rev. **24**, 502 (1924).
[6] H. B. Wahlin, Phys. Rev. **25**, 630 (1925).

work is now in progress with another form of apparatus and when results are secured the resolving power of both methods will be discussed.

Further Experiments

Long corona tube. As previously stated, a short corona tube was used so that all ions would have about the same age on entering the ion chamber. In order that the effect of a long corona tube might be noted one was constructed having a length of 30 cm, and a curve was taken on CO_2. As the distance between the corona tube and the ion chamber was the same as previously used, namely 25 cm, the curve should repeat itself in shape, only for greater corona current the ion current should increase. The youngest ions in the case of the long corona tube would be no older than the youngest ions of the short tube, but the

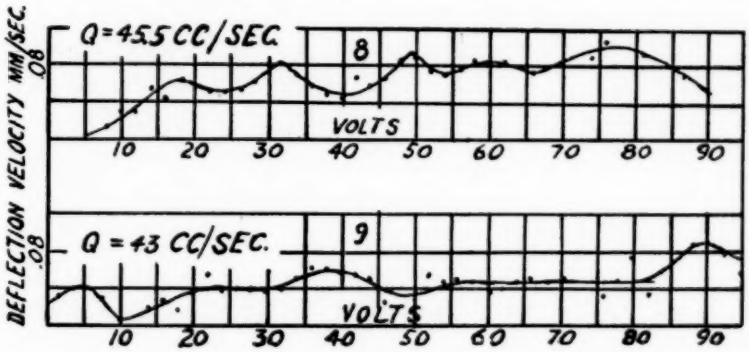

Fig. 6. Ion current in carbon dioxide. Curve 8, 115 cm between corona tube and ion chamber. Curve 9, 76 cm between corona tube and ion chamber.

oldest ions would have the greater age for the long tube. These expectations were realized and maxima were obtained which gave, quite exactly, mobilities previously obtained. The corona current for the long tube was 2.08 times that used in the short tube. The ion current increased about four times.

Variable distance from corona tube to ion chamber. As a final test the distance between corona tube and ion chamber was varied to note the effect on the mobilities present. Two curves were taken at each of the distances 115 cm and 76 cm and curves are reproduced, Fig. 6, showing the maxima obtained. The long corona tube and short ion chamber were used in order that the more rapidly moving ions might be observed and that the ion current might be large. The table shows the variation of the mobilities for carbon dioxide

115 cm: 2.2×10^{-2} 1.2×10^{-2} 8.2×10^{-3} 6.7×10^{-3} 5.2×10^{-3}
76 cm: 7.7×10^{-2} 1.7×10^{-2} 1.0×10^{-2} 4.3×10^{-3}

It is thought that one grouping of ions, when the corona tube and ion chamber are separated by a short distance (25 cm) at which most of the tests were made, is unstable and goes over into another when the distance is increased. In other words the grouping of the atoms and molecules in the ions changes with time and tends toward the formation of larger clusters of ions having smaller mobility. This is in accord with the recent results of Erikson,[4] Wahlin,[7] and others.

Point discharge. After measurements had been made on the mobilities of the ions in the corona discharge, the same apparatus was used and a few rough curves were taken on the point discharge merely to confirm the values found by Chattock. In this case it was interesting to note that the ion current for each gas had about two maxima, a weak one yielding the value of mobility determined by Chattock and a strong one giving a value considerably less.

Chattock gave a value of 1.3 cm/sec per volt/cm as the mobility for positive O_2 ions. This method yielded, for rough measurements, the two mobilities 1.27 and .284 cm/sec per volt/cm. The mobility corresponding to that given by Chattock is defined by a rather weak maximum on the curve, whereas, the second mobility is very strongly defined.

Conclusions

It should be first noted that no mobilities of ions were obtained greater than .716 cm/sec per volt/cm for nitrogen. Others have found that the initial ion changes over into one of smaller mobility as time is increased. In all the measurements recorded in this paper the ions had an age of 2.5 sec or more. Most of the tests were made on ions of age about 5 sec and this is greater than the life of the initial ion of Erikson.

The measurements show that ions generated in the corona discharge have small mobilities and that nearly all mobilities can be found of a value less than 10^{-2}. These ions seem to be in about equal numbers because of the small average value of the ion current, except now and then a greater number of a certain mobility are formed. This fact is manifest on the maxima of the curves.

Nearly all ions are of very low mobility at atmospheric pressure at which measurements were made.

Assuming the mobility of the ion to depend on the charge, evidence can be found of ions which contain different charges. Also if it can be assumed that the mass influences the mobility, then ions may be picked out having the same charge but whose mobility varies inversely as

[7] H. B. Wahlin, Phil. Mag. 49, 566 (1925).

the square root of the molecular weight. If these ions are gaseous then a comparison of the mobilities found shows evidence of the formation of oxygen and carbon monoxide in carbon dioxide. These may be identified by comparing mobilities of nitrogen and oxygen with those of carbon dioxide. Identical mobilities should appear for ions of the same charge and mass since nitrogen has the same molecular weight as carbon monoxide.

It was noted before that no single mobilities of ions have been found which alone account for the corona pressure from which J. Kunz calculated his mobilities. The pressure could be obtained probably by taking the sum of the impact energies of all ions generated by the corona but as apparently only a few of the ions were found in these measurements, no attempt was made at such a calculation. This matter will be taken up again in the near future.

The writer desires to express his appreciation to Dr. J. Kunz for his many helpful suggestions and keen interest in the work, and to Professor A. P. Carman for his interest and for the use of the laboratory and facilities.

DEPARTMENT OF PHYSICS,
UNIVERSITY OF ILLINOIS.
December 22, 1925.

A THREE INDUCTOR STATIC MACHINE

A. W. SIMON[1]

ABSTRACT

The quantitative theory of a three inductor static machine of the Holtz type is given. It is shown that such a machine is essentially a three phase electrostatic alternator, and that it can be star or mesh connected. A method for demonstrating the action of the machine visually by means of the glow in discharge tubes is described.

MULTIPLE inductor static machines of the Holtz type have been studied very little before either theoretically or experimentally. Holtz constructed a machine of this type with twenty inductors, and found that the quantity of electricity was greatly increased but that such a machine was very liable to reverse its polarity.[2] The latter point is significant in the light of our present considerations.

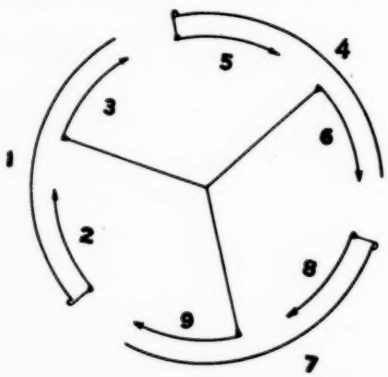

Fig. 1. A three inductor Holtz machine, Y connected.

Since the ordinary Toepler Holtz static machine is a two inductor machine, it is logical in the study of multiple inductor machines to consider next a three inductor machine of this type, and this is the object of our present paper.

A three inductor static machine of the Holtz type is illustrated in Fig. 1. It consists of three fixed inductors 1, 4, 7; and six revolving carriers 2, 3, 5, 6, 8, 9; and operates in a manner readily seen from the figure. In order to simplify the theory we shall assume that the three neutralizing rods are connected together and grounded.

[1] National Research Fellow.

[2] V. E. Johnson, "High Speed Influence Machines," p. 115.

I. Theory of a three Inductor Static Machine

If we use the same notation and general method explained in detail in a previous paper,[3] we have as the fundamental equations for the charges:

$$Q_1(n+1)+Q_2(n+1)=Q_1(n)+Q_9(n),$$
$$Q_4(n+1)+Q_5(n+1)=Q_4(n)+Q_3(n),$$
$$Q_7(n+1)+Q_8(n+1)=Q_7(n)+Q_6(n).$$

If next we eliminate the charges in the usual way by substituting for each charge its value in terms of the electric coefficients and the corresponding potentials, we have a set of three equations, in which the matrix of the coefficients of the left members (which involve as unknowns $V_1(n+1)$, $V_4(n+1)$, $V_7(n+1)$, in order), is conveniently represented as follows:

	1,2	4,5	7,8
1,2	a	c	b
4,5	b	a	c
7,8	c	b	a

and the matrix of the coefficients of the right members (which involve as unknowns $V_1(n)$, $V_4(n)$, $V_7(n)$) similarly by:

	1,2	4,5	7,8
1,9	a'	c'	b'
4,3	b'	a'	c'
7,6	c'	b'	a'

The definition of this representation is as follows:

Any cell of the square represents the coefficient occupying the corresponding place in the matrix of the coefficients of the potential equations; and this coefficient is obtained in terms of the fundamental electric coefficients (coefficients of capacity and of induction) by combining the numbers at the head of the column with the numbers at the head of the row in which the coefficient stands according to the notation:

$$a_{pq,\,rs}\equiv a_{pr}+a_{ps}+a_{qr}+a_{qs}$$

the significance of which has already been given in a previous paper.[4]

[3] A. W. Simon, Phys. Rev. **25**, 368 (1925).
[4] A. W. Simon, l.c.[3]

In order to solve these equations we make use of another matrix

$$\begin{matrix} \omega_0^0 & \omega_0^1 & \omega_0^2 \\ \omega_1^0 & \omega_1^1 & \omega_1^2 \\ \omega_2^0 & \omega_2^1 & \omega_2^2 \end{matrix}$$

where ω_j is the cube root of unity corresponding to an amplitude of $j2\pi/3$. The detailed solution is carried out in accordance with the method already outlined in the preceding paper for the case of an eight inductor electrostatic alternator. We have, provided the initial potentials satisfy the relations:

$$V_1(0) = V_1(0)\cos(0),\ V_4(0) = V_1(0)\cos(-2\pi/3),\ V_7(0) = V_1(0)\cos(-4\pi/3),$$

as the solutions:

$$\begin{aligned} V_1(n) &= \rho^n V_1(0)\cos(n\theta - 0), \\ V_4(n) &= \rho^n V_1(0)\cos(n\theta - 2\pi/3), \\ V_7(n) &= \rho^n V_1(0)\cos(n\theta - 4\pi/3). \end{aligned}$$

From these equations we see directly that a three inductor static machine of the Holtz type is an electrostatic alternator; in particular, it is essentially a *three phase electrostatic alternator*—a most remarkable result. This conclusion also shows that the Holtz machine of the ordinary two inductor type really belongs to a family of electrostatic alternators, and is a direct current machine only by accident, so to speak. The fundamental matrix of the Holtz machine is

$$\begin{matrix} \omega_0^0 & \omega_0^1 \\ \omega_1^0 & \omega_1^1 \end{matrix}$$

where ω_0, ω_1 are square roots of unity with an amplitude of 0 and π respectively, and are therefore both real instead of complex, being equal to 1 and -1. respectively.

It is interesting to inquire whether the analogy of a three phase alternator can be carried farther to include star and mesh (Y and delta) connections. The answer is that it can (if resistances are inserted in the brush circuits) the case illustrated in Fig. 1 being a star connection, while the case given in Fig. 2 would represent a mesh connection.

II. Experimental Verification of the Theory

Experimentally these two connections can be demonstrated very strikingly in the following way: Between each brush and the neutral point in the case of the star connection, or between each pair of ad-

jacent brushes in the case of the mesh connection, straight discharge tubes, (neon, helium, or nitrogen) are inserted, and shortcircuited for a moment until the machine has built up. The fact that the polarity reverses, as well as the fact that a wave travels around the machine, can then be detected readily by the glow in the tubes. Particularly striking is the delta connection, in which the tubes light up in succession, and a wave can be seen to travel around the circuit formed by the delta.

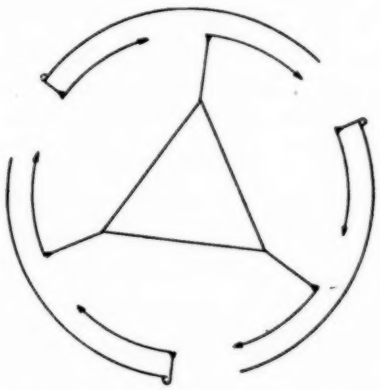

Fig. 2. A three inductor Holtz machine, delta connected.

The machine just discussed corresponds, of course, to a Holtz machine with collector brushes and Leyden jars removed, and a discharge tube inserted in the neutralizing rod. Vice versa, we can add neutralizing rods, and Leyden jars to the three inductor machine, and perform a variety of new experiments.

The theory and experiments just given can be extended to machines with more than three inductors and various types of connections.

In conclusion I wish to express my thanks to Mr. G. Forster of the Department of Electrical Engineering, for carrying out the experimental work just described.

NORMAN BRIDGE LABORATORY,
CALIFORNIA INSTITUTE OF TECHNOLOGY,
PASADENA, CALIFORNIA.
March 1, 1926.

MAGNETOSTRICTION IN PERMALLOY

By L. W. McKeehan and P. P. Cioffi

Abstract

The *materials* studied comprised *iron*, *nickel*, and *permalloys* containing 46, 64, 74, 78, 80, 84 and 89 percent nickel. The method permitted simultaneous measurement of *magnetization* and *magnetostriction* in about 12 cm at the middle of a 40 cm wire, 1 mm in diameter, in an approximately uniform field not exceeding 40 gauss, and either with or without applied *tension* (within the elastic limit).

The *magnetostriction* was measured by a combination of a mechanical lever, an optical lever, a multiple slit and a photoelectric cell. The magnifying power of this combination, as used, was about 2×10^6, and magnetostrictive strains from 2×10^{-9} to 3×10^{-5} were detected and measured without changing the sensitivity.

The *magnetostriction-magnetization* curve has initial slope zero in all the cases studied. When the attainable field was sufficient for magnetic saturation the magnetostriction reached a limiting value. In *iron* there is evidence for the existence of a Villari reversal in fields too great to be attained in the apparatus. In *nickel* there is no sign of such reversal. In the *permalloys with more than 81 percent Ni* the magnetostriction is a *contraction*. In the *permalloys with less than 81 percent Ni* the magnetostriction is an *expansion*. The limiting values of magnetostriction, when plotted against chemical composition, fall on a smooth curve.

Tension increases magnetostrictive contraction and diminishes magnetostrictive expansion. It causes a reversal in the sign of magnetostriction in permalloy with 80 percent Ni, a small contraction preceding the final small expansion.

Introduction

THE effects of tension upon the magnetization and hysteresis of permalloy[1] indicate with certainty that its magnetostriction in weak fields must change sign in the vicinity of 80 percent nickel and 20 percent iron. Honda and Kido,[2] who used cast ellipsoids, found such a change in this region of composition, but their experiments have nothing to say in regard to magnetostriction in weak fields. The present paper reports the results of simultaneous measurements of magnetization and magnetostriction, the latter by a new and precise method, in a series of well-annealed wires, including iron, nickel and permalloy in seven different compositions. The alloys contained, by analysis, in the form used, the following amounts of nickel in weight percent: 45.57, 64.44, 74.17, 78.07, 80.35, 84.41, 89.43. They have the same crystal structure (face-centered cubic) as nickel, the dimensions of

[1] Buckley, O. E., McKeehan, L. W., Phys. Rev. (2) **26** 261–273 (1925).
[2] Honda, K., Kido, K., Tohoku Univ. Sci. Rep. **9** 221–232 (1920).

the unit of structure increasing slightly as the nickel content diminishes.[3] In what follows the composition will be given only to the nearest percent. The iron and nickel wires were of comparable purity, cast from the same stock metals, and worked into wire in the same manner as the alloys. Nickel and permalloy wires were annealed for 20 hours in vacuum at 1200°C; the iron wire was kept at 1000°C for one hour and then at 850°C for two hours. During and after heat-treatment the wires were kept straight and free from over-strain of any kind.

The magnetostriction under no tension was measured for all the samples; the magnetostriction of the permalloys containing 74, 80 and 84 percent Ni was also measured under an applied tension of about 3600 lbs/in.^{2} (2.5×10^8 dyn/cm^2), due to a dead load of 4.5 lbs. hung at the lower end of the wire.

Apparatus and Method of Measurement

The principal parts of the apparatus are shown schematically in Fig. 1, which is distorted in order to show with equal clearness parts differing widely in dimensions. The wire under test was about 1 mm in diameter and 40 cm in length. It was hung vertically from a helical spring and was stretched, when desired, by loading its lower end. Magnetic fields were applied by passing currents through one or both of the two windings (#16 enameled wire) of a solenoid, 52 cm long and 3.1 cm in average diameter, coaxial with the sample and wound on the outside of a tubular glass jacket with two walls. These walls were silvered and the space between them was evacuated to reduce the radial flow of heat. The inside diameter of the jacket was 1.3 cm.

One of the windings of the solenoid was used for demagnetizing the specimen before each measurement of magnetization and magnetostriction.

The part of the wire in which the magnetostriction was measured was the middle 12 cm of its length. This was clamped at the top to the lower end of a rigidly supported brass sleeve and at the bottom to the upper end of a similar sleeve, the lower end of which projected from the magnetizing coil and rested on the shorter arm of a duralumin lever. The upper sleeve was 24 cm long, the lower, 21.5 cm. Both were of 1.6 mm inside, and 3.2 mm outside diameter, and were clamped onto the wire by small three-jawed brass chucks of the same outside diameter. The sleeves were slit longitudinally to reduce eddy currents. The upper sleeve was not fixed to its brass support until the wire and its supporting spring had been stretched by any applied load. (The

[3] McKeehan, L. W., Phys. Rev. (2) **21**, 402–407 (1923).

weight of the lower sleeve was balanced by the lever.) The helical spring then ensured that magnetostrictive strains in the upper part of the wire did not create appreciable differences in tension within it, above and below the plane of attachment of the upper chuck.

The duralumin lever was 22 cm long and its arms had the ratio 1 : 10. Its cross-section was rectangular, of width 3 mm and of height

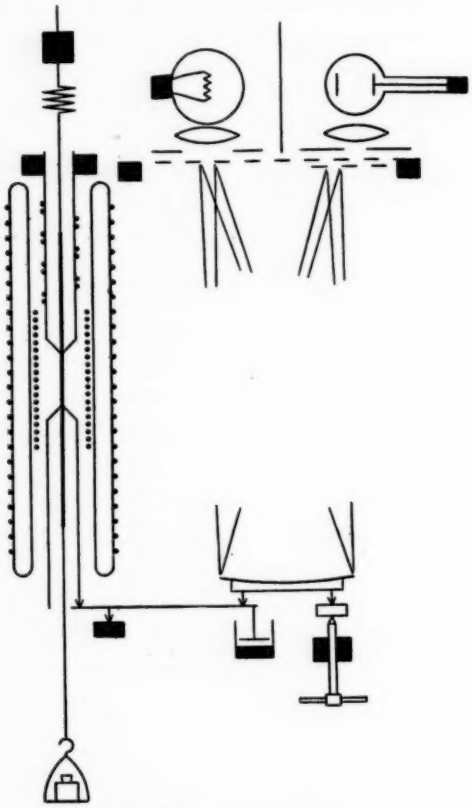

Fig. 1. Diagram of apparatus.

tapering from 5 mm to 2 mm. The lever rocked on an agate knife-edge, 2 cm long, resting on an agate plate. Its long arm had cemented on its top a slip of glass on which rested the free foot of an optical lever. It also carried, for mechanical damping, a plunger traveling freely in a dash-pot that could be filled with oil when especially sudden displacements were to be measured. Magnetostrictive displacements did not generally require the use of this dash-pot. The other two feet of the optical lever, on a line 0.794 cm from the free foot, rested in small glass cups on a brass arm which could be bent slightly by a stout

screw in a more rigid member so as to adjust the height of the axis of tilt. One of the cups was set in the end of a set screw to permit leveling this axis.

The optical lever carried upon its nearly horizontal upper surface a selected concave glass mirror, 1.3 cm in diameter and with a radius of curvature of 1 meter, front-silvered in vacuum by evaporation. The mirror was stabilized by grinding the metal support to fit its back. A glass screen on which black lines 0.0508 cm wide were accurately engraved 0.0508 cm apart, was set horizontally one meter above the mirror and with its lines parallel to the axis of tilt. A small lens condensed the light, from a 14-volt gas-filled incandescent lamp with coiled tungsten filament, upon the screen so as to cover a circle about 1.5 cm in diameter and to form an image of the filament on the concave mirror. The mirror was then adjusted to project an image of the illuminated part of the screen onto an otherwise unilluminated part of the same screen. A lens set just above this image collected the transmitted light into a photoelectric cell connected through a dry-cell battery (70 volts) to a galvanometer.[4] The tilting of the optical lever caused the bright stripes of the image to travel across the equally-spaced transparent stripes of the screen. The change in the transmitted light was nearly proportional to the change in length of the section of wire between the two sleeves. The galvanometer (Leeds and Northrup, Type #2285, period on open circuit 7 sec) in series with the photoelectric cell was critically damped and adjusted to give a deflection of about 50 cm (at a distance of 120 cm) for the change from full transmission to full cut-off. An iris diaphram in the collecting system was used for this adjustment, its normal opening being such that the maximum transmission was practically independent of image position over a wide range. The lamp, operated on portable storage batteries. without series resistance, gave a sufficiently steady source of light, Under these conditions 1 mm on the scale of the galvanometer corresponded roughly to a total change in length of the object, in this case 12 cm of wire, of 4×10^{-8} cm. For changes in length greater than about 2×10^{-5} cm account had to be taken of the opposite variation of galvanometer deflection and length during successive half-millimeters of the motion of the image on the screen. Changes in length greater than about 4×10^{-4} cm caused such large displacements of the image that the photoelectric cell ceased properly to integrate the transmitted light, but this limit was not exceeded in the final measurements.

[4] The lamp and photoelectric cell were those used in these laboratories for the telephonic transmission of pictures. H. E. Ives, Bell System Tech. J. **5**, 320–336 (1926).

The multiple slit and photoelectric integrator are similar in principle to an arrangement used by Rankine[5] for detecting rapid vibrations. Their use in the manner here described has the effect of giving to the length-measuring galvanometer a nearly uniform scale, some 10 meters long, folded into a space of less than 50 cm.

The principal assembly of apparatus (corresponding to Fig. 1) was mounted on a two-inch oak plank hung vertically on a Julius suspension with damped springs.[6] A felt-lined cabinet standing on the floor and high enough to surround the suspended system further reduced the effects of air currents and other sources of mechanical and thermal disturbances. The galvanometer was separately suspended.

The length-measuring galvanometer was calibrated by propping up the long arm of the duralumin lever at a point a few centimeters from its bearing, and then allowing a succession of drops of oil, fed under constant pressure through a small nozzle, to fall into a pan so hung as to bend the free end of the lever. The interval between drops was so adjusted that the galvanometer index came to rest in each interval, permitting accurate reading of its position on the scale. The drops being of equal weight, and the greatest stress in the lever being well within its elastic limit, it could safely be assumed that the consecutive positions of the image on the screen (about 2×10^{-3} cm apart) were equally spaced. A representative calibration curve, obtained in this way, is shown in Fig. 2. The points are plotted as read, without any sort of smoothing. Along the upper edge of Fig. 2 four diagrams are placed which show how the image, as seen from the upper side of the screen, travels across the field of the photo-electric cell (the smaller circle of the diagrams) as the lever is bent. The diagrams correspond to the points on the calibration curve directly beneath them, but the number of stripes in the image has been reduced to make the changes in its appearance more conspicuous. The background, consisting of both opaque and transparent stripes, is shown black in these diagrams.

The relation between image position and reading on the galvanometer scale is nearly enough linear over about 85 percent of the total range on the scale, but optical defects cause a deviation from linearity near the positions corresponding to greatest and least transmission. This could be taken into account in the interpretation of scale readings in the affected regions, but it was better to avoid such readings by a method to be described below.

[5] Rankine, A. O., Proc. Phys. Soc. **31**, 242–264 (1919).
[6] Johnsrud, A. L., J. O. S. A. & R. S. I. **10**, 609–11 (1925).

Since heat is generated in the wire and its attachments by the eddy currents set up during changes in magnetization and since a rise of temperature of only 0.001°C causes thermal expansion (in the 12 cm of wire alone) sufficient to change the galvanometer reading by about 50 mm, the drift due to imperfect thermal equilibrium within the nearly heat-tight enclosure would have been troublesome. To eliminate drift, a non-inductive winding was imbedded in the upper brass sleeve, and such a current—a few milli-amperes—was passed through this winding, that its equilibrium temperature was raised a few hundredths of a degree. This current was then regulated, just before each reading, until the drift was compensated. This process was made nearly instantaneous by reducing the thermal capacity of the sleeve and its winding to

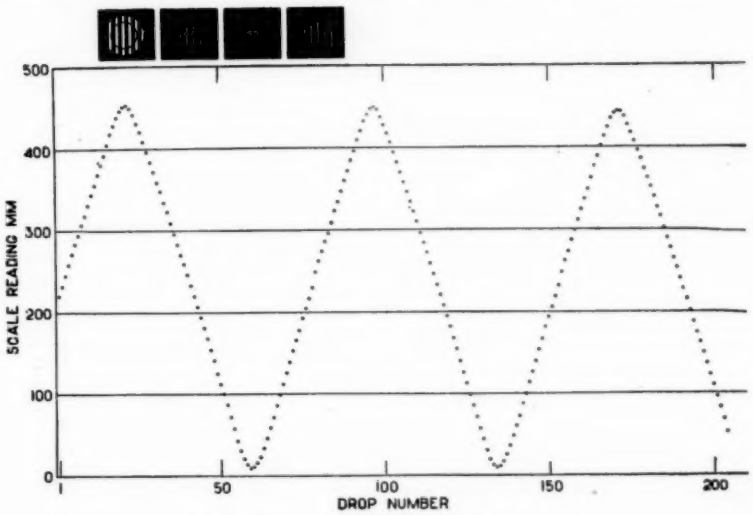

Fig. 2. Representative calibration curve.

the smallest practicable value. In the absence of magnetic changes it was possible in this way for a practiced observer to keep the galvanometer index steady within a range of one millimeter as long as desired and deflections could be taken from a zero chosen, for greater accuracy so that both the initial and final readings fell within the linear part of the scale. The same artifice made it convenient to check the constancy of the maximum photoelectric current, i. e. the constancy of the lamp and photoelectric cell, before each reading, by varying the length of the system slowly through a value corresponding to maximum galvanometer deflection (upper turning-point). The sign of a change in length was determined by noting in which direction an increase in the drift-correcting current—corresponding to increase in length—moved

the galvanometer index. The number of maxima and minima traversed in a large change in length was sometimes checked by making the change in applied field take place so slowly that the galvanometer had time to go through the successive turning-points. In all cases where the initial and final readings lay between different pairs of turning-points the upper turning-point was determined after, as well as before, the

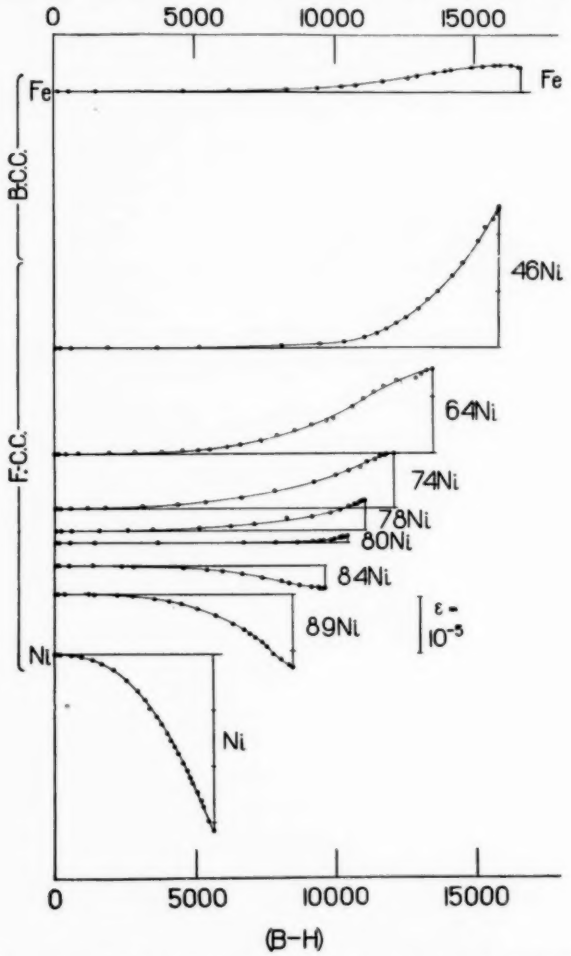

Fig. 3. Dependence of the relative change in length upon the ferric induction.

deflection occurred. The lower turning-point, it should be noted, was practically independent of the state of the optical and photoelectric systems.

Changes in magnetization were measured in the usual way.[7] The search-coil, mounted in the jacket at the center of the length of the

[7] Cioffi, P. P., J.O.S.A. & R.S.I. 9, 53–60 (1924).

specimen, was wound on 15.2 cm of the length of a hard rubber spool 17 cm long, of 3.6 mm inside, and 11 mm outside diameter. It comprised 17,735 turns of #40 single-silk-covered wire, and the maximum sensitivity of the ballistic galvanometer (Leeds and Northrup, Type 2285) in series with it was such that small changes in $(B-H)$ were measured within about one gauss.

The compensation of the vertical component of the earth's magnetic field was frequently checked, by noting the equality of changes in magnetization for equal positive and negative field increments.[8] The uncompensated poles at the ends of the specimen made the field within it less than the applied field. The true magnetization-field curves were accordingly determined, in advance, in shielded apparatus[1] wherein the pole effect was eliminated, and it was assumed that at the same values of B the values of H within the sample in the unshielded apparatus were those more accurately determined in the shielded apparatus. The correction to be subtracted from the applied field was, over most of the range in $(B-H)$ for each specimen, $(B-H)\times 40\times 10^{-6}$. It was determined by experiment that when a non-magnetic wire was tested there was no change in length due to the application of magnetic fields and, in other experiments, that the forces on the ends of a magnetic wire due to the unavoidable non-uniformity of the magnetic fields near its ends did not change the length of a non-magnetic segment between the chucks.

Results

The dependence of the relative change in length, i. e. the strain, ε, upon the ferric induction, $(B-H)$, is shown, for all unstretched specimens, in Fig. 3. The scale for $(B-H)$, which is abscissa, is common to all the curves of Fig. 3, but the zero ordinate for each curve is set at a height which depends upon the composition of the specimen.

The range /ε was so great, and the precision in its measurement so high, that graphical presentation, as in Fig. 3, cannot easily do justice to the data. Representative data and calculations for a few cases are therefore presented in Table I.

The applied field was carried to an upper limit of about 40 gauss. This was sufficient to saturate all the permalloys, but was insufficient to saturate either nickel or iron alone. The magnetostrictive strain was found to approach a limiting, or saturation, value whenever magnetic saturation was effected. Fig. 4 gives ε as a function of H

[8] McKeehan, L. W., Cioffi, P. P., J.O.S.A. & R.S.I. **9**, 479–485 (1924).

TABLE I

Illustrative data and calculated quantities

i, magnetizing current, amperes; H, magnetizing field, gauss; d, ballistic galvanometer deflection, mm; $(B-H)$, magnetization, gauss; δ, length-measuring galvanometer deflection, mm; n, number of turning-points traversed; ε, magnetostrictive strain (cm/cm), A horizontal row of dashes calls attention to the omission of a series of points from the table.

Material, and region considered.	i	H	d	$(B-H)$	δ	n	ε
Ni, Initial region and last point.	0.005	0.044	4.0	11	0	0	0
	0.010	0.089	8.3	22	0	0	0
	0.020	0.177	20.6	58	−1	0	-3×10^{-6}
	0.030	0.263	59.	114	−2	0	-7×10^{-6}
	0.040	0.349	70.	214	−12	0	-41×10^{-6}
	0.060	0.513	188.	603	−66	0	-230×10^{-6}
	3.50	31.3	67.3*	5630	−206	19	-31620×10^{-6}
80 Ni (without tension), initial region and last point.	0.002	0.016	11.6	39	0	0	0
	0.006	0.047	47.7	163	0	0	0
	0.012	0.085	163.	564	0	0	0
	0.020	0.121	56.8*	1440	0	0	0
	0.040	0.210	147.	3690	0	0	0
	0.080	0.447	58.2*	6720	+2	0	$+7\times10^{-6}$
	4.48	40.0	111.1	10400	+311	0	$+1150\times10^{-6}$
80 Ni (with tension) first point, reversal region, and last point.	0.010	0.076	96	329	0	0	0
	0.200	1.63	75.5*	8680	−24	0	-88×10^{-6}
	0.300	2.68	82	9390	−23	0	-84×10^{-6}
	0.350	3.13	83.2	9480	−14	0	-51×10^{-6}
	0.400	3.58	84	9560	−7	0	-26×10^{-6}
	0.500	4.48	86	9730	+12	0	$+44\times10^{-6}$
	0.600	5.38	88	9920	+29	0	$+107\times10^{-6}$
	4.57	40.9	112.2	10480	+173	0	$+661\times10^{-6}$
Fe, maximum expansion.	0.050	0.441	60.5	184	0	0	0
	1.00	8.95	131.6	14920	+250	2	$+426\times10^{-6}$
	1.40	12.54	137.0	15300	+288	2	$+440\times10^{-6}$
	1.90	17.00	142.9	15720	+333	2	$+460\times10^{-6}$
	2.46	22.0	147.4	15940	+314	2	$+452\times10^{-6}$
	3.08	27.6	153.8	16320	+311	2	$+451\times10^{-6}$
	3.64	32.6	158.8	16580	+276	2	$+436\times10^{-6}$
	4.40	39.4	162.8	16650	+228	2	$+420\times10^{-6}$

* Change in sensitivity of ballistic galvanometer.

(corrected) for a few cases only. Fig. 5 shows how the greatest observed strains depended upon the composition.

The results for magnetostriction in stretched permalloys are shown in Fig. 6, in which, for comparison, have been included also the results for the same wires when unstretched. The scale for ε has been made much more open in Fig. 6 than in Fig. 3. In the case of permalloy with 80 percent Ni curves have been drawn through points (dots) with ordinates ten times greater than those plotted on the standard scale,

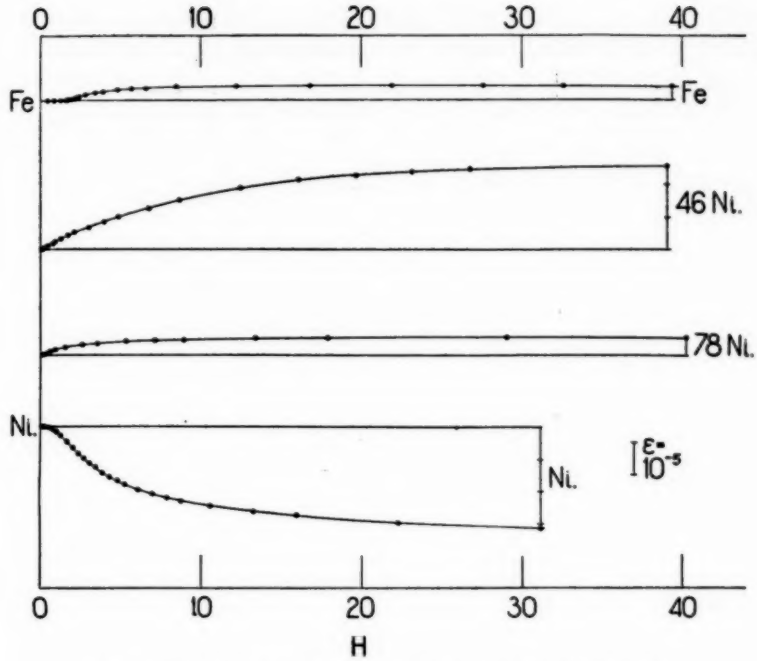

Fig. 4. The strain ε as a function of magnetic field strength.

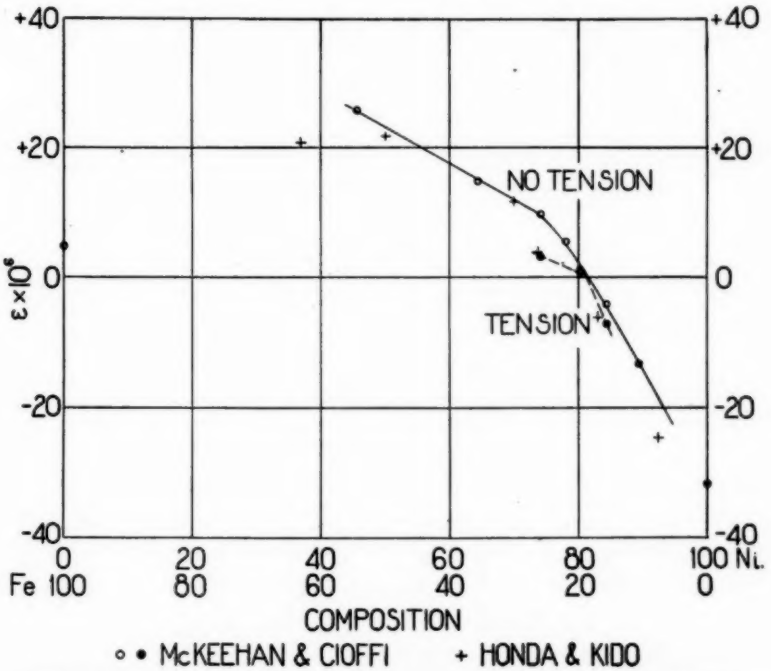

Fig. 5. Dependence of the greatest observed strains upon composition.

in order to show more clearly the changes in $\mathfrak{E}$ produced by tension. A still larger scale for $\mathfrak{E}$ would have been justified by the precision of the readings (cf. Table I).

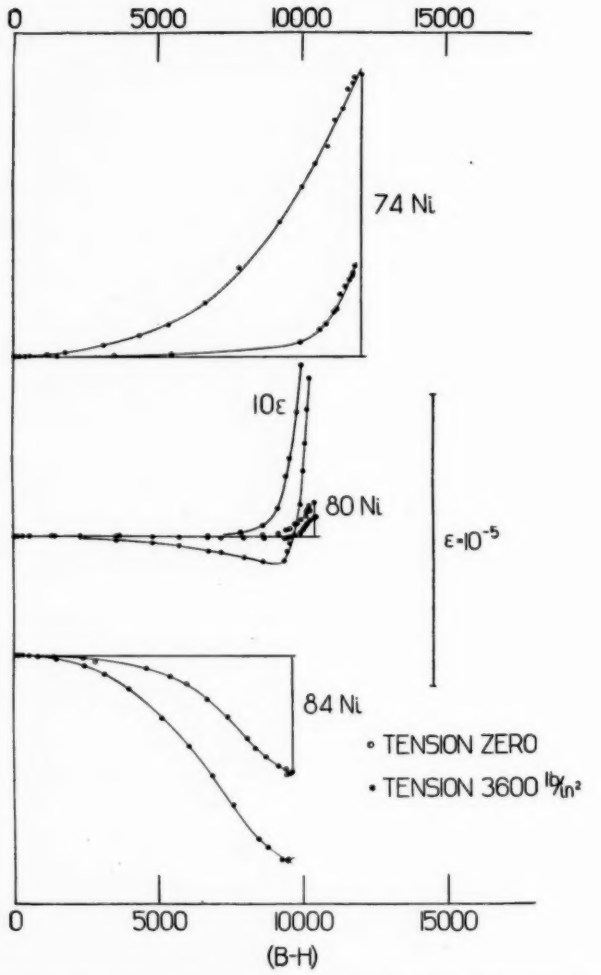

Fig. 6. Showing results for magnetostriction in stretched permalloys.

Discussion of Results

The greatest magnetostrictive strains recorded by Honda and Kido[2] for alloys in the range of compositions here studied have been plotted in Fig. 5. The lowest field applied in their experiments was 10.5 gauss, the highest, 590.5 gauss. The discrepancies between our results and theirs are not greater than might be expected from the differences in methods of preparation and experiment.

The behavior of iron, as far as it could be studied in our apparatus, is similar to that usually reported in having a maximum expansion followed by lower values at higher magnetizations.

The theoretical bearings of the experimental results here obtained, and others, are discussed by one of us in the following paper.[9]

We desire to express our appreciation of the alertness and accuracy of Mr. R. H. Raguse as second observer in all the experiments here described.

BELL TELEPHONE LABORATORIES, INC.,
NEW YORK CITY.
April 17, 1926.

[9] McKeehan, L. W., Phys. Rev. (2), **28** 158–166 (1926).

THE SIGNIFICANCE OF MAGNETOSTRICTION IN PERMALLOY

By L. W. McKeehan

Abstract

Magnetostriction in permalloy, measured by McKeehan and Cioffi,[1] confirms qualitatively the existence of atomic magnetostriction, as previously proposed, and the explanation, based thereon, for high magnetic permeability and low hysteresis in these alloys. The effect of tension upon magnetostriction suggests that orientation of the magnetic axes of iron and nickel atoms precisely like that due to the application of magnetic fields may be effected by mechanical stresses within the elastic limit. Acceptance of this view makes it possible to explain the large effects of tension upon magnetic hysteresis and the observed relation between the changes in electrical resistance produced by tension and by magnetization. The occurrence of a reversal of magnetostriction in a stretched wire containing 80 percent Ni is covered by the same explanation. A connection between magnetic hysteresis and mechanical hysteresis is suggested and the molecular field postulated by Weiss is interpreted as the integrated effect of local mechanical stresses.

Introduction

THE preceding paper[1] reports measurements on the magnetostriction of permalloys covering a wide range in composition, and the effect of tension upon the magnetostriction of permalloys covering a narrower range. This paper will discuss the results of these experiments, and of others previously reported, in the light of a theory[2] which attributes changes in the external dimensions of a body during its magnetization to changes in the immediate neighborhood of individual atoms as these atoms contribute to the magnetization by aligning their magnetic axes. Such atomic magnetostriction was assumed by the author to explain the loss of energy in magnetic hysteresis. It served at the same time to connect the intra-atomic changes—in orientation and energy—which the theory assumed to be basic, with inter-atomic changes like those due to gross mechanical strains and to the more local strains associated with cold-working, alloying, and other processes which alter the mechanical and magnetic properties of metals. This theory will be referred to herein as the theory of atomic magnetostriction, or more briefly, as the theory.

The theory of atomic magnetostriction is found adequate to explain the newly discovered facts of experiment, and gains in definiteness by including them in its field of application.

[1] McKeehan, L. W., Cioffi, P. P., Phys. Rev. (2), **28** 146–157 (1926).
[2] McKeehan, L. W., Phys. Rev. (2), **26**, 274–279 (1925).

Discussion

The first point to be emphasized is that in pure nickel (and *a fortiori* in the other materials tested) magnetization reaches considerable values before magnetostriction becomes perceptible. The apparatus used measures small changes in length so accurately that the data (cf. Table I)[1] establish this fact beyond question.

The theory demands that magnetostriction should begin in this way in all cases. For, at the beginning of magnetization only widely separated atoms are supposed to respond to the applied field. Although intense local stresses are set up about these oriented[3] atoms, the matrix of quite unmodified atoms offers to such local stresses an almost unyielding resistance. As, however, the continuity of the original structure is destroyed at more and more points, motion of the boundaries, with relief of accumulated stresses, occurs more and more readily.

The second thing to which attention will be directed is the curve in Fig. 5[1] showing the dependence of maximal magnetostriction upon the chemical composition (iron and nickel content) of unstretched permalloy. The second basic assumption of the theory is that atomic magnetostriction, i. e. the changes in the equilibrium positions of adjacent atom-centers due to changes in direction of the magnetic axis of the atom considered, are independent of the nature of the neighboring atoms. The theory views the greatest observable magnetostriction in any of these alloys as the net result of an expansion along the axis of magnetization, due to the orientation of all its iron atoms and a contraction along the same axis due to the orientation of all its nickel atoms. To a first approximation, therefore, the net magnetostriction should be a linear function of the concentration of either component (Fe or Ni). The approximation of the plotted points to a straight line justifies the second basic assumption of the theory.[4] The course of the curve suggests that face-centered cubic iron (as in austenitic steel) should, if it could be magnetically saturated, exhibit a magneto-

[3] An atom will be said to be oriented in a given direction when its magnetic axis is parallel to that direction, and to be unoriented when its magnetic axis has any other direction. It is not to be assumed that the magnetic moment of the unoriented atom is zero, and, as far as this paper goes, it is not necessary to suppose that the atomic magnetic moment is modified (except in the direction of its axis) by magnetic fields or other agencies.

[4] A second approximation calls for a defect from linearity in the magnetostriction-vs.-composition curve in the critical region, requiring nearly compensated alloys to show less expansion or contraction than that called for by the first approximation. There is some slight tendency for the points in Fig. 5[1] to deviate in this sense from the straight line there drawn.

strictive expansion greater than any magnetostrictive strain yet measured.

The smooth passage of the magnetostriction-vs.-composition curve through zero magnetostriction is in striking contrast to the abruptness of the changes in the magnetizability of stretched wires[5] in the same range of composition. This difference in the character of the two effects was to be expected, for, on general grounds,[6] the sensitiveness to strain should vary inversely as the magnetostriction, and where the latter passes through zero the strain-sensitivity should change discontinuously from its greatest positive to its greatest negative value. The observed variations in strain-sensitivity in the critical region are very great. That they are not infinite is not surprising in view of the unavoidable variations in local composition within a specimen of any alloy.

The third point of interest is the composition for which the net magnetostriction is zero. This can now be established as lying very close to 81 percent Ni, 19 percent Fe, and this is also the composition for which (in well-annealed alloys) hysteresis has its very low minimum value. The theory assumes that those groups of nickel and iron atoms in which atomic magnetostrictions are so compensated that hysteresis vanishes, are very small groups. If these groups were large the residuum of atoms left between groups organized at haphazard points within the alloy would frequently be ungroupable, and would give rise to considerable hysteresis even in that alloy for which the net magnetostriction is zero. The very low hysteresis observed in this alloy therefore substantiates the hypothesis of small groups.

The smallest group consistent with the critical composition thus indicated has four nickel atoms and one iron atom (80.6 percent Ni, 19.4 percent Fe). In a face-centered cubic solid solution the most compact and symmetrical arrangement of five atoms, four of one kind and one of another kind, is that in which the four like atoms form a rectangle lying in a (111) plane, with the fifth atom at its center. If a is the edge of the unit cube the sides of this rectangle are $a\sqrt{2}/2$ and $a\sqrt{6}/2$. A single iron atom completely surrounded by nickel atoms can be grouped in this fashion with four of its twelve neighbors in six different ways, so that even if it be essential to the proper functioning of such a group that the long edges of its rectangle lie nearly parallel to the applied field there is nevertheless a good chance of finding a suitably oriented group.

[5] Buckley, O. E., McKeehan, L. W., Phys. Rev. (2), **26**, 261–273 (1925).
[6] Kirchhoff, G., Berl. Ber. **47** 1155–1170 (1884).

While the hypothesis that this simple group is that in which atomic magnetostrictions are compensated is an attractive and tenable one in view of the present evidence, it cannot be considered proved. The important point at this stage is that a small group is required by the theory, and that a group of as few as five atoms (4 of Ni and 1 of Fe) will fit the observed critical composition.

The fourth problem which confronts the theory of atomic magnetostriction comprises the effects of tension on permalloys with notably more or less nickel than the critical amount (81 percent). These are the most interesting of the newly discovered facts, and they merit the most careful analysis (see Fig. 6[1]). In discussing the results observed in particular alloys it will be convenient to distinguish between atoms so grouped that all the atoms in a group become oriented (and magnetized) simultaneously, without magnetostriction or much energy loss, and atoms not so grouped. The former will be referred to as compensated atoms, the latter, as uncompensated. It is clearly the uncompensated atoms alone concerning which measurements of magnetostriction give direct evidence. Compensated atoms can only affect the results indirectly by offering resistance to the stresses set up around uncompensated atoms.[4]

It is to be kept in mind that there need be nothing essentially permanent about the grouping of compensated atoms. The same atom may, in different magnetic cycles, be compensated in one and uncompensated in another, depending upon chance variation of local conditions in the different cases. In any one case, however, the classification will be unique. The impossibility of predicting the classification of particular atoms will lead to no confusion in the present analysis.

In the permalloy wire containing 74 percent Ni tension diminishes the magnetostrictive expansion. It is clear that most of the uncompensated atoms in this alloy must be iron atoms. The theory says that the magnetic properties of the compensated atoms will not be affected by tension, and therefore that the observed change in magnetostriction must be due to something which affects the uncompensated (Fe) atoms alone. But the theory says just as positively that the atomic magnetostriction of iron (compensated or uncompensated) in face-centered cubic crystals cannot be altered, either in kind or in magnitude, by external agents such as tension. There is only one way of escape from this dilemma. The magnetostriction that occurs when a strong magnetic field is applied to a stretched demagnetized wire must be only part of the whole change in length producible by atomic orientation. Stretching the wire must, therefore, have oriented some of its

atoms. It is found by direct experiment[5] that application of a strong field to a demagnetized wire produces the same change in magnetization with and without tension. Furthermore this change is half the change produced by reversing the field. These facts mean that in the magnetostriction experiments the initial magnetization is zero and the final magnetization has the same (saturation) value with and without tension. A little consideration shows that, if tension orients the same number of atoms in each of the two possible directions along the wire-axis, the whole change in magnetization when all are subsequently oriented in a single direction, will be the same as if the original state had been one of random orientation, as it is assumed to be in the annealed unstretched wire. The same invariance will not be shown by the magnetostriction, for the atoms oriented axially by tension have already contributed their quota to the change in length. Whether or not the applied magnetic field reverses their magnetic polarity the length of the wire is not altered. They are magnetizable but not magnetostrictive.

Precisely the same type of reasoning applies to the effect of tension on permalloy with 84 percent Ni. Tension orients the uncompensated (Ni) atoms transversely to the axis of the wire (but not all parallel to any particular diameter). Each atom so oriented should contribute a maximal quota to the magnetostriction later observed when strong fields produce magnetic saturation by orienting all the atoms parallel to the axis of the wire.

If sufficient tension can be applied to complete the axial type of orientation there will be no further change in length upon magnetizing permalloy with less than 81 percent Ni. In permalloy with more than 81 percent Ni, however, if complete transverse orientation can be produced by tension the characteristic contraction upon magnetizing should reach a limit somewhat greater than that in an unstretched specimen. That the limit should not be much greater is reasonable because the magnetostriction due to turning through 90° the axes of all the uncompensated nickel atoms, cannot be a large multiple of that due to turning them through angles ranging at random from 0° to 90°. The slope of a magnetostriction-vs.-composition curve plotted from data taken under any fixed tension should therefore change abruptly at the critical composition, being steeper on the high-nickel side. The broken line in Fig. 5[1] exhibits this effect of tension.

The effects of tension upon magnetizability[5] are also in agreement with this analysis. In the lower range of nickel content weak applied fields should suffice to reverse the orientation of uncompensated iron

atoms which have, by tension alone, been oriented in the "wrong" direction. Atoms not oriented by tension alone should be oriented by weaker fields than if tension was absent. Both circumstances should raise the observed permeability and the first, in particular, should make the magnetization-vs.-field curves rise very abruptly. As far as compensated atoms are concerned the theory does not predict any change of behavior with tension. In the upper range of nickel content stronger fields should be required to orient axially the uncompensated Ni atoms which have, by tension alone, been oriented transversely. The range in stability of obliquely directed atoms should also be greater. Both circumstances should reduce the observed permeability and the magnetization-vs.-field curves under tension should rise less abruptly.

So far in this discussion it has always been assumed that magnetic fields have been applied to demagnetized specimens, so that the changes considered have been those taking place along the normal magnetization curve. The effects on hysteresis loops are simpler, for at saturation there are only two sorts of uncompensated atoms to consider, those oriented parallel to the applied field by tension alone and those so oriented under the cooperating (Fe) or opposing (Ni) effects of tension and applied field. In low-nickel permalloys, at sufficient values of the tension, only the first sort should be present, and reversal of their orientation should occur within a very narrow range of reversed magnetic field. The sharp corners and precipitous sides of the hysteresis loops corresponding to these conditions[5] are just what the theory demands. In high-nickel permalloys, on the other hand, only the second sort of uncompensated atoms are to be expected and the whole contour of the hysteresis loops under tension should be less angular, as experiment[5] shows it to be. In both cases, of course, the effect of uncompensated atoms is to be thought of as superposed upon the smooth but narrow hysteresis loop characteristic of compensated atoms, and best exhibited by permalloy with 81 percent Ni.[5] In low-nickel permalloys tension keeps iron atoms axially oriented so that the magnetic energy to be furnished for this purpose in each half-cycle is greatly diminished. The area of the magnetic hysteresis loop is correspondingly decreased. In high-nickel permalloys tension, whenever the applied field falls too low, orients nickel atoms transversely, wasting mechanical energy at the moment and requiring an extra supply of energy from the magnetic field to reorient the atoms axially at a later stage in the same half-cycle. The area of the magnetic hysteresis loop is correspondingly increased.

The mechanical nature of magnetic hysteresis, upon which the theory insists, is perhaps most evident in this type of experiment where a change in mechanical conditions alters magnetic energy losses.

The conclusions in regard to atomic orientation by tension are so novel that independent evidence on this point is highly desirable. Fortunately, such evidence exists. Experiments[7] in these laboratories have shown that the electrical resistivity of permalloy wires containing 78.5 percent Ni may be raised about as much (2 percent) by tension within the elastic limit as by magnetization to saturation, and that a combination of these causes produces no greater limiting change in resistivity than either cause alone. The theory of atomic magnetostriction suggests the following explanation for both sets of facts.

Change in resistivity in permalloy (at constant temperature) is due principally to atomic orientation and hardly at all to changes in dimensions (or distances between atom-centers). Magnetization and magnetostriction are due entirely to atomic orientation. In zero magnetic field tension produces atomic orientation equally in two opposite directions parallel to the tension—or, equally in all directions at right angles to the tension—and thereby produces change in resistivity and magnetostriction, but no measurable magnetizaton. Starting from any condition, the further change in resistivity producible by applying more tension or by increasing the applied magnetic field, and the further magnetostriction producible by increasing the magnetic field, measure the same thing, the extent to which the alignment of atomic axes (in uncompensated atoms) was incomplete at the start.

The fifth of the newly reported experimental results which will here be dealt with is the reversal in magnetostriction in stretched permalloy containing 80 percent Ni (Fig. 6[1]). This alloy is, on the average, so nearly compensated that the composition in small regions may lie on either side of the critical composition. Uncompensated atoms of both iron and nickel should therefore be present in the specimen. In the unstretched alloy it is experimentally evident that in the first stages of the process of magnetizing the net magnetostriction is zero, so that the uncompensated atoms, if oriented at all during this stage, must be oriented in nearly the compensating ratio. This quasi-compensation is different from the true compensation previously defined, in depending on events non-adjacent in time or in space, and should not therefore entail abnormally low hysteresis losses. It is also different from true compensation in being upset by tension, because tension orients and disables from subsequent magnetostrictive action a large fraction of the

[7] Arnold, H. D., McKeehan, L. W., Phys. Rev. (2) **23**, 114 (1924).

uncompensated iron atoms, leaving the uncompensated nickel atoms to control the observed magnetostriction in low fields, and enhancing their average contribution thereto in the manner already described. It is apparent that with tension sufficient to orient all uncompensated iron atoms the only observable magnetostriction should be a contraction. In the case examined the tension was not so great as this, and a final expanson of small amount betrays the presence of uncompensated iron atoms not oriented by the applied tension alone.

The experiments of Webster[8] on magnetostriction in single iron crystals show that even in these simplest of structures magnetic processes are quite analogous to those in crystal aggregates, upon the behavior of which the theory of atomic magnetostriction has been based. This is not surprising, because even the smallest crystal in an annealed aggregate contains so many atoms that inter-atomic actions should be practically independent of crystal size. (Intra-atomic actions are, by definition, independent thereof.) The dependence of magnetostriction upon direction of magnetization is, in the body-centered crystals studied by Webster, very complicated. In explaining magnetostriction in the aggregates of face-centered crystals examined by McKeehan and Cioffi[1] it has not been found necessary to assume different magnetostrictive properties in different directions within each crystal. The study of magnetostriction in single nickel crystals would be of great interest in this connection.

The equivalence of tension and magnetic fields in orienting ferromagnetic atoms supplies a clue to the nature of the "molecular" field postulated by Weiss[9] to account for magnetic retentivity. The more or less random stresses in ordinary metals would, in accordance with the views here expressed, do that for which this molecular field was evoked, for they would in the case of all but favorably oriented atoms tend to maintain the established direction of magnetization against small disturbances, and thus confer upon magnetization that stability which the simple interaction of freely turning magnets cannot furnish. The development of specialized atomic orientation by tension also requires in ferromagnetic metals, far below the elastic limit, a defect of proportionality between stress and strain, a dissipation of energy as in magnetic hysteresis, and the same opportunities for lag and after-effects that occur in such changes of atomic orientation as can be followed by magnetic measurements alone. Mechanical hysteresis in

[8] Webster, W. L., Proc. Roy. Soc. **109A**, 570–584 (1925).

[9] Weiss, P., J. de phys. (4) **6**, 661–690 (1907); Ann. de physique (9) **1**, 134–162 (1914); Arch. des sci. (4) **37**, 105–116, 201–213 (1914); (5) **6**, 417–418 (1924).

ferromagnetic metals (except in permalloy with 81 percent Ni) should therefore be abnormally high.

Conclusion

The theory of atomic magnetostriction is found to suggest an adequate explanation for magnetostriction in permalloy and establishes a close correspondence between magnetostriction and the changes in resistivity which accompany magnetization and tension. It suggests that the orientation of the magnetic axes of ferromagnetic atoms may be affected by mechanical as well as by magnetic forces, makes more rational the molecular field postulated by Weiss, and should prove useful as a guide in attacks upon unsolved problems in ferro-magnetism.

Bell Telephone Laboratories, Incorporated,
New York City.
April 17, 1926.

THE ROLE OF MAGNETISM IN VALENCE

By E. H. Williams

Abstract

A brief statement concerning the electrochemical and magnetochemical theories is made, together with a description of some of the phenomena for which the electrochemical theory does not give a satisfactory explanation. It is pointed out that one of the tests in favor of the magnetochemical theory would be the changing of a paramagnetic substance to a diamagnetic substance when the valence is modified so as to change the molecule from one of odd molecular number to one of even molecular number. To test this point measurements were made of the magnetic susceptibilities of a number of carefully prepared compounds of variable valence such as CuO and Cu_2O. The results show that the compounds of Cu, Bi, Pb and Sn of odd molecular number are paramagnetic while those of even molecular number are diamagnetic. On the other hand MnO (odd) and Mn_2O_3 (even) are both paramagnetic, the former slightly more so. CoO (odd) is strongly ferro-magnetic while Co_2O_3 (even) is paramagnetic. AgO and Ag_2O are both diamagnetic suggesting that possibly AgO is of the form Ag_2O_2 (even).

THE electrochemical theory has, for many years, been the predominating theory in the science of chemistry. It explains very beautifully the type of chemical phenomena met with in electrolytes, especially those of inorganic compounds. There are, however, other fundamental phenomena in chemistry and physics for which the electrochemical theory, in its present form at least, does not give a satisfactory explanation. For example, the symmetrical grouping of electrons which is of so common occurrence in molecules, the fact that the majority of chemical compounds, especially the organic compounds, are diamagnetic and the formation of chemical bonds by the coupling of electrons are phenomena that are difficult to explain by the electrochemical theory alone.

In order to account for some of the phenomena for which the electrochemical theory does not give a satisfactory explanation, various magnetochemical theories have been proposed from time to time, but thus far very little experimental evidence has been brought forth either to prove or to disprove these theories. Among those who have advocated some form of magnetochemical theory may be mentioned A. L. Parson,[1] G. N. Lewis,[2] J. Dorfmann,[3] B. H. Wilsdon,[4] and E. C. Stoner.[5]

[1] A. L. Parson, Smithsonian Misc. Coll. **65**, 11 (1916).
[2] G. N. Lewis, Am. Chem. Soc. Mon. Ser. (1923); Chem. Rev. **1**, 231 (1924).
[3] J. Dorfmann, Zeits. f. Physik **23**, 286 (1924).
[4] B. H. Wilsdon, Phil. Mag. **49**, 354, 900, 1145 (1925).
[5] E. C. Stoner, Phil. Mag. **49**, 1289 (1925).

If one examines the chemical compounds that may be obtained he is surprised at the frequency with which even molecules occur and the scarcity of odd molecules. (By odd molecules is meant molecules having an odd number of electrons.) Furthermore one is struck by the marked differences in the physical phenomena exhibited by odd and even atoms and molecules. First may be mentioned ionization potential or the work required to eject an electron from an atom. With very few exceptions elements with odd atomic number have a lower ionizing potential than those with even atomic number. The relations between ionization potentials and atomic numbers have been very clearly summed up by F. A. Saunders[6] who shows that in general, the ionizing potentials are higher by several volts for atoms with an even number of electrons than for those with an odd number.

Spectroscopy also shows striking differences between atoms and molecules with odd and even numbers. For example, doublets of spectral lines, such as the D lines of sodium, are characteristic of atoms with odd numbers of electrons such as those appearing in column I of the periodic table. Those elements appearing in column II give spectral lines that are either singlets or triplets while those odd numbered elements appearing in column III give doublets and quadruplets. Again, when new atoms are created by the removal of one or more electrons from an atom the spectral properties of these temporary atoms depend on whether the new atom has an odd or an even number of electrons left. Thus the spectral properties of Al^{++}, Mg^{+} and Na are similar, each having eleven electrons. Likewise the spectral properties of Al^{+} and Mg, each with twelve electrons, resemble each other. From the above and other physical phenomena we are led to conclude that whether the atom or molecule contains an odd or an even number of electrons determines in large measure many of the phenomena connected with it.

If we are to accept the Bohr atom with its revolving electrons we must assume that each revolving electron constitutes a magnet just as any circular current does. According to this theory every molecule must be regarded as containing within it a number of electrons, each of which is an elementary magnet. As has been shown by Parson and others, these magnets may be so related to each other that the molecule as a whole has little or no magnetic moment which apparently is the case in the great majority of chemical molecules. In a few substances, however, the molecule may have one or more unneutralized

[6] F. A. Saunders, Science **59**, 47 (1924).

elementary magnets. Such substances exhibit paramagnetic properties and when placed in a magnetic field the molecule tends to orient itself in such manner as to diminish the net magnetic field in its neighborhood.

The lack of accurate magnetic data makes it difficult to predict the behavior or grouping of electrons from the point of view of magnetism. One may assume that any arrangement of the electrons that is symmetrical will produce diamagnetic conditions whereas unsymmetrical arrangements will produce paramagnetism. Also one may assume that if there is an even number of electrons in the atom they will group themselves in pairs in such manner as to neutralize each other and thus produce diamagnetism whereas if the atom contains an odd number of electrons there will necessarily be one that cannot be paired and this will produce external effects if not neutralized by an electron in some other atom.

It is in this connection that the possibility of magnetism being one of the factors in valence comes in. That the odd electron has something to do with valence is undoubtedly true. Whether the forces are electric or magnetic, or both, is the question that has to be answered. Any solution must necessarily take into account the fact that the electric forces due to the charges must be several thousand times greater than the magnetic forces due to the revolving electrons if we can apply the laws of electromagnetics. The fact that the electrochemical theory which has been held in the past fails to explain some of the important phenomena of chemistry and physics suggests the problem of studying in more detail the electromagnetic theory. The present investigation was undertaken in order to get additional data bearing on this phenomenon and to determine, if possible, the role of magnetic forces in valence.

One method of joining of two electronic orbits is suggested in Figs. 1 and 2. A revolving electron is equivalent to a magnet with polarity as shown in Fig. 1. Two such electromagnets approaching each other, as in Fig. 2, will be drawn together with a magnetic force which depends on some inverse function of the distance apart. There is nothing to prevent the electronic orbits overlapping each other and thus making the distance between effective poles very small. If the atom contains an even number of electrons one might expect, according to the magnetochemical theory, that they would all pair off and thus form a diamagnetic substance. However, one does not have to look far to find substances of even atomic number that are not diamagnetic. Two of the most magnetic substances known, namely, iron and nickel,

are of even atomic number as is oxygen which is also quite strongly magnetic. However, it must be remembered that oxygen is exceptional in its behavior in many other instances[7] and that iron and nickel may be produced in the non-magnetic state according to recent results by L. R. Ingersoll and S. S. DeVinney.[8]

In making a magnetic test between the electrochemical and the magnetochemical theories of valence, it is necessary to experiment on substances of odd atomic number in order to obtain positive evidence. Take for example the oxides of copper, CuO and Cu_2O. The atomic number of copper being 29 and that of oxygen 8, it is seen that CuO has a molecular number 37 which is odd. The copper atom may be

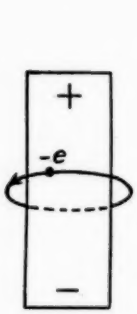

Fig. 1.

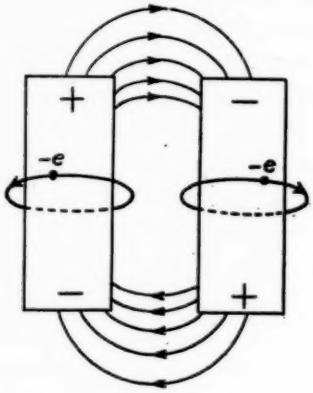

Fig. 2.

thought of as having 14 pairs and one odd electron and the oxygen atom 4 pairs while the compound CuO has 18 pairs and one odd electron. CuO then, should be paramagnetic which is found to be the case. If now, one more atom of copper with its 14 pairs and one odd electron be added to the CuO molecule one should expect one of two things to happen. Either the odd electron of the added copper atom would manifest its magnetism by making the substance Cu_2O more magnetic or the odd electron of the CuO would combine with the odd electron of the added copper atom forming another pair and thus neutralizing the magnetic effect of both. If the latter case were true the substance Cu_2O should be diamagnetic and the magnetic force could easily be thought of as the valence bond or at least as contributing to it. Experiments show that Cu_2O is diamagnetic.

[7] G. N. Lewis, J. Amer. Chem. Soc. **46**, 2027 (1924).
[8] L. R. Ingersoll and S. S. DeVinney, Phys. Rev. **26**, 86 (1925).

Since in the case of elements with even atomic number there are no odd electrons, one may ask whence comes the valence bond? Evidently, as Parson has shown in another connection, two pairs may be joined together to form a stable non-magnetic configuration.

As stated above it is the tendency for electrons to occur in symmetrical groups or in pairs and for this reason it is difficult to obtain many substances of odd molecular number. To make the test that the author is trying to make an element of odd atomic number must be obtained in two compounds; one where the element has a valence of two and the other where the valence is one or three. The author is indebted to B. S. Hopkins of the Chemistry Department of this University under whose direction most of the substances thus far used have been prepared. Care has been taken to eliminate ferromagnetic substances and where there has been any question as to purity a second or even a third sample has been prepared.

The method used was the same as that used by the author in previous magnetic investigations on rare earth oxides, namely, the Curie balance method. The balance was calibrated from time to time but throughout the investigation it has remained practically constant. The amount of the sample used in each test varied from about 40 mg in the case of MnO to 180 mg when some of the diamagnetic substances were being tested.

TABLE I

Magnetic Susceptibilities

Substance	$\chi \times 10^6$ dyne cm per gm.
CuO (odd)	+1.35
Cu_2O (even)	− .34
$CuCl_2$ (odd)	+8.77
CuCl (even)	− .41
$CuBr_2$ (odd)	+2.71
CuBr (even)	− .34
BiO_2 (odd)	+1.55
Bi_2O_3 (even)	− .26
PbO (even)	− .19
PbO_2 (even)	− .20
SnO (even)	− .14
SnO_2 (even)	− .14

Results have been grouped under two tables. Each value is the mean of a large number of determinations with fields varying from 2000 to 4500 lines per sq. cm and for two or more samples for any given material. In Table I are placed those substances which can be said to

be in agreement with the magnetochemical theory in that the odd molecule is paramagnetic and the even molecule is diamagnetic thus indicating that the odd electrons have been paired to help form the valence bond. Many other illustrations similar to the oxides of lead and tin where both molecules are even could be given. In Table II are placed those substances the magnetic measurements for which do not give good evidence in favor of the magnetochemical theory. Lewis, in the article referred to above, quotes the results of Soné for nitrogen and its oxides which are in agreement with the results shown in Table I.

Results given in Table II require special consideration. Manganese, atomic number 25, is very close to the ferromagnetic group, iron, cobalt and nickel, atomic numbers 26, 27 and 28. Two different samples of the oxides of manganese were prepared by different chemists

TABLE II

Magnetic susceptibilities

Substance			$\chi \times 10^6$ dyne cm per gm.
MnO	(odd)		+66.3
Mn_2O_3	(even)		+63.1
CoO	(odd)	(H = 1190 c.g.s. units)	+630.0
Co_2O_3	(even)		+27.5
AgO	(odd)		− .14
Ag_2O	(even)		− .58

and both gave approximately the same results both in magnitude and in having a lower value for the even than for the odd molecule. One advocating the magnetochemical theory might argue that inasmuch as the even molecule has smaller magnetic susceptibility there is evidence of some pairing of electrons when the manganese atom with its odd electron is added to MnO.

Oxides of one of the ferromagnetic elements, cobalt, were used. These showed interesting properties in that the compound CoO (odd) was not only highly magnetic but showed very decided ferromagnetic properties, the susceptibility varying from about 940×10^{-6} dyne cm per gm for a field of about 15 gauss, the lowest field at which the apparatus could be used, down to 265×10^{-6} dyne cm per gm for a field of 4245 gauss. The magnetic susceptibility of Co_2O_3, on the other hand, was practically constant and was very small compared with CoO.

The compounds of silver were peculiar in that both the odd and the even molecule gave diamagnetic susceptibilities. This suggests

the possibility that the AgO (odd) was of the form Ag_2O_2 (even). Further work is to be done in the near future on this substance as well as on other substances of this type.[9]

PHYSICS LABORATORY,
UNIVERSITY OF ILLINOIS,
URBANA, ILLINOIS.
February 10, 1926.

[9] Since submitting this work to the PHYSICAL REVIEW, papers in the same field by S. S. Shaffer and N. W. Taylor (J. Am. Chem. Soc. **48,** 843 (1926)) and by N. W. Taylor (Ibid., **48,** 854 (1926)) have appeared. These experimenters, working with different substances and using a different method, arrived at conclusions essentially the same as the author's.

SPECTRAL EMISSIVITIES OF TANTALUM, PLATINUM, NICKEL AND GOLD AS A FUNCTION OF TEMPERATURE, AND THE MELTING POINT OF TANTALUM

By A. G. Worthing

Abstract

Spectral emissivities of Ta at 0.665μ and 0.463μ have been determined by (a) the tubular filament, (b) the reflectivity and (c) the comparison at contact methods. For 0.665μ the smoothed values at 300°K, 1500°K, and 2700°K are 0.493, 0.438, and 0.394; for 0.463μ, 0.56, 0.50, and 0.43. While agreeing at 300°K with the results of Wartenberg and of Coblentz, at incandescence the present values are lower than previous values. Probable sources of error in emissivity determinations are such as to indicate that these lower values are the more reliable. *Temperature scale for Ta.*—For 0.665μ, the above emissivities lead to the following differences between brightness temperature and true temperature as a function of the brightness temperature: 57° at 1200°K, 107° at 1600°K, 179° at 2000°K, 278° at 2400°K, and 406° at 2800°K. *Melting point of Ta.*—Two determinations by the contact method, using tungsten as the known material yielded 3300°K. This is higher than previously reported values.

Spectral emissivity of Pt was found to vary linearly with temperature. For 0.665μ, the emissivities at 1200°K and 1850°K are 0.295 and 0.310; for 0.535μ at 1200°K and 1600°K, 0.325 and 0.335; for 0.460μ at 1600°K and 1850°K, 0.375 and 0.390. The emissivity at 0.665μ combined with an observed brightness temperature of 1842°K checks Hoffman's careful melting-point determination exactly.

Spectral emissivity of Ni (98.8% pure) was found not to change with temperature. For 0.665μ, 0.535μ, and 0.460μ, emissivities of 0.375, 0.425, and 0.450 were obtained.

Spectral emissivity of Au for 0.665μ was found to increase from 0.062 at 300°K to 0.145 at 1300°K, for 0.535μ to increase from 0.352 at 300°K to 0.450 at 1300°K, for 0.460μ to remain constant at 0.633.

Introduction

A CONSIDERABLE amount of work has been done, mostly from the standpoint of optical constants, in studying emissivities or reflectivities at room temeratures. A moderate amount of work has been done in studying the variations with temperature. The results show great discrepancies. While in the writer's opinion, the variations in the visible for tungsten and molybdenum are well established, there does not seem yet to be a general agreement as to this among workers using these metals. Some still cherish the belief that the optical constants of metals for the visible region are independent of temperatures.

With a desire to find out further facts regarding the emissivity variations of other metals, and to determine the high temperature scales for certain ones likely to be used in other high temperature studies, a study has been made of tantalum, platinum, nickel and gold.

TANTALUM

Emissivity Methods. Three methods[1] have been employed in determining spectral emissivities, namely, (a) the tubular filament method, (b) the reflectivity method, and (c) the comparison at contact method.

By the first method, a comparison of surface brightness with interior brightness as seen through a hole in the side wall of the tubular filament of tantalum yielded an emissivity directly. As in the study of molybdenum, the tube was formed by winding ribbon in a closed helix. Only one workable tube was thus obtained from the limited supply of pre-war tantalum wire, and only at rather high temperatures did it show a uniformity of surface brightness such as to justify inclusion of the data obtained on it in the final average.

By the second method, a comparison of the brightness of an unreflected image of a bright source with its image formed at and reflected by the polished surface of a tantalum ribbon filament mounted in a lamp bulb, yielded a reflectivity (1.00—emissivity). When the ribbon filament was incandescent, its natural brightness was first subtracted from the apparent reflected brightness. Polished flat surfaces were obtained by rolling down wire, the final stage being between two polished safety razor blades. With this method surface pittings, resulting from operating at high temperatures, are liable to reduce the apparent brightness of a reflected image and to lead to too high emissivities. Freedom from this source of error may be assumed when the reflected image for the area studied shows no added detail over the unreflected image. While probably not a perfect criterion, its use insures a certain freedom from error. Quite in contrast, excepting cases where the pits are deep, the other methods, through depending on natural brightness measurements, are free from errors of this type.

By the third method, a comparison was made of the brightness of a metal of known emissivity with that of tantalum in contact, when the junction was heated to incandescence. To obtain reliable results by this method, it is necessary to have a fused contact with the boundary layer of alloy very thin. Obtaining such a layer involved

[1] Worthing, (a) Phys. Rev. **10**, 377 (1916); (b) Zeits. f. Physik **22**, 9 (1924); (c) Phys. Rev. **25**, 846 (1925).

considerable preparation and usually, in the case of tantalum, such attempts resulted in failure. In fact, only one lamp was obtained in which the junction layer was sufficiently thin (not over 1/10 the diameter of the filaments) to justify inclusion of emissivity results obtained with it. The metal having the known emissivity in this case was molybdenum. At the melting point of tantalum there was a slight modification of method. In this case, the brightness of a tungsten filament at the contact end to end with a tantalum filament in one

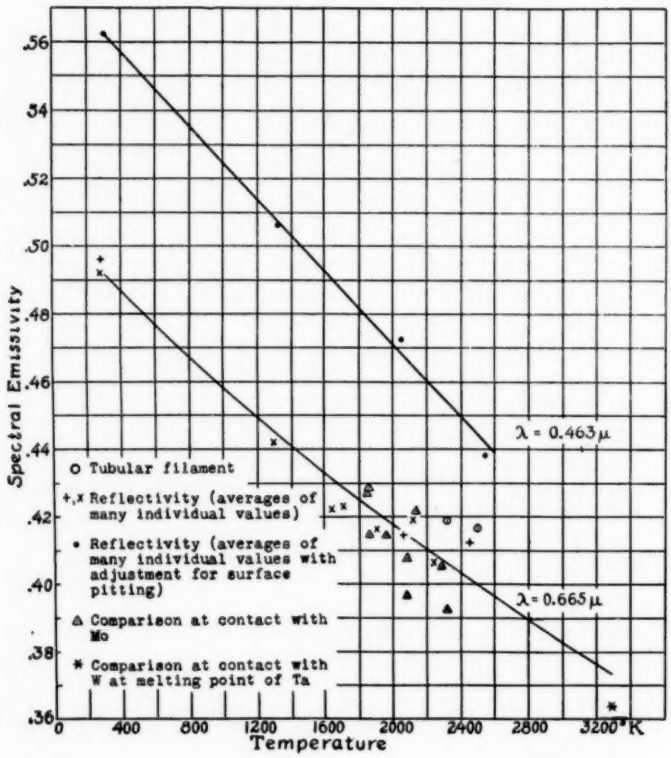

Fig. 1. Spectral emissivities of tantalum as obtained from various methods.

lamp was compared with the surface brightness of a short all tantalum filament at the melting point in another lamp.

Residual gases in the lamp bulb and gases apparently emitted by the tantalum on heating had to be guarded against much more than in the case of tungsten or of molybdenum. Except when the tantalum filament had been operated at a high temperature, say 2400°K, for a considerable time while connected to a mercury condensation pump, there was a tendency for the tantalum surface to lose its luster and to

deteriorate rather rapidly. This was not due to mere surface pittings, for the natural luster of the surface once dimmed as judged by reflectivity measurements, could be largely restored by repeating the above heating and evacuating process.

Emissivity results. Emissivities obtained for 0.665μ and 0.463μ are shown in Fig. 1. As shown, only two determinations were obtained under satisfactory conditions by the tubular filament method. For the most part the reflectivity method was used. Further, all such points represent averages of many determinations. In this work, for 0.665μ, the errors due to shallow pittings have presumably been largely eliminated by limiting the accepted results to that period for which no appreciable changes were noticeable in the measured reflectivities at room temperature. The emissivities for 0.463μ, however, were determined on tantalum showing distinct pitting. Corrections were made, however, in accord with some reflectivities for 0.665μ measured at the same time. Emissivities for 0.463μ are less dependable than those for 0.665μ.

The few results obtained by the comparison at contact method are all shown in Fig. 1. The molybdenum emissivities used were taken from recently published result. The single value plotted at the melting point represents the result obtained from the averages of two tungsten and of two tantalum brightnesses, the tantalum and tungsten brightnesses being obtained in different lamps, as explained above. Due to the actual brightness settings on the tantalum being slightly off from the place where melts actually occurred, the computed spectral emissivity is expected to be low.

Altogether, the data are not as satisfactory as were similar data obtained for tungsten and molybdenum. However, it is probable that the curve for 0.665μ as drawn is correct to within 0.01 or at most 0.02. For 0.463μ the uncertainty is probably over twice as great. It is interesting to note that tantalum shows not only the same type of variation with temperature that tungsten and molybdenum show, but that its actual variation is of the same order. Between room temperature and the melting point for 0.665μ, each shows a decrease, tungsten about 14.5 prcent, molybdenum 22 percent, and tantalum 24 percent.

Comparisons with published results. Previously published results on tantalum for the visible region together with those here presented are shown in Table I. At room temperature, considering the range of interpolation using Coblentz's data, it seems that the results of Wartenberg, Coblentz and the present writer are in fair agreement.

Henning's results do not fit well with the others. How much of the differences is due to impurities is difficult to say. Coblentz found great variations in his specimens. The present writer's specimens, however, obtained at two different times (once from Siemens and Halske) of pre-war origin, and intended for incandescent lamp filaments, yielded essentially the same results. Perhaps their operation several times at very high temperatures, through freeing them from absorbed gases and cleaning the surfaces may have been the determining factor.

TABLE I

Published data on spectral emissivities of tantalum in the visible region.

Author	Method	λ	e_λ	Remarks
		At room temperature		
Wartenberg[2] (1910	Optical constant	.579μ	56.2%	
Henning[3] (1910)	Spectral pyrometer	.665	55	Interpolated from curve
Coblentz[4] (1911)	Thermocouple	.665	48	Interpolated from curve (Wartenberg's sample)
Worthing (1925)	Optical pyrometer	.665	49.3	
		At incandescent temperatures		
Pirani[5] (1910)	Various	.65(?)μ	49%	Assumed constant—disregarded in later work
Mendenhall and Forsythe[6] (1913)	Open wedge	.658	61	1400°K
			49	2100
			47	2800
McCauley[7] (1913)	Open Wedge	.658	59	1400
			47	2100
			46	2800
Worthing (1925)	Tubular filament	.665	44.2	1400
	Reflectivity		41.5	2100
	Mo-Ta contact		39.0	2800

At incandescent temperatures, as also shown in Table I, there are great variations. Pirani had little faith in his determinations and later used for all temperatures 56 percent, the average of Wartenberg's and Henning's results at room temperature. Mendenhall and Forsythe, and also McCauley working under Mendenhall, using the open wedge method, obtained results considerably higher than those presented in this paper. Since all ordinary errors in pyrometry measurements, such as those due to residual gases (Mendenhall and Forsythe do not mention trouble of this kind), pitted surfaces, and failure to obtain complete blackness for the black body radiation, separately

[2] Wartenberg, Verh. Deut. Phys. Gesell. **12**, 105 (1910).
[3] Henning, Zeits. f. Instrumentenk **30**, 61 (1910).
[4] Coblentz, Bull. Bur. Standards, **7**, 197 (1911).
[5] Pirani, Verh. Deut. Phys. Gesell. **12**, 301 (1910).
[6] Mendenhall and Forsythe, Astrophys. J. **37**, 380 (1913).
[7] McCauley, Astrophys. J. **37**, 164 (1913).

tend toward emissivities that are too high, it follows that, other things being the same, the lower values (in this case the present writer's) of emissivity are the more probable. Data on the rate of variation of radiation intensity with temperature, as will be noted in the following paper, point to the same conclusion.

Henning,[8] on the supposition of constancy for his factor θ, obtained at incandescence a minimum value for emissivity, which at about 2500°K in the case of his tantalum band amounted to 30 percent. (His 27 percent for tantalum wire must be discarded because of the errors due to diffraction[8] in pyrometry which may have entered in that case.) This minimum is really an approximation to what is now termed color emissivity,[9] and is in close agreement with the 29 percent which may be deduced from Forsythe's[10] color temperature-brightness temperature data, and with the 32 percent which may be deduced from the above data by means of the equation

$$\log e_c = \frac{\lambda' \log e' - \lambda'' \log e''}{\lambda' - \lambda''}$$

where e_c is the color emissivity and e' and e'' the spectral emissivities at wave-length λ' and λ''.

As a whole, the data of Table I do not show satisfactory agreement. However, for the establishing of a temperature scale at incandescence a selection must be made. In doing so the present author has disregarded previously published results. He has felt justified in so doing (1) because his different methods have checked reasonably well, and (2) because, on the basis of errors at incandescent temperatures arising from imperfect black body conditions, pitted surfaces, and surfaces altered by residual gases, his results seem to be the more nearly free from suspicion.

Temperature scale. The temperature scale of tantalum which follows from the foregoing emissivity at 0.665μ is shown in curve *A*, Fig. 2. The corresponding color temperature scale (curve *B*), however, fairly closely in accord beyond $S=1600$°K with a constant color emissivity of 0.29, is taken from data referred to above obtained by the writer's colleague, W. E. Forsythe.

Melting Point. Only two melting point determinaions have been made. Both have depended upon the determination of the tempera-

[8] Worthing and Forsythe, Phys. Rev. **4**, 163 (1914).

[9] Worthing, Bull. Am. Inst. Mining Met. Eng. No. 153, 1925 (1919); Forsythe and Worthing, Astrophys. J. **61**, 146 (1925).

[10] Forsythe, J.O.S.A. **7**, 1115 (1923).

ture of tungsten filaments at the contact end to end with tantalum filaments as the tantalum was heated to the melting point. These values were 3275°K and 3315°K, the latter having the greater certainty. They give an approximate average of 3300°K.

Previous data are summarized in Table II. Taken altogether there is not a reasonable agreement. Extended extrapolations, based on determinations of currents of small filaments at burnouts, are always subject to considerable uncertainty. Pirani and Meyer's result assumed an emissivity of 0.56 at 0.64μ to apply at all temperatures, but they concluded that the tantalum, when once melted, had a much lower apparent emissivity. This probably means that their

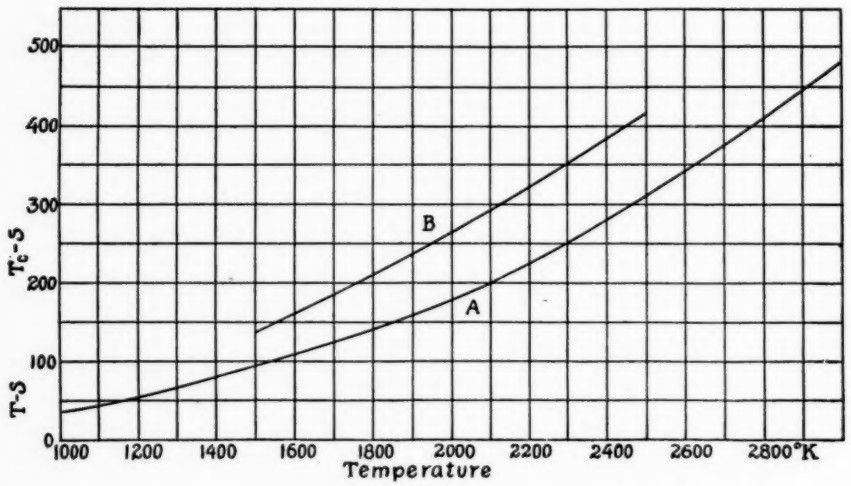

Fig. 2. Temperature scales for tantalum. A. (T−S) scale represents result of present study. B. (T_e−S) scale represents results published by Forsythe.

specimens had roughened surfaces, in which case the application of any supposed emissivity is questionable. The method used by Forsythe seems fundamentally sound. But it is to be said that a discussion of the results for both molybdenum and tantalum emissivities (tungsten also, though the cause for difference in that case was very apparent) obtained by the open wedge method, in contrast to those obtained by the tubular filament, the reflectivity and the contact methods, leads to the belief that the open wedge has not yielded completely black radiation. For this reason Forsythe's 3160°K is probably too low. It is interesting to note that if a lack of blackness of the open wedge radiation occurred, sufficient to account for a measured 0.47 near the melting point as determined by Mendenhall and Forsythe instead

of the present author's 0.375, Forsythe's value for the melting point when corrected would be 3270°K as against the present author's

TABLE II

Published values for the melting point of tantalum.

Observer	Method	c_2	M.P. of Pt.	No. of Trials	Melting Point.	Average Deviation	Melting point $c^2=14330\mu$ deg $T_{Au}=1336°K$ or $T_{Pd}=1829°K$
Waidner and Burgess[11] (1907)	Extrapolation	14500	2026°K	5	3180°K	..	3230‡
Pirani[5] (1910)	Extrapolation	14200	2018	..	3270	..	3230‡
Pirani and Meyer[12] (1911)	Brightness temp. at melt.	14200	*	14	3123	30°K	3106
Forsythe[13] (1911)	Open wedge	14500	2028	8	3071	13	3160♯
Worthing (1925)	Contact with tungsten	14330	....	2	3300	20	3300

*M.P. of Pd taken as 1828°K
♯Correction made for change in effective wave-length (Hyde, Cady, Forsythe, Astrophys. J., **42**, 294 (1915))
‡Adjusted for change in c_2 only

3300°K. Regarding his own result, the writer feels that the temperature scale for tungsten is so nearly agreed upon that the greatest objection to his 3300°K is the smallness of the number of trials. A reasonably precise value for the melting point cannot be stated.

SPECTRAL EMISSIVITY OF PLATINUM

A portion of the platinum used was obtained from Heraeus. Originally in wire form, it was rolled into a ribbon and wound into a tube as had previously been done with molybdenum. Another portion of the platinum was obtained from Baker & Co. Ltd. It was originally tubular. Small holes were drilled through the side walls. These tubes were much like those previously used in the study of tungsten. In all cases the tubes were mounted as filaments in incandescent lamp bulbs with commercial argon as used in incandescent lamps as the contained atmosphere. No reflectivity measurements were made in the case of platinum.

The spectral emissivities obtained for platinum for wave-lengths 0.665μ and 0.460μ by three observers are shown in Fig. 3. The agreement is not good. Nevertheless, for 0.665μ, there is sufficient definite-

[11] Waidner and Burgess, J. Phys. **6**, 830 (1907).
[12] Pirani and Meyer, Verh. Deut. Phys. Gesell. **13**, 540 (1911).
[13] Forsythe, Astrophys. J., **34**, 353 (1911).

ness to justify their presentation. With increase in temperature, there seems to be an increase in spectral emissivity. If this is real, platinum differs in this respect from tungsten, molybdenum, and tantalum for which decided decreases have been found.

As a whole, published results for platinum as presented in Fig. 4 show a wide variation. Relatively, the writer's results are low at low temperatures and about an average at high temperatures.

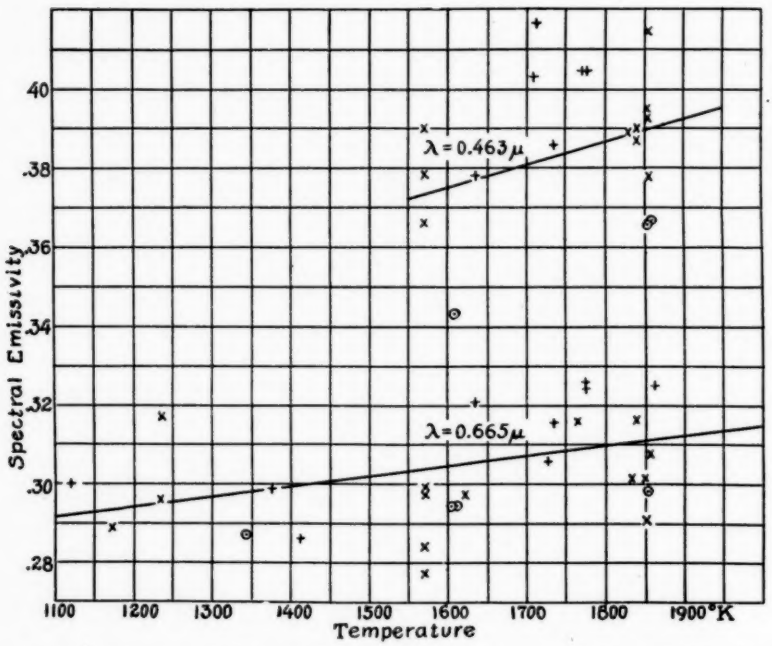

Fig. 3. Spectral emissivity of platinum. Results by three different observers, using the tubular filament method.

There are certain indications, however, which show that considerable confidence may well be given the writer's data. These are his determinations of the melting point which are based in part on the line of Fig. 3 for 0.665μ extrapolated to 2040°K of thereabouts. Using short platinum wires mounted in Λ-shape with the peak considerably reduced in cross-section to make the location of melt definite, eight determinations of the brightness temperature at melt gave 1842°K,*

* At melt the emissivity of platinum, as has been pointed out by Burgess and Waltenberg, increases by about 15%. With wire shaped as stated, it was possible to keep a short length of wire in a semi-molten state. About the small area under observation a boundary line between a dark and a bright portion could be seen to shift slowly back and forth. The dark portion was taken to be the solid phase. Brightness temperature readings on this solid phase were apparently affected by the shifting, for the readings t_n the liquid phase, which gave a brightness temperature of 1864°K, showed only an ^{a}verage deviation of 2°.

the average deviation being 6°. With 0.316 as the emissivity at 0.665μ, a melting point temperature of 2043°K is obtained. This is in

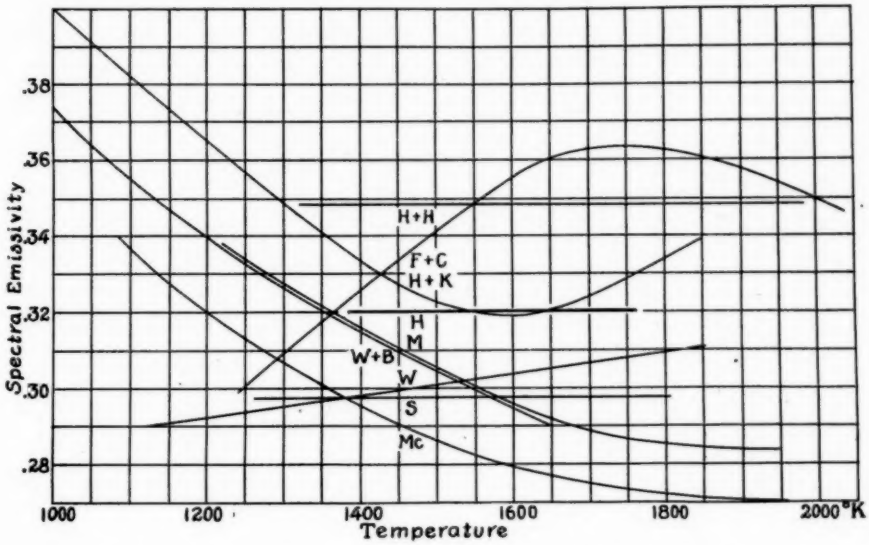

Fig. 4. Published spectral emissivities of platinum for red light at incandescent temperatures as obtained by various experimenters.

Curve	Author	Year	λ
H & K	Holborn and Kurlbaum	1903	.65μ
W & B	Waidner and Burgess	1907	.66
L & M	Laue and Martens	1907	.63
F & C	Fery and Cheneveau	1909	.629
H	Henning	1910	.665*
M	Mendenhall	1911	.658
Mc	McCauley	1913	.658
S	Spence	1913	.658
H & H	Henning and Heuse	1923	.647
W	Worthing	1925	.665

* Interpolated from results for 0.680μ and 0.627μ.

excellent agreement with the value recently obtained by Hoffman[2] in a very careful study. His 2044°K when corrected for a change in[1] c_2 from 14300μ deg. to 14330μ deg. yields 2043°K. On the other hand,

[14] Holborn and Kurlbaum, Ann. d. Physik **10**, 225 (1903).
[15] Waidner and Burgess, Bull. Bur. Standards **3**, 163 (1907).
[16] Laue and Martens, Physik Zeits **8**, 853 (1907).
[17] Fery and Cheneveau, Comptes Rendus **148**, 401 (1909).
[18] Mendenhall, Astrophys. J. **33**, 91 (1911).
[19] Spence, Astrophys. J., **37**, 194 (1913).
[20] Henning and Heuse, Zeits f. Physik **16**, 63 (1923).
[21] Hoffman, Zeits. f. Physik **27**, 285 (1924).

there are the results of Nernst and Wartenberg[22] and of Waidner and Burgess[15] which point to 2035 °K. To check this value either the brightness temperature 1842 °K must be reduced by 6°, the emissivity must be increased to 0.330, or some combination of their partial changes must be made. Further study of platinum is needed.

Spectral Emissivity of Nickel

The nickel used is the same as that used for leads in commercial vacuum incandescent lamps (98.8 percent Ni, 0.75 percent Fe, 0.15 percent each of Cu, Mn, and Si and traces of S, P, and C). The impurities may well affect the melting point but probably are of little consequence in affecting spectral emissivities. For incandescent temperatures, the nickel was formed into tubes as in the case of molybdenum. For room temperature reflectivity measurements, the nickel was in polished ribbon form. In all cases the nickel was mounted as filaments in lamp bulbs baked out in a furnace at a temperature of about 275 °C. Finally the bulbs were filled with commercial argon.

At incandescence, spectral emissivities were taken over the range 1300 °K to 1660 °K. No indication of a change with temperature was found, the average, in fact, agreeing with the two values obtained at room temperature by reflectivity. For 0.665μ, eight determinations gave $0.375 \pm .006$ (average deviation from the mean); for 0.535μ, five determinations gave $0.425 \pm .006$; for 0.460μ, fifteen determinations gave $0.450 \pm .013$.

The above together with previously published spectral emissivities are shown in Table III. The fact that the two single values obtained by the reflectivity method at room temperature are higher than all other values may mean that there was some deterioration of polish due to heating; though, in contrast with others, it may have produced a surface freeer from impurities. The uncertainty in the measurements could hardly by themselves account for the difference.

At incendescence there is a complete failure to check the results of Bidwell. From the standpoint of probable errors of pyrometry, Bidwell's lower values might seem preferable; but in substatiation of the present author's results, some melting point determinations may be quoted. A single determination sighting on the hole of a nickel tube gave 1723 °K, while the average of five groups using the method described for platinum gave 1720 ± 3 °K. Considering impurities this is not a bad check with 1725 ± 2 °K, which the work of

[22] Nernst and Wartenberg, Verh. Deut. Phys. Gesell. **8**, 48 (1906).

TABLE III

Published data on spectral emissivities of nickel in the visible region.

Author	Method	Red		Green		Blue		Remarks
		λ	e_λ	λ	e_λ	λ	e_λ	
		Roon temperatures						
Quincke[23] (1874)	Optical constant	.650μ	.336	.525μ	.396	.450μ	.437	As reported by Rubens.
Rubens[24] (1889)	Bolometric	.665	.340	.535	.385	.460	.390	From smoothed curve.
Drude[25] (1890)	Optical constant	.63	.363	.59	.380	....	....	
Hagen and Rubens[26] (1902)	Thermocouple	.665	.326	.535	.380	.460	.408	From smoothed curve
Hagen and Rubens[26] (1903)	Thermocouple	.65	.328	....	....	....	....	
Bernoulli[27] (1909)	Optical constant	....	....	.535	.365	.460	.378	From smoothed curve.
Henning[3] (1910)	Spectral-pyrometer	.665	.365	.535	.430	....	....	From smoothed curve.
Meier[28] (1910)	Optical constant	.665	.318	.535	.367	.460	.413	From smoothed curve.
Tool[29] (1910)	Optical constant	.665	.333	.535	.383	.460	.430	From smoothed curve.
Ingersoll[30] (1910)	Optical constant	.65	.322	....	....	....	....	
Bureau Standards[31] (1920)		.665	.340	.535	.377	....	....	From smoothed curve.
Worthing 1925)	Pyrometer	.665	.375	....	....	.460	.450	From smoothed curve.
		Incandescent temperatures						
Bidwell[32] (1914)	Pyrometer	.660	.250	....	....	....	....	T = 1200°K (solid)
		.660	.215	....	....	....	....	T = 1700°K (solid)
		.660	.215	....	....	....	....	Liquid at M.P.
Worthing (1925)	Pyrometer	.665	.375	.535	.425	.460	.450	1200°K < T < 1650°K.

Holborn,[33] Day and Sosman,[34] and Burgess and Waltenberg[35] has standardized. To have obtained this value in the present case would

[23] Quincke, Ann. d. Physik **1,** 336 (1874).
[24] Rubens, Ann. d. Physik **37,** 249 (1889).
[25] Drude, Ann. d. Physik **39,** 481 (1890).
[26] Hagen and Rubens, Ann. d. Physik **8,** 1 (1902); **11,** 873 (1903).
[27] Bernoulli, Ann. d. Physik, **29,** 585 (1909).
[28] Meier, Ann. d. Physik **31,** 1017 (1910).
[29] Tool, Phys. Rev. **31,** 1 (1910).
[30] Ingersoll, Astrophys. J. **32,** 265 (1910).
[31] Bureau of Standards, Chem. Met. Eng. **24,** 73 (1921).
[32] Bidwell, Phys. Rev. **3,** 439 (1914).
[33] Holborn, Ann. d. Physik **56,** 361 (1895) (corr. by Ruer, Zeits. anorg. Chem. **51,** 224 (1906).
[34] Day and Sosman, Am. J. Sci. **29,** 93 (1910).
[35] Burgess and Waltenberg, Bull. Bur. Standards **10,** 79 (1914).

have necessitated using an emissivity 0.360 in place of 0.375 for 0.665μ. Were Bidwell's spectral emissivities used, a value of about 1800°K would have been obtained for the melting point. No other conclusion seems possible than that Bidwell's results are considerably in error, and that the present writer's results at incandescence, together with published careful determinations of the melting point, have a consisency which indicates their substantial correctness.

Spectral Emissivity of Gold

The gold used in this study was obtained in sheet form from Eimer and Amend. It was stated to be very pure and suitable for temperature standardizing. The gold for direct emissivity determinations was formed from a portion of the sheet rolled into a closed tube; the gold for reflectivity determinations was formed from small polished strips. All specimens tested at incandescence were mounted and operated like gas-filled lamp filaments. The results obtained for gold are shown in Fig. 5.

Much difficulty was experienced in handling gold. In polishing with rouge, the polishing material became embedded in the gold; and when such a polished strip was heated to incandescence, the presence of the embedded material was manifested at first by numerous bright specks on a comparatively dark background. These rapidly disappeared when the temperature was increased to about 1200 or 1300°K. It has been assumed for the filaments so polished that with such heating the embedded material was either driven off or diffused into the body of the ribbon leaving an essentially pure gold surface. In this report all values for rouge polished filaments refer to surfaces thus cleaned. When operated at about 1200°K, gold etches rapidly due to uneven vaporization, the surface tends to become mottled, and true reflectivity determinations are made difficult even when the etching lines are shallow. All reflectivity determinations made on rouge polished filaments in this work were subject to this difficulty. No such difficulty, however, is experienced in the direct emissivity determinations (*points of Fig. 5) using the tubular filament. The only error due to shallow etching lines would result from the variation from Lambert's cosine law, and for gold, when the lines are shallow, that error is negligible.

In a test of a suspected change in emissivity with heat treatment of gold (none was found), a great many careful reflectivity measurements at room temperature were made. In these cases the surface of the gold was scraped or shaved with a sharp razor blade and then the

specimen was rolled between two other polished razor blades. In all cases the surface was highly polished and under a high power microscope showed no indications of any embedded particles. The average of twelve determinations for 0.665μ gave for the reflectivity $0.938 \pm .010$ (average deviation from mean); the average of two for 0.535μ gave 0.648 ± 0.018; and the average of twelve for 0.460μ gave $0.367 \pm .014$.

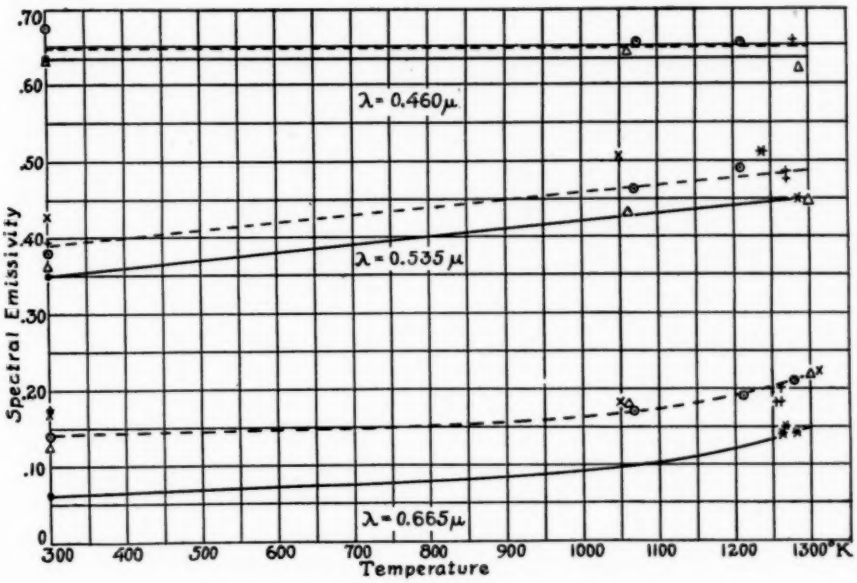

Fig. 5. Spectral emissivity of gold as a function of temperature.

X,Θ,+,Δ values obtained by reflectivity method on rouge polished ribbon filaments showing etching due to heating

* values obtained by direct method on tubular filament

*averages of many determinations by reflectivity method using ribbon filaments, which though highly polished were not contaminated with polishing material

---- averages of X,Θ,+, and Δ values, no corrections being made for effects due to etching

——— expected averages for uncontaminated material

These results (*points of Fig. 5) have been assumed to be the correct reflectivities for gold at room temperature.

The full line curves, representing expected emissivities, have been drawn in accord with the assumption that the observed reflectivities using etched filaments (dashed curves) should be increased throughout by the ratio necessary to yield the more dependable values at room temperature. It is quite satisfying to note that the curve thus obtained for 0.665μ agrees very well at incandescence with the directly

observed emissivities using the tubular filament. At 0.535μ one of the two directly observed emissivities falls on the corrected curve, but the other falls considerably off. A possible explanation is that, in this case, the orientation of the tubular filament, along whose length there ran a narrow slit, was such in this particular instance as to prevent the complete blackening of the radiation from the interior in the direction from which it was viewed.

TABLE IV

Published data on spectral emissivities of gold in the visible region.

Author	Method	Red		Green		Blue		Remarks
		λ	e_λ	λ	e_λ	λ	e_λ	
		Room temperature						
Quincke[23] (1874)	Optical constant	.65 μ	.086	.525μ	.293	.450μ	.652	As reported by Rubens.
Rubens[24] (1889)	Bolometric	.665	.128	.535	.335	.460	.566	From smoothed curve.
Drude[25] (1890)	Optical constant	.63	.105	....	....	....	....	
		.59	.149	....	....	..	....	
Hagen and Rubens[26] (1902)	Thermocouple	.665	.098	.535	.330	.460	.650	From smoothed curve.
Hagen and Rubens[26] (1903)	Thermocouple	.650	.108	....	....	....	....	
Meier[18] (1910)	Optical constant	.665	.120	.535	.335	.460	.565	From smoothed curve.
Tool[29] (1910)	Optical constant	.665	.082	.535	.315	.460	.640	From smoothed curve.
Tate[36] (1912)	Photometric Opt. const.	.665	.160	.535	.395	.460	.635	From smoothed curve.
Försterling and Friederickz[37] (1913)	Optical constant	.67	.045	....	....	....	....	
Worthing (1925)	Pyrometer	.665	.062	.535	.352	.460	.635	
		Incandescent temperatures						
Stubbs and Prideaux[38] (1912)	Photometric	.665	.120	.535	.410	.495	.531	Solid just below M.P.
		.665	.208	.535	.405	.495	.473	Liquid just above M.P.
Bidwell[32] (1914)	Pyrometer	.660	.125	....	....	....	....	Solid and liquid near M. P.
Burgess and Waltenberg[39] (1914)	Pyrometer	.650	.145	.550	.38	....	....	Solid at 1275°K
		.650	.219	.550	.38	....	....	Liquid just above M.P.
Worthing (1925)	Pyrometer	.665	.140	.535	.448	.460	.632	Solid at 1275°K

A comparison of the emissivities obtained with previously published data is shown in Table IV. At room temperature, viewed from the reflectivity standpoint (unity less emissivity), there is general excellent

[36] Tate, Phys. Rev. **34**, 321 (1912).

[37] Försterling and Friederickz, Ann. d. Physik **40**, 201 (1913).

[38] Stubbs and Prideaux, Proc. Roy. Soc. **87A**, 451 (1912).

[39] Burgess and Waltenberg, Bull. Bur. Standards **11**, 591 (1914).

agreement between published values. From the emissivity standpoint, however, the checks on a percentage basis are not good. The present author's value for 0.665μ with a single exception is lower than that of others. Whether or not the polishing by pressure, rather than by means of the more common method employing rouge with its possibilities of embedding polishing material in the gold, is the explanation cannot well be stated. That the differences shown in the table for 0.535μ should not only relatively but numerically be generally less and those for 0.460μ still less, is in agreement with the supposition of embedded polishing material as a source for discrepancies. Thus, some unintentional confirming tests with rouge-embedded gold specimens indicated an apparent change in emissivity for the specimens which at 0.655μ was over five times as great as at 0.460μ.

At incandescence, at 0.665μ, there is a moderately good agreement in published emissivities. For the green and blue regions of the spectrum the agreement does not seem to be quite so good, though due to the diversities of wave-lengths it is difficult to say so definitely. Altogether, the writer has considerable confidence in the results which he has presented.

An interesting point which may be with or without significance is to be seen when comparisons of emissivity variations with temperature are made for gold and tungsten. Weniger and Pfund[40] found for tungsten that at 1.27μ there was no change in emissivity with temperature, while for longer wave-lengths there was a definite progressive increase in emissivity with increase in temperature, and for shorter wave-lengths, as was known before, a definite progressive decrease. The present work suggests a similar relation for gold with 0.460μ as the wave-length corresponding to 1.27μ; and it is interesting to note, though it may be a mere coincidence, that these wave-lengths are in direct proportion to the melting point temperatures. Thus $1.27\mu/0.46\mu$ equals 2.76, while 3655°K/1336°K equals 2.74.

In conclusion the writer wishes herewith to acknowledge his indebtedness at different times in the progress of the work to Lester Boss, Ruth Sublett Haas, Pauline Perkins, and John Kirschner.

NELA RESEARCH LABORATORY,
August, 1925.*

[40] Weniger and Pfund, Phys. Rev. **14**, 427 (1919).

* Received April 5, 1926.

PHYSICAL PROPERTIES OF WELL SEASONED MOLYBDENUM AND TANTALUM AS A FUNCTION OF TEMPERATURE

By A. G. Worthing

Abstract

Spectral emissivity, spectral reflectivity, resistivity, radiation intensity, and thermal expansion measurements as a function of temperature have been made for well seasoned molybdenum and tantalum. From the data thus obtained values for many other physical quantities as functions of temperature have been computed. As such physical quantities, *average visible emissivity, color emissivity, total emissivity, brightness temperature, color temperature, radiation temperature, normal brightness, luminous efficiency,* and certain temperature variation coefficients have been included. Comparison measurements on moderatly pure and very pure molybdenum showed no appreciable variation in radiation properties, though appreciable variations appeared in their resistivities. The results for very pure molybdenum and moderately pure tantalum are incorporated in tables giving values where known for every 200 degrees between room temperature and the melting points.

Molybdenum

Introduction. Once given the temperature scale[1] for molybdenum, a determination of some of the physical properties naturally follows. Herewith are presented measurements of resistance, total radiation and thermal expansion. From these, with the aid of the temperature scale, various physical properties as a function of temperature have been derived.

The data have been obtained from two lamps. Both lamps had long cylindrical filaments bent into squared U-forms with fine pick-off leads spot welded to the main filaments for the elimination of end loss effects. Both lamps were well evacuated by means of a condensation pump operating through a liquid air trap. The familiar coil test showed high vacua in both cases.

During their lives, both lamps were operated at such high temperatures that on account of vaporization they had to be opened up three or four times to remove the deposit on the inside of the bulb. Finally, after having found the highest temperatures for safe operation, a series of measurements was obtained on each, the lamps opened and the filaments measured. The dimensions obtained were, therefore, strictly applicable to the filaments as used in obtaining the data to be reported.

[1] Worthing, Phys. Rev., 25, 846, 1925.

Mechanical data relating to the filaments are given in Table I. The filament of 2-W-37 was supplied by the Cleveland Wire Division of the National Lamp Works. It was drawn from the most nearly

TABLE I

Mechanical data relating to molybdenum filaments in the lamps studied.

Lamp	Radius	Overall length	Length between pot. leads	Surface	Maximum end loss correction	Filament purity
2–W–46	0.262mm	39.8cm	31.6cm	5.20cm²	0.3%	Commercial
2–W–37	0.120	41.2	30.1	2.27	0.0	Very pure

pure slug that that division had been able to obtain. Results on the temperature coefficient of resistance, as will be reported, bear out this claim for purity.

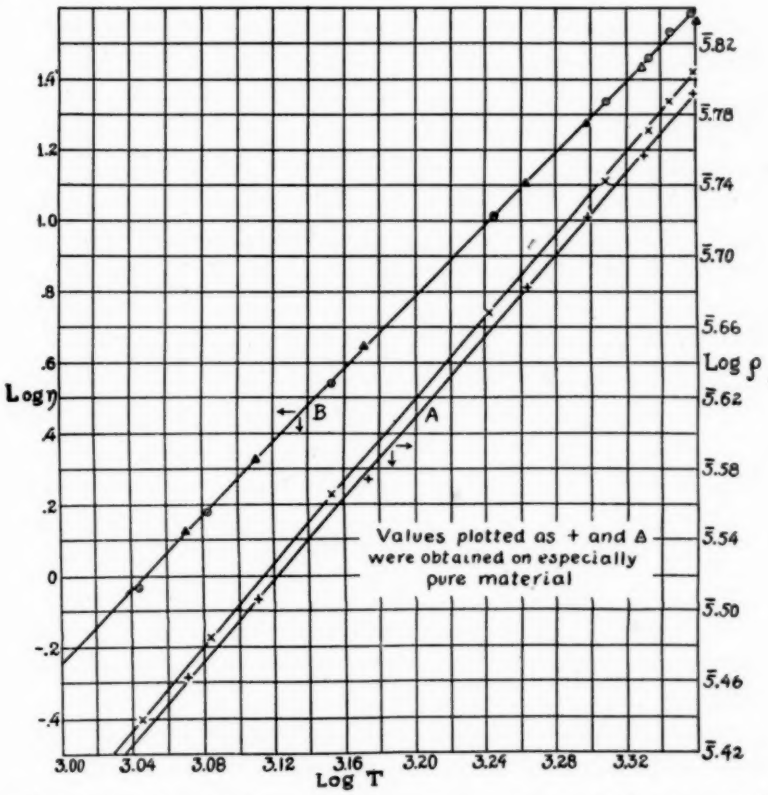

Fig. 1. Variation of resistivity ρ in ohm cms (Curve *A*) and radiation intensity η in watts/cm² (Curve *B*) with temperature T in °K for well seasoned molybdenum.

Resistivity, radiation intensity, and thermal expansion measurements. Measurements of resistance and of the total radiation rate at high

temperatures were made simultaneously. Temperatures were obtained with a disappearing filament pyrometer. Settings were made at several points along the filaments. The observed resistivities and radiation intensities are shown in Fig. 1. The individual data on radiation intensity for the two lamps fall very closely on the same curve. The resistivity curves for the two specimens of wire differ, however. While the resistivities at incandescence show the same variation with temperature, there is a definite difference at any one temperature, the resistivity of the pure material being less by about 2 percent. As with tungsten, the plot showing $\log\rho$ as a function of $\log T$ is a straight

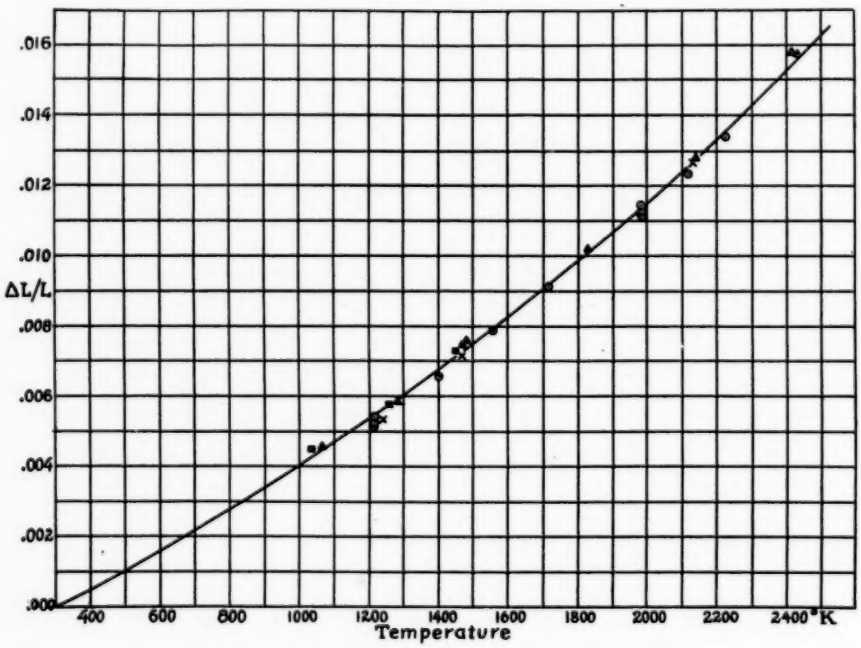

Fig. 2. Thermal expansion of molybdenum.

line. Its slope, which gives the percentage change in resistance due to one percent change in temperature, is less for molybdenum, however, being about 1.145, against 1.200 for tungsten.

Thermal expansion measurements were made with the aid of a position microscope and a micrometer microscope. Small scratches made on the filaments before mounting were used as reference marks. The data on thermal expansion (see Fig. 2) are the results of four runs. In each set some low incandescent temperature was selected as a condition to which references were frequently made to assure freedom from instrumental variations. In each set at the beginning, one meas-

urement of expansion between room temperature and this reference temperature was taken. Because of the long time required by a filament in vacuo to reach temperature equilibrium at room temperature after being once heated to incandescence, the usual check back could not be carried out for this step. The equation obtained for the curve of Fig. 2 is

$$L/L_{300}=5.00\times10^{-6}(T-300)+10.5\times10^{-10}(T-300)^2.$$

The first coefficient is greater than that obtained for tungsten, namely 4.44×10^{-6} deg.$^{-1}$. It is less, however, than the 5.08×10^{-6} deg.$^{-1}$ which is obtained from the equation giving the carefully determined results of Schad and Hidnert,[2] though well within the range of the recently determined coefficients of Hidnert and Gero[3] for various specimens having different coarseness of grains. The check is quite satisfactory.

Measurements of resistance at low temperatures were made by a Kelvin double bridge method with the filament immersed in a high grade lubricating oil and heated externally. Temperatures were determined with mercury in glass thermometers which were calibrated in melting ice and in steam and compared elsewhere with the indications of a standard calibrated Pt, Pt+10 percent Rh thermocouple.

Purity of the molybdenum in lamp 2-W-37. Giess and van Liempt[4] showed from a study of alloys of tungsten and molybdenum that the average temperature coefficient of resistance between 0°C and 100°C, α, for any specimen gave a very good index of its purity. In a plot of α as a function of atomic percent of Mo, they found $\alpha\times10^5$ in deg.$^{-1}$, starting with 100 percent W and 0 percent Mo, to have a value of 482, to decrease rapidly with increasing Mo content to a minimum of 290 at 35 percent Mo and thereafter to increase at first slowly and then more rapidly to 457 for 100 percent Mo. Later, in a personal letter, Dr. van Liempt states that he has obtained still purer Mo with $\alpha\times10^5$ equal to 463. Apparently for nearly pure Mo a change of 1 percent in the tungsten content means approximately a change of 10 in this quantity.

The writer, in his measurements made previous to Giess and van Liempt's publication, obtained three values at different temperatures which can be used in checking purity. Using the formula

$$\alpha=\frac{R_1-R_2}{R_2t_1-R_1t_2} \tag{1}$$

[2] Schad and Hidnert, Bull. Bur. Stds., **15,** 31, 1919.
[3] Hidnert and Gero, Bull. Bur. Stds., p. 429, 1924.
[4] Giess and van Liempt, Z. für Anorg. u. Allg. Chem., **128,** 355, 1923.

where α refers to the temperature range 0° to 100°C and R_1 and R_2 the resistances of the specimen at two temperatures, t_1 and t_2, expressed in °C, he obtained three values for $\alpha \times 10^5$ in deg.$^{-1}$, namely, 463, 464, and 464. The check with van Lempt's later result for pure Mo is excellent and indicative of the supposed purity of the specimen. The foregoing indicates that for Mo for $0°C < t < 100°C$

$$R = R_0(1 + 0.00464t) \ . \qquad (2)$$

For the range $0°C < t < 200°C$ additional readings (see Table II) indicated the best value for α should be decreased by about 2 in the

TABLE II

Resistance temperature data for a pure molybdenum specimen at low temperatures.

t	R	.3417 (1+.000464t)	.3418 (1+.000462t)
30.80°C	.3905 ohms	.3905 ohms	.3905 ohms
52.10	.4242	.4243	.4241
100.85	.5015	.5014	.5011
155.7	.5872	.5887	.5876
181.7	.6287	.6299	.6287
206.5	.6681	.6692	.6679

last place. This may only mean that the temperature measurements are more uncertain in the range $100°C < t < 200°C$, or that the departure from the linear relation is more evident over the longer range.

Unfortunately, the variation in resistance with temperature at low temperatures was not determined for lamp 2-W-46. From a careful comparison of the variation between low incandescence and room temperature, for the two lamps, it is certain that, at low temperatures, the temperature coefficient of 2-W-46 was much lower than for the pure material of 2-W-37. Whereas, as shown in Fig. 1, at incandescent temperatures the resistivity of the pure specimen was about 2 percent less than for the other specimen, at room temperature it was about 11 percent less. These values are in agreement with what is expected from a consideration of Giess and van Liempt's results and the known purities of the wires used.

Collected data. From the data presented in the paper on the temperature scale, together with that presented above, it is possible to compute values for various other properties. In Table III at equal temperature intervals from room temperature, values for the observed and computed properties are given. The meaning of some of the terms and the manner of their obtaining follow.

Color emissivity, e_c, and color temperature, T_c, have significance for a source only when its light may be matched with that from a black

TABLE III

Properties of well seasoned molybdenum for various temperatures

($c_2 = 14330\mu$ deg., $T_{au} = 1336°K$)

Temperature T °K	Spectral Emissivity $e_{.665\mu}$	Spectral Emissivity $e_{.475\mu}$	Average Visible Emissivity e_v §	Color Emissivity e_c §	Total Emissivity e_t	Brightness Temperature $S_{.665\mu}$ °K	Color Temperature T_c °K	Radiation Temperature T_r °K	Relative Length L/L_0	Resistivity ρ μ-ohm cm. * ‡	$\frac{T}{\rho}\frac{d\rho}{dT}$ * ‡	Brightness normally B_n candles/cm²	$\frac{T}{B_n}\frac{dB_n}{dT}$	Radiation Intensity η watts/cm²	$\frac{T}{\eta}\frac{d\eta}{dT}$	Luminous Efficiency eff lumens/watt † §
273	.420	.425	....	....	....	....	.....	....	.....	5.14	1.265	.....	....	.....	....	.....
300	.419	.424	....	....	....	....	....	....	1.00000	5.78	1.235	.....	....	.....	....	.....
400	.415	.421	....	....	....	....	....	....	.....	8.15	1.170	.....	....	.....	....	.....
600	.406	.415	....	....	....	....	....	....	.....	.....	.....	.....	....	.....	....	.....
800	.398	.409	....	....	....	....	.....	....	.....	.....	.....	.....	....	.....	....	.....
1000	.390	.403	.393	.361	.096	958	1004	557	1.0041	23.9	1.145	.00010	22.3	.55	5.32	.....
1200	.382	.398	.386	.347	.121	1139	1207	708	1.0054	29.5	1.145	.0050	19.2	1.43	5.23	.....
1400	.375	.393	.379	.333	.145	1316	1411	864	1.0068	35.2	1.145	.089	16.9	3.18	5.16	.093
1600	.367	.388	.373	.321	.168	1489	1616	1024	1.0083	41.1	1.145	0.765	15.1	6.30	5.10	.40
1800	.360	.383	.367	.309	.189	1658	1823	1187	1.0099	47.0	1.145	4.13	13.6	11.3	5.04	1.22
2000	.353	.379	.362	.297	.210	1824	2032	1354	1.0115	53.1	1.145	15.9	12.4	19.2	4.99	2.75
2200	.347	.375	.357	.287	.230	1986	2244	1523	1.0133	59.2	1.145	48.5	11.3	30.7	4.94	5.28
2400	.341	.371	.352	.277	.248	2143	2456	1693	1.0151	65.5	1.145	123.	10.4	47.0	4.90	8.70
2600	.336	.368	.348	.268	.265	2297	2672	1866	.....	71.8	1.145	270.	9.6	69.5	4.86	13.0
2800	.331	.365	.344	.260	.281	2448	2891	2039	.....	78.2	1.145	540.	8.9	98.	4.83	18.4
2895¶	.328	.363	.342	.255	.290	2519	2997	2122	.....	81.4	1.145	730.	8.6	116.	4.81	.....

* Values given for ρ and $\frac{T}{\rho}\frac{d\rho}{dT}$ assume the dimensions possessed at 300°K. All other quantities have been corrected when necessary so as to be in strict accord with definitions.

‡ For the range 0°C < to < 200°C, the resistivity is given by the equation $\rho_t = \rho_0 (1 + 0.00462t)$. The molybdenum wire used was especially pure.

† Luminous efficiencies were obtained by applying the relation $\left[\text{eff} = 1.06_\pi \frac{B_n}{\eta}\right]$. The factor 1.06 was introduced to account for the deviation of molybdenum from Lambert's cosine law.

§ Values given for e_v, e_c, T_c, and eff presuppose an acurate color match between molybdenum at T and a black body at T_c.

¶ Melting point.

body. This is the case with molybdenum. Quantitatively for a source at a temperature, T, the color emissivity is the ratio of the brightness of the source to that of a black body at color match that is at T_c. Mathematically the relation is given by

$$ln\ e_c = \frac{c_2}{\lambda}\left(\frac{1}{T_c} - \frac{1}{S}\right)$$

where e and S are the spectral emissivity and brightness temperature for wave-length λ and c_2 the Wien-Planck constant.

Brightness may be computed in either one of two ways; either as the product of e_c and the brightness of a black body at temperature T_c, or as the product of the average visible emissivity, e_v, and the brightness of a black body at temperature T. In equation form,

$$ln\frac{e_v}{e_c} = \frac{c_2}{\lambda_0}\left(\frac{1}{T} - \frac{1}{T_c}\right)$$

where λ_0 is the Crova wave-length for black body radiation.

Total emissivity, e_t, and radiation temperature, T_r, corresponding to any temperature, T, have been computed from the defining equations

$$\eta = e_t\sigma T^4 = \sigma T_r^4$$

where η is the radiation intensity expressed here in watts/cm^2, and σ the Stefan-Boltzmann constant.

Luminous efficiencies have been computed from the normal brightness and radiation intensities, with a correction of 6 per cent (to be published later) for deviation from Lambert's cosine law.

The more nearly constant factors

$$\frac{Td\rho}{\rho dT},\ \frac{TdB_n}{B_n dT},\ \text{and}\ \frac{Td\eta}{\eta dT}$$

are the slopes on corresponding log plots.

There are very little published data for molybdenum on the properties at incandescence which are considered here. Greenslade[5] has published in an abstract spectral energy curves for various temperatures, but the plots are in such a form that comparisons cannot well be made. Somerville[6] has studied the resistance change with temperature between room temperature and 1000°C. The results do not check with what is given here. The cause is probably due to impurities in Somerville's molybdenum which was prepared when the metallurgy

[5] Greenslade, Phys. Rev., **15**, 150, 1920.
[6] Somerville, Phys. Rev., **31**, 261, 1910.

of molybdenum was much less well developed. In contrast with the temperature coefficient of resistance between 0°C and 100°C, α_{0-100}, of 0.00463 1/deg. as obtained by Giess and van Liempt and by the present author, as reported above, Somerville obtained 0.0033 1/deg. More recently Blom[7] has published resistivity results for the range 0°C to 2000°C. Unfortunately the check here is not good. Perhaps here also lack of purity of the specimens used is the cause for discrepancy. Expressed in micro-ohm cm, he found 4.4 as the resistivity at 0°C, as against 5.78 for the very pure and 6.41 for the commercial specimens used by the present author. For α_{0-100}, Blom obtained 0.00414 1/deg. as against 0.00463 1/deg. Reduced to the temperature scale employed here, Blom's results give for $\frac{T}{\rho}\frac{d\rho}{dT}$ values which increase gradually from 1.11 at 0°C to 1.23 at 1600° to 2000°K; whereas the present work gives results which starting with 1.265 at 0°C decrease gradually to the constant value of 1.145 which applies above 1000°K. From the standpoint of variations in α_{0-100} and in $T/\rho\ d\rho/dT$, the differences might be explained by assuming Blom's wire to have been less pure than the present author's. The actual resistivities found at room temperature do not fit in with this explanation, however.

Tantalum

From some of the same wire that was used in the spectral emissivity work (see preceding paper), a lamp with voltage pick-offs of fine tungsten wire was made. This lamp had a good vacuum. The filament was well aged at a temperature of about 2700°K, and its surface, during the measurements made on it, was well polished and quite free from pits and any apparent damage resulting from any residual gases. The dimensions of the part between the potential leads were: diameter, 0.496 mm; length, 30.5 mm. At 23°C its resistance was 0.0228 oms.

Determinations of temperature distribution along the length of the filament were made for four widely separated temperatures to take account of variations due to lack of constancy in diameter. Then for several currents, resistance, wattage and thermal expansion measurements were made. Methods and precautions were the same as in the study of molybdenum.

Resistivity. In curve *A*, Fig. 3, resistivity as a function of temperature ($1500°K < T < 2800°K$) is shown on a logarithm scale. The locus is nearly a straight line with the slope $\frac{T}{\rho}\frac{d\rho}{dT}$ equal to 0.785. Pirani's[8]

[7] Blom, Phys. Rev., **13**, 309, 1919.

[8] Pirani, Verh. Deut. Phys. Gesell., **12**, 301, 1910.

data plotted similarly gives a noticeably greater slope, namely, 0.86. This difference cannot be ascribed to a difference in temperature scales. It may be found, perhaps, in Pirani's method of eliminating cooling effects due to leads. He used the method of differences as obtained from two filaments of unequal length. This method is good in case the filaments have the same cross-section, but such a coincidence occurs too seldom according to the present writer's experience, and instead he has used the potential lead method.

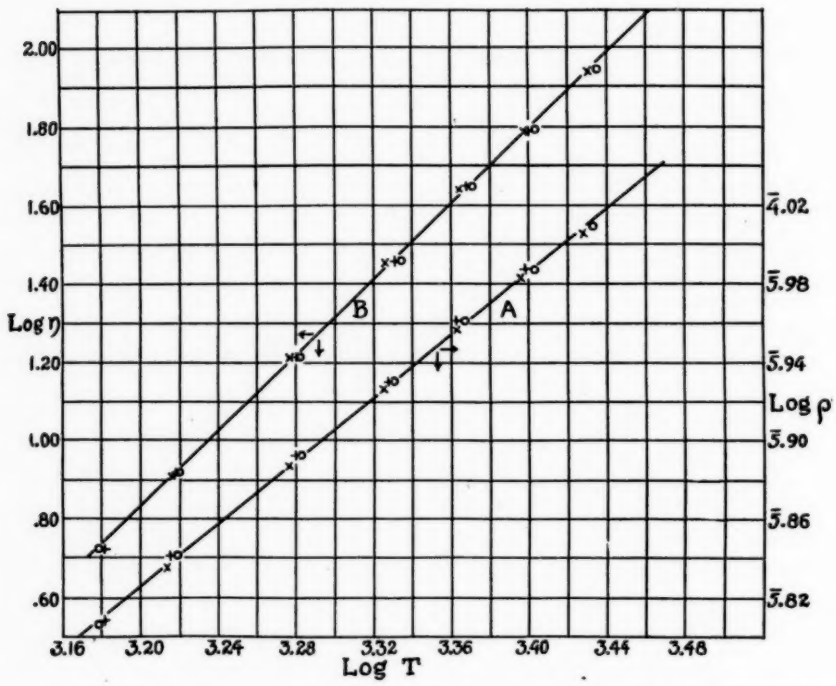

Fig. 3. Variation of resistivity ρ in ohm cms (Curve A) and radiation intensity η in watts/cm² (Curve B) with temperature T in °K for well seasoned tantalum.

At the lowest temperature shown in Fig. 3, there is indication of an increase in the slope $\frac{T}{\rho}\frac{d\rho}{dT}$. This is consistent with the average slope of .915 between room temperature and 1500°K which is obtainable from the data given. This low temperature value agrees satisfactorily with Holborn's[9] data and also with Pirani's for this range, but not with Bridgman's[10] as is indictated by Holborn's comparison.

[9] Holborn, Ann. Physik, 59, 145, 1919.
[10] Bridgman, Proc. Nat. Acad. Sci., 3, 10, 1917.

The resistivity of 14.6 microohm-cm. at 300°K does not check with Pecheux's[11] 17.5 microohm-cms.

In contrast with tungsten and molybdenum, for which $\frac{T}{\rho}\frac{d\rho}{dT}$ at incandescent temperatures are 1.200 and 1.145, this quantity for tantalum is lower than unity, being about 0.78.

Radiation intensity. In curve *B*, Fig. 3, the variation in the radiation intensity of tantalum with temperature is shown. Three sets of measurements taken in the order ×, +, o are indicated. Just why

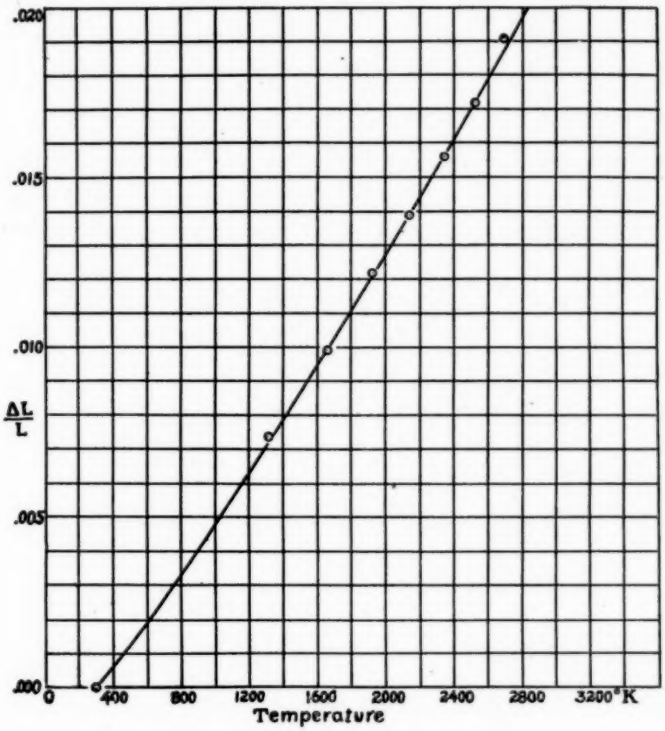

Fig. 4. Thermal expansion of tantalum.

the O values of curve *B* should lie so much further from the × and + values than in case of curve *A* is uncertain. The supposition of an error of determination of the temperature combined with an appreciable filament vaporization between sets does not fit. The supposition of deleterious effects due to residual gases is also eliminated, for the filament surface maintained a high polish throughout. Taken al-

[11] Pecheux, Comptes Rendus, **153**, 1140, 1911.

together, there is an indication of some change in resistivity or in radiation intensity or both.

All three sets of measurements show separately the same percentage change in wattage for a given percentage change in temperature, $\frac{T}{\eta}\frac{d\eta}{dT}$ amounting to 4.80. Theoretically with increase in T, $\frac{T}{\eta}\frac{d\eta}{dT}$ must finally decrease to 4, the black body value. That line *B*, Fig. 3, is straight may indicate an error in the locating of the spectral emissivity curve as presented in the preceding paper. This does not tend, however, to indicate essential correctness in other reported temperature scales for tantalum such as those resulting from Mendenhall's and Forsythe's or McCauley's emissivity data, for on their temperature scales an appreciable increase in $\frac{T}{\eta}\frac{d\eta}{dT}$ with temperature would follow.

The same comments with regard to published data that are made above relative to resistivity at incandescent temperatures apply equally here.

TABLE IV

Physical properties of well seasoned tantalum.

Temperature T °K	Spectral emissivity at 0.665μ	Spectral emissivity at 0.463μ	Brightness Temp. °K $S_{0.665\mu}$	Color Temp.* T_c °K	Resistivity ρ μ-ohm-cm	$\frac{T}{\rho}\frac{d\rho}{dT}$	Radiation Intensity η watts/cm^2	$\frac{T}{\eta}\frac{d\eta}{dT}$	Total Emissivity e_t	Radiation Temperature T_r °K
300	.493	.56	....	....	.....	.....	.....	....	....	....
1000	.459	.52	966	....	.....	.....	.....	....	....	....
1200	.450	.51	1149	....	.....	.....	.....	....	....	....
1400	.442	.50	1329	....	.....	.....	.....	....	....	....
1600	.434	.49	1506	1642	67.6	0.785	1.65	4.80	.194	1062
1800	.426	.48	1680	1859	74.1	0.785	2.90	4.80	.213	1222
2000	.418	.47	1851	2075	80.5	0.785	4.81	4.80	.232	1390
2200	.411	.46	2018	2288	86.9	0.785	7.60	4.80	.251	1556
2400	.404	.45	2180	2497	92.9	0.785	11.5	4.80	.269	1730
2600	.397	.44	2339	2705	99.1	0.785	16.9	4.80	.287	1901
2800	.390	...	2495	2911	105.0	0.785	24.2	4.80	.304	2080
3000	.384	...	2647	....	.....	.....	.....	....	....	....
3300mp	.375	...	2870	....	.....	.....	.....	....	....	....

*As determined by Forsythe.

Thermal expansion. The data for a particular run are shown in Fig. 4. The curve is represented with considerable accuracy by the equation

$$\frac{\Delta l}{l} = 6.60\times10^{-6}(T-300°)+5.2\times10^{-10}(T-300°)^2,$$

For 0°C this yields a coefficient of 6.57×10^{-6} deg.$^{-1}$. This is in good agreement with Disch's[12] equation for the range $0°C<t<400°C$, obtained by the Fizeau method,

$$\frac{\Delta l}{l}=6.46\times10^{-6}t+9.0\times10^{-10}t^2.$$

Collected data. In Table IV data on properties of tantalum between room temperature and the melting point where known with reasonable certainty are shown at 200° intervals.

The writer is greatly indebted to Lester Boss, Ruth Sublett Haas, C. H. Prescott Jr. and Pauline Perkins for aid in carrying out the experimental work.

NELA RESEARCH LABORATORY,
NELA PARK, CLEVELAND,
September, 1925.

[12] Disch, Z. Physik, **5**, 173, 1921.

A TEMPERATURE SCALE FOR TUNGSTEN

By H. A. Jones

Abstract

Temperature variation of the resistance of tungsten from 273°K to 3655°K.—In the range from 273°K to 1500°K measurements were made of the resistance of coils of pure, well-aged, tungsten filaments (diam. 2.61 mils) placed in the center of a constant temperature compartment of an alundum resistance furnace through which a stream of pure dry hydrogen was continuously passed. Temperatures were measured by a carefully standardized chromel-alumel thermocouple. In the range 1200°K to 3655°K tungsten filaments (V shape, length 40–50 cm, diam. 2.61, 5.00 and 9.85 mils) were mounted in lamp bulbs and their resistances measured. Temperatures were determined by pyrometering against a standard lamp. The specific resistance of tungsten was found to vary from 5.00×10^{-6} ohm cm at 273°K to 117.1×10^{-6} at 3655°K.

Temperature variation of the rate of radiation from tungsten filaments.—Lamps of the above type were also used to determine the variation with temperature of the energy radiated per cm² of the tungsten filaments. Temperatures from 300°K to 1500°K were measured by the resistance method, from 1500°K to 3655°K by the optical pyrometer. The rate of radiation varied from .000016 watts/cm² at 300°K to 399.4 at 3655°K.

A LARGE number of investigations on electrical discharges in gases involve the use of a "cold" cathode whose temperature is less than 1500°K. Since temperatures cannot be estimated with any great accuracy in the range 1500°K to 273°K by the usual pyrometric or photometric methods, the resistance method of determining temperatures finds valuable application here. In this paper a temperature scale for pure tungsten, based primarily upon accurate resistance measurements, is presented for the range 273°K to 1500°K. For the sake of completeness the measurements are continued up to 3655°K and observations are made on the rate of radiation from tungsten filaments for the temperature range 300°K to 3655°K.

The ratio of the resistance at the temperature T to that at 0°C, or at a known room temperature, affords a simple and convenient estimate of the temperature of tungsten filaments. If ρ is the resistivity of tungsten in ohm cm at the temperature T, the resistance R of a cylindrical filament at this temperature will be $4\rho l/\pi d^2$, where d and l are expressed in cm. Putting $R'=4\rho/\pi$, we have $R'=Rd^2/l$. R', the resistance of a filament of unit length and unit diameter is a function of the temperature alone and may be used as a measure of the temperature.

The resistance method of measuring temperatures has the advantage that it can be used when the filament is surrounded by a gas or when

its surface is tarnished by oxidation. On the other hand it has the disadvantage that the resistance and its temperature coefficient are very sensitive to traces of impurities, and also that at low temperatures the resistance of a filament is often so low that errors due to lead and contact resistances are apt to play a large role.

Measurements of the ratio of hot to cold resistance of tungsten have been made by Somerville,[1] Pirani,[2] Langmuir,[3] Holborn,[4] Forsythe and Worthing,[5] and Zwikker.[6]

Measurements of the Ratio of Hot to Cold Resistance

Three different tungsten wires were used, all drawn from the same rod of metal which was of unusual purity. The wires, which we will designate W_1, W_2 and W_3 were 2.61, 5.00 and 9.85 mils in diameter, respectively. The diameters were determined from the density and the weight per unit length, using the value 19.35 gm/cc which has been accepted for the density of well aged, pure tungsten. This value has been determined at the Phillips Glowlamp Works in Holland[7] from an extensive series of density measurements on aged tungsten filaments. (It is interesting to note that the latest x-ray work on single crystal tungsten gives a value of $19.32 \pm .02$ as an upper limit for the density, while experimental measurements on the wires used in the present work gave 19.39.) The diameters obtained by the above method agree within the experimental error with the results of a series of measurements made with a sensitive micrometer.

Several lengths of the wire W_1 (each having a resistance of approximately 8 ohms at 0°C) were coiled on a 10 mil mandrel; each length was electrically welded to 30 mil molybdenum leads and sealed into a bulb. These lamps were then well exhausted (residual gas pressure less than 0.0006 bar), the glass being baked out at 360°C while the filaments were heated for about 5 minutes at 2800°K. After seal-off the coils were further aged by heating to 2400°K for twenty-four hours. They were then removed from the bulbs and used for the subsequent resistance measurements.

[1] A. A. Somerville, Phys. Rev. **30**, 433 (1910).
[2] Pirani, Verh. d. Phys. Ges. **12**, 301 (1910); Phys. Zeits. **13**, 753 (1912).
[3] Langmuir, Phys. Rev. **7**, 302 (1916).
[4] Holborn, Ann. d. Physik **59**, 145 (1919).
[5] Forsythe and Worthing Astrophys. J. (Jan. 1925).
[6] Zwikker, Koninklijke Akademie Van Wetenschappen Te Amsterdam Deel 34, No. 5.
[7] Private communication.

In this case the coils were welded to 120 mil Mo leads and correction made for the resistance of the latter by making a separate determination of the resistance of similar Mo leads.

The resistance of the coil at 0°C measured by the Wheatstone bridge method was obtained before and after a set of data by immersing in well stirred distilled water maintained at 0°C by a surrounding ice and salt bath. To obtain values of the hot resistance, the coiled filament was placed in the center of a constant temperature compartment which in turn was placed in the center of the alundum tube in a resistance furnace through which a constant slow stream of pure dry hydrogen was continuously passed.

The constant temperature compartment consisted of two alundum discs spaced 4 inches apart and held firmly in position by means of heavy molybdenum wires passing through them, while a cylindrica molybdenum shield co-axial with the alundum furnace tube and having one half inch clearance from it fit snugly between them. As a precautionary measure, two radiation shields were placed at equal distances from each end of the central heating compartment, six being used altogether to divide the furnace tube into zones. It was observed that for any constant setting of the current through the resistance coil of the furnace the temperature at any point within the central compartment was constant.

The temperature was determined by the potential difference, as measured on a potentiometer, between the hot and cold (0°C) junctions of a well-aged chromel-alumel thermocouple. The latter was calibrated before and after a set of data against a well aged standard platinum, platinum-rhodium couple.

The curve for the platinum couple was obtained by calibrating against a newly standardized Bureau of Standards platinum couple while the melting points of the purest obtainable tin, aluminum, gold and copper were also used for fixed points at which the thermocouple millivolts and the resistance of the tungsten coil were measured simultaneously in the hydrogen furnace. The thermocouple was also checked at the gold point in air immediately after each set of measurements.

Hot resistance measurements were obtained on a number of different coils both on the ascending and descending temperature curves with the temperature in the central heating compartment brought to a constant value for each reading.

As a check on the accuracy of the data obtained in the hydrogen furnace, resistance data were obtained on some coils up to 250°C in an

oil bath. These data agreed well with those from the furnace measurements.

The resistivity of tungsten at 0°C was obtained from measurements on a number of coils by the Wheatstone bridge method and also from measurements on straight pieces of each of the well aged wires W_1, W_2 and W_3 by the current voltage method using a laboratory standard potentiometer. The value obtained at 0°C expressed as the resistance of a cylindrical wire 1 cm long and 1 cm in diameter agrees with Langmuir's value, i.e.,

$$R' = 6.37 \times 10^{-6} \pm .01$$

The results of the measurements, expressed in terms of the function R', were plotted on a large scale against temperature and the most probable curve drawn through the data. The data from all the coils measured were found to lie very closely along this smooth curve from which the data in the table were obtained.

The data for the resistivity of tungsten were then used to estimate the temperatures in a determination of the energy radiated in watts per unit area of surface for the range 1500°K to 293°K.

Three lamps, each of which had a cocoanut charcoal side tube attached, which was immersed in liquid air to insure good vacuum, were used for this experiment. The lamps contained two V-shaped filaments, one 40 cm and the other 50 cm long of W_1, W_2 and W_3 wires respectively. The filaments were arc-welded to equal lengths of 40 mil molybdenum leads, and were degassed and aged according to the schedule described previously.

The volt-ampere characteristics were measured for the two different lengths of each size of filament and the watts radiated per unit area calculated by the method of differences to eliminate lead losses. This method was found to be more consistently reproducible than that involving the use of fine wire potential leads welded to a measured length of filament (although this method was also used in several check experiments).

Direct experimental determinations of the watts radiated per cm^2 were thus obtained down to 600°K below which temperature errors due to lead losses could not be eliminated. The watts radiated per cm^2 below 600°K were calculated by the method of Davisson and Weekes.[8] The complete data expressed as watts input necessary to maintain one cm^2 of tungsten at the temperature T are given in the table.

[8] Davisson and Weekes, J.O.S.A. **8** (May, 1924).

These same lamps were subsequently used to measure the watts radiated per unit area and the resistivity of tungsten in the range 1200° to 3000°K. The filament temperatures, at which the electrical characteristics were obtained for the two lengths of each wire, were estimated by pyrometering against a standard lamp. This lamp was

TABLE I

Resistance and radiation data on tungsten filaments. R' is the resistance of a filament 1 cm long and 1 cm in diam.; ρ is the specific resistance in ohm cm; W' is the number of watts radiated from 1 cm length of a filament 1 cm in diam.; W is radiation from the surface in watts per cm.²

The data are based on filament dimensions measured at room temperature.

	Jones				Zwikker		Forsythe and Worthing	
T°K	$R'+10^6$	W'	$\rho+10^6$	W	$\rho+10^6$	W	$\rho+10^6$	W
273	6.37	0.0	5.00	0.0	.....	.....	.....	.....
293	6.99	0.0	5.49	0.0	.....	.....	.....	.....
300	7.20	0.0000501	5.65	0.000016	.....	.....	.....	.....
400	10.26	0.00619	8.05	0.00197	.....	.....	.....	.....
500	13.45	0.0304	10.56	0.00970	.....	.....	.....	.....
600	16.85	0.0953	13.23	0.0304	.....	.....	.....	.....
700	20.49	0.240	16.10	0.0764	.....	.....	.....	.....
800	24.19	0.529	18.99	0.169	.....	.....	.....	.....
900	27.94	1.04	21.94	0.331	.....	.....	.....	.....
1000	31.74	1.89	24.90	0.602	.....	.....	.....	.....
1100	35.58	3.24	28.10	1.030	.....	.....	.....	.....
1200	39.46	5.24	31.96	1.67	30.9	1.70	32.02	1.70
1300	43.40	8.10	34.10	2.58	34.0	2.70	35.24	2.60
1400	47.37	12.1	37.18	3.86	37.1	3.94	38.52	3.86
1500	51.40	17.4	40.35	5.54	40.2	5.52	41.85	5.61
1600	55.46	24.4	43.50	7.77	43.4	7.90	45.22	7.86
1700	59.58	33.3	46.78	10.6	46.7	10.7	48.63	10.73
1800	63.74	44.4	50.00	14.2	49.9	14.1	52.08	14.46
1900	67.94	58.2	53.30	18.6	53.2	18.6	55.57	18.6
2000	72.19	75.0	56.67	23.9	56.7	24.0	59.10	24.1
2100	76.49	95.1	60.00	30.3	60.1	30.5	62.65	30.4
2200	80.83	119.0	63.40	37.9	63.5	38.2	66.25	38.1
2300	85.22	147.2	66.85	46.8	66.9	47.2	69.90	47.0
2400	89.65	179.9	70.38	57.3	70.5	57.3	73.55	57.0
2500	94.13	217.4	73.83	69.2	74.0	69.4	77.25	69.2
2600	98.66	260.6	77.38	83.0	77.6	83.5	81.0	83.0
2700	103.2	310.1	81.00	98.8	81.2	100.5	84.7	98.9
2800	107.9	366.4	84.69	116.7	84.8	119.0	88.5	116.5
2900	112.5	430.3	88.30	137.2	88.5	139	92.3	136.5
3000	117.2	502.6	92.00	160.1	92.3	162	96.2	159.6
3100	122.0	583.9	95.74	186.1	97.0	189	100.0	184.2
3200	126.8	675.2	99.55	215.0	99.9	221	103.8	211
3300	131.6	777.5	103.3	247.6	103.8	254	107.8	242
3400	136.5	891.9	107.2	284.0	107.8	291	111.7	276
3500	141.4	1020	111.1	325.0	.....	.....	115.7	314
3600	146.4	1164	115.0	371.0	.....	.....	.....	.....
3655	149.2	1253	117.1	399.4	.....	.....	121.8	376

standardized through the kindness of Dr. W. E. Forsythe of the Nela Research Laboratory, to whom I am further indebted for checking temperatures and electrical characteristics on several of the experimental lamps.

The temperature scale used in the pyrometrey determinations is one recently adopted by the General Electric Company's research laboratories. On this scale the gold point is the Day and Sosman[9] value of 1336°K and C_2 of Wien's equation is taken as 1.433 cm deg. (the value adopted for the forthcoming International Critical Tables). On this scale the palladium point is 1829°K,[10] and the melting point of tungsten comes out to be 3655°K.[5]

Worthing's determination[11] of the spectral emissive power for tungsten, upon which the standard lamp temperatures were based has been independently verified by Zwikker.[6]

Zwikker's comprehensive paper was published subsequently to the completion of our work. The values given by him for watts radiated and resistance are tabulated in columns 6 and 7 in the table. The agreement with our values is excellent in the temperature range in which the efforts were duplicated.

Forsythe and Worthing[5] have recently published a summary of the properties of tungsten as a function of temperature. Their values for the watts radiated and the resistivity of tungsten are also given in columns 8 and 9 in the table. Since their values for the resistivity of tungsten are somewhat higher than the more recent determinations by Zwikker, and the writer (compare values in Table I) new values for the various functions which have been found convenient for estimating the temperature of tungsten filaments will be published in the near future in the General Electric Review.

The writer extends his thanks to Dr. Langmuir and to Dr. S. Dushman for many helpful suggestions during the course of the work.

RESEARCH LABORATORY,
GENERAL ELECTRIC COMPANY,
SCHENECTADY, NEW YORK.
March 15, 1926.

[9] Day and Sosman, Amer. Jour. of Sci. **29**, 93 (1910).
[10] Hyde and Forsythe, Astrophys. J. **51**, 244 (1920).
[11] Worthing, Phys. Rev. **10**, 377 (1917).

THE VAPOR PRESSURE OF SOLID SODIUM AND SOLID POTASSIUM AMALGAMS

By Franklin E. Poindexter

Abstract

The vapor pressure of solid sodium and potassium amalgams.—A Buckley ionization gauge was used to measure the vapor pressure of eight sodium amalgams ranging in concentration from 1 : 1 to 15 : 1 mol ratio of Hg to Na and of 3 potassium amalgams whose concentrations were 5 : 1, 10 : 1 and 21 : 1, Hg : K. The vapor pressure of each amalgam was measured at a number of temperatures which were determined by means of a platinum resistance thermometer. The pressures measured varied from approximately 10^{-8} mm to 10^{-3} mm over a maximum temperature range of from $-56°$ to 90°C. *The log p vs $1/T$ graphs for the different amalgams were found to be approximately straight lines.* The difference between the free energy calculated by R. H. Gerke and the internal energy change as calculated in this work shows that the log p vs $1/T$ graphs can be expected to be straight within the experimental error. The heats of reaction were calculated by means of the Van't Hoff reaction isochore, the pressures at different temperatures for these calculations being taken from the log p vs $1/T$ graphs. These heats of reaction for the sodium amalgams varied from 15,000 cal. in the case of the amalgams rich in Hg to 14,000 cal. for the 2 : 1 amalgam. This small heat difference over such a wide range of concentrations indicates that most of the heat of reaction between Na and Hg is liberated in the formation of the initial compounds. The heats of reaction for the potassium amalgams were calculated to be 25,500 cal.

Duration of the efficiency of a sodium mercury vapor trap.—The vapor pressure of 1 : 1 sodium amalgam was extrapolated to 20°C and found to be 3×10^{-8} mm. The time necessary for sufficient mercury to diffuse through 100 cm of tubing having an internal diameter of 1 cm to form a 1 : 1 amalgam with 10 g. of sodium was found to be 1554 days. That is, a sodium mercury vapor trap containing 10 g. of sodium should hold the mercury vapor beyond the trap down to 10^{-8} mm for 1500 days under the prescribed conditions.

The relation between the free and internal energy changes of potassium and sodium.—The internal energy change of potassium as calculated from the log p vs $1/T$ graphs are somewhat greater than the free energy change as calculated by R. H. Gerke. This indicates that the temperature gradient of the e m.f. of concentration cells should be small and negative. There seems to be no experimental data with which to check this prediction. For sodium Richards and Conant found that the temperature gradient of the e.m.f. of concentration cells was comparatively large and positive, thus indicating that the free energy change is considerably greater than the internal energy change. R. H. Gerke calculated the free energy change from electrochemical data for a 5 : 1, Hg : Na sodium amalgam to be 18,300 cal. which is of the order of 3,000 cal. greater than the internal energy change as calculated from the log p vs $1/T$ graphs. That is, the present work is in agreement with the above.

THE vapor pressure of each of a number of solid sodium and potassium amalgams has been measured at a series of temperatures and the heat of formation calculated by means of the Van't Hoff Reaction Isochore. Notwithstanding the fact that the literature is practically devoid of data on the heats of reaction between these alkalies and mercury, yet, in the case of sodium amalgams, agreement is found both with Cady's work on heat of dilution and with that of Richards and Conant[1] on the e.m.f. of concentration cells.That is, the present work indicates that the heat of dilution is small compared to the heat of reaction involved in the formation of the initial compounds, and also that the heat of reaction, or total internal energy change U, is considerably less than the change in free energy as indicated by the comparatively large temperature gradient of the e.m.f. of concentration cells. In the case of potassium, no work has been done on the heat of dilution or on the e.m.f. of concentration cells and, consequently, no comparisons can be made. The present work indicates, however, that the temperature gradient of the e.m.f. of concentration cells of potassium in mercury may be expected to be small and negative.

There is also a matter of very practical importance involved in the study of the vapor pressure of the amalgams rich in these alkalies. This has been brought about by the recent discovery[2,3] in this laboratory that a sodium or potassium trap is almost, if not quite, as effective as a liquid air trap for stopping mercury vapor. A knowledge of the vapor pressure of an amalgam enables one to calculate the time that must elaspse for sufficient mercury to diffuse into the trap to form this amalgam. That is, the time it takes for the mercury vapor beyond the trap to reach a given value can be estimated with a fair degree of accuracy. Such a calculation has been made for a sodium trap.

Apparatus

The apparatus used is shown diagramatically in Fig. 1, the essential features consisting of a Buckley[4] ionization gauge B, an amalgam reservoir R, a potassium mercury vapor trap T and a McLeod gauge with a high vacuum mercury diffusion pump and a Cenco rotary fore-pump. The McLeod gauge and pumps are not shown

[1] A fairly complete bibliography on Na amalgams will be found in a paper by Richards and Conant, J. Am. Chem. Soc. **44**, 610 (1922).

[2] F. E. Poindexter, J.O.S.A. & R.S.I. **9**, 629 (1924).

[3] Hughes and Poindexter, Phil. Mag. **50**, 432 (1925).

[4] Buckley, Proc. Nat. Acad. Sci. **2**, 683 (1916).

in the diagram. The most important part of this set-up is the ionization gauge and its accessories. Since it was found desirable to modify the type of Buckley gauge as used by Dushman[5] and others, it is thought desirable to describe the gauge here used in some detail.

The action of the ionization gauge depends upon the ionization of the gas molecules by electrons which are driven from the filament F, to the plate P, the ions thus formed being collected by the grid G. Now Dushman,[5] in his extended research, finds that the straight line relation between the ionization and the electron current (within

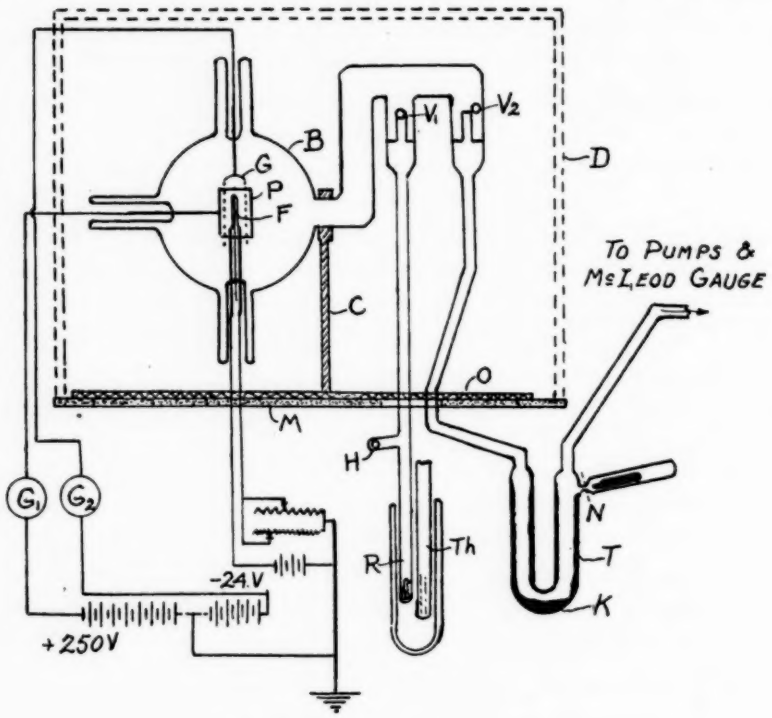

Fig. 1. Diagram of apparatus.

certain limits) holds only when the paths of all of the electrons are the same length. He also calls attention to the importance of separating the lead-in wires as much as possible in order to prevent electrical leakage over the glass. The present structure incorporates these features. However, the ion collecting grid G, is not a filament as Dushman[5] found necessary in his modification by reason of the outgassing difficulties. It was found in this and the three[2,3,6] pre-

[5] S. Dushman, Phys. Rev. **17**, 7 (1921).
[6] F. E. Poindexter, Phys. Rev. **26**, 859 (1925).

ceding researches that after a few days spent in alternately baking at 400°C, and bombarding the plate at red heat, the evolution of gas was below the limit of the gauge, i. e. less than 4×10^{-9} mm. The present design has the added, very important advantage that a filament may be replaced very easily without disturbing the remaining parts. In the writer's[6] work on mercury vapor pressure, an ionization gauge was described wherein protecting collars were used about the plate and grid stems in order to prevent electrical leakage. These collars are not necessary if mercury vapor is carefully excluded during the bombardment of the plate, sputtering being thus prevented.

The filament F, is a straight loop of 10 mil tungsten wire braced by means of a 20 mil tungsten wire thrust into the glass between the leads. The grid is a spiral of 7 mil tungsten wire carried by a 10 mil tungsten frame extending down each side, each end of the spiral being welded to the supporting frame. The plate P is of nickel and somewhat longer than the filament while the grid G is longer than the plate. This extra length in the plate and grid is a precaution against stray ions or electrons collecting upon the glass walls of the gauge which may give erratic results. The main part of the gauge is a one liter Pyrex flask. It is made large so that its temperature while the gauge is in use is considerably lower than the outgassing temperature.

The plate P was maintained at $+250$ volts relative to the filament F, by means of a storage battery. The galvanometer G_1, used to measure the electron current from filament to plate was a Leeds and Northrup type P galvanometer having a sensitivity of 2.66×10^{-8} amp. per scale division. A universal shunt was used with G_1 which multiplied the electron current readings in steps of 10. The deflection of G_1 was held at 100 scale divisions throughout the experiment, the shunt being set at 10 to 1, 100 to 1, and 1000 to 1. This eliminated any possibility of error due to non-uniformity of the galvanometer scale. The grid G was maintained at -25 volts with respect to the filament. The positive ions formed by the collision of electrons with the molecules of gas between F and P were collected on the grid G. The ion current from G was measured by the highly sensitive, critically damped, Leeds and Northrup type R galvanometer G_2, having a sensitivity of 8×10^{-10} amp per scale division. The sensitivity of this galvanometer was found to be constant over all parts of the scale.

The amalgam reservoir R, and the mercury vapor trap T, were connected to the ionization gauge through the steel ball valves V_1 and V_2. The glass seats of these valves were repeatedly ground and polished with similar steel balls and the finest of emery flour—obtained by

means of fractional settling in water—to the point where the dry seats would hold the 1/2″ ball in an inverted position for 5 minutes when partially exhausted by suction. The leakage of these valves was negligible at the pressures used in this work. The valves were opened and closed by means of an electromagnet.

A *U*-tube mercury vapor trap *T* was placed between the apparatus and the McLeod gauge. Clean potassium was driven into the trap and the empty container sealed off as indicated at *N*.

A platinum resistance thermometer of approximately 25 ohms resistance and carrying a current of .01 amperes was used to determine the temperatures. The potentiometer balance method against a standard resistance held at constant temperature was used, the balance being obtained through a Leeds and Northrup type *R* galvanometer. The platinum thermometer was calibrated three times at the ice, steam, and liquid oxygen points, at intervals of a few weeks. These calibrations checked. The constants and Pt differences found by Callender and others[7] were in close agreement with those of this thermometer, and it is thought that the temperatures are probably correct to 1/100°.

Preparation of Materials

The mercury used to prepare the amalgams was twice distilled in a current of air in a modified Hulett still. The purification of the alkali metal is more important than the redistillation of the mercury. In the first place, the oil in which sodium or potassium has been packed must be removed down to the last trace before introduction

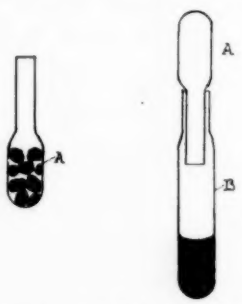

Fig. 2. Apparatus for cleaning the alkali metals.

into a high vacuum system. Secondly, these metals take up and retain gases in large quantities. While it seems that these gases can not be removed absolutely, yet much can be done by reflux distilla-

[7] E. Vanstone, J. Chem. Soc. (London) **105**, 2617 (1914).

tion. In order to remove the oil referred to above, the metal was washed and rinsed in benzol. Then it was placed in a large Pyrex test tube to which a smaller tube was sealed as shown at *A*, Fig. 2. This entire tube was heated in a bunsen flame till the oils were driven out and the alkali vapor began to burn at the mouth of the tube. The tube *A* was then permitted to cool and placed in juxtaposition with a second tube *B* into which the metal was driven by heating.

The outgassing and bottling arrangement for the alkali metals is shown in Fig. 3. The tube *B* of Fig. 3 was sealed on to the bottle system at *C*, through a thick walled capillary having an internal

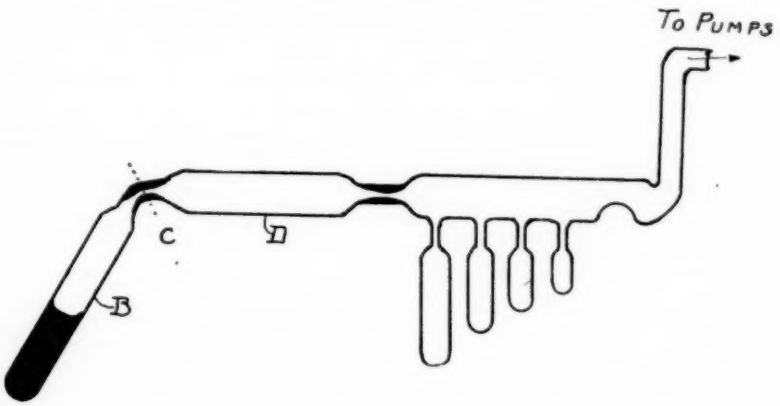

Fig. 3. Arrangement for bottling the alkali metals.

diameter of approximately1 mm. After outgassing the glass parts of the system by heating with a hand burner, the lower end of the tube *B* was heated so that the alkali metal condensed in the upper part and ran back. This reflux condensation was continued for an hour or more, then the metal was evaporated into *D* and *B* sealed off at *C*. The clean metal was then driven through another capillary into the bottles which were sealed off with a hand blow torch. The weights of the empty bottles together with the weight per cm of the necks were recorded. In this way, the weight of the alkali metal in each bottle was determined to within .01 g.

Preparation of the Amalgams

It is a comparatively easy matter to prepare an amalgam of known composition by using one of the above described weighed bottles of alkali. Fig. 4 shows the necessary set up. A weighed quantity of mercury was run into the flask *A* and the bottle of alkali *B* sealed into the side neck *C*. The apparatus was exhausted through a flexible

connection E and the different parts outgassed by baking with a hand blow torch. The mercury was then run into the thin walled bottles D and the alkali metal run into A, the side neck C, being sealed off at F and the whole arrangement allowed to cool. The mercury was then run in on the sodium or potassium in small quantities by tilting A. As soon as all the mercury was mixed with the alkali, and still hot from the reaction, the flask A was sealed off at G. The whole was carefully heated in a large bunsen flame until the amalgam was entirely molten, care being taken not to heat it too much since it might have exploded from the mercury vapor pressure.*

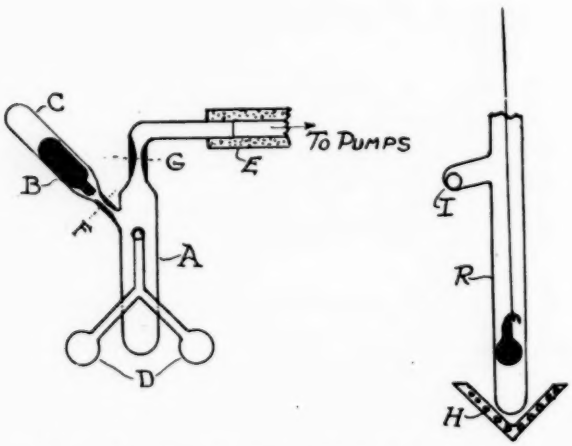

Fig. 4. Apparatus for preparations of the amalgams.

The molten amalgam was run into the thin walled bottles D, one of which was immediately sealed off and lowered into the electrically heated reservoir R, by means of a wire. In this way the amalgam was kept molten till the whole apparatus, Fig. 1, was outgassed and ready to run. When a concentrated amalgam solidifies, it usually breaks the bottle, hence the necessity of keeping the reservoir hot till the outgassing is completed. The glass bottle containing the amalgam was broken by dropping the steel ball I upon it, the ball being manipulated by means of an electromagnet.

Experimental Method

Probably the most important part of the experimental procedure was the outgassing. There were four sources of gas; the metal parts

* All of the amalgams appear to be dissociated in the liquid state. In fact, the mercury begins to distill out before the melting point is reached in the case of concentrated amalgams. On this account it was necessary to seal off the mixing chamber at G, Fig. 4.

in the system, the glass walls, the bottle of amalgam, and the mercury vapor trap. The base of an electric oven is shown at *m*, Fig. 1, upon which a clamp *C* was mounted to support the apparatus. An asbestos lined, removable metal box, represented by the broken line *D*, served as the oven in which the ionization gauge and the steel ball valves were subjected to prolonged baking at 400°C. In this manner the gas was removed from the glass walls and partially removed from the metal parts. After from 6 to 12 hours baking, the oven was removed and the plate subjected to electron bombardment from the filament by means of a 1/2 k.w. 10,000 volt transformer. This outgassing by electron bombardment was continued for several hours until the gas pressure was less than 10^{-5} mm while hot. Then the oven was placed in position and the baking at 400°C resumed and continued till the pressure was less than 10^{-5} mm. During the baking, the other glass parts, including the McLeod gauge, were outgassed by means of a hand blow torch.

The outgassed alkali metal used in the mercury vapor trap *T* was prepared in the same manner as that used in preparing the amalgams. After a bottle of this metal (potassium in this case) was driven into the trap and the side neck sealed off, as indicated at *N*, Fig. 1, it was subjected to additional reflux distillation, the upper parts of the trap serving as the condenser. While it seems impossible to drive all of the gas out of the potassium yet in this way it was reduced to such an extent that it did not interfere with the work as long as the trap was at room temperature. Whenever it was necessary to let air into the apparatus, the reflux distillation was repeated. (However, the letting in of air does not impair the efficiency of the mercury vapor trap as a trap.[3]) The test which was used in conjunction with the ionization gauge readings to determine the thoroughness of the outgassing of the whole apparatus was that the mercury should stick in the top of the reading tube of the McLeod gauge after twelve hours standing with the pumps shut off, i. e., $p<10^{-5}$ mm.

The temperatures were controlled by means of a thermos bottle bath about the amalgam reservoir. This bottle was cooled to such a temperature that the vapor pressure was below the limit of the gauge, and then warmed up in steps to 5° to 10° by the addition of small quantities of warmer liquid. Forty minutes were allowed for the equalization of the temperature, and twenty minutes for the equilizaton of pressure. That is, valve V_1, Fig. 1, was closed and valve V_2 opened during the first 20 min. Then V_1 was opened and V_2 closed and the pressure allowed to build up for 20 min. In most cases, the pressure became steady in ten minutes.

It was necessary in some instances to correct for an intial gas effect. This correction was determined by cooling the amalgam to such a temperature that its vapor pressure was below the limit of the gauge and then allowing the pressure to build up for a period of 20 minutes at a time at consecutively increased temperatures. These pressures were approximately constant until the temperature was reached at which the vapor pressure of the amalgam began to play a part. This initial, constant pressure was subtracted from the pressure that built up in the subsequent periods. The correction was negligible in all of the amalgams with the exception of numbers 1, 2 and 3 (see col. 4 Table XII) and these will be discussed under Gas Effects.

The amalgams were analyzed for sodium or potassium by titrating the excess of dilute H_2SO_4 used to acidify the amalgam, with NaOH, using phenophthalein as indicator, the acid solution being boiled before neutralization.* The mercury was weighed direct. In all cases the mercury broke up into fine permanent globules indicating the complete removal of the alkali as noted by Richards and Daniels.[8]

Data and Results

The ionization gauge is particularly well adapted for pressures below 10^{-2} mm. However, it is an indirect method and the ionization for a given electron current will be different for different gases. It is, thereore, necessary to calibrate the gauge at some one temperature for mercury vapor. Then the ratio of the ionization in that gas at any other temperaure to that at the calibrating temperature is equal to the ratio of the respective pressures. That is, the vapor pressure, P', in the ionization gauge G, is proportional to the ratio of the positive ion current I, to the electron current E, i. e.

$$P' = KI/E$$

Knudsen's[9] value of $P = .0001846$ mm at 0°C was used to calibrate the gauge. When P' is in mm of mercury, I in scale divisions and $E = 1000$ scale divisions, then

$$K = 3.38 \times 10^{-6} \text{ mm/1 scale division of ion current.}$$

The experimental data are given in Tables I to III. The values of P' in mm of mercury are given in column 3 of the tables as uncorrected pressures, because the pressures above the mercury in the amalgam reservoir are not directly in the ratio of the positive ion

* The writer wishes to thank Prof. R. W. Pilcher of the Chemistry Department for making up the standard solutions used and for valuable suggestions as to the analysis.

[8] Richards and Daniels, J. Am. Chem. Soc. **41**, 1736 (1919).

[9] Knudsen, Ann. d. Physik **29**, 179 (1909).

current on account of the phenomenon of thermal effusion as pointed out by Knudsen,[10] West,[11] and others.

Thermal effusion correction. A correction of the pressure for thermal effusion between two regions of different temperature in a system is

TABLE I

Vapor pressures of sodium-mercury amalgams.

Electron current scale divs.	Ion current scale divs.	Uncorrected pressure P'	True pressure P	Temp. of amalgams
		(1) Hg:Na = .985:1		
100,000	12	2.88×10^{-7}	2.90×10^{-7}	44.6°C
"	17	4.08×10^{-7}	4.12×10^{-7}	47.5
"	33	7.92×10^{-7}	8.12×10^{-7}	57.1
"	78	1.87×10^{-6}	1.95×10^{-6}	67.3
"	118	2.83×10^{-6}	2.97×10^{-6}	72.2
"	230	5.52×10^{-6}	5.85×10^{-6}	79.9
"	513	1.23×10^{-5}	1.32×10^{-5}	90.8
		(2) Hg:Na = 1.19:1		
100,000	11.0	2.64×10^{-7}	2.66×10^{-7}	46.3
"	23.7	5.69×10^{-7}	5.78×10^{-7}	51.4
"	38.5	9.24×10^{-7}	9.46×10^{-7}	56.4
"	71.3	1.71×10^{-6}	1.75×10^{-6}	61.4
"	104.7	2.51×10^{-6}	2.61×10^{-6}	66.0
"	188.0	4.51×10^{-6}	4.73×10^{-6}	72.0
"	295.0	7.32×10^{-6}	7.48×10^{-6}	77.0
"	707.0	1.70×10^{-5}	1.82×10^{-5}	84.3
		(3) Hg:Na = 1.63:1		
100,000	2.5	8.45×10^{-8}	8.08×10^{-8}	9.58
"	7.0	2.36×10^{-7}	2.28×10^{-7}	14.46
"	12.0	4.06×10^{-7}	3.96×10^{-7}	21.39
"	25.5	8.63×10^{-7}	8.47×10^{-7}	25.86
"	41.0	1.385×10^{-6}	1.38×10^{-6}	31.08
"	65.5	2.20×10^{-6}	2.21×10^{-6}	36.31
"	101.5	3.43×10^{-6}	3.45×10^{-6}	40.85
"	157.0	5.31×10^{-6}	5.45×10^{-6}	48.45
"	389.5	1.32×10^{-5}	1.36×10^{-5}	59.75
		(4) Hg:Na = 1.96:1		
100,000	23.0	5.52×10^{-7}	5.01×10^{-7}	−14.17
"	34.7	8.33×10^{-7}	7.62×10^{-7}	−10.36
"	36.0	8.64×10^{-7}	7.96×10^{-7}	−6.02
"	51.0	1.22×10^{-6}	1.13×10^{-7}	− 3.67
"	75.5	1.81×10^{-6}	1.69×10^{-6}	− .08
"	90.8	2.18×10^{-6}	2.04×10^{-6}	+ 1.41
"	126.5	3.07×10^{-6}	2.86×10^{-6}	6.07
"	155.0	3.72×10^{-6}	3.52×10^{-6}	7.40
"	230.0	5.52×10^{-6}	5.24×10^{-6}	10.61
"	282.0	6.77×10^{-6}	6.47×10^{-6}	13.89
"	374.0	8.98×10^{-6}	8.58×10^{-6}	14.37
10,000	69.4	1.67×10^{-5}	1.70×10^{-5}	18.93
"	134.0	3.23×10^{-5}	3.31×10^{-5}	23.30
"	149.0	3.58×10^{-5}	3.69×10^{-5}	24.15
"	240.0	5.76×10^{-5}	5.98×10^{-5}	28.63
"	431.5	1.03×10^{-4}	1.08×10^{-4}	33.79
1,000	100.0	2.40×10^{-4}	2.57×10^{-4}	40.64
"	247.0	5.93×10^{-4}	6.41×10^{-4}	45.09
"	378.0	9.07×10^{-4}	9.91×10^{-4}	51.80

[10] M. Knudsen, Ann. d. Physik **31**, 205 and 33, 1435 (1910).

[11] G. D. West, Proc. Phys. Soc. **31**, 278 (1919).

TABLE I (continued)

Electron current scale divs.	Ion current scale divs.	Uncorrected pressure P'	True pressure P	Temp. of amalgams
		(5) Hg:Na = 3.41:1		
10,000	43.5	1.04×10^{-5}	1.02×10^{-5}	− 8.83°C
"	55.5	1.33×10^{-5}	1.30×10^{-5}	− 3.72
"	99.5	2.39×10^{-5}	2.38×10^{-5}	4.38
"	168.0	4.03×10^{-5}	4.04×10^{-5}	7.59
"	280.0	6.72×10^{-5}	6.80×10^{-5}	14.10
1,000	85.0	2.04×10^{-4}	2.13×10^{-4}	23.68
"	185.5	4.44×10^{-4}	4.68×10^{-4}	28.63
"	253.5	6.07×10^{-4}	6.48×10^{-4}	35.74
		(6) Hg:Na = 5.86:1		
100,000	16.0	3.84×10^{-7}	3.25×10^{-7}	−47.68
"	64.0	1.54×10^{-6}	1.33×10^{-6}	−36.74
"	168.0	4.06×10^{-6}	3.56×10^{-6}	−27.72
"	419.0	1.01×10^{-5}	9.02×10^{-6}	−19.26
10,000	156.0	3.74×10^{-5}	3.63×10^{-5}	−10.09
"	173.0	4.15×10^{-5}	4.02×10^{-5}	− 9.67
"	363.0	8.72×10^{-5}	8.58×10^{-5}	− 1.71
1,000	77.0	1.85×10^{-4}	1.86×10^{-4}	4.14
"	234.0	5.62×10^{-4}	5.75×10^{-4}	12.16
"	312.0	7.49×10^{-4}	$7.69\times10^{-}$	14.15
		(7) Hg:Na = 5.78:1		
100,000	8.5	2.04×10^{-7}	1.72×10^{-7}	−49.77
"	32.0	7.68×10^{-7}	6.58×10^{-7}	−42.43
"	133.5	3.20×10^{-6}	2.81×10^{-6}	−31.82
"	383.5	9.21×10^{-6}	8.22×10^{-6}	−22.64
10,000	103.5	2.48×10^{-5}	2.38×10^{-5}	−15.14
"	172.0	4.13×10^{-5}	4.02×10^{-5}	− 7.42
"	374.0	8.98×10^{-5}	8.86×10^{-5}	− .51
1,000	77.0	1.85×10^{-4}	1.87×10^{-4}	4.83
"	187.0	4.49×10^{-4}	4.57×10^{-4}	9.20
"	289.0	6.94×10^{-4}	7.12×10^{-4}	13.72
"	385.0	9.24×10^{-4}	9.53×10^{-4}	16.98
		(8) Hg:Na = 15.71:1		
100,000	1.5	3.60×10^{-8}	2.99×10^{-8}	−56.68
"	13.0	3.12×10^{-7}	2.66×10^{-7}	−45.29
"	59.5	1.43×10^{-6}	1.24×10^{-6}	−35.43
"	76.0	1.82×10^{-6}	1.55×10^{-6}	−34.94
"	173.5	4.17×10^{-6}	3.69×10^{-6}	−26.55
"	365.0	8.76×10^{-6}	7.85×10^{-6}	−21.20
"	410.0	9.84×10^{-6}	8.84×10^{-6}	−19.08
10,000	92.5	2.22×10^{-5}	2.13×10^{-5}	−14.58
"	144.0	3.46×10^{-5}	3.35×10^{-5}	−10.48
"	168.5	4.05×10^{-5}	3.93×10^{-5}	− 8.72
"	268.5	6.46×10^{-5}	6.32×10^{-5}	− 4.22
"	309.0	7.42×10^{-5}	7.30×10^{-5}	− 2.86
"	395.0	9.48×10^{-5}	9.36×10^{-5}	− .04
1,000	56.5	1.36×10^{-4}	1.36×10^{-4}	2.62
"	56.0	1.34×10^{-4}	1.35×10^{-4}	2.65
"	73.0	1.75×10^{-4}	1.77×10^{-4}	4.88
"	158.0	3.79×10^{-4}	3.85×10^{-4}	7.27
"	159.0	3.82×10^{-4}	3.87×10^{-4}	7.40
"	189.0	4.54×10^{-4}	4.62×10^{-4}	9.41
"	221.0	5.30×10^{-4}	5.42×10^{-4}	11.34
"	256.5	6.16×10^{-4}	6.31×10^{-4}	12.90
"	317.0	7.61×10^{-4}	7.83×10^{-4}	15.27
"	407.0	9.77×10^{-4}	1.01×10^{-3}	18.26

necessary when the mean free path is great compared to the dimensions of the parts connecting the two regions. In this research the tube

connecting the amalgam reservoir to the ionization gauge was approximately 1 cm in diameter and since the mean free path at the highest pressures measured (1.2×10^{-3} mm) was of the order of 2 cm, it was necessary to make this correction. This correction for a similar gauge was discussed in detail in a recent paper[6] and the reader is referred to that discussion for the details.

TABLE II

Vapor pressures of potassium-mercury amalgams.

Electron current scale divs.	Ion current scale divs.	Uncorrected pressure P'	True pressure P	Temp. of amalgams
		(9) Hg:K = 5.226:1		
100,000	258.0	8.72×10^{-6}	7.96×10^{-6}	−13.61
"	425.0	1.436×10^{-5}	1.33×10^{-5}	− 7.16
10,000	94.5	3.19×10^{-5}	3.16×10^{-5}	− 2.95
"	161.0	5.42×10^{-5}	5.42×10^{-5}	2.11
"	282.0	9.54×10^{-5}	9.59×10^{-5}	7.15
"	475.5	1.61×10^{-4}	1.65×10^{-4}	11.46
1,000	86.0	2.92×10^{-4}	3.01×10^{-4}	15.70
		(10) Hg:K = 10.667:1		
100,000	377.5	1.28×10^{-6}	1.15×10^{-6}	−19.51
10,000	60.0	2.03×10^{-5}	2.00×10^{-5}	− 2.45
"	111.5	3.77×10^{-5}	3.76×10^{-5}	1.88
"	181.5	6.13×10^{-5}	6.14×10^{-5}	6.43
"	283.5	9.58×10^{-5}	9.69×10^{-5}	10.72
"	457.0	1.545×10^{-4}	1.57×10^{-4}	14.20
1,000	76.0	2.57×10^{-4}	2.67×10^{-4}	18.15
"	114.6	3.87×10^{-4}	4.05×10^{-4}	21.93
		(11) Hg:K = 20.833:1		
100,000	207.0	6.96×10^{-6}	6.26×10^{-6}	−24.03
10,000	89.0	3.01×10^{-5}	2.90×10^{-5}	−14.43
"	161.0	5.44×10^{-5}	5.31×10^{-5}	− 9.05
"	297.0	1.005×10^{-4}	9.89×10^{-4}	− 3.25
1,000	54.0	1.825×10^{-4}	1.84×10^{-4}	1.28
"	87.5	2.96×10^{-4}	3.01×10^{-4}	5.77
"	150.0	5.07×10^{-4}	5.20×10^{-4}	10.86

The experimental data and results are displayed in Tables I, II, III, and in the $\log p$ *vs* $1/T$ graphs of Figs. 5 and 6. In Tables I and II the electron and ion currents, columns 1 and 2, are given in scale divisions. These may be converted to amperes by multiplying by the sensitivities of the electron and ion current galvanometers, 2.66×10^{-8} and 8×10^{-10} respectively. The uncorrected pressures P', in column 3, are the pressures in the ionization gauge. To get the true pressure, P in column 4 of the tables, in the amalgam reservoir, it was necessary to correct for thermal effusion as mentioned above. These corrected pressures are found in column 4. The molecular ratio of mercury to alkali, the heat for formation U, and the initial gas effect are shown in Table III, in which the amalgam numbers correspond to those of Tables I and II. The $\log p$ *vs* $1/T$ graphs in

Figs. 5 and 6 for pure mercury were plotted from data previously published by the writer.[6]

Discussion of Results

Gas effects. There were three sources of gas back of the valve V_2, Fig. 1; the ionization gauge, the walls of the amalgam reservoir or amalgam bottle and the amalgam. These effects are made manifest in a striking manner in some of the graphs. Let us first examine the graphs of amalgams numbered 1 and 2, Fig. 5. The initial gas effects (col. 4 Table III) in the case of numbers 1 and 2 were 22 and 26 scale

Table III

The internal energy change, U, and the initial gas effect for Hg, Na and Hg,K amalgams.

Amalgam No.	Mol Ratio Hg:Alkali	Internal energy change U	Initial gas effect in scale divs.
	Sodium amalgams		
1	.985:1	19,000	22
2	1.19 :1	21,500	26
3	1.63 :1	15,800	11
4	1.96 :1	14,000	0
5	3.41 :1	14,300	2
6	5.86 :1	upper curve	0
7	5.78 :1	14,500	0
8	15.71 :1	lower curve	
		15,500	1.5
	Potassium amalgams		
9	5.226:1	25,500	0
10	10.667:1	25,500	0
11	20.833:1	.....	0

divisions of ion current respectively.* The graphs of these two amalgams have slopes that are too steep (as indicated by the high** heat values) and the one with the greater slope gave the greater initial gas correction. The slope of the graph number 3 is but slightly steeper than it should be (judging from the slopes of the graphs of the amalgams whose heats gradually increase with dilution and whose initial gas effects were negligible)yet its initial gas effects were approximately half that of number 1 and 2. This is accounted for by the fact that it became necessary to install a new filament in the ionization gauge just prior to the run on number 3. A new filament will continue to give off small quantities of gas in diminishing quantities for a number of days. Since we have no reason to believe that the evolution of gas from the filament would increase with a rise in temperature of the

* See section on "Experimental method" for initial gas effect correction.

** Since there is a positive heat of dilution for the amalgams, the total heat of reaction should be greater the greater the dilution.

amalgam, the slope of the graph should not be affected. It is not surprising that there was a slight evolution of gas in the case of these three amalgams since their mercury vapor pressure became readlabe at temperatures considerably above that of the room.

The break in the graph of amalgam number 4 near room temperature is an example of the extreme care necessary in outgassing. This

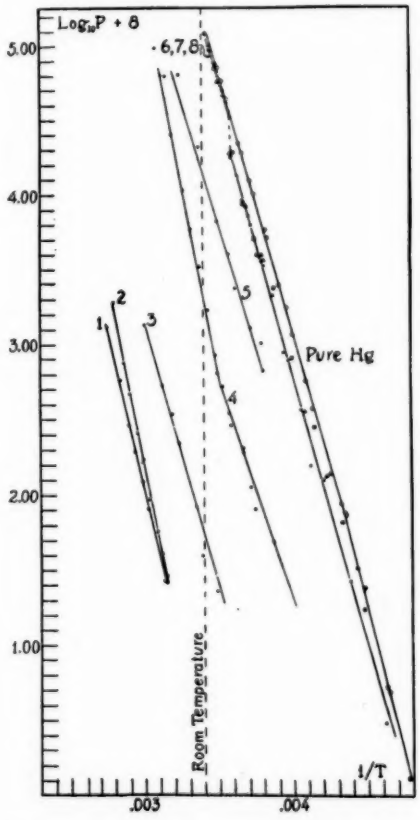

Fig. 5. Graphs for the sodium amalgams.

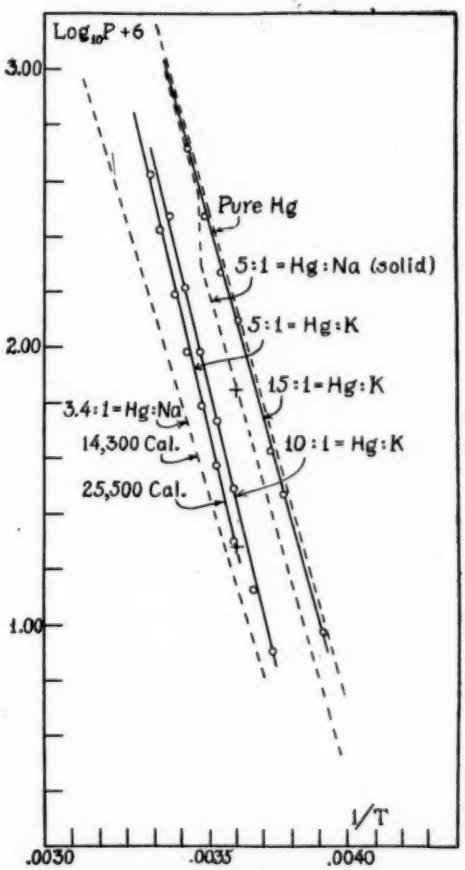

Fig. 6. Graphs for the potassium amalgams. (Some sodium amalgams are shownfor comparison.)

bottle of amalgam was introduced cold. When the amalgam reservoir was warmed up the bottle broke and consequently neither the reservoir nor the outside of the bottle could be properly outgassed. There was no initial gas correction and the lower part of this graph gives a heat of reaction that is thought to be reliable.

Graphs of amalgams numbered 6, 7 and 8. The fact that the graphs of these three amalgams coincide is explainable on the basis of a saturated

solution in mercury of an amalgam whose formula is $NaHg_5$. A number of experimenters[8] have identified this well defined crystalline amalgam at ordinary temperatures. Between 4° and 5°C, however, the whole mass of amalgam and mother liquor solidifies, even in the case of amalgam number 8 which had a mol ratio 15.7 : 1 = Hg : Na, and the vapor pressure suddenly drops. Evidently an amalgam can exist below say 4°C which has a formula of $NaHg_x$ where $x > 15.7$. This behavior together with the two facts, first, that mercury is easily driven out of a solid amalgam far below its melting point, and second, that cooling curves have shown such a large number of compounds between mercury and sodium [7,12,13] inclines one to the thought that the role played by the greater part of the mercury in these amalgams is of the nature of that played by water in a large number of our common crystalline compounds. (See especially Roozeboom's work on ferric chloride.[14]) That is, we may well call this excess of mercury, above, say, Na_2Hg, mercury of crystallization.

It is also worthy of note that the vapor pressure of the partially liquid amalgam is but little below that of pure mercury. R. H. Gerke,[15] in a very interesting paper based upon the electrochemical measurements of a number of different observers, made the surprising prediction that this could be expected. He deduced that in the formation of a gram mol. of $NaHg_5$ the reduction in the free energy of the gram atom of sodium amounted to 18,046 cal. while the reduction in free energy of a gram atom of the mercury was only 61 cal. His words on this point are:

"The most striking and unexpected conclusion which can be drawn from these data, is that the mercury does not greatly change in free energy when it enters into chemical combination with a more electropositive metal. In other words, the vapor pressure of a pure liquid mercury is only very slightly greater than the partial pressure of mercury from an amalgam saturated with a mercuride."

This, also, adds weight to the theory that liquid amalgams are dissociated and that the greater part of the mercury even in $NaHg_5$ is held as mercury of crystallization. Vanstone[7] concluded from electrical conductivity and specific volume measurements that all liquid amalgams are probably completely dissociated. From Smith and Bennett's work[16] we see that at 5°C the mercury and sodium in a saturated

[12] E. Vanstone, Chem. News **103**, 182 (1921).
[13] A. Schüller, Zeits. Anorg. Chem. **40**, 385 (1904).
[14] B. Roozeboom, Zeits. Phys. Chem. **10**, 477 (1892).
[15] R. H. Gerke, J. Am. Chem. Soc. **45**, 2508 (1923).
[16] G. McP. Smith and H. C. Bennett, J. Am. Chem. Soc. **32**, 622 (1910).

solution of $NaHg_5$ is approximately in the mol ratio of 20 : 1. If these molecules are dissolved in mercury then the mol ratio of solvent to solute is 15 : 1 and consequently the vapor pressure should be lowered some 6 percent. Suppose, however, that the solute is Na_2Hg, Na_3Hg or Na_4Hg, then it is readily seen that the vapor pressure would be lowered by a very small amount; i. e., it would be approximately 1 percent in the case of Na_4Hg.

The graphs of 9, 10 *and* 11. These are potassium amalgams. It will be observed that 9 and 10, Fig. 6, have a greater slope than the corresponding sodium amalgams which are plotted for the sake of comparison. This, of course, means that the heat of reaction between potassium and mercury is greater than that for sodium and mercury (the ratio is approximately 5 to 3). In the case, however, of number 11, we have a striking departure from the behavior of the sodium amalgams. This amalgam was partially liquid at the lowest temperature used and its vapor pressure differs but slightly from that of pure mercury. There is a well defined potassium amalgam whose formula according to Smith and Bennett[16] and others is KHg_{12}. Number 11 was evidently a saturated solution of these crystals in mercury.

Heats of reaction. The heats shown in column 3 of Table XII were calculated by applying the integrated Van't Hoff isochore[17] to large scale graphs similar to those shown in Figs. 5 and 6, that is

$$\mathrm{Ln}\frac{p_2}{T_2} - \mathrm{Ln}\frac{p_1}{T_1} = \frac{U}{R}\left(\frac{1}{T_1} - \frac{1}{T_2}\right) \qquad (1)$$

where p_1 and p_2 are the saturated mercury vapor pressure of the amalgams, T_1 and T_2 are the respective temperatures on absolute scale, R is the gas constant and U is the total change of internal energy when a gram molecule of the amalgam is formed, i. e., U is the heat of reaction at constant volume and is assumed constant over the range of temperature T_1 to T_2. The vapor at these low vapor pressures can not depart appreciably from an ideal gas and, since the gas law is the only other simplified assumption involved in these calculations it is thought that the heats thus obtained are accurate to within say ± 200 cal.*

[17] W. Nernst, Theoretical Chemistry, p. 747 (1923 edition).

* The heats could not be calculated from the log p *vs* $1/T$ graphs with a greater accuracy than ± 200 cal. It is thought that the pressures as obtained from the smooth graphs of the amalgams of low or zero gas effect are accurate to within one percent. This error in the pressures introduces an additional error of approximately ± 200 cal. in the heats.

It will be noticed in Table III that the difference in the internal energy changes U, involved in the formation of the different amalgams is comparatively small. This means that the greater part of the heat of reaction is evolved in the initial compounds formed, i. e., Na_3Hg, Na_2Hg, etc. It also follows that the heat of dilution is comparatively small. Unfortunately the literature is practically devoid of data on the heats of dilution or reaction of sodium and potassium amalgams. There is considerable electrochemical data on the subject, which, however, cannot be directly applied[18] to the calculation of the heats of dilution as pointed out by Richards and Conant[1] p. 609 in their paper on the Electrochemical Behavior of Liquid Sodium Amalgams, in which they have this to say:

"Aside from a few rough experiments by Berthelot[19] and a few more of Cady[20] on heats of dilution, there has been no thermochemical study of sodium amalgalms. It has been shown that these data are not directly applicable to the thermodynamic considerations of the electrochemical results, because the latter involve not dilution but rather transfer of sodium from a more concentrated to a more dilute amalgam."

The heat of reaction between sodium and mercury in the formation of a 10 percent by weight amalgam ($NaHg_2$) was found by Berthelot to be 10,300 cal. per gram molecule of amalgam. For a 7 percent by weight potassium amalgam (approximately HKg_5) the same author found the heat of reaction per gram molecule of amalgam to be 20,800 cal. The method used by Berthelot was an indirect calorimetric process in which little confidence can be placed, yet, apparently, it is all we have with which to compare the heats calculated in the present work. In the case of the sodium amalgam, the heat of reaction as herein calculated is 140 percent of that found by Berthelot and for the potassium amalgam it is 125 percent. Notwithstanding the fact that the heats calculated in the present paper are a maximum (an increasing evolution of gas would increase the slope of the log p $vs\,1/T$ graph) it is thought that, with the exception of amalgams number 1, 2 and 3, the heats given in Table III are correct to ± 400 cal.

The heats given in Table III also indicate that the internal energy change is considerable less than the free energy change as calculated by Gerke.[15] This is in agreement with the work of Richards and Co-

[18] See Richards and Daniels[8] p. 1761, for a complete discussion of this point in connection with their work on Thallium Amalgams.

[19] Berthelot, Am. Chem. Phys. **5**, 18, 442 (1879).

[20] Cady, J., Phys. Chem. **2**, 560 (1898).

nant[1] on the temperature gradient of concentration cells of sodium amalgams. They found that the temperature gradient of the e.m.f. was positive and comparatively large giving a considerable difference between the free and internal energy change.

The change in internal energy for the potassium amalgams was calculated from the $\log p$ vs $1/T$ graphs to be 25,500 cal. According to Gerke,[15] the free energy change in the formation of a KHg_{12} amalgam should be 24,200 cal., assuming that the free energy change of the mercury is the same (-61 cal.) as in the formation of sodium amalgams. Accordingly, then, we may expect the temperature gradient of the e.m.f. of potassium amalgam concentration cells to be small and negative. Unfortunately the writer has not been able to find experimental data with which to check this conclusion.

Straight line graphs. The integrated Van't Hoff relation, Eq. (1), may be written in the form

$$U=\frac{R(\ln p_2-\ln p_1)}{1/T_1-1/T_2}-\frac{R(\ln T_2-\ln T_1)}{1/T_1-1/T_2}. \tag{2}$$

Taking 10° intervals, the variation with the temperature of the last term of this equation from 10°C to -30°C is but 81 cal. i. e., this term amounts to 405 cal. at 10° and 486 cal. at -30°. This variation is well within the experimental error and, therefore, may be neglected. It follows then, from the fact that the best possible graph in all cases was a straight line, that the heat of reaction was constant within the experimental error (± 400 cal.).

The heat of reaction, U, may be expressed as a function of the temperature as,

$$U=U_0+\alpha T+\beta T^2+\gamma T^3+\cdots \tag{3}$$

where U_0 is the heat of reaction at 0°K and α, β, γ, etc., are constants. This gives

$$dU/dT=\alpha+2\beta T+3\gamma T^2+\cdots \tag{4}$$

The integration of the Gibbs-Helmholtz relation

$$A-U=TdA/dT \tag{5}$$

and the substitution of the value of U as given in equation (3) gives,

$$A=U_0+aT-\alpha T\ln T-\beta T^2-\tfrac{1}{2}\gamma T^3-\cdots \tag{6}$$

where a is the constant of integration and A is the free energy change. Differentiating this last equation with respect to T we get,

$$dA/dT=a-\alpha-\alpha\ln T-2\beta T-3/2\gamma T^2\cdots \tag{7}$$

According to the Nernst theorem,

$$dA/dT = dU/dT = 0 \tag{8}$$

at 0°K. For this to be true both a and α must be zero. Therefore we have

$$U = U_0 + \beta T^2 + \gamma T^3 + \cdots \tag{9}$$

and

$$A = U_0 - \beta T^2 - \tfrac{1}{2}\gamma T^3 \cdots \tag{10}$$

Neglecting terms in γ and beyond, we get upon subtracting (9) from (10).

$$A - U = -2\beta T^2 \tag{11}$$

Substituting 18,300 cal. for A as calculated by Gerke, and 14,500 for U as calculated from the log p vs $1/T$ graph, we get the value of β at 280°C to be $-.024$. From Eq. (4) we have $dU/dT = 2\beta T = -13.44$ cal. per degree. According to the Nernst hypothesis, dU/dT diminishes in our case with decreasing temperature, but if it were constant over a range of say 40°, the variation in U would be approximately -500 cal. But the effect of the last term in Van't Hoff relation discussed in the preceeding paragraph was to diminish the value of U by 80 cal. over this range. Therefore the variation of slope was of the order of 400 cal. which is still within our error of ± 400 cal. Thus we can expect the log p vs $1/T$ graphs to be straight lines.

Parallelism of graphs. Since the slope of the log p vs $1/T$ graphs determine the heat of reaction, the parallelism means that the heat of dilution is comparatively small. This is in agreement with the work of Cady[20] who found the average heat of dilution of a 20 : 1 mol ratio of Hg : Na amalgam when diluted to 86.7 : 1 to be 136 cal. per gram mol. of mercury added. That is, the greater part of the heat of reaction is liberated in the initial compounds of mercury with sodium or potassium. In making up the amalgams, it was necessary to add the mercury very cautiously since the initial mercury always reacted with explosive violence, the heat liberated being sufficient to vaporize the alkali and mercury and scatter the whole over the walls of the mixing chamber.

Duration of efficiency of sodium trap. When mercury is first added to an alkali, it reacts violently. The violence of this reaction diminishes rapidly as the mercury content increases, the point being soon reached, at approximately a 1 : 1 mol ratio, at which the additional mercury is quietly soaked up. A drop of mercury on the wall of a vessel containing an amalgam whose mol ratio of Hg : Na is less than 5 : 1, i. e.,

solid amalgam, will disappear in a short time. A sodium or potassium trap between an apparatus and a source of mercury vapor will gradually turn black on the side next to the source of mercury vapor. This discoloration creeps but slowly along the trap, the farthermost parts remaining perfectly bright for weeks. These facts indicate that the action between the mercury and the sodium is not a surface effect but is rather a mass action. That is, that the mercury is distributed more or less evenly throughout the mass of the amalgam formed. We will assume that it is a mass action in the following calculation.

Two facts are necessary to such a calculation. First, we must know the vapor pressure of a limiting amalgam. In this instance, we will take an amalgam whose molecular ratio of Hg to Na is 1 : 1. By drawing the best mean straight line through the three lowest points for amalgam number 1 parallel to the graph of amalgam 3 (gas effect in number 3 being small) the vapor pressure of a 1 : 1 amalgam was extrapolated to be 3×10^{-8} mm at 20°C. Then if we place 10 g. of sodium in a trap, 87 g. of mercury must diffuse into this trap in order for the mercury vapor pressure in the trap to be as much as 3×10^{-8} mm.

Secondly, we must know the rate of flow of mercury vapor through the connecting tubes under working conditions. The flow of gases at low pressures has been worked out both theoretically and experimentally by M. Smoluchowshky, M. Knudsen and W. Gaede who have published a large number of papers on this subject since 1908. The following treatment is from S. Dushman's book on High Vacuum.[21] When the mean free path of the molecule is large compared to the diameter D, of the tube through which the gas is flowing, then the quantity, Q, (measured in pressure volume units) which flows through the tube of length, l, in 1 sec. is related to the driving pressure, P_2-P_1, by the equation

$$Q=\frac{P_2-P_1}{(W_1+W_2)\sqrt{\rho_1}},$$

where $w_1=6l/\sqrt{2\pi}D^3=2.394l/D^3$; $w_2=\sqrt{2\pi}/A$ (A = Area of cross-section of tube); and $\rho_1=m/83.15\times10^6T$ is the density at 1 bar pressure and at the temperature of the tube.

Let us assume a room temperature of 20°C and that the trap is separated from the source of mercury vapor by 100 cm of tubing whose diameter is 1 cm i. e., $l=100$ and $D=1$. Then we have $w_1+w_2=242.6$. For mercury $\rho_1=82\times10^{-10}$ at 20°C. The vapor pressure of

[21] Production and Measurements of High Vacuum by S. Dushman, General Electric Review (1922).

mercury at 20°C is .00121 mm and the back pressure of 3×10^{-8} mm is negligible compared to it. Therefore, we have, finally $Q=73.4$ cc/sec. That is, there are 73.4 cc of mercury vapor at a pressure of 1 bar entering the trap each sec. This amounts to .056 g. per day. This means that it would require 87/.056 or 1554 days for the pressure from the trap to reach 3×10^{-8} mm. During the first 2 years of this time the formula for the amalgam would be richer in sodium than Na_2Hg, and since it appears that the greater part of the energy of reaction is liberated in the formation of these initial amalgams, there is no telling how low the pressure really is.

The writer wishes to thank Professor A. L. Hughes for his interest and helpful suggestions throughout this research.

PHYSICS LABORATORIES,
WASHINGTON UNIVERSITY,
ST. LOUIS, MISSOURI.
February 26, 1926.

A NOTE ON THE TRANSVERSE VIBRATION OF STRINGS

By Satyendra Ray

Abstract

The investigation of the velocity of propagation of transverse waves in strings is generally made under the assumption that the wave form is very flat. It is shown here that the velocity is a function of the dimensionless quantity α/λ where α is the amplitude of vibration and λ the wave-length. When α/λ is constant, or the waves are geometrically similar, the velocity of propagation is a constant, but not otherwise.

THE transverse vibration of strings is generally investigated for a case in which the wave form is very flat. An attempt is made here to determine the correction necessary for the departure from this condition in actual practice.

Let l be the length of the string when there is no tension on it whatsoever, and let m be the mass of the string. Then by Hooke's Law the tension is given by the relation

$$T=\gamma\delta l/l$$

and ρ the mass per unit length of the wire is given by the expression $\rho=m/(l+\delta l)$.

For the velocity of the disturbance along the string we have the expression

$$v=\sqrt{T/\rho}=\sqrt{\frac{\gamma\delta l/l}{m/(l+\delta l)}}=\sqrt{\frac{\gamma}{m}\frac{(l+\delta l)\delta l}{l}}$$

or, neglecting the square of δl, we have for a first approximation

$$v=\sqrt{\gamma\delta l/m}=\sqrt{\gamma\delta l/\rho_0 l}=\sqrt{\gamma\epsilon/\rho_0}$$

where $\rho_0=m/l$ and $\epsilon=\delta l/l$.

The velocity of propagation along the string varies as the square root of the elongation per unit length and is constant only if this elongation remains constant.

In a "plane polarized wave" the elongation ϵ varies with the time, but in a "circularly polarized wave" the length and therefore the elongation remains constant during the vibration of the string if the amplitude remains constant. This circularly polarized wave is in fact easier to generate in a rope than the plane polarized wave. If we grip the lower end of a rope hanging from the roof and give it a circular

motion in a horizontal plane, by adjusting the speed of rotation we can throw the rope into stationary vibration with any number of nodes and loops that we like. And during this stationary motion the length of the string remains constant. We shall therefore find ϵ for this simple case, where

$$x = a \sin 2\pi(t/\tau - z/\lambda) + a \sin (t/\tau + z/\lambda)$$
$$y = a \cos 2\pi(t/\tau - z/\lambda) + a \cos (t/\tau + z/\lambda)$$

Simplifying we get

$$x = 2a \cos (2\pi z/\lambda) \sin (2\pi t/\tau)$$
$$y = 2a \cos (2\pi z/\lambda) \cos (2\pi t/\tau)$$

For the form of vibration at distance z we have

$$x^2 + y^2 = 4a^2 \cos^2 2\pi z/\lambda$$

which is a circle of radius $r = 2a\cos 2\pi z/\lambda$ where z is measured from a loop. The string therefore forms a sine curve given by the equation

$$r = 2a \sin 2\pi z/\lambda \ .$$

and the plane of the curve rotates about the axis of z with a period equal to the period of vibration, the length of the string remaining unaltered.

We now proceed to find the elongation per unit length, $\epsilon (= \delta l/l)$ in terms of the amplitude for the string bent into a sine curve of equation $y = \alpha \sin 2\pi z/\lambda$. The formula for rectification is

$$l + \delta l = \int_{z=0}^{z=\lambda/2} ds = \int_0^{\lambda/2} \left(1 + \frac{4\pi^2\alpha^2}{\lambda^2} \cos^2 2\pi z/\lambda\right)^{\frac{1}{2}} dz$$

Strangely enough this integral is not given in any textbook of integral calculus on which the present author could lay his hands either as a solved example or as an exercise. We note however from the physical conditions of the experiment that the integral is finite for finite values of the amplitude. Expanding the expression under the radical sign and integrating we have on setting $4\pi^2\alpha^2/\lambda^2 = e$ and $2\pi z/\lambda = \theta$,

$$l + \delta l = \frac{\lambda}{2\pi} \int_0^{\lambda/2} \left(1 + \frac{4\pi^2\alpha^2}{\lambda^2} \cos^2 2\pi z/\lambda\right)^{\frac{1}{2}} d(2\pi z/\lambda)$$

$$=\frac{\lambda}{2\pi}\int_0^{\pi}\left(1+\frac{1}{2}e^2\cos^2\theta-\frac{\frac{1}{2}\cdot\frac{1}{2}}{1\cdot 2}e^4\cos^4\theta\right.$$

$$\left.+\frac{\frac{1}{2}\cdot\frac{1}{2}\cdot\frac{3}{2}}{1\cdot 2\cdot 3}e^6\cos^6\theta-\cdots\right)d\theta$$

$$=\frac{1}{2}\lambda+\frac{1}{2}\lambda\left[\frac{e^2}{2^2}-\left(\frac{1}{2}\right)^2\cdot\frac{3e^4}{4^2}+\left(\frac{1\cdot 3}{2\cdot 4}\right)^2\frac{5e}{6^2}-\right.$$

$$\left.-\left(\frac{1\cdot 3\cdot 5}{2\cdot 4\cdot 6}\right)^2\frac{7e^8}{8^2}+\cdots\right]$$

or

$$\delta l/l=\epsilon=\left[\frac{e^2}{2^2}-\left(\frac{1}{2}\right)^2\cdot\frac{3e^4}{4^2}+\left(\frac{1\cdot 3}{2\cdot 4}\right)^2\cdot\frac{5e^6}{6^2}-\cdots\right]=\Phi(\alpha/\lambda)$$

We note immediately that when α/λ is constant the velocity of the disturbance along the string is constant but not otherwise. This is a result identical with that obtained by the present author for waves along tubes of electric force.[1]

LUCKNOW UNIVERSITY,
February 6, 1926.

[1] Ray, Zeits. f. Physik **8**, 112 (1922).

BOOK REVIEWS

Atomzertrümmerung. [*Verwandlung der Elemente durch Bestrahlung mit α-Teilchen*]—HANS PETTERSSON und GERHARD KIRSCH.—The authors are well known contributors from the Radium Institute in Vienna to the field of radioactivity and within the last few years to the field of artificial disintegration of atoms. The memoir of 244 pages is divided into eight sections. In the first is given a comprehensive history of attempts, experimental and theoretical, bearing on transmutation of elements, starting with the dream of the mediaeval alchemists and passing through the period of the discovery of radioactivity and noting some of the "transmutations" of elements that were erroneously supposed to have been accomplished by radiations from radioactive substances. Section two presents a review of the essentially necessary facts concerning α rays, the nuclear atom and in particular the phenomenon of scattering of the α-particles as well as the discovery of the *H* rays. The experiments of Rutherford and his collaborators showing that the *H* ray (hydrogen nucleus) is not a product of radioactive disintegration but a product of the action of α rays on hydrogen or hydrogen compounds are fully discussed. The following three sections deal in detail with the experiments, experimental methods and the results of artificial disintegration. Firstly, the pioneer experiments of Rutherford are reviewed and this is following by a detailed, description of the contributions made by the workers at the Vienna Radium Institute, which researches have been directed by one of the authors. Experiments dealing with the study of the long range α-particles are all reviewed in a critical manner. The results of studies of proton emission from various elements are tabulated and discussed. It may be noted in particular that Pettersson-Kirsch definitely report emission of protons from carbon while Rutherford-Chadwich quite as definitely report no protons from this element when it is bombarded by α-particles. The scintillation method of counting was used in all these experiments and the various methods used by Rutherford and Chadwich and by the authors are discussed in detail as are also the optical arrangements necessary for accurate work. The experiments of Blackett and others using the Wilson cloud method are also discussed in full detail. In section seven the authors consider the theoretical bearing of all known experiments, including those of β-γ ray emission, on the conceptions of the nuclear structure. The memoir concludes with a full bibliography of original papers and standard works.—vii+247 pp., 61 figs. Akademische Verlagsgesellschaft M. B. H., Leipzig, Germany, 1926.

ALOIS F. KOVARIK

The Theory of Sound. (Vol. 1, second ed., reprinted). LORD RAYLEIGH.—To the small but growing group of workers in acoustics, Lord Rayleigh's two volumes on the Theory of Sound has been an indispensible aid in the mathematics of this troublesome subject. The 1894 edition was exhausted several years ago, and it is a tribute to the lasting quality of this great treatise that the demand after more than thirty years is great enough to justify a reprinting. Thanks are due the publishers for making this work once more available in a substantial and attractive volume.—xiv+480 pp., 53 Figs., Macmillan and Co., New York City, N. Y., 1926.

PAUL E. SABINE

Lehrbuch der Technischen Physik. Bd. II. Optik, Elektrik.—GEORG GEHLHOFF.—This is the second and concluding volume of this work, and is almost twice the size of the first. (For review of first volume see Phys. Rev., **26**, 141, 1925.) About one-third of the book is devoted to optics and the remainder to electricity, which is handled

at greater length than any of the other subjects. As stated in the preface, the difference in treatment between this and the ordinary physics text is more evident in the present volume than in the first. Much of the section on electricity deals with topics ordinarily found only in treatises on electrical engineering. There are in addition, however, chapters on gaseous discharge, high vacuum production and measurement, and x-rays, which round the book out and add greatly to its value. The section on light deals chiefly, as might be expected, with matters connected with illumination and with optical instruments, but application in the fields of interference, diffraction, and polarization are not neglected, and there is a special chapter on spectral analysis, with a good discussion of high-resolution spectroscopes. On the whole, it is a very useful and fairly up-to-date treatise. One looks in vain for discussion of such subjects of recent interest as the manifold new applications of ultra-violet light or the quartz crystal stabilized transmitter in radio work, but such omissions are excusable because the issuing of this volume has been considerably delayed on account of the death of two of the collaborators. The two volumes together make a work well worth a place on the shelves of every library of physics.—Pp. xx+761. Johann Barth, Leipzig, 1926. Price 45 R.M.

L. R. INGERSOLL

Astronomical Physics. F. J. M. STRATTON.—This book, by one of the younger English astrophysicists, is intended, mainly for the serious student. It covers almost the whole field of modern astrophysics and contains a great amount of information upon astrophysical matters, supplemented by a very valuable set of references, throughout, to original papers and memoirs. The data which are given are reliable, and usually brought well up to the date of writing—or to that of correcting the proof—and the cases where observations are apparently inconsistent, or opinions are conflicting, are fairly and judicially presented. The arrangement of the material is somewhat less fortunate, and suggests that lecture notes or similar material have been utilized when time was not fully available for reworking them into a connected account—which may be attributed to the pressure of teaching duties to which the author refers in his preface. While this would make the book rather hard reading for the student who acquired his first acquaintance with the facts through its means, it does not detract at all from its usefulness as collateral reading for university lecturers, or by advanced students,—for which it is heartily to be commended. Of special value to the professional astronomer as well as the student are the admirable chapter on Novæ—(of which the author is well known to have exceptional knowledge,)—and the list of lines of unknown origin, appearing in various astrophysical spectra, which has been compiled by Mr. Baxandall. Errors are few, and usually in matters not affecting the main discussion—for example, in the formula for correcting radial velocity for the influence of the solar motion, on p. 89. The historical summaries which are occasionally introduced are of interest. It may be mentioned that it was Hertzsprung, and not the present reviewer, who first called attention to the relation between the spectral peculiarities of the stars and their real brightness; and it is surprising that in the discussion of the hypothesis of the origin of the solar system by the action of a passing star upon the sun, no reference should be made to Chamberlin and Moulton, who originated this theory many years ago—as is frankly acknowledged in the work of the later English workers upon the subject. Pp. xi+213, 32 figs., E. P. Dutton and Co., New York City, N. Y., 1924. Price $5.00.

HENRY NORRIS RUSSELL

Modern Astrophysics. HERBERT DINGLE.—This volume represents a successful attempt to present the results of modern astrophysical research in a form intelligible and attractive to the general reader. Formal mathematical developments are omitted or subordinated, but the physical significance of the phenomena is clearly explained. The

guiding principle of presentation is thoroughly modern, opening with four chapters on Spectroscopy, which deal not only with the experimental facts but with their interpretation in terms of atomic structure, excitation and ionization. The second section of the work treats of the characteristics of the stars and the correlations between them, dealing mainly with the observed facts, and gives a very good account of the state of knowledge at the time the book was completed. A summary is also included of the theory of stellar evolution (as advanced by the writer of this review, previous to Eddington's important work, which appeared just too late to be included in the book). The third section "Varieties of Cosmic Bodies" discusses the sun, the stars, the nebulæ, and star-clusters, from the standpoint of astrophysical theory—dealing with the problems of sun-spots, of ionization in the solar atmosphere, of the sequence of stellar spectra, of variable stars, and the like. The existence of dark nebulæ, and the probability that galactic nebulæ are excited to shine by the radiation of neighboring stars, are fully recognized, as is the importance of star-clusters in determining the extent of the visible universe. The last three chapters, on the Universe "as it is," "as it was" and "as it will be" discuss its extent, origin and ultimate physical destiny—maintaining a judicious agnosticism upon the last two questions. In a popular survey of so extensive a field, occasional errors are almost inevitable—for example, the statement (p. 124) that "if we could assume that the universe is in what is called dynamically a steady state, we could determine the mass of a star directly from its velocity with respect to the center of gravity of the universe" is at best true only statistically, of large groups of similar stars. But these slips are of minor importance, and not numerous. More serious exception might be taken to the relatively large space given to some of the older theories, and the small space allotted to such important matters as Saha's theory of ionization. It may be remarked also, that Lockyer's theoretical recognition of the existence of stars of rising and falling temperature had a more direct influence upon the later work of the reviewer than would be gathered from the present work (p. 154). The style is clear and readable, and gains from the occasional short and appropriate literary allusions, and the stimulating discussions of the philosophical implications of the more general principles and conclusions of the science—should be of value to the student as well as the general reader. Pp. XXVIII+420, Macmillan Company, New York City, 1924. Price $8.50.

HENRY NORRIS RUSSELL